The tolerance of wheat (*Triticum aestivum* L.) to Septori tritici blotch

La tolérance du blé (*Triticum aestivum* L.) à la septoriose

A thesis submitted to:

the University of Nottingham, School of Bioscience (Sutton Bonington, United Kingdom)

and

l'École doctorale Agriculture, Alimentation, Biologie, Environnement et Santé — ABIES, AgroParisTech (Paris, France).

Prepared by François Collin for the dual-award of

the degree of Doctor of Philosophy

and

the grade of Docteur de l'Institut agronomique, vétérinaire et forestier de France.

October 2017

Acknowledgments

This work would not have been possible without the participation of Arvalis, the University of Nottingham and the UMR ECOSYS (AgroParisTech, INRA). I am proud to have been part of these organisations which carry project, support research and provide an environment for scientific achievement.

Firstly, I am grateful to Marie-Odile and Pierre Bancal and John Foulkes who supervised the PhD project. They provided effective guidance and support. They have also taught me complementary methods and approaches which, I hope, spread through this study. Besides, they encouraged my participation in conferences which were good opportunities to communicate about my work and to confront with the scientific community. If I obviously have a profound respect for them as scientists, I also appreciate their sympathy, kindness and encouragement which are an inspiration for me. Thank you very much.

My participation in this project would not have been possible if I had not met Jean-Charles Deswarte and David Gouache. They showed a large enthusiasm for my participation in this project and helped for a smooth and effective transition from my former position to this study. They regularly contributed to the project, bringing ideas and complementary standpoint on the project. Beyond the scientific input they provided, they also helped me to take confidence in my work and emphasised the professional relevancy of it.

In addition, many people fed the scientific discussion and helped us during the French steering committees, the ADAS meetings of the tolerance project restitution and other meetings. I am therefore grateful to Neil Paveley, Julie Smith, Femke van den Berg, David Causeur, Frank van den Bosch, Pierre Casadebaig, Bénédicte Quilot-Turion, Mickaël Chelle for their respective contributions.

Moreover, I want to thank Larissa Ondo, Julie Rodrigues, Maxime Marques, Fabrice Duhamel for their implication in the glasshouse experiment. I am thankful for the assistance and the good company of Dennis Churchill and James Durnford during my stay for the field experiment in Hereford. I thank Jayalath De Silva who organised effective technical assistance and training in Sutton Bonington as well as Dongfang Li who has been very kind and helpful for the chemical analysis.

Finally, the PhD project was personally demanding because of the alternate periods in

the UK and in France. However, it was also an incredible enrichment. I would never have imagined that I would meet so many people from so many shores in such a short time. They have been supportive, helping colleagues, supporting friends, housemates, tourists (!), I am keen to thank: Marion, Gita, Helena, Maike, Verena, Alfonso, Becca, Kate, Ajit, Shadia, Kamal, Letizia, Iride and Anna.

Thank you, merci and dziękuję!

Abstract

The Septoria tritici blotch disease (STB, pathogen *Zymoseptoria tritici*) is the most damaging foliar infection of wheat crops in Europe. Disease management strategies include cultivar resistance, disease escape strategy and fungicides. However, these strategies have failed to provide a complete protection of wheat crops. The STB tolerance is a complementary approach which aims to maintain yield in the presence of the symptoms.

The tolerance of STB relies on plant physiology and source/sink balance: the sink demand (the grain growth) must be satisfied in spite of reduced source availability (photosynthetic capacity as affected by the STB symptoms on the leaves). The green canopy area, the senescence timing and the grain yield components are interesting potential sources of tolerance that were studied in this project.

A data-mining study, one glasshouse experiment and two field experiments were carried out providing complementary insights on STB tolerance mechanisms. The genotype × environment interaction effects on tolerance traits were investigated for two seasons × five locations × nine cultivars datasets. The nitrogen nutrition and metabolism of four doubled-haploid (DH) lines contrasting for STB tolerance were examined in a controlled-glasshouse experiment at UMR ECOSYS (INRA,AgroParisTech) Grignon, France. The source/sink balance of six DH lines contrasting for STB tolerance was also examined according to their responses to a spikelet removal treatment, applied in a field experiment in Hereford, UK. Finally, a field experiment with two fungicide regimes (full disease control and non-target (STB) disease control) probed the STB tolerance of six modern UK winter wheat cultivars in Leicestershire, UK. The main objective was to verify identified potential STB tolerance traits in commercial cultivars.

Putative STB tolerance traits have been identified such as the early heading date, the low degree of grain-source availability of healthy crops during the grain filling phase, the vertical canopy distribution favouring a relatively larger flag-leaf. Results showed these traits might be selectable in wheat breeding without a trade-off with the potential yield. Finally, the project also discussed the need for alternative STB tolerance quantification methods, as well as the importance of environmental variations which have to be taken into account to study genetic variation in tolerance, but which could also be used to discriminate tolerant environment.

Contents

1 Introduction and Literature Review **1**
1.1 Introduction . . . 1
1.2 Literature Review . . . 2
1.2.1 Potential yield . . . 3
1.2.1.1 Overview of the wheat physiology: growth and development 4
The wheat development until anthesis . . . 4
The grain filling phase . . . 6
The source/sink manipulations and grain yield limitation . 6
1.2.1.2 Fate of Nitrogen and Carbon fluxes during the senescence 7
The end of nitrogen uptake . . . 8
Senescence and N remobilisation . . . 10
Senescence and reduction of carbon assimilation . . . 13
1.2.1.3 An equation for potential yield . . . 15
1.2.2 Stress, strain and tolerance of Septoria tritici blotch . . . 17
1.2.2.1 The Septoria tritici blotch: a biotic stress of wheat crops 18
Life cycle of *Zymoseptori tritici* . . . 19
Plant × pathogen interactions . . . 20
1.2.2.2 Methods for crop control of STB . . . 21
Breeding for resistance . . . 21
Avoidance and sanitary measures . . . 22
Fungicide-based control . . . 23
1.2.2.3 Quantify the tolerance of Septoria tritici blotch . . . 25
1.2.3 Identification of STB tolerance traits . . . 25
1.3 Rationale, objectives and hypotheses . . . 29
References . . . 30

2 Materials and methods **43**
2.1 Introduction . . . 43
Introduction . . . 43
2.2 Overview of the study methods . . . 44
2.2.1 Data mining . . . 44
2.2.2 Field experiment 2014-15 . . . 45
2.2.3 Glasshouse experiment 2014-15 . . . 45
2.2.4 Field experiment 2015-16 . . . 46
2.3 Selection of genotypes or cultivars . . . 46
2.4 Growth analysis . . . 47
2.5 The Healthy Area Duration (HAD) . . . 48
2.5.1 Leaf lamina area and green leaf lamina area . . . 49
2.5.2 Post-heading green leaf lamina area kinetics . . . 50

2.5.3 Healthy Area Duration . . . 51
2.6 Source / sink ratio and tolerance . . . 51
References . . . 52

3 Genotype and environment effect on senescence and grain weight 53
3.1 Introduction . . . 53
3.2 Materials and methods . . . 57
3.2.1 Dataset, response and explanatory variables . . . 57
3.2.1.1 E, G and G×E . . . 57
3.2.1.2 The response variables: the senescence timing and the Thousand Grain Weight (TGW) . . . 59
3.2.1.3 Explanatory variables . . . 60
3.2.2 Statistical analysis . . . 61
3.2.2.1 Classification of explanatory variables by Random Forest models . . . 61
3.2.2.2 Linear model selection . . . 63
3.2.2.3 Random effects: E, G and G×E . . . 65
3.2.3 External validation. . . . 65
3.2.4 Softwares . . . 65
3.3 Results . . . 66
3.3.1 Identifying the main explanatory variables using Random Forest modeling . . . 66
3.3.1.1 Fitting the Random Forest models . . . 66
3.3.1.2 Ranking of explanatory variables according to their contribution . . . 68
3.3.2 Multiple regression models . . . 70
3.3.3 Identifying the origin of G, E or G×E . . . 74
3.3.3.1 Variance component analysis . . . 74
3.3.3.2 Partial regressions . . . 77
3.3.4 External validation . . . 87
3.3.4.1 Validation of the Random Forest models . . . 87
3.3.4.2 Validation of the linear models . . . 88
3.4 Discussion . . . 90
3.4.1 Method . . . 92
3.4.2 Senescence timings . . . 93
3.4.3 The TGW . . . 97
3.4.4 Hypotheses to improve tolerance of STB . . . 97
References . . . 99

4 Field experiment at Hereford, 2014-15 104
Abstract . . . 104
4.1 Introduction . . . 105
4.2 Materials and methods . . . 107
4.2.1 Genotypes screened for tolerance . . . 107
4.2.2 Experimental design and treatments . . . 108
4.2.3 Crop measurements . . . 109
4.2.4 Data analysis . . . 110
4.3 Results . . . 111
4.3.1 The tolerance grade of the genotypes . . . 111
4.3.2 Variability of grain filling source traits . . . 112

4.3.3 Variability of grain sink traits . . . 115
4.3.4 Source-sink balance . . . 116
4.3.5 Tolerance prediction using source and sink traits . . . 118
4.4 Discussion . . . 119
4.4.1 Tolerance and yield . . . 119
4.4.2 TGW was co-limited by source and sink . . . 120
4.4.3 Low source limitation is a genotype tolerance trait . . . 120
4.4.4 The grain source? . . . 121
4.4.5 Tolerance estimation in healthy crops . . . 122
4.5 Conclusion . . . 123
4.6 Acknowledgements . . . 123
References . . . 123

5 Glasshouse experiment at Grignon, 2014-15 127
5.1 Introduction . . . 127
5.2 Materials and methods . . . 128
5.2.1 Experimental design . . . 128
5.2.1.1 Genotype materials . . . 128
5.2.1.2 Obtaining a field-like crop in the glasshouse . . . 128
5.2.1.3 Experimental treatments . . . 129
5.2.1.4 Growth analysis . . . 131
5.2.2 Data analysis . . . 133
5.2.2.1 Population settings . . . 133
5.2.2.2 The grain yield . . . 134
5.2.2.3 The Healthy Area Duration (HAD) . . . 134
5.2.2.4 Dry matter weight and Nitrogen amounts . . . 135
5.2.2.5 Tolerance estimation . . . 135
5.2.3 Statistics . . . 136
5.3 Results . . . 137
5.3.1 From source:sink characterisation to tolerance . . . 137
5.3.1.1 Development rate . . . 137
5.3.1.2 The source traits for grain filling . . . 137
5.3.1.3 The grain sink traits . . . 142
5.3.1.4 Relation between the grain yield and HAD . . . 146
5.3.2 Analysis of dry-matter and nitrogen balance behaviour of cultivars 150
5.3.2.1 Dry-matter fluxes . . . 150
5.3.2.2 Nitrogen fluxes . . . 154
5.4 Discussion . . . 158
5.4.1 Obtaining a field-like canopy in the glasshouse. . . . 158
5.4.2 Traits associated with the putative tolerance of the genotypes. . . . 159
5.4.3 GNe tolerance of the genotypes . . . 161
5.4.4 Nitrogen and tolerance of the genotypes . . . 162
5.5 Conclusion . . . 163
References . . . 164
5.A Appendix . . . 165
5.A.1 Composition of nutrient solution . . . 165

6 Field experiment at Sutton Bonington, 2015-16 **167**
6.1 Introduction . . . 167
6.2 Materials and methods . . . 168
6.2.1 Experimental design and treatment . . . 168
6.2.2 Measurements . . . 169
6.2.3 Data analysis . . . 171
6.2.3.1 Senescence kinetics and healthy area duration . . . 171
6.2.3.2 Tolerance/intolerance . . . 172
6.2.3.3 Statistics . . . 173
6.3 Results . . . 174
6.3.1 Development rate . . . 174
6.3.2 The sources for grain filling . . . 175
6.3.2.1 Leaf area characterisation . . . 175
6.3.2.2 The senescence parameters . . . 175
6.3.2.3 The healthy area duration . . . 179
6.3.2.4 Alternative sources: the dry matter remobilisation . . . 179
6.3.3 The grain sink . . . 180
6.3.3.1 Yield and yield losses . . . 180
6.3.3.2 Yield and grain number . . . 181
6.3.3.3 Grain weight . . . 183
6.3.4 Source-sink relationship, HAD and yield . . . 185
6.3.5 Tolerance . . . 187
6.3.5.1 Cultivar tolerance estimation . . . 187
6.3.5.2 Tolerance and healthy crop traits . . . 190
6.4 Discussion . . . 194
6.4.1 Range of potential tolerance traits . . . 194
6.4.2 Insights on the estimation of tolerance . . . 196
6.4.3 Main results on tolerance and tolerance traits . . . 198
6.5 Conclusion . . . 200
References . . . 200
6.A Appendix . . . 202
6.A.1 Healthy trait correlation with tolerance estimates . . . 202

7 Discussion **205**
7.1 Highlights of the results . . . 205
7.2 The range of source/sink balance generated . . . 206
7.3 The quantification of tolerance and the scale . . . 208
7.3.1 Limits of the single slope-based estimation of tolerance . . . 208
7.3.2 Improve the tolerance estimation . . . 209
7.3.3 The grain scale relevance . . . 211
7.4 The STB-tolerance traits . . . 212
7.4.1 Comparison of the experimental results . . . 212
7.4.2 Tolerance traits . . . 214
7.4.3 Grain-source availability . . . 218
7.4.4 Interaction between tolerance traits . . . 218
7.5 Environment effect . . . 219
7.6 Tolerance and trade-off . . . 220
7.7 Perspectives . . . 221
References . . . 223

8 Synthèse du manuscrit en français **227**
8.1 Introduction . . . 227
8.2 Les études réalisées . . . 228
8.2.1 Présentation générale du matériel et des méthodes . . . 228
8.2.2 Datamining : effets du génotype et de l'environnement sur la sénescence et le poids des grains . . . 231
8.2.3 Champ 2014-15 (C2015) . . . 233
8.2.4 Serre 2014-15 (S2015) . . . 234
8.2.5 Champ 2014-16 (C2016) . . . 235
8.3 Discussion . . . 236
8.4 Conclusion . . . 239
Références . . . 239

Glossary and list of acronyms **246**

Complete list of references **247**

List of Figures

1.1 Main nitrogen metabolic pathways 9
1.2 Theoretical green blade area kinetic 15
1.3 Theoretical source/sink potential curve 17
1.4 The Septoria tritici blotch symptoms 18

2.1 Post-anthesis green area kinetics: the Gomptertz's function 50

3.1 Localisation of the expriments 58
3.2 The Gompertz's function 59
3.3 Relationship between observations and random forest predictions of the senescence timing of at the canopy level 67
3.4 Relationship between observations and random forest predictions of the TGW 68
3.5 Relationship between the fraction of flag leaf and heading date 73
3.6 Variance component analysis 75
3.7 Synthesis of the response variance explain/unexplained by the models . . 76
3.8 TGW: Synthesis of the variances explain/unexplained by the models . . . 76
3.9 Relationships between TGW and grain number per m^2: raw data and residuals of partial regressions 79
3.10 Relationships between $I1$ and heading date: raw data and residuals of partial regressions 81
3.11 Relation between heading date and I 87
3.12 External validation: observations, predictions and estimations of I 88
3.13 External validation: observations, predictions and estimations of TGW . 89

4.1 Disease severity 113
4.2 TGW at maturity 115
4.3 Relationship between relative increase in grain dry weight and relative increase in assimilate availability from the time of spikelet removal 117
4.4 TGW versus HADg 118

5.1 Intolerance estimation of the six doubled-haploid lines selected for the field trial based on three previous experiments 129
5.2 Illustration of the phases of the glasshouse experiment 130
5.3 Sampling schedule of greenhouse experiments applied to each genotype . 130
5.4 Daily temperature and global radiation exposition 132
5.5 Kinetics of fraction of Green leaf lamina area 140
5.6 Evolution of the vegetative dry-matter 141
5.7 Grain filling kinetics 145
5.8 The crop grain yield in relation to HADm 147

5.9 Relationship between the crop grain yield and the healthy area duration at the crop scale . . . 147
5.10 Comparison of tolerance estimations at grain and crop scale. . . . 149
5.11 Dry matter or Nitrogen balance per shoot . . . 151
5.12 Origin of grain dry-matter per ear-bearing shoot . . . 153
5.13 Nitrogen yield (N grain per shoot) in relation to the true N uptake and the remobilisation . . . 156
5.14 Nitrogen balance of vegetative organs since GS44 per organ . . . 156
5.15 Origin of grain dry-matter and nitrogen per ear-bearing shoot . . . 157
5.16 Comparison of glasshouse TGW, grain yield and HADm with the field observations . . . 160

6.1 TGW from hand-harvested versus combine grain samples . . . 171
6.2 Zadoks's growth stage assessment . . . 174
6.3 Evolution of post-heading green leaf lamina area. . . . 177
6.4 Relative senescence and disease evolution since heading stage. . . . 178
6.5 Average grain yield per treatment . . . 181
6.6 Linear relationship between grain yield and grain number . . . 184
6.7 Source/sink relation at square metre, shoot and grain scale. . . . 186
6.8 Grain yield per m^2 regarding the HADm (HAD per m2), per cultivar and per block . . . 187
6.9 Tolerance per m^2 or per grain . . . 189
6.10 Correlation of healthy traits with average of normalized tolerance values (Ts) and with tolerance values (Tm1, Tg1, Tm2, Tg2) . . . 191

7.1 Source/sink balance comparison between experiments . . . 207
7.2 The Yield to HAD potential curve for tolerance of STB estimation . . . 210

List of Tables

2.1 Summary of the experiments and studies 44

3.1 Relative importance of 40 most important variables for each leaf layer to explain the senescence timings or the grain weight 69
3.2 Partial regression: individual E and G intercept and slopes from the relationships between partial residuals of the inflexion point of canopy senescence and the explaining variables 83
3.3 Partial regression: individual E and G intercept and slopes from the relationships between partial residuals of the inflexion point of flag leaf senescence and the explaining variables 84
3.4 Partial regression: individual E and G intercept and slopes from the relationships between partial residuals of the inflexion point of leaf 4 senescence and the explaining variables 85
3.5 Partial regressions: individual slopes corresponding to partial correlation between the grain weight and explaining variables 86

4.1 Estimation of the genotype tolerance 112
4.2 Analysis of variance of grain source traits 114
4.3 Correlation between tolerance and grain tolerance and grain source or grain sink traits 119

5.1 Analysis of variance of the grain source trait responses 138
5.2 Values for grain source traits 138
5.3 Analysis of variance of the grain yield component responses 143
5.4 Values for grain sink traits 143
5.5 Tolerance estimations 148
5.6 Analysis of variance: nitrogen balance at the ear-bearing shoot scale . . . 154
5.7 Composition of the stock solution (i) 165
5.8 Composition of the stock solutions (ii) 165
5.9 N P K balance of the nutrient solutions 166

6.1 Inputs applied in the Field 2015-16 experiment 170
6.2 Analysis of variance of different grain source traits 176
6.3 Grain source traits observations 176
6.4 Analysis of variance of Dry Matter fluxes 180
6.5 Analysis of variance of different grain sink traits 182
6.6 Grain sink traits observations 182
6.7 Pearson's correlation coefficient between source and with sink traits estimated on the treated and untreated plots 185
6.8 Tolerance estimations 188
6.9 Correlation matrix of tolerance estimations 190

6.10 Healthy trait correlations with tolerance estimations 192
6.11 Best multiple linear correlation combinations explaining the tolerance estimations 193
6.12 Healthy trait correlations with tolerance estimations 202

7.1 Tolerance values across experiments 214
7.2 Summary of the correlations between tolerance and genotype traits . . . 215

Chapter 1

Introduction and Literature Review

1.1 Introduction

Wheat (*Triticum aestivum* L.) is genetically complex (hexaploid genome AABBDD). It is the result of a selection/hybridisation process, initiated in the Fertile Crescent, which involves the fusion of the complete genomes of three different species. It started 500,000 years ago by the hybridisation between the diploid wild wheat *Triticum urtatu* (genome AA) and an unidentified *Aegilops sp* (genome BB) resulting in the wild tetraploid wheat *Triticum turgidum* (genome AABB). The latter was domesticated 10,000 years ago, and is the ancestor, among others, of the durum wheat (*T. turgidum durum*). A second hybridisation happened 9,000 years ago between *T. turgidum* and *Aegilops tauschii* (genome DD) resulting in the ancestor of the current most widely grown bread wheat: the hexaploid wheat *T. aestivum* L. (Shewry, 2009).

The worldwide wheat crops (95% being the hexaploid wheat, Shewry 2009) rank amongst the most important for cereal production, after maize and rice: 745 million tonnes produced in 2013 FAO (2015). Wheat is largely used in food production but is also a key ingredient in animal feed. The wheat quality, mainly based on protein content, determines the end use: the best quality is used in the food industry for making breads and biscuits. The worldwide demand is increasing to support a growing population, raising concerns about the ability to meet the demand in the next decades (Godfray 2014; quantified demand increase per annum, see Hall and Richards 2013). The demand increase is also an increase of the consumption *per capita* (Curtis and Halford, 2014). In China, the population has doubled between 1962 and 2013, the wheat consumption has increased sixfold, explained by an increase in meat consumption (wheat feeds the animals) (Curtis and Halford, 2014; FAO, 2015). The increasing production of bioethanol also increases the pressure on the wheat demand (Curtis and Halford, 2014; FAO, 2015) in addition with the loss of growing land to urbanisation (FAO, 2015).

In Europe wheat production is important. In 2012, 13 of the 20 highest wheat pro-

ducing countries (per capita) were European FAO (2015). In 2014, Europe produced 249 million tonnes. France, Germany and the United Kingdom represent more than 50% of the European Union wheat production (respectively, in million tonnes: 40.0, 27.8 and 16.6, FAOSTAT 2017). The high yield observed in these countries is supported by important inputs (fertiliser and pesticides).

Septoria tritici blotch (STB, *Zymoseptoria tritici*) is responsible for important grain yield loss of wheat crops in Europe (Burke and Dunne, 2006; Fones and Gurr, 2015). Genotype resistances to the disease are sparse and subject to circumvention by the pathogen. Likewise, the fungicide-based strategies are marked by a sharp increase in pathogen resistance. In Northern France, Quinone outside Inhibitors (QoI, strobilurines, azoles) were the principal STB-inhibiting molecules. According to Cheval et al. (2017), 83% of *Z. tritici* isolates collected from naturally infected leaves were resistant to QoI in 2005, almost 100% since 2009. QoI resistance was detected as early as 2001 in the UK (Fraaije et al., 2003).

At the same time, economic, environmental and sociological contexts demand the reduced use of inputs on wheat crops in Europe. Given these pressures and genotype resistances or fungicide adaptation, tolerance (i.e. maintaining the crop yield in the presence of expressed disease (Ney et al., 2013)) is a relevant approach to protect the yield in presence of probably more frequent and severe STB symptoms.

This thesis presents the results of a PhD study targeting tolerance of STB in wheat crops. Based on ecophysiological approaches and working on wheat crops, the aim was to understand the plant mechanisms which affect STB tolerance. The final purpose was to propose strategic wheat crop traits as targets to improve tolerance of STB. This thesis manuscript is composed of a literature review. The state of the art of STB tolerance knowledge was drawn to: define the concept, explain the physiological basis, illustrate the interest of tolerance. Of course, this state of the art also identifies the knowledge gap and justifies the scientific targets which need to be investigated. Then, four chapters describe the study conducted. Finally a discussion is proposed to emphasize the important new facts, to access the limits of the present project and to show the subsequent perspectives.

1.2 Literature Review

Wheat (*Triticum aestivum* L.) is a monocarpic species. As such, its life cycle follows two main phases. The first period, from sowing to anthesis, achieves the vegetative growth while the second is associated with the reproductive growth. The two periods overlap a little, as rapid ear growth occurs from the beginning of booting to anthesis. Around anthesis, the size of the vegetative organs of the plants is set. The leaves, roots and the whole canopy architecture will not change significantly and the plant functions are then mainly oriented toward the grain filling. Since most of the significant damage caused by

Septoria tritici blotch (STB) is usually linked to the symptoms on upper leaf layers during the grain filling period — wheat as a monocarpic species and late stage disease — the tolerance of STB is a question which can be addressed primarily during the post-anthesis period. Therefore, the literature review focuses mainly on the post-anthesis period.

The tolerance of STB is the study of the crop performance reduction regarding a biological stress. The bibliography proposes a review of the following questions:

1. The potential grain yield is the relevant crop performance here and is explained in a first section. During the grain filling period, the nitrogen and carbon metabolism evolve along with the progressive senescence of the photosynthetic area. The genotype and environmental variability in healthy crops is reviewed, the quantification of the crop grain yield performance is also addressed.

2. The tolerance and resistance are two distinct properties. A clear distinction is based on the definition of the stress and the strain on crops. The STB is the biological stress in question here and is therefore extensively described. The questions that tolerance of STB quantification raise are also addressed.

3. The tolerance can be improved. Studies demonstrated potential mechanisms and genotype traits which are based on reviews or experiments. The different strategies proposed are explained in this section.

4. The potential traits and mechanisms which can be involved in tolerance can be simulated. Are there models that can be used to address the question of tolerance of STB?

The literature review is concluded by the rationale of the thesis project. The scientific gaps are identified, and hypotheses on tolerance are developed here. They are addressed by four studies which were run during this PhD project.

1.2.1 Potential yield

The tolerance of wheat is a relative property, quantifying a yield loss. The potential yield is therefore explained in the current section as the reference yield, in the absence of disease. The potential yield is generally the highest wheat grain yield attainable by a crop (Fischer, 2007). From a breeding standpoint, studies have investigated from a source/sink approach the causes of the yield limitation. In this ecophysiological approach, the source designates the organs for which the main function is the export of assimilate (e.g. the mature leaves export carbon or nitrogen) while the sink designates the organs for which the main function is the import of assimilate (e.g. the organs which provide storage capacity to support the growth). In this perspective in relation to grain growth, wheat can be described through the development of the source, the demand from the sink, respectively

the vegetative organs of the wheat shoot and the grains (Section 1.2.1.1). The source/sink relation involves transfer from source to sink, mostly carbon and nitrogen. These fluxes can be described as antagonist: as the carbon is mostly associated with anabolic functions while the nitrogen fluxes are the results of catabolic functions. The senescence is the visual evidence of these antagonist relationships, its impacts on the attainable yield are therefore described (Section 1.2.1.2). Taking a step back, the source/sink balance has been studied on multiple genotypes, in most of the wheat-growing regions, during many years and using variable crop management and source/sink manipulation strategies. Theoretically, the collection and accumulation of the source/sink data in conjunction with statistical methods may therefore define the population of possible source/sink balance and consequently may define the limit of the relationship. This limit defining the yield potential through site×year×genotype is also reviewed (Section 1.2.1.3).

1.2.1.1 Overview of the wheat physiology: growth and development

The wheat grain sink is described by the numerical components: ear number per square metre, grain number per ear and potential grain weight. This description is convenient but does not take into account the interactions between components and give sufficient insight in sink development stage organisation (Slafer et al., 2014). The determination of the different yield components is therefore explained hereafter within the physiological cycle description. The distinction was made between pre- and post-anthesis phases as the tolerance of STB is mainly associated with post-anthesis expression of STB.

- **The wheat development until anthesis**

The wheat developmental stages are visually characterised by four main phases. Development starts with the seed germination and the development and growth of the first leaves as the leaf lamina are unfolded. It is followed by the development of tillers — growth stage 20 (GS20, Zadoks et al. 1974) — which are the ramifications of the main shoot. Later, the stem elongates, the upper internodes extend and grow, the ear grows and finally pushes through the flag-leaf sheath until complete emergence. All the tillers do not develop ears, some abort, which determines the final number of ears per square metre. Finally, the flowering starts and is followed by the grain filling phase. The vegetative growth phase from a single seed results in a plant composed of several ear-bearing shoots at anthesis. The term "fertile shoot" refers to a single ear-bearing shoot from a wheat plant. The shoots of a single plant compete for the resources (e.g. solar radiation, water, nutrient) but there is no assimilate flux (although there is a N flux) from a shoot to another and they can therefore be considered as independent.

Winter wheat needs a period of cold temperatures before triggering the reproductive phase of development. In temperate climates, wheat can therefore withstand the cold win-

ter temperatures for an extended period of time as the apical meristem remains insulated below ground. Spring wheat does not require vernalisation to trigger reproductive development and can therefore be cultivated either in spring sowings in the regions where the winter is too cold (Siberia, Canada) or in autumns sowings in regions with warm winters where vernalisation is not possible (e.g. Mexico, India).

Each shoot is composed of successive phytomers (functional unit of a plant). The peduncle and ear sit above the phytomers. Each phytomer exposed to the light is composed of a node, an axillary bud, an internode and a leaf (sheath and lamina). The internode extends only for the upper phytomers and only the upper part of the internode is visible as the lower part is wrapped inside the leaf sheath. The phytomers (and respective organs) are usually numbered downward by agronomists, the phytomer 1 being the top phytomer, below the peduncle. The ear is the reproductive organ composed of a central rachis (stem-like structure) opposing two rows of spikelets. Each spikelet is composed of two bracts (the glumes) surrounding the florets (2-4 per spikelet). Each floret is enclosed between a lower and upper bract (lemma+awn and palea). The rachis, glumes, lemma and palea form the chaff.

The ear formation starts early during the plant development. Indeed, before the stem extension, the floral transition of the apex, which has until then initiated vegetative phytomers, occurs. The apex, which is then located at approximately 1 cm above the ground surface within the stem, initiates the spikelets of the ear. The ear develops and grows during the stem extension and eventually emerges from the flag-leaf sheath. Several factors, endogenous or external, during the ear development determine the final number of fertile/aborted florets, the production of pollen, the grain set and consequently the grain number per ear. Nutrition status and assimilate availability during the ear formation alter the grain number. For instance, at the shoot scale, during stem extension, the stem growth rate is maximum and competition for carbohydrate assimilate between stem growth and ear growth could explain floret death (Kirby, 1988). At the plant scale, the ears compete for resource availability, there is a balance between ear number and grain number per ear which affects the grain number per square metre. Environmental factors may also be considered. For instance, meiosis during the boot stage (when the ear is still enclosed in the first leaf sheath) is disturbed by low radiation inducing male sterility (Fischer and Stockman, 1980; Demotes-Mainard et al., 1995, 1996) reducing the pollen production (more about the relationship between temperature and wheat development, see **???**). More generally, excluding environmental "accidents", the plasticity of the grain number per square metre may be an heritable trait of wheat genotypes, acting as a "coarse tuning parameter" of the grain wheat yield as proposed by Slafer et al. (2014): high resource availability promoting high grain density per ear (e.g. because of an exceptional environment, or explained by a low inter-shoot competition because of low ear density).

Finally, at anthesis the fertilisation of the ovule occurs: the wheat florets are cleistogamic which results in a largely predominant autogamy — Rieben et al. (2011) quantified 3% of the wheat seeds resulted from cross pollination in a field experiment. Given the wheat development programme, at the end of anthesis the number of ears per square metre and the number of grains per ear are already set. Besides, the vegetative biomass is then close to maximal as, later, the reproductive organ will be the main sink.

- **The grain filling phase**

After anthesis, the grain is the main sink of wheat shoots. During grain filling, the grain itself undergoes successive physiological processes. It first operates morphological changes, then initiates the dry matter accumulation and finally achieves dessication.

At the grain level, anthesis is followed by an intense multiplication of the endosperm cells, without substantial evolution of the grain dry weight, but a gain in water content (Shewry et al., 2012). The number of endosperm cells is directly linked to the potential of the grain for starch and protein deposition (Jenner et al., 1991). Therefore the endosperm cell division influences the potential grain size. This phase is also designated as the slow grain growth phase, during approximately 250 degree-days after anthesis. The rapid grain filling phase comes next. Most of the starch and protein is deposited during this phase. The starch represents 60-70% of the mature grain weight and is mainly provided by the current photosynthesis during that phase, but is also translocated from soluble carbohydrate reserves which accumulate in the stem. The proteins represent 8-15% of the mature grain weight, most of the nitrogen has been taken up before anthesis and remobilised during the senescence process which occurs during grain filling. The grain dry weight increases nearly linearly with thermal time during the rapid grain filling phase, and the relative water content decreases. Below 45% grain moisture content, the dry matter is stabilised, the grain has reached physiological maturity and further water content is lost following passive dessication.

If the grain number, set before anthesis, may be described as a "coarse tuning parameter" of the grain yield, Slafer et al. (2014) also highlighted the plasticity of the individual grain weight. They consider the grain weight plasticity is a heritable trait that can be perceived, in comparison to the grain number plasticity, as a "fine tuning parameter" of the grain yield. This is consistent with general representation of the yield being primarily dependent on the grain number, and secondarily on the individual grain weight.

- **The source/sink manipulations and grain yield limitation**

To study the source/sink balance is to investigate the relationship between the organs whose main function is the export (the source) with the organs whose main function is the import (the sink) of assimilate. More generally, it describes the functions which support

growth and development of the wheat shoots. After anthesis, the main sink is the grain, while the source is composed of the vegetative organs. A critical question of interest in wheat physiology is to understand what limits the grain yield. Do the vegetative organs supply enough assimilate to fill the grain? Do the grain have the capacity to store all the available assimilate? Answers to these questions indicate the direction for wheat yield potential improvement for instance in the breeding strategy.

An application of this approach led to reduced wheat growth investment in the straw and leaves to increase grain growth in the semi-dwarf genotypes, which partition more assimilate to ears, increasing the grain number per unit area and the harvest index (ratio of the grain yield dry matter to the above-ground dry matter) (Austin et al., 1980) and also reducing lodging risk. This success is referred to as the "Green Revolution" (Evenson and Gollin, 2003). This major physiological change was not associated with a substantial increase of the biomass production but rather a better partitioning of the assimilate toward the grain (Slafer and Andrade, 1991). The sharp decrease in source/sink ratio led to a more balanced situation between the potential for C assimilation by the source and sink capacity. Slafer and Andrade (1991) concluded there is a need to increase the grain number (increase the sink) and simultaneously the source potential for further improvement of the grain yield. In Spain, Sanchez-Garcia et al. (2013) studied the grain yield improvement during the 20th century on a collection of 26 cultivars. They confirmed the increase in the harvest index during the 1950s, and a further improvement of the HI associated with the introduction of the semi-dwarf germplasm during the 1970s. The source/sink approach can therefore help to identify the possible levers to improve the wheat yield.

Source/sink manipulations after grain setting (i.e. shading, defoliation, ear trimming, etc) have been used to understand the source/sink balance effect on grain growth and identify ways to increase the yield of wheat (Serrago et al., 2013; Slafer and Savin, 1994b; Ma et al., 1996) or barley (Cartelle et al., 2006) or soybean (Egli and Bruening, 2001), either by manipulating the source or the sink potential. The results of these studies mostly agree: the grain yields of wheat crops in Europe are mostly sink limited or co-limited under favourable conditions the grain growth is limited by sink in the early grain filling and by the source in later grain filling phase (Acreche and Slafer, 2009; Slafer and Savin, 1994b; Cartelle et al., 2006). Consequently, the increased source availability increases only slightly the grain growth, if it does. In this perspective, the potential attainable grain yield limited by the sink size, is expected to be reached in absence of disease in European conditions.

1.2.1.2 Fate of Nitrogen and Carbon fluxes during the senescence

After water, nitrogen is the most limiting factor of wheat crop growth (Vitousek, 1994; Sanchez-Bragado et al., 2017), and an essential factor of the grain quality and productivity

(Passioura, 2002). Nitrogen is the main element of proteins and a substantial component of the biomass. Besides, more than 70% of proteins of wheat crops are linked to photosynthesis. Up to 75% of the reduced N in cereal leaves is located in the mesophyll cells, mainly as Ribulose-Bisphosphate-Carboxylase-Oxygenase (Rubisco), and is involved in photosynthetic processes (Evans, 1989). So nitrogen plays also a central role in carbon assimilation, the fate of carbon and nitrogen fluxes are closely linked, and their interaction is closely linked to the grain yield (Zhang et al., 2014).

In the previous section, the post-anthesis physiology description focuses on the grain development and growth, through the deposition of carbohydrates and proteins. However, the canopy is the main source of carbon and nitrogen for grain filling. The senescence of the canopy is the visual evidence of major modification of the fluxes within the shoot happening during grain filling:

- The end of nitrogen uptake;
- The net remobilisation of nitrogen;
- The reduction of carbon assimilation.

- **The end of nitrogen uptake**

Nitrogen comes from the soil complex and nitrogen uptake by the plant relies on environmental characteristics (soil type, water content, climate, *etc*) and capacity of the species (Masclaux-Daubresse et al., 2010). Ammonium NH_4^+ and nitrate NO_3^- are the main forms of usable nitrogen compounds by plants. Nonetheless, wheat preferentially absorbs nitrates. Physicochemical reactions depending on edaphic and weather conditions lead to N loss by volatilisation or leaching (Recous et al., 1997). Moreover, microorganisms are responsible for nitrogen immobilisation. Lastly, plants compete for nitrogen. In response, wheat crops are able to uptake high amount of nitrogen in a short time span that will be used later. This two-step metabolism is emphasized because beyond genetic improvement through plant breeding to improve nitrogen uptake (root architecture: depth, root hair density and localisation, *etc*), agronomists work on nitrogen fertilisation management to boost nitrogen nutrition, deciding the most appropriate timing and split of fertilisation as well as applied fertiliser amount (Spiertz and Devos 1983; Borghi et al. 1997 in Aranjuelo et al. 2013). Nitrogen Efficiency cannot satisfactorily be assessed only by the N-Use Efficiency (NUE) which quantifies the grain dry matter yield increase for an amount of N available, from the soil and/or N fertiliser. NUE is rather decomposed into two terms. The first, being the N-Uptake Efficiency (NUpE), which is the nitrogen uptake per unit of nitrogen available. The second is the N-Utilisation Efficiency (NUtE) which is the grain dry matter production per unit of nitrogen uptake. From a physiologist's standpoint, this decomposition is relevant as it deals with two distinct processes involved in nitrogen use: uptake and then utilisation linked to carbon assimilation.

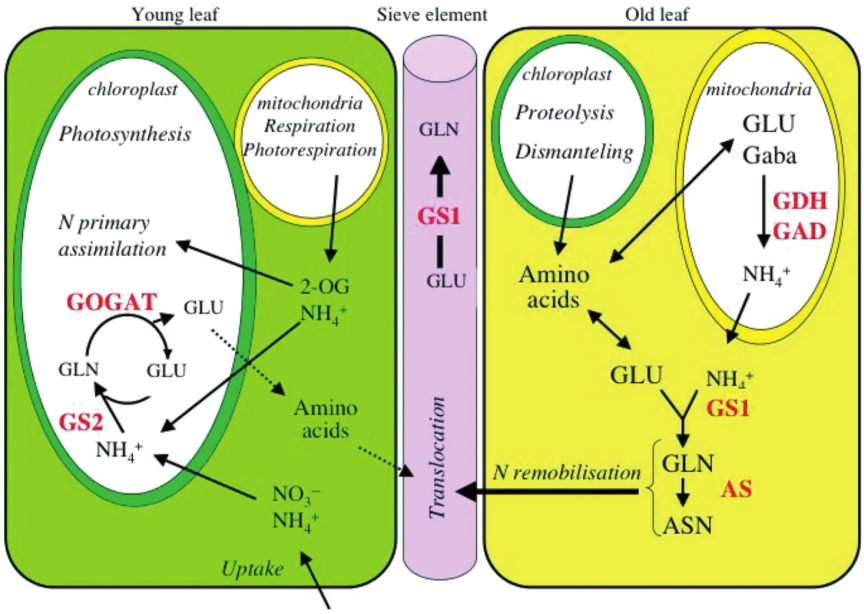


Figure 1.1: Main nitrogen metabolic pathways (Masclaux-Daubresse et al., 2008).

Nitrogen-uptake efficiency relies on root architecture traits but also the cells properties and biochemical mechanisms for absorption (Cormier et al., 2016). Absorption of nitrogen occurs at the absorbent root hair level. It involves two transport systems: a low affinity transport system and a high affinity transport system respectively coded by NRT1 and NRT2 genes, and respectively enabled in case of high or low soil nitrogen availability according to a trade-off between affinity transport and energetic cost. Ammonium absorption relies on different transporters coded by AMT (Ammonium transporter) genes (Masclaux-Daubresse et al., 2010). Assimilation of nitrogen in organic matter can be described in four steps (Fig. 1.1, *young leaf*). First, the reduction of nitrate into nitrite requiring nitrate reductase occurs in the cytosol and is then followed by a reduction into ammonium by nitrite reductase in the plastids. Ammonium is fixed to Glutamate initially by glutamine synthethase to form the amino acid glutamine which, in turn, reacts with the 2-oxoglutarate catalysed by the glutamate synthase (Masclaux-Daubresse et al., 2010). The resulting glutamate molecules join the sap and are driven to the sinks.

Before anthesis, the uptake and assimilation of nitrogen influences source/sink balance in many ways. For instance, it modifies plant architecture. Indeed, an increase in nitrogen absorption causes an increase of the leaf lamina area so that before senescence the variability in specific leaf nitrogen (nitrogen per unit leaf area) is largely buffered. In addition, agronomic practices are important. Indeed, if increasing the nitrogen fertilisation generally improves the growth rate, an excessive input can also be damaging. For instance, an excessively dense canopy because of nitrogen not only is favourable to crop infection, but also increases the susceptibility to water stresses as evapotranspiration is enhanced by a large leaf area. It can even cause yield losses because of haying-off (Hall

et al., 2014): the vigorous vegetative growth enhanced by the large N fertilisation increase the canopy area and therefore increases water consumption beyond environmental availability. Nitrogen not only had direct effects on sources, during ear growth pre-anthesis the ear N concentration might positively interact with floret fertility and the grain number (Sinclair and Jamieson, 2006). In addition, the lodging risk increases with a high shoot density at high N inputs.

The supply of nitrogen relies on the volume of soil explored by the growing roots. However, after anthesis the net root growth ceases (Foulkes et al., 2009) and as the nitrogen availability for the plant decreases the nitrogen uptake is decreased. Aranjuelo et al. (2013) reported that low nitrogen availability during the post-anthesis period induced early nitrogen remobilisation (bread wheat, cv. Califa). Although the post-anthesis nitrogen uptake is not the main source of nitrogen for nitrogen grain filling, it remains as substantial as $1\,\mathrm{kg}\cdot\mathrm{ha}^{-1}\cdot\mathrm{day}^{-1}$ (Gooding et al., 2005).

In European farming practices, approximately a third of the nitrogen found in grain has been incorporated during the post-anthesis period, the complementary N coming from remobilisation of already incorporated nitrogen (Bancal et al., 2008). Besides Bancal et al. (2008) found that variability in grain N uptake at harvest was better correlated to variation of post-anthesis nitrogen uptake than to remobilized nitrogen (cv. Soissons in four experiments). Thus, despite remobilized nitrogen being the main source of grain nitrogen, it does not explain all variation of grain nitrogen content (Barbottin et al., 2005; Bancal et al., 2008). This is also highlighted by the correlation between grain protein content and nitrate reductase activity (which catalyses nitrate reduction) during the post-anthesis period (Kichey et al., 2007). Finally, this can be confirmed by agronomic practices as Hébrard (1999) observed an association between late N fertilisation and increase grain protein content.

- **Senescence and N remobilisation**

The majority (60% to 85%) of nitrogen grain sink demand after anthesis is fulfilled by the remobilisation of nitrogen accumulated in stem and leaves prior to anthesis (Kichey et al., 2007). Nitrogen remobilisation is linked to senescence.

Far from being a simple and disorganized cell death, senescence is an evolutionary strategy which improves growth-limiting nutrient economy by remobilisation for organ growth (Dawson et al., 2008). In *Arabidospsisi* sp. two strategies can be observed: early senescence and high reproductive effort in opposition to late senescence and low reproductive effort (Wingler et al., 2006). Within monocarpic species, and especially for the wheat, sequential senescence is first observed for juvenile shoots: upper leaf growth is counterweighted by lower and older leaf senescence. Shading effect and modification of light quality might be a signal for senescence onset of lower and older leaves. Canopy

senescence happens after heading, then senescence and ongoing N remobilisation contribute to the grain growth. Leaf senescence is visually characterised by the chlorophyll degradation but may happen earlier and relies firstly on biochemical signals leading to transdifferentiation of cells. Indeed, senescence is not a cell decay, it is a modification of cell functions that, in annual crops such as wheat, is linked to nutrient remobilisation (Gregersen et al., 2013). Leaf function shifts from photosynthesis to remobilisation; from mainly anabolic to mainly catabolic functions. Chloroplasts are no longer maintained and active biochemical reactions result in metabolite export. At first, senescence can be reversed and the yellowing leaf can become green again, until a certain limit when reversion is no longer possible, and the leaf actually dies (Gregersen et al., 2013). Senescence timing is of major interest to wheat grain production.

The relation between surrounding environmental factors and genetic-dependent responses describes the high effect of Genotype × Environment interaction (G×E). Genes accountable for senescence and mechanisms have been identified. Endogenous factors such as transcription factors NAC and WRKY are involved in sugar signalling (Wingler et al., 2006) and Senescence Associated Gene activation. Phytohormones such as abscissic acid, jasmonic acid and cytokinins are also associated with senescence regulation. Finally, the nutritional state and the source/sink balance also influence the life time of leaves. These factors are influenced by the surrounding environment which makes senescence a highly plastic trait (Wingler et al., 2006). Shading (Weaver and Amasino, 2001), light intensity (Noodén et al., 1996), light quality (Rousseaux et al., 1996; Causin et al., 2006) and water or nutrient availability (Ono et al., 1996; Thomas and de Villiers, 1996; Crafts-Brandner et al., 1998; Ding et al., 2005) modify the senescence pattern. For instance, the relocation of N content of lower leaves to the top leaves within dense canopies confers competing advantage of tobacco wild type Boonman et al. (2006). In *Arabidopsis*, the individual shading of a leaf accelerated its senescence (Weaver and Amasino, 2001). However the shading induced several alteration of the micro leaf environment and can be decomposed in a reduction of the light intensity (part of the light is intercepted) and modification of its quality according to the leaf-pigment properties. And indeed, the light quality affect the senescence as blue light exposition treatment applied on wheat plants was associated with delayed senescence, probably explained by a maintained catalase activity within the leaf (Causin et al., 2006). Rousseaux et al. (1996) observed that the decrease in Red/Far-red light composition ratio enhanced the senescence of lower leaves of sunflower (*Helianthus annuus L.*). The senescence of *Arabidopsis thaliana* plants was found mainly promoted by the light intensity rather than the photoperiod (Noodén et al., 1996). The accumulation of carbohydrate were also associated with earlier senescence of hydrid maize (Crafts-Brandner et al., 1984); in a field winter-wheat experiment a steam-girdled treatment applied of the flag leaf also initiated rapid senescence supposedly caused by

the accumulation of assimilates (Fröhlich and Feller, 1991). In addition to abiotic factors, biotic factors can provoke senescence. However, if abiotic stresses are considered as funnelled into a common senescence pathway (Guo and Gan, 2012), it is not so clear for biotic stresses. From a source/sink perspective, the STB is an additional sink. Indeed, as for the plant, nitrogen is a key element for pathogen development. For instance, an increased availability of nitrogen in the leaves can raise the incidence of the STB as for other late-season diseases (Ben Slimane, 2010).

Remobilized nitrogen is provided by protein hydrolysis which funnels into an amino acid / oligo peptides flux in the sap toward the sink (Feller and Fischer, 1994; Masclaux-Daubresse et al., 2010). In the ear, nitrogen is converted into metabolic and structural proteins or in storage form. Metabolic and structural proteins are accumulated earlier in the cycle than storage forms, and their source/sink characterisation likely differs (Pask, 2009). At the plant level, it is possible that determinism of N metabolism therefore shifts during grain filling. Gaju et al. (2014) used Nitrogen Remobilisation Efficiency (proportion of N in the plant components at anthesis remobilized to the grain at harvest; NRE) to quantify the potential for remobilisation, which varies between genotypes (Cox et al., 1985; Vansanford and MacKown, 1987; Kichey et al., 2007; Gaju et al., 2011, 2014). Although, NRE varies to a higher extent between plant organs, possibly according to the properties of protein in the various tissues. Indeed, Pask et al. (2012) suggested that nitrogen in wheat plants is found in three main forms: i) structural (supporting tissues and vascular system, mostly in the stem, low remobilisation efficiency), ii) photosynthetic (mostly in the leaves where Rubisco comprises about 70% of leaf protein (Parry et al., 2001) high remobilisation efficiency because of well organised degradation) and iii) reserve (i.e. not photosynthetic, not structural, buffering N grain source/sink balance). Pask et al. (2012) estimated the N leaf lamina remobilisation efficiency was up to 76%; in comparison, although the internodes represent half of remobilized nitrogen and most of the N reserve pool, NRE was only 48%. Pask et al. (2012) assumed these proteins are necessary for transport and mechanical functions.

The net nitrogen remobilisation increases when nitrogen uptake decreases in cereals (Aranjuelo et al., 2013), while the rate of nitrogen grain filling remains constant. Barneix (2007) proposed a model in which N uptake and remobilisation are excluding one another. More generally the literature commonly describes N uptake and N remobilisation as two successive steps which is a clear simplification as at the plant level the young active organs are present together with old senescing ones. Moreover, plant N uptake may end several weeks after N is declining in every plant vegetative organ indicating remobilisation for these plant organs. A clear characterisation of interactions between net mobilisation and uptake could be addressed using sequential labelling and fine dissections which to our knowledge is not yet published.

At the plant level, senescence can be delayed: post anthesis fertilisation commonly results in extended plant life. In addition, stay-green genotypes show extended green leaf life (sorghum, Borrell and Hammer 2000; rice, Fu and Lee 2008; maize, Echarte et al. 2008; Martin et al. 2005; Ding et al. 2005; Rajcan and Tollenaar 1999; durum wheat, Spano et al. 2003; wheat, Chen et al. 2010; Derkx et al. 2012). According to the genetic modifications, stay-green effect is sometimes referred as "cosmetic": the degradation of chlorophyll is impeded, the leaf stays green, but the carbon fixation has been stopped (Thomas and Howarth, 2000). In the case of functional stay-green, a strong association with nitrogen metabolism — or photosynthesis parameters which depend on nitrogen metabolism — is often indicated. Stay-green genotypes have been associated with: higher leaf nitrogen concentration at anthesis in sorghum (Borrell and Hammer, 2000) and wheat (flag leaf, Derkx et al. 2012), higher N absorption and storage in the shoot in maize (Martin et al., 2005), maintained post-silking N uptake in maize (Rajcan and Tollenaar, 1999), higher N uptake in wheat (Derkx et al., 2012), delayed and slower degradation rate of photosystem II in rice (Fu and Lee, 2008) (i.e. N remobilisation), maintained leaf carbon exchange rate in maize (Echarte et al., 2008) or photosynthetic capacity in maize (Ding et al., 2005) and durum wheat (Spano et al., 2003), lower Reactive Oxygen Species (ROS, especially H_2O_2) peak values in wheat (Chen et al., 2010). The functional stay-green is associated with an increase in grain yield generally limited to stress conditions such as drought (Borrell and Hammer, 2000) or nitrogen deficiency (Derkx et al., 2012); possibly because of sink limitation in non stressed conditions (Derkx et al., 2012). Efficient stay-green could also improve the yield when exposed to biotic stresses (pathosystem Spring wheat × spot blotch, *Bipolaris sorokiniana*, Joshi et al. 2007).

- **Senescence and reduction of carbon assimilation**

In leaf laminas, 70% of the protein is linked to photosynthetic functions: carbon and nitrogen fate are closely linked. During the grain filling phase, photosynthesis is the main source of carbon. Consequently, maintained photosynthesis during grain filling is expected to increase the photoassimilate availability in an extended grain-filling phase. Unlike carbon, nitrogen is mainly remobilized and late senescence decreases by dilution the nitrogen concentration of the grain (Gregersen, 2011), that is a quality criterion of wheat production, and a trade-off is generally understood between the grain yield and the protein concentration of the grain.

Independently from nitrogen, the photosynthesis potential relies on genotype traits describing the canopy architecture determining light capture or biochemical pathways involved in photosynthesis. The photosynthesis efficiency first relies on the light interception. The Leaf Area Index (LAI) represents the ratio of leaf lamina area per unit of soil area. For a wheat crop maximal light interception is reached for LAI around 3 to 4

(Gouache et al., 2014), leaf shading then limiting the increase of light interception. However, the LAI does not give information about the lamina leaf profile. The light extinction coefficient k describes the extent to which radiation is transmitted to the lower leaf layers (Eq. 1.1). A large extinction coefficient implies a high fraction of light interception by the upper leaf layers and low light level lower down the canopy (Bingham and Topp, 2009). Extinction coefficient can be manipulated through architecture traits including leaf inclination (Angus et al. 1972 in Bingham et al. 2009). Then, genetic variation exists for radiation-use efficiency (above-ground dry matter per unit radiation interception): the intercepted amount of light can be more or less efficiently used for carbon assimilation, and grain filling.

$$F = 1 - \exp^{-k \cdot LAI} \tag{1.1}$$

With: F, the intercepted fraction of light; LAI, the Leaf Area Index; k, the light extinction coefficient.

During grain filling, the upper leaf layers are the main sources of carbon assimilation. The contribution of the two top leaf layers is estimated at 50% of carbon grain filling while ear photosynthesis could also be a non-negligible source of C during grain filling (Tambussi et al., 2007). Nonetheless, quantifications did not reach a consensus. Based on carbon isotope and six Mexican CIMMYT spring wheat genotypes in a field experiment, Sanchez-Bragado et al. (2014) estimated the relative contribution to grain filling: flag leaf contribution ranged between 8-18% while the ear photosynthesis represented in average 70%. In comparison, Aranjuelo et al. (2011) worked with durum wheat (cv. Regallo) and concluded with its labelled carbon field experiment in spain that the ear photosynthesis does not contribute substantially during the beginning of the post-anthesis phase. Photosynthesis of non-lamina organs obviously leads to tolerance to leaf attack by pathogens. So, the efficiency of the photosynthesis relies on architecture traits, photosynthetic biochemical potential, as well as source/sink balance.

The reduction of carbon assimilation can be compensated by the remobilisation of pre-anthesis stored carbon. Pre-anthesis carbon is stored preferentially in internodes and translocation contributes to grain filling. However, the pre-anthesis stored carbon may be preferentially used for respiration than grain filling (Aranjuelo et al., 2013). Ruuska et al. (2006) identified large genetic variation of the water-soluble carbohydrate (WSC) accumulation in the stem (112 to 213 $mg \cdot g^{-1}$) associated with large broad-sense heritability (H = 0.90±0.12).

* * *

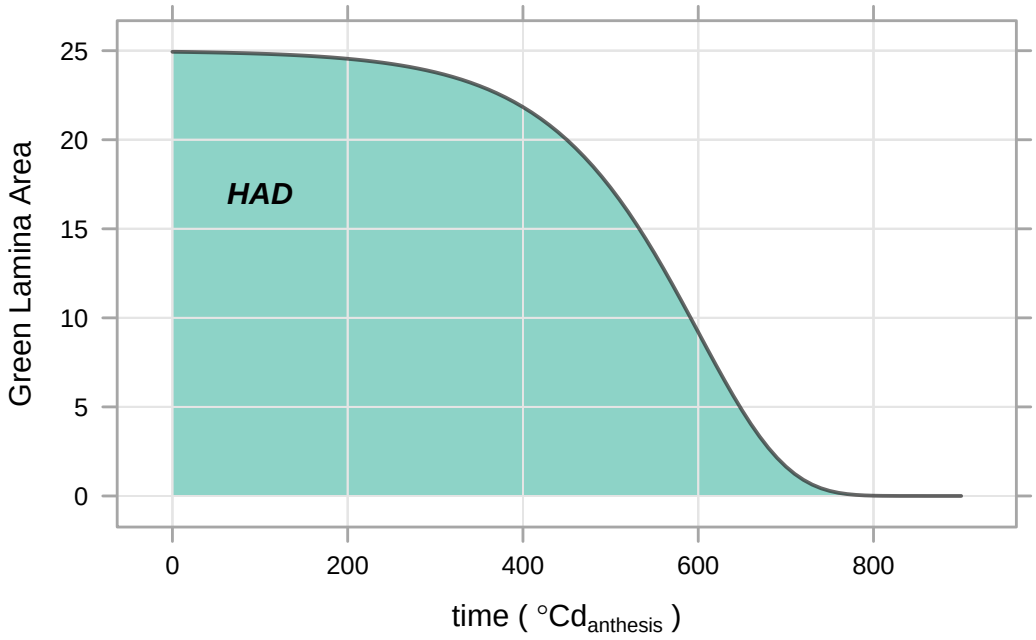


Figure 1.2: Theoretical green blade area kinetic. Since heading date, green area kinetic follows a sigmoid pattern, the area under the curve quantifies the available green area during grain filling period and so the volume of source. Given the relation, a first approximation of the Healthy Area Duration (HAD) can be obtained through multiplication of the Leaf Area Index (LAI) and the onset of senescence.

The attainable yield is therefore the result of this evolution along with the grain filling of these antagonist fluxes: reduction of nitrogen uptake, increasing of nitrogen remobilisation and reduction of carbon assimilation. The potential yield appears as a trade-off between remobilisation flux and maintenance of the photosynthetic potential.

1.2.1.3 An equation for potential yield

The potential yield is defined in this project as the maximum attainable grain sink weight for a given source extent. The potential carbon assimilation is linked to the potential photosynthesis associated with large availability of green leaf lamina area during the grain filling period.

The remaining green area of the leaf lamina can be assessed at different times from anthesis to maturity. The kinetic provides an estimation of the complete evolution of the green area during grain filling and its integration from anthesis to maturity (Healthy Area Duration, HAD; Fig. 1.2) informs about the green lamina area available during the grain filling period. The relevance of HAD is confirmed by the radiation-use efficiency which is relatively conservative, although limited RUE genetic variation was observed in winter wheat (Shearman et al., 2005). The HAD is an appropriate physiological estimation of

the grain source availability.

The calculation of the HAD still raises methodological questions. First of all, the HAD calculation is based on a non-linear kinetic, i.e. the evolution of green leaf lamina area from heading to maturity follows a sigmoid which includes a relatively sharp sudden decrease. The methods to estimate the area under the curve influence the HAD estimation. The less complex method is the trapezoidal estimation, a non-parametric method. For each time-step, green area evolution is supposed linear, the area under the curve is therefore trapezoidal and can be simply computed. The successive time-step trapeze are cumulated from heading stage to maturity. Parametric methods can be used, relying on the definition of an equation. The equation can vary, but the parameters of the equation are fitted to the observed data through converging algorithm. The quality of the HAD estimation depends mainly on the frequency of the observations, knowing that the rapid senescence phase typically lasts from 100 to 350 degree-days in the UK conditions (Gaju et al., 2011). Not only the estimation methods, but the HAD can also vary according the scale of calculation. The HAD is possibly estimated for each leaf layer or for the cumulated top leaf layers (canopy); the HAD results from individual shoot observation, but can be expressed per single grain or at the crop scale (per square metre).

Gouache et al. (2014) proposed a statistical definition of the potential grain yield regarding the grain source availability, the principle is explained hereafter. A yield observation coupled with the HAD is an indicator of the crop performance: how much yield per unit of HAD can be achieved. Using a large sample of observed yield/HAD building on many genotypes × sites × seasons, it is possible to estimate the range of attainable yields for any range of HAD observed, the highest attainable yield being the potential yield. Instead of a discrete definition, Gouache et al. (2014) proposed to fit the boundary line which links the potential yields over the whole range of observed HAD. Because the light interception saturates with the increase in leaf area, it is also expected that the relationship between the potential yield and the HAD reaches an asymptote: once all the light has been intercepted, an increase in HAD is not expected to be associated with a significant yield gain. It is generally admitted that 90% of the light is intercepted for LAI ranging 3 to 4. Therefore, the potential yield curve was defined by a saturating equation (theoretical representation, Fig. 1.3). Mathematically, the positive marginal yield gain decreases with the HAD increase. Physiologically, the grain source limitation decreases with the HAD increase: the yield gain is largely responsive to HAD increase for low values of HAD; the yield gain does not respond to HAD increase for large values of HAD.

The potential yield described by the equation may be considered as a physiological limit observed in any cultivated situation. Consequently, the absence of disease does not guarantee that the crop will achieve its potential yield. The deviation below the curve can be explained by an inadequate combination of environment × genotype × agronomic

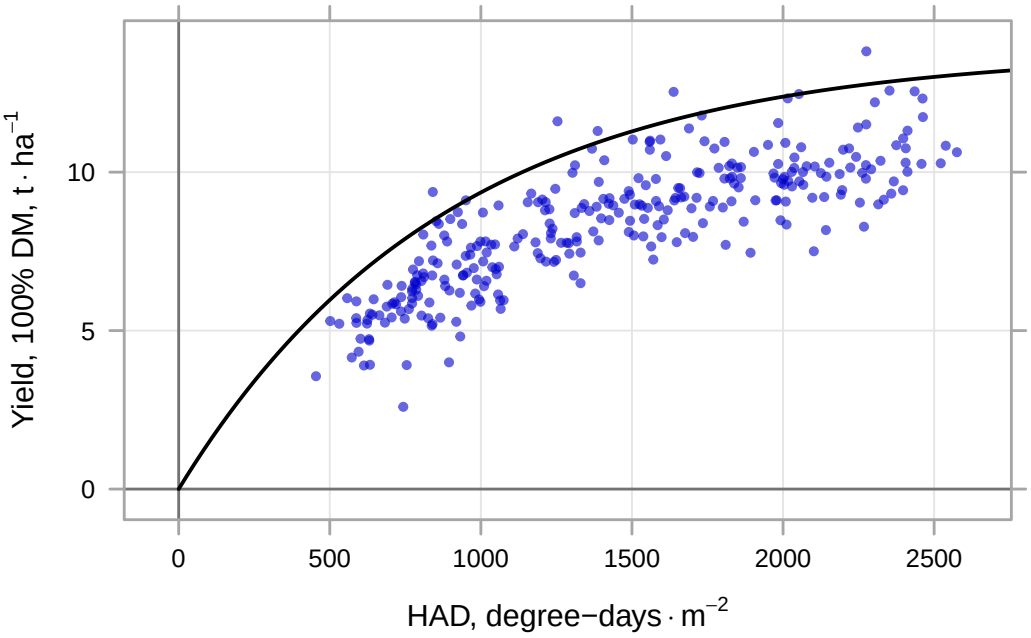


Figure 1.3: Theoretical source/sink potential curve. Couples of grain yield/HAD were simulated (n = 150, each blue dot). The HAD is estimated from anthesis to maturity. The quantile regression was used to fit a boundary line, defining the potential yield over the range of simulated HAD ($\tau = 0.98$, the equation is an asymptotic regression defined as follow: $y = 13.8(\pm 1.2) \times (1 - exp(-exp(-6.8(\pm 0.2)) \cdot x))$. The potential curve shows that the grain yield gain decreases with the grain source limitation.

practices, or more directly from uneven potential between genotypes or even between environments.

1.2.2 Stress, strain and tolerance of Septoria tritici blotch

The preceding section described the yield components, the associated major fluxes along with the monocarpic senescence, and finally proposed a definition of the potential yield regarding the source availability. It was stated that, because of environment or genotype potential, the yield observed in healthy crops often remains below its potential considering the associated HAD. In addition, the pressure caused by a disease or an abiotic stress lowers the attainable yield. This pressure can be decomposed into the stress and the strain: the stress leading to a specific strain exerted on the crop (Levitt, 1972). The stress is defined as any environmental factor (e.g. a drought, nutrient deficiency, airborne spores concentration) with the capacity to elicit from the plants a harmful chemical or physical change. The change is the strain (e.g. reduction of cell turgor, reduction of nitrogen content, disease symptoms).

The distinction between stress and strain circumscribes tolerance to a specific area

of the plant protection strategies. In the domain of crop protection and working at the level of the genotype, in order to avoid crop losses, the most direct strategy is to avoid the stress by avoidance or escape strategies. This can be achieved, for instance, by modifying the architecture of the plant or imposing modification of the growth and development rate. If the stress can not be avoided, then two options can be developed. The first is to reduce the strain, the symptoms in the case of biotic stress, this is the resistance strategy. The second solution is to tolerate the strain which is precisely the definition of tolerance studied within the project: the ability of a plant to maintain performance in the presence of expressed disease (Ney et al., 2013).

The PhD project focuses on the tolerance of wheat to the STB, as a biotic stress. Therefore, in this section the essential information about STB is provided. Then, the quantification methods of tolerance of STB are proposed. Finally, previous studies providing evidence and hypotheses for the identification of genotype tolerance traits.

1.2.2.1 The Septoria tritici blotch: a biotic stress of wheat crops

The Septoria tritici blotch (STB) is a leaf disease of wheat (Eyal et al., 1987), characterised by large necrotic area dotted by black pycnidia emerging from the leaf stomatae (further description of the symptoms, Fig. 1.4). It is caused by the Ascomycetes *Zymoseptoria tritici* (Desm.), also formerly known as *Mycosphaerella graminicola* (Fückel).

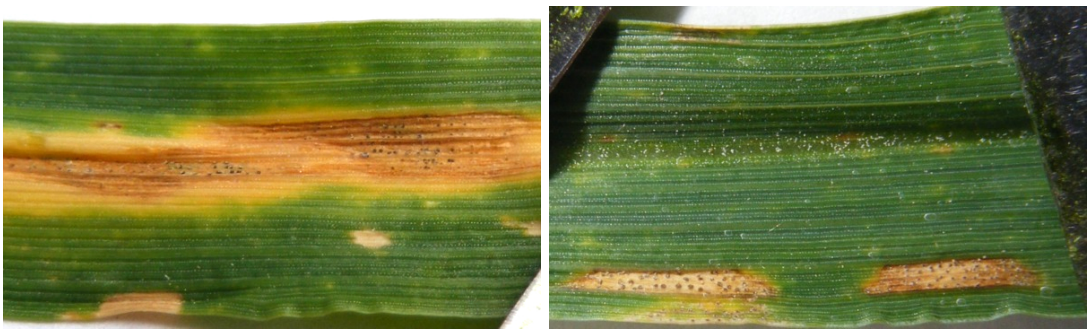


Figure 1.4: The Septoria tritici blotch symptoms. The STB forms necrotic area on the leaves, rectangular or elliptic brown blotch, surrounded by yellowed area, dotted with dark spots. The necrotic area can also be circumvented, well delimited and lighter, where black spots also develop. The black spots are pycnidia, they contain the spores propagating the disease by rain splash effect.

The prevalence of STB was relatively low prior to the 1960s-70s (Eyal et al., 1987) in Western Europe (Torriani et al., 2015). Since then, the breeding strategies increased the potential yield of wheat varieties and also increasing STB incidence appeared. The introduction of early maturing and semi-dwarf varieties (Eyal et al., 1987) and priority given to yield increase (Torriani et al., 2015) was inadvertently associated with higher STB yield loss. This was illustrated in Syngenta trials reported by Torriani et al. (2015) as a strong negative association of varietal resistance with yield potential that may explain the increase in yield susceptibility to STB.

The STB is today certainly the most important disease of wheat crops in the European Union (Burke and Dunne, 2006; Cools and Fraaije, 2013; Fones and Gurr, 2015). In a disease management guide, the AHDB (2016) described STB as the most damaging foliar disease in the UK where yield loss ranging 30-50% has been reported (the average yield loss in untreated trials being 20%). According to Fones and Gurr (2015), the STB loss is worth in the order of billions euros for each of the three main wheat growing countries in Europe (France, Germany, UK). Its economic damage can be illustrated by 70% of the wheat EU fungicide market that STB represents worth in 2014 (about 1bn euros) (Torriani et al., 2015).

- **Life cycle of *Zymoseptori tritici***

Z. tritici is a polycyclic hemibiotroph (or "latent necrotroph" Sánchez-Vallet et al. 2015) pathogen. The fungus achieves several life-cycles during the wheat crop. The primary inoculum composed of spores dispersed by the wind or rain-splashed develops on the seedlings infected during the autumn or the early spring. The infection followed by the production of macroconidiospores is marked by an imperative switch from a biotroph/endophyte to necrotroph metabolism (Sánchez-Vallet et al., 2015). The life cycle description hereafter outlines the main feature of the pathogen starting from the infection. More information can be found in the review paper (among others) of Steinberg (2015) or Sánchez-Vallet et al. (2015).

1. The infection (12h to 48h after inoculation). The spore germinates at the surface of the leaf, *Z. tritici*. The germination requires moisture and optimal temperatures range from 20 to 25 °C (min. 2 °C; max. 37 °C, Eyal et al. 1987). The mycelium grows and mainly penetrates the leaf through the stomates (Kema et al., 1996; Duncan and Howard, 2000) that are reached randomly (Kema et al., 1996) or maybe based on a thigmotropic signal (Duncan and Howard, 2000). It colonises the substomatal cavity within 12 to 48 h after inoculation (Kema et al., 1996; Duncan and Howard, 2000).

2. Endophyte/biotroph metabolism (from infection to 10 days after inoculation). The hyphal growth carries on within the leaf mesophyll and the mycelium spreads within the apoplast (Kema et al., 1996; Duncan and Howard, 2000). The hyphae accumulate in the substomatic cavities and initiate pre-pycnidia (Kema et al., 1996; Duncan and Howard, 2000). At this stage the infection remains asymptomatic (Kema et al., 1996). In addition, the biotroph or endophyte metabolism has not been elucidated yet. Indeed, Keon et al. (2007) reported no feeding structure was identified at this stage, no fungal biomass increases were detected by, and the apoplast content composition was not found to be modified in the presence of the fungus, all suggesting

an endophyte metabolism.

3. Necrotroph (10 to 12 days after inoculation). The development of the fruiting bodies is concomitant with the first lesions appearing 10 to 12 days after inoculation (Kema et al., 1996; Duncan and Howard, 2000; Keon et al., 2007). Host cells are disintegrated, associated with extensive cell death (Kema et al., 1996) similar to an hypersentive response which involves reactive oxygen species (Keon et al., 2007) and probably triggered by the pathogen (Keon et al., 2007). The cell content is released and the concentrations of apoplast metabolites sharply increase followed by an increase in pathogen growth (Keon et al., 2007). The fungus forms mature pycnidia containing the macropycnidiospores. The macropycnidiospores are dispersed by rain-splash up the canopy within a short distance range.

4. Saprophyte (25 to 30 days after infection). Saprophytic growth is observed on dead tissues, followed by the production of pseudothecia (sexual fruiting bodies) (Sánchez-Vallet et al., 2015). The pseudothecia initiates sexual reproduction. The ascospores therefore produced ensure the overseasoning of the inoculum and the important gene flow of the STB population (Zhan and McDonald, 2004): at the season end, the sexual reproduction constitutes up to 30% of the *Z. tritici* population (Eriksen et al. 2001 in Fones and Gurr 2015).

The dispersion of the macropycnidiospores is mainly associated with rain-splash events, and therefore limited to the neighboring plants. The rain-splash dispersion induces the progress of the infections from the bottom leaves to the top leaves. The ascospores contained in the pseudothecia are mainly airborne and responsible for long range dispersion. Fones and Gurr (2015) reported the genetic characteristics and remarkable plasticity of *Z. tritici*. In conjunction with modern agricultural practices, Fones and Gurr (2015) estimated the potential production of spores per season being as high as $10^{10\text{-}11}$ spores per hectare, concluding that "emergence of new fungal strains is of grave concern".

- **Plant × pathogen interactions**

The STB is mainly a late stage disease of wheat. Indeed, the monocarpic senescence of wheat leads to the termination of leaf initiation and growth, while the ear becomes the principal sink. After anthesis during the grain filling period, the STB symptoms spread along the upper leaves, causing a net reduction of photosynthetic leaf area, consequently a reduction of the grain source availability of carbon assimilates. The severity of the damage depends on various factors involved in the plant × pathogen interactions, and the effect of the nitrogen has been investigated as associated with the photosynthetic potential.

At the crop scale, the high nitrogen availability in the soil can favor the production of tillers or large leaves. The lush canopy modifies micro-climatic conditions, higher humidity condition increase the fungi fitness (Savary et al., 1995)).

If nitrogen is a key element for the plant growth, the fungus also requires nitrogen compounds for growth. The necrotroph phase of the disease induces the liberation of these compound in addition to the fungus proteases so the nitrogen becomes available for the fungus growth. The nitrogen metabolism of the plant and the nitrogen fertilisation applied to the crop influences the disease epidemics. It is commonly observed that an increase in the nitrogen leaf concentration also increases the disease severity or the susceptibility to the fungi (Bancal, 2008). However, insufficient nitrogen nutrition is also associated with lower defence response of the plant to the disease, and therefore, a nitrogen nutrition deficiency can also increase STB disease epidemics.

The effect of STB on nitrogen fluxes was investigated by Bancal et al. (2008). Although the STB symptoms can cause disruption in the vascular system, blocking the remobilisation of the nitrogen beyond/within the necrotic area (Bastiaans, 1993; Kremer and Hoffmann, 1993), the nitrogen yield reduction was found to be better linked to post-anthesis nitrogen uptake than to nitrogen remobilisation (Bancal et al., 2008).

1.2.2.2 Methods for crop control of STB

The curative solutions against STB are sparse, the control of STB relies on prevention strategies. Cultural practices can help in STB prevention, but the main tools are the genotype resistances and the fungicide applications.

- **Breeding for resistance**

Currently, cultivars present partial resistance to STB. In the UK Recommended List, the winter wheat cultivars are assessed for their resistance of disease (1 to 9, low to high resistance). For instance, in the most recent Recommended List (AHDB, 2017), varieties of grade 9 resistance are available against mildew (e.g. cv. KWS Siskin), yellow rust (e.g. cv. RGT Illustrious) or brown rust (e.g. cv. Skyfall). In comparison, the achieved resistance of STB ranged from 4.3 up to 7.3 for the most recently proposed cv. LG Sundance (AHDB, 2017). However, the current partial resistance opposed to the STB is susceptible to decline (AHDB, 2016) as *Z. tritici* is characterised by an important gene-flow (Eriksen et al. 2001 in Fones and Gurr 2015) favoring the emergence of fungi strains able to circumvent the plant resistance.

Although prone to circumvention by the pathogen, the wheat resistance contributes substantially to the control of STB by a reduction of the lesion extent and/or a reduction of the leaf area covered in pycnidia (Eyal et al., 1987; Kema et al., 1996; Somasco et al., 1996). In phytopathology, the plant resistance can be: total, qualitative, race-specific,

narrow spectrum, or a gene-specific response (to the pathogen); it involves a high selection pressure and the pathogen may adapt (Cowger et al., 2000). Contrarily, the resistance can be partial, quantitative, non-specific, or broad spectrum, and involve more than one gene; because it is polygenic and mitigates results, breeding for partial resistance is more difficult.

Resistance of STB genes has been identified *Stb1* to *Stb15*, *Stb16q*, *Stb17*, *Stb18*, *StbWW* and *TmStb1* (see the literature review of Brown et al. 2015). The identification relies on several methods. For instance, the loci *Stb1-3* were identified in the wheat varieties Bulgaria, Veranopolis and Israel 493, respectively, through natural infection process while probably exposed to a mixture of pathogen genotypes (Wilson 1985 in Chartrain et al. 2004). In comparison, using specific *Z. tritici* strains, the loci *Stb4-8* were identified in cv. Tadinia, Synthetic 6x, Flame, Estanzuela Federal and the synthetic wheat W7984 using defined isolates of the pathogen (Chartrain et al., 2004; Somasco et al., 1996; Arraiano et al., 2001; Brading et al., 2002; McCartney et al., 2002; Adhikari et al., 2003). Different types of resistance have been selected. The *Stb6* gene is an example of gene-for-gene relationship (Brading et al., 2002). The locus *Stb17* provides quantitative resistance, a QTL for adult plant resistance (Tabib Ghaffary et al., 2012). The duration of STB control by resistance genes is variable and poorly understood, but is nonetheless associated with: *Z. tritici* gene flow, total or quantitative resistance, and generally the resulting selection pressure. For instance, the vertical resistance of cv. Gene (i.e. strain specific) selected for *Z. tritici* was overcome within five years (Cowger et al., 2000). The *Stb4* locus of the spring wheat cv. Tadinia single dominant gene) exhibited resistance of the seedlings as well as adult plants to STB (Adhikari et al., 2004) and achieved control of STB in California since 1975 for more than 30 years (Somasco et al., 1996).

- **Avoidance and sanitary measures**

Avoidance or disease escape can be achieved by limiting the contact pathogen × host, modifying environmental condition of the pathogen, or impeding the triggering of the infection process (Ando et al., 2007). Initially, studies suggested a possible genetic link between the wheat resistance of STB and the plant height (Baltazar et al., 1990) or heading date (Rosielle and Boyd, 1985; Eyal et al., 1981). These genetic associations seem rather unlikely as Simón et al. (2005), based on 16 cultivars tested in glasshouse, showed no evidence supporting the genetic association, and concluded the association may be due to environmental and epidemiological factor modification associated with plant height and heading date.

About heading stage, Murray et al. (1990) demonstrated a positive correlation between the number of days between sowing and heading stage and STB severity, the late sowing date was therefore likely to decrease STB epidemics. They proposed the key expla-

nation of this relation was the reduction of the primary infection rate caused by adverse environmental conditions for the pathogen associated with late sowings. Limiting the primary infection would reduce multiplication of the inoculum and probability of later infection resulting on lower observed severity of STB. Later, Shaw and Royle (1993) proposed an alternative explanation relying on the longer-lasting maturation of early-sown crops which is likely to: increase the number of infection cycles per leaf layer, multiplying the inoculum and increase the chances for upper-leaf infection.

The tall plants could generate unfavourable environment conditions for epidemics which could explain the generally lower severity observed for tall plants (Simón et al., 2005; Baccar et al., 2011). The infection and pathogen spore dispersal is also dependent on the distance between the source of inoculum and healthy leaves. Lovell et al. (1997) suggest the high stem extension rate might avoid the infection of younger leaves. This was presented by Baccar et al. (2011) as a "race" for vertical progress between the progression of the disease and the growth of the new leaves. Lovell et al. (1997) also highlighted the position of the leaves: erect diseased leaves favour the propagation to the upper leaves. The criteria of rate of plant development was highlighted by the model Septo3D (Robert et al., 2008).

The canopy density might be a factor increasing foliar disease severity (Gan et al., 2007; Baccar et al., 2011) through an increase of the relative humidity within the canopy with increasing density (Tompkins et al., 1993) or modification of canopy architecture (Baccar et al., 2011).

Consequently, cultural management can reduce STB severity. The STB prevention relies mostly on low susceptibility of the preceding crop and later sowing. In the UK, the AHDB (2016) generally recommended to avoid early sowing especially for susceptible varieties. Considering the rain splash-dispersal method of the STB, when the wheat crop is irrigated, overhead irrigation should be avoided.

- **Fungicide-based control**

In the EU, 70% of the annual use of fungicide is employed to address the STB epidemics (Fones and Gurr, 2015). In the UK, it was the highest of all the foliar diseases in 2015 (AHDB, 2016). The fungicide control can be satisfactory but only few curative solutions exist (Fones and Gurr, 2015), therefore the fungicide-based strategies aim at preventing the appearance of STB lesions.

The first endophyte/biotroph phase increases the difficulty of STB control by fungicides (Fones and Gurr, 2015) as the pathogen is protected within the leaf and not exposed to the fungicide application. This phase duration is affected by the temperature and moisture conditions, lasting from 14 to 28 days in the UK (AHDB, 2016) while the fungicide application targeting STB is effective for about 7 days (AHDB, 2016). Therefore, asymp-

tomatic leaves may not be free of STB infection and lesions can appear later.

Best fungicide-based practice relies on protection of the three top leaves protection through a first application when leaf 3 is fully emerged (GS31-33) followed by an additional application at the emergence of the flag leaf (AHDB, 2016). Additional protection may rely an early spraying during tillering before onset of stem extension to delay STB development in complement to other disease prevention such as mildews, rust or eyespot. For particularly susceptible cultivars, a last application may be considered at anthesis to control infection on the flag leaf and the ear (AHDB, 2016). With regard to cultivars, the optimal fungicide rate was not found to be consistently different in Ireland for cultivars exhibiting variable range of STB resistance (Lynch et al., 2017).

The fungicide protection relies on a mixture of fungicides. The AHDB (2016) recommends the use of azole in mixture with fungicides which include demethylation inhibitors (DMIs), Quinone outside Inhibitors (QoI), succinate dehydrogenase inhibitors (SDHI) and protective multi-site inhibitor such as chlorothalonil (Fraaije et al., 2012; Lynch et al., 2017). In addition, seed treatment may control the early steps of the epidemic, relying on azole again (e.g. fluquinconazole, AHDB 2016). The strobilurins don't provide adequate control in the UK anymore (AHDB, 2016).

However, the STB shows a remarkable adaptation to the fungicides. The pathogen strains acquire resistance to fungicide, partly explained by the important *Z. tritici*. Similarly to Griffin and Fischer in 1985 who studied the development of *Z. tritici* resistance to the benzimidazole fungicides, the STB strains resistance to QoI has increased (Fraaije et al., 2005). According to Cheval et al. (2017), 83% of *Z. tritici* isolates collected from naturally infected leaves were resistant to Qol in 2005, almost 100% since 2009. The QoI resistance was detected as early as 2001 in the UK (Fraaije et al., 2003). In addition, the gradual decline of triazole efficacy raises concerns (Cools and Fraaije, 2008; Fraaije et al., 2012; Dooley et al., 2016a). Finally, given the mechanism specific target of SDHI (inhibition of the succinate dehydrogenase of the mitochondrial respiratory chain) the fungicide resistance predicted by Fraaije et al. (2012) has been observed recently in *Z. tritici* isolates from Irish experiments and a related fungus mutation identified (Dooley et al., 2016b). The use of active ingredients with different modes of actions may, however, delay the evolution of the pathogen resistance to the azoles (Dooley et al., 2016a).

* * *

Because of its worldwide economical importance (Burke and Dunne, 2006; Fones and Gurr, 2015) and its biology cycle as well as the already acquired knowledge about this disease, STB is a well suited model to study the tolerance to biotic stress.

1.2.2.3 Quantify the tolerance of Septoria tritici blotch

Formerly, Schafer (1971) considered tolerance as a relative property, evident by comparison of crops exposed to comparable severity disease (Bingham et al., 2009). Several attempts to quantify tolerance have been developed. Kramer et al. (1980) or Inglese and Paul (2006) considered the tolerance based on estimation of the disease severity (respectively leaf rust, *Puccinia hordei* on barley and alien rust fungi on groundsel, *Senecio vulgaris*). They used the relationship between the Area Under the Disease Progress Curve (AUDPC) and the yield to quantify the tolerance. However, the disease information (AUDPC) is relative and does not take into account the absolute size of the grain source, likely to change between sites, seasons and genotypes. Instead of the AUDPC, the present study considers the effect of STB on the healthy area duration (HAD, the area under the green leaf lamina area progress curve). The HAD summarises the variability of the canopy size across genotypes and sites and seasons (Parker et al., 2004). For instance Bryson et al. (1997) evidenced that HAD conversion into grain yield depended also on the level of radiation that characterise the environment. The STB symptoms on the upper leaves reduce the HAD, and therefore the grain yield loss per unit of HAD reduction was used as a quantitative trait of the wheat crops for STB intolerance in tolerance studies (Parker et al., 2004; Foulkes et al., 2006; Castro and Simón, 2016).

Thus the ratio $\frac{\Delta Y}{\Delta HAD}$ quantifies the intolerance: a high value implies high yield loss for small source reduction (intolerant crop). Whereas a low value implies a small yield loss associated for a high source reduction (tolerant crop). Alternatively, based on the potential curve (Figure 1.3, Gouache et al. 2014), the potential yield reduction for a given source reduction (independently from the observed yield variation) is as a reference situation: what the expected yield loss is in such circumstances. This tolerance component is called hereafter the generic tolerance. Then, the comparison between the generic tolerance and the observed tolerance is an alternative tolerance quantification which might be called the specific tolerance (Eq. 1.2). In other words: is the observed yield loss worse or better than the theoretical potential yield loss for a given HAD reduction?

$$Tol_{Specific} = \frac{Tol_{Obs}}{Tol_{Generic}} = \frac{\Delta Y_{obs}}{\Delta HAD_{obs}} \times \frac{\Delta HAD_{obs}}{\Delta Y_{pot}} \tag{1.2}$$

1.2.3 Identification of STB tolerance traits

Evidence of a genetic basis for tolerance exists as yield response variability has long been observed for a given source reduction caused by STB. For instance, the cv. Fulhard hard wheat in Kansas (USA) could withstand severe leaf rust symptoms (*Puccinia recondita*, Salmon and Laude 1932), or the spring wheat cultivar Miriam in Israel endured severe

STB symptoms but reduced yield loss in comparison to three other genotypes (Ziv and Eyal, 1978). Historically, physiological assumptions to explain tolerance have pointed to source/sink relations. For instance, Ellis (1954) assumed a sink limitation buffered the effect of source reduction by leaf-rust *Puccina polysora* on a low-yielding maize genotype.

The yield components could influence tolerance of STB through sink demand. Foulkes et al. (2006) detected a negative correlation between STB tolerance and grain sink capacity based on three pairs of Near Isogenic Lines (NILs), through an increase in grains $\cdot$ m^{-2} while maintaining equivalent potential size, consistently with the UK breeding trends for increased grain density (Shearman et al., 2005). They explained higher grain density could decrease the sink limitation of the modern genotypes and confer higher susceptibility in yield loss when exposed to source limitation because of a disease. While studying traits favourable to wheat yield losses due to STB, Bancal et al. (2015) also identified a positive correlation with yield loss per unit HAD and grains $\cdot$ m^{-2} in healthy crops. In addition to grain density, Bancal et al. (2015) also indicated TGW as linked to tolerance, they actually suggested a negative correlation. However, the data base reported by Bancal et al. (2015) included a N fertilisation effect. When restricting to crops receiving a standard N fertilisation, they no longer observed any TGW effect on tolerance.

Source traits have also been found to be correlated with STB tolerance in wheat. Parker et al. (2004) hypothesised that increased radiation-use efficiency associated with the 1BL/1RS chromosome translocation reduced tolerance: the loss of green area and light interception may cause larger source reduction in genotypes with higher RUE. The green canopy area, light extinction coefficient and leaf photosynthetic traits were proposed to be candidate traits for tolerance of STB (Parker et al., 2004; Bingham et al., 2009). Parker et al. (2004) proposed that an increase in the canopy size could result in maintenance of green area. The upward propagation of the STB infection make the infection of the flag leaf less probable. Therefore, an increase in the contribution of upper leaf-layers to the light interception could reduce the impact of lower-leaf infections on photosynthesis (Lovell et al., 1997). Therefore, Parker et al. (2004) and later Bingham et al. (2009) suggest the increase light-extinction coefficient (k) as a tolerant trait. However, Bingham et al. (2009) also signified that if k could improve barley tolerance of *Rhynchosporium* leaf scald, that lever would be more difficult to use on wheat tolerance of STB because the genetic variation of k in barley is substantially larger than that of wheat. Foulkes et al. (2006) identified on wheat near-isogenic lines (NILs) that the flag-leaf area was positively correlated with tolerance of STB, which could be related to the upward movement of the pathogen through the canopy leaf layers by rain-splash events with an advantage for those genotypes with relatively more light interception in the flag-leaf layer. Bancal et al. (2015) did not observe a significant effect of flag-leaf area, but they confirmed its interest through the timing of senescence: crops with later flag-leaf senescence exhibited greater tolerance.

Complexity increases as source and sink may be involved in interactions with effects on tolerance. It is possible that up-regulation of photosynthesis in remaining healthy tissues may compensate partial source reduction caused by STB. Indeed, Scharen and Krupkinsk (1969) identified a positive relationship between CO_2 absorption and tolerance of wheat to *Septoria nodorum* infection. The tolerant spring wheat cv. Miriam (Ziv and Eyal, 1978) showed an enhanced carbon fixation by the healthy tissues (Zuckerman et al., 1997). Furthermore, Reynolds et al. (2005) identified a positive correlation of post-anthesis RUE with sink demand in spring wheat, where grains $\cdot$ m^{-2} was increased by row opening during booting, compared to a control treatment. Although investigated but not validated yet, tolerance could rely on post-anthesis RUE increase in response to lower assimilate availability relative to sink strength (investigated in the UK for cv Miriam and Barkai by Bingham et al. 2009; also in NILs lines by Foulkes et al. 2006). At the organ level, Bastiaans (1991, 1993) identified that the metabolism of the green area surrounding the visually identified symptoms was also altered in the case of rice leaf blast. The modification could result in a local increase in the RUE, which origin is still unclear as it could result from a local decrease in the source/sink balance stimulating the photosynthesis (e.g. increase in energy consumption for plant defense response, pathogen nutrient consumption as an additional sink), or a direct diversion of cell metabolism by the pathogen. More recently, Zhang et al. (2014) suggested a positive feedback from the sink strength on sources at the shoot level: an altered source/sink balance, decreased by ear shading or increased by spikelet-removal treatments in wheat, led to either up-regulation or down-regulation of flag leaf photosynthetic rate. This confirmed the work of Slafer and Savin (1994a) who found a positive correlation between sink strength and green area duration during grain filling.

The compensation of carbon assimilation, due to the reduction of HAD, by the remobilisation of stored components could also be a source of tolerance (Parker et al., 2004; Bingham et al., 2009). Therefore the carbohydrates, mainly stored in the internodes, could also buffer the HAD reduction. Using a pair of NILs contrasting for internode length, Foulkes et al. (2006) studied carbohydrate remobilisation but could not link higher carbohydrate remobilisation to STB tolerance (NILs: cv. Weston versus cv. Chaucer). However, Shearman et al. (2005) concluded that modern UK cultivars were associated with high remobilisation of carbohydrate, which might limit the extent of the remobilisation increase in a disease crop. To address the relationship between tolerance of STB and carbohydrate remobilisation, the genotypes/cultivars should therefore express a wide range of carbohydrate remobilisation patterns, involving not only modern UK cultivars.

The source/sink ratio estimates source availability relative to sink size and allows comparison with previous work. Still this ratio is complex, as its expression varies with the scales which can depend on methodological choices (HAD per grain, HAD per shoot or

per m^2, per grain weight or yield unit). Besides, hypotheses linked to individual leaf layer contributions also support the importance of understanding the effects of individual leaf layer HAD estimations to genetic variation in STB tolerance (Bancal et al., 2015; Bingham et al., 2009). The source to sink relation at the crop scale follows a saturating pattern (linked to the saturation of light interception), whereby the increase of grain sources tends to result in an asymptote sink size determining grain growth. Grain yields of wheat crops in Europe are mostly sink limited or co-limited under favourable conditions (Acreche and Slafer, 2009; Slafer and Savin, 1994b; Cartelle et al., 2006), i.e. close to the asymptote, the increased source availability increases only slightly the grain growth or not at all. The source/sink ratio can be modified through source/sink manipulations. Source/sink manipulations after grain setting (e.g. shading, defoliation, ear trimming) have been used to understand the source/sink ratio effect on grain growth and identify ways to increase the yield (Serrago et al., 2013; Slafer and Savin, 1994a; Egli and Bruening, 2001; Cartelle et al., 2006). However, the results of source/sink manipulation are complex. For instance, in their studies, Serrago et al. (2013); Slafer and Savin (1994a); Egli and Bruening (2001); Cartelle et al. (2006) all applied source/sink treatments which generated variations of the grain source availability. They discussed at the crop scale the sink limitation observed at the grain scale, while their work rather demonstrated the variability of the grain source limitation at the crop scale. Although implying a complex discussion, the usefulness of the source/sink manipulation treatments are indicated in the tolerance of STB, given the link between tolerance and source or sink described above.

Bancal et al. (2015) linked physiological traits of non-diseased shoots to yield loss regarding disease pressure in an environment. The linear relation exposed underlines effects of senescence pattern parameters and yield components on potential tolerance. Bancal et al. (2015) pointed out that higher maximum leaf lamina area could increase yield loss while a delayed senescence increases HAD and increases disease tolerance. An explanation can be proposed: an increased leaf area could increase disease severity unlike delayed senescence increasing the HAD (where a first approximation of HAD is computed by multiplication of leaf lamina area and onset of senescence). Indeed epidemics are accelerated by dense canopies (Lovell et al., 1997). And senescence advance is highly correlated with HAD and the area under the disease progress curve. Thus, delayed senescence onset appears to be of major interest as a lever to increase the ability of the crop to maintain the yield in presence of expressed disease. However, the response between factors and "stress-induced" senescence is qualitatively partially described, the understanding of quantitative effect of G×E on leaf senescence is sparse. For example, if it is well known that water stress can trigger senescence, the rainfall regimen and stage effects on leaf senescence onset has not been explored. As a second example, if the leaf shading is affecting hormone distribution and then senescence, the effect of canopy

density on senescence onset has not been quantified either.

1.3 Rationale, objectives and hypotheses

The aim of the PhD project is to identify traits and associated mechanisms which can improve the wheat tolerance of STB. The objectives of the project rely on studies developed to understand and model the ecophysiological processes associated to STB tolerance. The project mainly focused on genetic variations, but also aimed to understand how environmental variations can alter the crop tolerance potential. Based on the literature review, tolerance is expected to be highly linked to a question of source/sink balance, the studies must therefore emphasise the effect and relationship between source and sink traits and tolerance of STB.

According to Bancal et al. (2015), the senescence time of the top leaf layers and the sink size are potential tolerance traits. The first study in this thesis investigates, based on historical datasets including several genotypes in multiple environments, the genotype traits or environmental effect which influence the senescence timing and the grain weight in healthy crops. With appropriate methods, G×E variations can be quantified to understand how much the senescence kinetics or the achieved grain weight are influenced by genotype or environmental variations. In addition, validation on a different database was attempted. Secondly, a field experiment and a glasshouse experiment were carried out to examine further the assumptions which come from the literature and the database exploration. Using genotype material contrasting for tolerance of STB, a detailed nitrogen-analysis protocol was applied in a glasshouse experiment to investigate the potential association between tolerance and nitrogen metabolism. The same rationale was followed for the choice of genotype material in a field experiment which addressed the source/sink balance through heavy grain sink manipulation in addition to a nitrogen treatment. Both experiments include a treatment to induce STB disease contrast, through a paintbrush inoculation in the glasshouse, or using dedicated fungicide programme in the field. These experiments explore deeply the source/sink balance (nitrogen or carbon) in association with tolerance of STB. A final field experiment, based on six commercial UK cultivars, aimed at providing additional data on independent genetic materials to evaluate and verify hypotheses and results of the previous studies.

A central assumption is that part of tolerance relies on genetically affected traits, therefore we can design experiments using contrasting tolerant lines. Tolerance is conferred by specific features of these lines which can be heritable traits, or combinations of traits; and tolerance is also affected by growth conditions affecting source/sink balance.

This has already been explored, and various crosses aiming at producing a wide range of genetic material have been developed and provide relevant lines for the study of tolerance.

A second hypothesis is that tolerance study observations and results are consistent in the glasshouse with field experiments. The results from both can be compiled and used to understand tolerance. Glasshouse studies are appropriate for examining accurately specific mechanisms, whereas field trials are well suited for wider experimental screening of tolerance in relation to yield loss per unit of disease symptoms.

A third hypothesis is that STB tolerance relies on physiological processes. For instance, this can be nitrogen metabolism or energetic transfer through water soluble carbohydrate. A better understanding of the physiology of the plant or crop is meaningful to identify related traits which could enhance tolerance. In this context, source-sink manipulation treatments are appropriate methods to investigate tolerance traits.

References

M. M. Acreche and G. A. Slafer. Variation of grain nitrogen content in relation with grain yield in old and modern Spanish wheats grown under a wide range of agronomic conditions in a Mediterranean region. *The Journal of Agricultural Science*, 147(6):657–667, 2009. doi: 10.1017/S0021859609990190 .

T. B. Adhikari, J. M. Anderson, and S. B. Goodwin. Identification and molecular mapping of a gene in wheat conferring resistance to Mycosphaerella graminicola. *Phytopathology*, 93(9):1158–1164, 2003. URL http://apsjournals.apsnet.org/doi/pdfplus/10.1094/PHYTO.2003.93.9.1158.

T. B. Adhikari, J. R. Cavaletto, J. Dubcovsky, J. O. Gieco, A. R. Schlatter, and S. B. Goodwin. Molecular mapping of the Stb4 gene for resistance to Septoria tritici blotch in wheat. *Phytopathology*, 2004. URL http://apsjournals.apsnet.org/doi/pdfplus/10.1094/PHYTO.2004.94.11.1198.

AHDB. *Wheat disease maagement guide.* AHDB, 2016. URL https://cereals.ahdb.org.uk/media/176167/g63-wheat-disease-management-guide-february-2016.pdf.

AHDB. Ahdb Recommended List for cereals and oilseed 2017/18. Internet, Stoneleigh Park, Warwickshire, CV8 2TL, UK, 2017. URL https://cereals.ahdb.org.uk/media/800462/lr-ahdb-recommended-list-2017-18.pdf. Accessed 2017-08-11.

K. Ando, R. Grumet, K. Terpstra, and J. D. Kelly. Manipulation of plant architecture to enhance crop disease control. *CABI*, 2(26):8 pp., 2007. ISSN 1749-8848. doi: 10.1079/PAVSNNR20072026 .

J. Angus, R. Jones, and J. Wilson. A comparison of barley cultivars with different leaf inclinations. *Crop and Pasture Science*, 23:945–957, 1972. doi: 10.1071/AR9720945 .

I. Aranjuelo, L. Cabrera-Bosquet, R. Morcuende, J. C. Avice, S. Nogués, J. L. Araus, R. Martínez-Carrasco, and P. Pérez. Does ear C sink strength contribute to overcoming photosynthetic acclimation of wheat plants exposed to elevated CO2? *Journal of Experimental Botany*, 62(11):3957–3969, 2011. doi: 10.1093/jxb/err095 .

I. Aranjuelo, L. Cabrera-Bosquet, J. L. Araus, and S. Noguès. Carbon and nitrogen partitioning during the post-anthesis period is conditioned by N fertilisation and sink strength in three cereals. *Plant Biology*, 15(1):135–143, 2013. ISSN 1438-8677. doi: 10.1111/j.1438-8677.2012.00593.x .

L. Arraiano, A. Worland, C. Ellerbrook, and J. Brown. Chromosomal location of a gene for resistance to Septoria tritici blotch (Mycosphaerella graminicola) in the hexaploid wheat 'Synthetic 6x'. *TAG Theoretical and Applied Genetics*, 103(5):758–764, 2001. doi: 10.1007/s001220100668 .

R. B. Austin, J. Bingham, R. D. Blackwell, L. T. Evans, M. A. Ford, C. L. Morgan, and M. Taylor. Genetic improvements in winter wheat yields since 1900 and associated physiological changes. *The Journal of Agricultural Science*, 94(3):675–689, 1980. doi: 10.1017/S0021859600028665 .

R. Baccar, C. Fournier, T. Dornbusch, B. Andrieu, D. Gouache, and C. Robert. Modelling the effect of wheat canopy architecture as affected by sowing density on Septoria tritici epidemics using a coupled epidemic × virtual plant model. *Annals of Botany*, 108(6): 1179–1194, 2011. doi: 10.1093/aob/mcr126 .

B. Baltazar, A. Scharen, and W. Kronstad. Association between dwarfing genes 'rht1'and 'rht2'and resistance to Septoria tritici blotch in winter wheat (Triticum aestivum L. em Thell). *Theoretical and applied genetics*, 79(3):422–426, 1990. doi: 10.1007/BF01186089 .

M.-O. Bancal, R. Roche, and P. Bancal. Late foliar diseases in wheat crops decrease nitrogen yield through N uptake rather than through variations in N remobilization. *Annals of Botany*, 102(4):579–590, Oct 2008. ISSN 0305-7364. doi: 10.1093/aob/mcn124 .

P. Bancal. Positive contribution of stem growth to grain number per spike in wheat. *Field Crops Research*, 105(1–2):27–39, 2008. doi: 10.1016/j.fcr.2007.06.008 .

P. Bancal, M.-O. Bancal, F. Collin, and D. Gouache. Identifying traits leading to tolerance of wheat to Septoria tritici blotch. *Field Crops Research*, 180:176–185, 2015. doi: 10.1016/j.fcr.2015.05.006 .

A. Barbottin, C. Lecomte, C. Bouchard, and M. H. Jeuffroy. Nitrogen remobilization during grain filling in wheat: Genotypic and environmental effects. *Crop Science*, 45(3): 1141–1150, May–Jun 2005. doi: 10.2135/cropsci2003.0361 .

A. J. Barneix. Physiology and biochemistry of source-regulated protein accumulation in the wheat grain. *Journal of plant physiology*, 164(5):581–590, May 2007. ISSN 0176-1617. doi: 10.1016/j.jplph.2006.03.009 .

L. Bastiaans. Ratio between virtual and visual lesion size as a measure to describe reduction in leaf photosynthesis of rice due to leaf blast. *Phytopathology*, 81:611–615, 1991. URL http://apsnet.org/publications/phytopathology/backissues/Documents/1991Articles/Phyto81n06_611.PDF.

L. Bastiaans. Effects of leaf blast on growth and production of a rice crop. 1. Determining the mechanism of yield reduction. *Netherland journal of plant pathology*, 99(5–6):323–334, 1993. ISSN 0028-2944. doi: 10.1007/BF01974313 .

R. Ben Slimane. *Effets de la septoriose foliaire sur la sénescence et les flux d'azote pendant le remplissage des grains chez le blé tendre.* PhD thesis, AgroParisTech, 2010. URL https://hal.archives-ouvertes.fr/pastel-00560282/.

I. J. Bingham and C. F. E. Topp. Potential contribution of selected canopy traits to the tolerance of foliar disease by spring barley. *Plant Pathology*, 58(6):1010–1020, Dec 2009. ISSN 0032-0862. doi: 10.1111/j.1365-3059.2009.02137.x .

I. J. Bingham, D. R. Walters, M. J. Foulkes, and N. D. Paveley. Crop traits and tolerance of wheat and barley to foliar disease. *Annals of Applied Biology*, 154:159–173, 2009. doi: 10.1111/j.1744-7348.2008.00291.x .

A. Boonman, N. P. R. Anten, T. A. Dueck, W. J. R. M. Jordi, A. van der Werf, L. A. C. J. Voesenek, and T. L. Pons. Functional significance of shade-induced leaf senescence in dense canopies: an experimental test using transgenic tobacco. *The American Naturalist*, 168(5):597–607, 2006. doi: 10.1086/508633 .

B. Borghi, M. Corbellini, C. Minoia, M. Palumbo, N. Di Fonzo, and M. Perenzin. Effects of Mediterranean climate on wheat bread-making quality. *European journal of agronomy*, 6(3-4):145–154, May 1997. ISSN 1161-0301. doi: 10.1016/S1161-0301(96)02040-0 .

A. K. Borrell and G. L. Hammer. Nitrogen dynamics and the physiological basis of stay-green in sorghum. *Crop science*, 40(5):1295–1307, 2000. doi: 10.2135/cropsci2000.4051295x .

P. A. Brading, E. C. Verstappen, G. H. Kema, and J. K. Brown. A gene-for-gene relationship between wheat and Mycosphaerella graminicola, the Septoria tritici blotch pathogen. *Phytopathology*, 92(4):439–445, 2002. URL http://apsjournals.apsnet.org/doi/pdfplus/10.1094/PHYTO.2002.92.4.439.

J. K. Brown, L. Chartrain, P. Lasserre-Zuber, and C. Saintenac. Genetics of resistance to Zymoseptoria tritici and applications to wheat breeding. *Fungal Genetics and Biology*, 79:33–41, 2015. doi: 10.1016/j.fgb.2015.04.017 .

R. J. Bryson, N. D. Paveley, W. S. Clark, R. Sylvester-Bradley, and R. K. Scott. Use of in-field measurements of green leaf area and incident radiation to estimate the effects of yellow rust epidemics on the yield of winter wheat. *European Journal of Agronomy*, 7: 53–62, 1997. doi: 10.1016/S1161-0301(97)00025-7 .

J. Burke and B. Dunne. Septoria tritici in winter wheat – to spray or not to spray? *Irish farmer*, pages 14–18, April 2006.

J. Cartelle, A. Pedró, R. Savin, and G. A. Slafer. Grain weight responses to post-anthesis spikelet-trimming in an old and a modern wheat under mediterranean conditions. *European Journal of Agronomy*, 25(4):365–371, 2006. ISSN 1161-0301. doi: 10.1016/j.eja.2006.07.004 .

A. C. Castro and M. R. Simón. Effect of tolerance to Septoria tritici blotch on grain yield, yield components and grain quality in Argentinean wheat cultivars. *Crop Protection*, 90: 66–76, 2016. ISSN 0261-2194. doi: 10.1016/j.cropro.2016.08.015 .

H. F. Causin, R. N. Jauregui, and A. J. Barneix. The effect of light spectral quality on leaf senescence and oxidative stress in wheat. *Plant Science*, 171(1):24–33, Jul 2006. ISSN 0168-9452. doi: 10.1016/j.plantsci.2006.02.009 .

L. Chartrain, P. A. Brading, J. C. Makepeace, and J. K. M. Brown. Sources of resistance to Septoria tritici blotch and implications for wheat breeding. *Plant Pathology*, 53(4): 454–460, 2004. ISSN 1365-3059. doi: 10.1111/j.1365-3059.2004.01052.x .

J. Chen, Y. Liang, X. Hu, X. Wang, F. Tan, H. Zhang, Z. Ren, and P. Luo. Physiological characterization of 'stay green'wheat cultivars during the grain filling stage under field growing conditions. *Acta physiologiae plantarum*, 32(5):875–882, 2010. doi: 10.1007/s11738-010-0475-0 .

P. Cheval, A. Siah, M. Bomble, A. D. Popper, P. Reignault, and P. Halama. Evolution of QoI resistance of the wheat pathogen *Zymoseptoria tritici* in Northern France. *Crop protection*, 92:131–133, Feb 2017. ISSN 0261-2194. doi: 10.1016/j.cropro.2016.10.017 .

H. J. Cools and B. A. Fraaije. Are azole fungicides losing ground against Septoria wheat disease? resistance mechanisms in Mycosphaerella graminicola. *Pest Management Science*, 64(7):681–684, 2008. ISSN 1526-4998. doi: 10.1002/ps.1568 .

H. J. Cools and B. A. Fraaije. Update on mechanisms of azole resistance in Mycosphaerella graminicola and implications for future control. *Pest management science*, 69(2):150–155, 2013. doi: 10.1002/ps.3348 .

F. Cormier, J. Foulkes, B. Hirel, D. Gouache, Y. Moënne-Loccoz, and J. Le Gouis. Breeding for increased nitrogen-use efficiency: a review for wheat T. aestivum L.). *Plant Breeding*, 135:255–278, 2016. doi: 10.1111/pbr.12371 .

C. Cowger, M. Hoffer, and C. Mundt. Specific adaptation by Mycosphaerella graminicola to a resistant wheat cultivar. *Plant Pathology*, 49(4):445–451, 2000. doi: 10.1046/j.1365-3059.2000.00472.x .

M. Cox, C. Qualset, and D. Rains. Genetic-variation for nitrogen assimilation and translocation in wheat. 2. Nitrogen assimilation in relation to grain-yield and protein. *Crop science*, 25(3):435–440, 1985. ISSN 0011-183X. doi: 10.2135/cropsci1985.0011183X002500030003x .

S. J. Crafts-Brandner, F. E. Below, V. A. Wittenbach, J. E. Harper, and R. H. Hageman. Differential senescence of maize hybrids following ear removal II. Selected leaf. *Plant Physiology*, 74(2):368–373, 1984. doi: 10.1104/pp.74.2.368 .

S. J. Crafts-Brandner, R. Hölzer, and U. Feller. Influence of nitrogen deficiency on senescence and the amounts of RNA and proteins in wheat leaves. *Physiologia Plantarum*, 102(2):192–200, 1998. ISSN 1399-3054. doi: 10.1034/j.1399-3054.1998.1020206.x .

T. Curtis and N. Halford. Food security: the challenge of increasing wheat yield and the importance of not compromising food safety. *Annals of applied biology*, 164(3):354–372, 2014. doi: 10.1111/aab.12108 .

J. C. Dawson, D. R. Huggins, and S. S. Jones. Characterizing nitrogen use efficiency in natural and agricultural ecosystems to improve the performance of cereal crops in low-input and organic agricultural systems. *Field Crops Research*, 107(2):89–101, 2008. doi: 10.1016/j.fcr.2008.01.001 .

S. Demotes-Mainard, G. Doussinault, and J. M. Meynard. Effects of low radiation and low temperature at meiosis on pollen viability and grain set in wheat. *Agronomie*, 15:357–365, 1995. URL `https://hal.archives-ouvertes.fr/hal-00885691/document`.

S. Demotes-Mainard, G. Doussinault, and J. M. Meynard. Abnormalities in the male developmental programme of winter wheat induced by climatic stess at meiosis. *Agronomie*, 15:357–365, 1996. URL https://hal.archives-ouvertes.fr/hal-00885813/document.

A. P. Derkx, S. Orford, S. Griffiths, M. J. Foulkes, and M. J. Hawkesford. Identification of differentially senescing mutants of wheat and impacts on yield, biomass and nitrogen partitioning. *Journal of integrative plant biology*, 54(8):555–566, Aug 2012. ISSN 1672-9072. doi: 10.1111/j.1744-7909.2012.01144.x .

L. Ding, K. Wang, G. Jiang, D. Biswas, H. Xu, L. Li, and Y. Li. Effects of nitrogen deficiency on photosynthetic traits of maize hybrids released in different years. *Annals of Botany*, 96(5):925–930, 2005. doi: 10.1093/aob/mci244 .

H. Dooley, M. Shaw, J. Spink, and S. Kildea. Effect of azole fungicide mixtures, alternations and dose on azole sensitivity in the wheat pathogen Zymoseptoria tritici. *Plant Pathology*, 65(1):124–136, 2016a. doi: 10.1111/ppa.12395 .

H. Dooley, M. W. Shaw, J. Mehenni-Ciz, J. Spink, and S. Kildea. Detection of Zymoseptoria tritici SDHI-insensitive field isolates carrying the SdhC-H152R and SdhD-R47W substitutions. *Pest management science*, 72(12):2203–2207, 2016b. doi: 10.1002/ps.4269 .

K. E. Duncan and R. J. Howard. Cytological analysis of wheat infection by the leaf blotch pathogen Mycosphaerella graminicola. *Mycological Research*, 104(9):1074 – 1082, 2000. ISSN 0953-7562. doi: 10.1017/S0953756299002294 .

L. Echarte, S. Rothstein, and M. Tollenaar. The response of leaf photosynthesis and dry matter accumulation to nitrogen supply in an older and a newer maize hybrid. *Crop Science*, 48(2):656–665, 2008. doi: 10.2135/cropsci2007.06.0366 .

D. B. Egli and W. P. Bruening. Source-sink relationships, seed sucrose levels and seed growth rates in soybean. *Annals of botany*, 88(2):235–242, Aug 2001. ISSN 0305-7364. doi: 10.1006/anbo.2001.1449 .

R. T. Ellis. Tolerance to the maize rust *Puccinia polysora* underw. *Nature*, 174:1021, 1954.

L. Eriksen, M. W. Shaw, and H. Østergård. A model of the effect of pseudothecia on genetic recombination and epidemic development in populations of Mycosphaerella graminicola. *Phytopathology*, 91(3):240–248, 2001. doi: 10.1094/PHYTO.2001.91.3.240 .

J. R. Evans. Photosynthesis and nitrogen relationships in leaves of C3 plants. *Oecologia*, 78: 9–19, 1989. URL https://link.springer.com/article/10.1007%2FBF00377192?LI=true.

R. E. Evenson and D. Gollin. Assessing the impact of the green revolution, 1960 to 2000. *Science*, 300(5620):758–762, 2003. doi: 10.1126/science.1078710 .

Z. Eyal, I. Maize, and W. I. Center. *The Septoria diseases of wheat : concepts and methods of disease management / International Maize and Wheat Improvement Center.* CIMMYT Mexico, D.F, 1987. ISBN 9686127062.

Z. Eyal et al. Integrated control of Septoria diseases of wheat. *Plant Disease*, 65(9):763–768, 1981.

FAO. *FAO Statistical pocketbook - World food and Agriculture*, chapter Crops, pages 28–29. Food and Agriculture Organization of the United Nations, Rome, 2015.

FAOSTAT. Faostat database. Internet, 2017. URL http://www.fao.org/faostat/. Accessed 2017-07-20.

U. Feller and A. Fischer. Nitrogen-metabolism in senescing leaves. *Critical reviews in plant sciences*, 13(3):241–273, 1994. ISSN 0735-2689. doi: 10.1080/713608059 .

R. A. Fischer. Understanding the physiological basis of yield potential in wheat. *The Journal of Agricultural Science*, 145(2):99–113, 2007. doi: 10.1017/S0021859607006843 .

R. A. Fischer and Y. M. Stockman. Kernel number per spike in wheat (*Triticum aestivum* l.): responses to preanthesis shading. *Australian Journal of Plant Physiology*, 7(2):169–180, 1980. doi: 10.1071/PP9800169 .

H. Fones and S. Gurr. The impact of Septoria tritici blotch disease on wheat: An EU perspective. *Fungal Genetics and Biology*, 79:3 – 7, 2015. ISSN 1087-1845. doi: 10.1016/j.fgb.2015.04.004 . Septoria tritici blotch disease of wheat: Tools and techniques to study the pathogen Zymoseptoria tritici.

M. J. Foulkes, N. D. Paveley, A. Worland, S. J. Welham, J. Thomas, and J. W. Snape. Major genetic changes in wheat with potential to affect disease tolerance. *Phytopathology*, 96:680–688, 2006. URL http://apsjournals.apsnet.org/doi/pdf/10.1094/PHYTO-96-0680.

M. J. Foulkes, M. J. Hawkesford, P. B. Barraclough, M. J. Holdsworth, S. Kerr, S. Kightley, and P. R. Shewry. Identifying traits to improve the nitrogen economy of wheat: Recent advances and future prospects. *Field crops research*, 114(3):329–342, Dec 2009. ISSN 0378-4290. doi: 10.1016/j.fcr.2009.09.005 .

B. Fraaije, H. Cools, J. Fountaine, D. Lovell, J. Motteram, J. West, and J. Lucas. Role of ascospores in further spread of QoI-resistant cytochrome b alleles (G143A) in field populations of Mycosphaerella graminicola. *Phytopathology*, 95(8):933–941, Aug 2005. ISSN 0031-949X. URL http://apsjournals.apsnet.org/doi/pdfplus/10.1094/PHYTO-95-0933.

B. A. Fraaije, J. A. Lucas, W. S. Clark, and F. J. Burnett. QoI resistance development in populations of cereal pathogens in the UK. In *Proceedings of the BCPC International Congress, Crop Science and Technology*, 689–694, Alton, Hampshire, UK, 2003. The British Crop Protection Council.

B. A. Fraaije, C. Bayon, S. Atkins, H. J. Cools, J. A. Lucas, and M. W. Fraaije. Risk assessment studies on succinate dehydrogenase inhibitors, the new weapons in the battle to control Septoria leaf blotch in wheat. *Molecular Plant Pathology*, 13(3):263–275, 2012. ISSN 1364-3703. doi: 10.1111/j.1364-3703.2011.00746.x . URL http://dx.doi.org/10.1111/j.1364-3703.2011.00746.x.

V. Fröhlich and U. Feller. Effect of phloem interruption on senescence and protein remobilization in the flag leaf of field-grown wheat. *Biochemie und Physiologie der Pflanzen*, 187(2):139–147, 1991. doi: 10.1016/S0015-3796(11)80118-6 .

J.-D. Fu and B.-W. Lee. Changes in photosynthetic characteristics during grain filling of a functional stay-green rice SNU-SG1 and its F1 hybrids. *Journal of crop science and biotechnology*, 11:75–82, 2008. URL http://www.cropbio.org/contribute/paperfiles/Jin-Dong%20Fu.pdf.

O. Gaju, V. Allard, P. Martre, J. W. Snape, E. Heumez, J. LeGouis, D. Moreau, M. Bogard, S. Griffiths, S. Orford, S. Hubbart, and M. J. Foulkes. Identification of traits to improve the nitrogen-use efficiency of wheat genotypes. *Field Crops Research*, 123(2):139 – 152, 2011. ISSN 0378-4290. doi: 10.1016/j.fcr.2011.05.010 .

O. Gaju, V. Allard, P. Martre, J. Le Gouis, D. Moreau, M. Bogard, S. Hubbart, and M. J. Foulkes. Nitrogen partitioning and remobilization in relation to leaf senescence, grain yield and grain nitrogen concentration in wheat cultivars. *Field Crops Research*, 155:213 – 223, 2014. ISSN 0378-4290. doi: 10.1016/j.fcr.2013.09.003 .

Y. Gan, B. D. Gossen, L. Li, G. Ford, and S. Banniza. Cultivar type, plant population, and Ascochyta blight in chickpea. *Agronomy journal*, 99(6):1463–1470, 2007. doi: 10.2134/agronj2007.0105 .

H. C. J. Godfray. The challenge of feeding 9–10 billion people equitably and sustainably. *The Journal of Agricultural Science*, 152(S1):2–8, 2014. doi: 10.1017/S0021859613000774 .

M. J. Gooding, P. J. Gregory, K. E. Ford, and S. Pepler. Fungicide and cultivar affect post-anthesis patterns of nitrogen uptake, remobilization and utilization efficiency in wheat. *Journal of Agricultural Science*, 143(6):503–518, Dec 2005. ISSN 0021-8596. doi: 10.1017/S002185960500568X .

D. Gouache, M. Bancal, B. de Solan, and P. Gate. Tolérance du blé tendre aux stress biotiques et abiotiques. *Innovations Agronomiques*, 35:75–87, 2014. URL https://hal.archives-ouvertes.fr/hal-01192469.

P. L. Gregersen. *The Molecular and Physiological Basis of Nutrient Use Efficiency in Crops*, chapter 5. Senescence and Nutrient Remobilization in Crop Plants, pages 83–102. Wiley-Blackwell, 2011. ISBN 9780470960707. doi: 10.1002/9780470960707.ch5 .

P. L. Gregersen, A. Culetic, L. Boschian, and K. Krupinska. Plant senescence and crop productivity. *Plant Molecular Biology*, 82(6):603–622, Aug 2013. ISSN 0167-4412. doi: 10.1007/s11103-013-0013-8 .

M. J. Griffin and N. Fischer. Laboratory studies on benzimidazole resistance in Septoria tritici. *EPPO Bulletin*, 15:505–511, 1985. doi: 10.1111/j.1365-2338.1985.tb00262.x .

Y. Guo and S.-S. Gan. Convergence and divergence in gene expression profiles induced by leaf senescence and 27 senescence-promoting hormonal, pathological and environmental stress treatments. *Plant, Cell & Environment*, 35(3):644–655, 2012. doi: 10.1111/j.1365-3040.2011.02442.x .

A. J. Hall and R. A. Richards. Prognosis for genetic improvement of yield potential and water-limited yield of major grain crops. *Field Crops Research*, 143:18–33, 2013. doi: 10.1016/j.fcr.2012.05.014 .

A. J. Hall, R. Savin, and G. A. Slafer. Is time to flowering in wheat and barley influenced by nitrogen? A critical appraisal of recent published reports. *European Journal of Agronomy*, 54:40–46, Mar 2014. ISSN 1161-0301. doi: 10.1016/j.eja.2013.11.006 .

J. P. Hébrard. Azote et qualité des blés: fractioner pour plus de protéines. *Perspectives Agricoles*, (68):21–29, 1999.

S. J. Inglese and N. D. Paul. Tolerance of Senecio vulgaris to infection and disease caused by native and alien rust fungi. *Phytopathology*, 96(7):718–726, 2006. URL http://apsjournals.apsnet.org/doi/pdf/10.1094/PHYTO-96-0718.

C. F. Jenner, T. D. Ugalde, and D. Aspinall. The physiology of starch and protein deposition in the endosperm of wheat. *Australian journal of plant physiology*, 18(3):211–226, 1991. ISSN 0310-7841. doi: 10.1071/PP9910211 .

A. K. Joshi, M. Kumari, V. P. Singh, C. M. Reddy, S. Kumar, J. Rane, and R. Chand. Stay green trait: variation, inheritance and its association with spot blotch resistance in spring wheat (Triticum aestivum L.). *Euphytica*, 153(1):59–71, 2007. ISSN 1573-5060. doi: 10.1007/s10681-006-9235-z .

G. H. J. Kema, D. Z. Yu, F. H. J. Rijkenberg, M. W. Shaw, and R. P. Baayen. Histology of the pathogenesis of Mycosphaerella graminicola in wheat. *Phytopathology*, 86(7):777–786, Jul 1996. ISSN 0031-949X. doi: 10.1094/Phyto-86-777 .

J. Keon, J. Antoniw, R. Carzaniga, S. Deller, J. L. Ward, J. M. Baker, M. H. Beale, K. Hammond-Kosack, and J. J. Rudd. Transcriptional adaptation of Mycosphaerella graminicola to programmed cell death (PCD) of its susceptible wheat host. *Molecular plant-microbe interactions*, 20(2):178–193, Feb 2007. ISSN 0894-0282. doi: 10.1094/MPMI-20-2-0178 .

T. Kichey, B. Hirel, E. Heumez, F. Dubois, and J. Le Gouis. In winter wheat (Triticum aestivum L.), post-anthesis nitrogen uptake and remobilisation to the grain correlates with agronomic traits and nitrogen physiological markers. *Field Crops Research*, 102(1): 22–32, Apr 2007. ISSN 0378-4290. doi: 10.1016/j.fcr.2007.01.002 .

E. J. M. Kirby. Analysis of leaf, stem and ear growth in wheat from terminal spikelet stage to anthesis. *Field Crops Research*, 18(2):127–140, 1988. ISSN 0378-4290. doi: 10.1016/0378-4290(88)90004-4 .

T. Kramer, B. H. Gildemacher, M. Van der Ster, and J. E. Parlevliet. Tolerance of spring barley cultivars to leaf rust, Puccinia hordei. *Euphytica*, 29(2):209–216, 1980. ISSN 1573-5060. doi: 10.1007/BF00025116 .

M. Kremer and G. M. Hoffmann. Effects of leaf infections of Drechslera tritici-repentis on the carbohydrate and nitrogen metabolism of wheat plants. *Journal of Plant Diseases and Protection*, 100(3):259–277, 1993. ISSN 0340-8159.

J. Levitt. *Stress and strain terminology*, chapter Chapter 1, pages 1–8. New York Academic Press Physiological Ecology, 1972.

D. J. Lovell, S. R. Parker, T. Hunter, D. J. Royle, and R. R. Coker. Influence of crop growth and structure on the risk of epidemics by Mycosphaerella graminicola (Septoria tritici) in winter wheat. *Plant Pathology*, 46(1):126–138, Feb 1997. ISSN 0032-0862. doi: 10.1046/j.1365-3059.1997.d01-206.x .

J. P. Lynch, E. Glynn, S. Kildea, and J. Spink. Yield and optimum fungicide dose rates for winter wheat (Triticum aestivum L.) varieties with contrasting ratings for resistance to Septoria tritici blotch. *Field Crops Research*, 204:89–100, 2017. doi: 10.1016/j.fcr.2017.01.012 .

Y.-Z. Ma, C. T. MacKown, and D. A. van Sanford. Differential effects of partial spikelet removal and defoliation on kernel growth and assimilate partitioning among wheat cultivars. *Field Crops Research*, 47:201–209, 1996. ISSN 0378-4290. doi: 10.1016/0378-4290(96)00016-0 .

A. Martin, X. Belastegui-Macadam, I. Quilleré, M. Floriot, M.-H. Valadier, B. Pommel, B. Andrieu, I. Donnison, and B. Hirel. Nitrogen management and senescence in two maize hybrids differing in the persistence of leaf greenness: agronomic, physiological and molecular aspects. *New Phytologist*, 167(2):483–492, 2005. doi: 10.1111/j.1469-8137.2005.01430.x .

C. Masclaux-Daubresse, M. Reisdorf-Cren, and M. Orsel. Leaf nitrogen remobilisation for plant development and grain filling. *Plant Biology*, 10:23–36, 2008. ISSN 1438-8677. doi: 10.1111/j.1438-8677.2008.00097.x .

C. Masclaux-Daubresse, F. Daniel-Vedele, J. Dechorgnat, F. Chardon, L. Gaufichon, and A. Suzuki. Nitrogen uptake, assimilation and remobilization in plants: challenges for sustainable and productive agriculture. *Annals of Botany*, 105(7):1141–1157, Jan 2010. ISSN 0305-7364, 1095-8290. doi: 10.1093/aob/mcq028 .

C. McCartney, A. Brûlé-Babel, and L. Lamari. Inheritance of race-specific resistance to Mycosphaerella graminicola in wheat. *Phytopathology*, 92(2):138–144, 2002. URL http://apsjournals.apsnet.org/doi/pdfplus/10.1094/PHYTO.2002.92.2.138.

G. M. Murray, R. H. Martin, and B. R. Cullis. Relationship of the severity of Septoria tritici blotch of wheat to sowing time, rainfall at heading and average susceptibility of wheat cultivars in the area. *Australian journal of agricultural research*, 41(2):307–315, 1990. doi: 10.1071/AR9900307 .

B. Ney, M.-O. Bancal, P. Bancal, I. J. Bingham, J. M. Foulkes, D. Gouache, N. D. Paveley, and J. Smith. Crop architecture and crop tolerance to fungal diseases and insect herbivory. Mechanisms to limit crop losses. *European Journal of Plant Pathology*, 135(3): 561–580, 2013. ISSN 0929-1873. doi: 10.1007/s10658-012-0125-z .

L. D. Noodén, J. W. Hillsberg, and M. J. Schneider. Induction of leaf senescence in Arabidopsis thaliana by long days through a light-dosage effect. *Physiologia Plantarum*, 96(3):491–495, 1996. ISSN 1399-3054. doi: 10.1111/j.1399-3054.1996.tb00463.x .

K. Ono, I. Terashima, and A. Watanabe. Interaction between nitrogen deficit of a plant and nitrogen content in the old leaves. *Plant and Cell Physiology*, 37(8):1083–1089, 1996. doi: 10.1093/oxfordjournals.pcp.a029057 .

S. R. Parker, S. Welham, N. Paveley, J. M. Foulkes, and R. K. Scott. Tolerance of Septoria leaf blotch in winter wheat. *Plant Pathology*, 53(1):1–10, 2004. doi: 10.1111/j.1365-3059.2004.00951.x .

Parry, M. Reynolds, M. Salvucci, C. Raines, P. Andralojc, X.-G. Zhu, D. Price, A. Condone, and R. Furbank. Raising yield potential of wheat. II. Increasing photosynthetic capacity and efficiency. *Journal of Experimental Botany*, 62:453–467, 2001. doi: 10.1093/jxb/erq30410.1093/jxb/erq304 .

A. Pask. *Optimising nitrogen storage in wheat canopies for genetic reduction in fertiliser nitrogen inputs*. PhD thesis, University of Nottingham, December 2009. URL http://eprints.nottingham.ac.uk/12567/.

A. J. D. Pask, R. Sylvester-Bradley, P. D. Jamieson, and M. J. Foulkes. Quantifying how winter wheat crops accumulate and use nitrogen reserves during growth. *Field crops research*, 126:104–118, Feb 2012. ISSN 0378-4290. doi: 10.1016/j.fcr.2011.09.021 .

J. B. Passioura. Soil conditions and plant growth. *Plant, Cell & Environment*, 25(2):311–318, 2002. doi: 10.1046/j.0016-8025.2001.00802.x .

I. Rajcan and M. Tollenaar. Source: sink ratio and leaf senescence in maize: II. Nitrogen metabolism during grain filling. *Field Crops Research*, 60(3):255–265, 1999. doi: 10.1016/S0378-4290(98)00143-9 .

S. Recous, P. Loiseau, J. M. Machet, and B. Mary. Transformations et devenir de l'azote de l'engrais sous cultures annuelles et sous prairies. *Les colloques de l'INRA*, 83:105–120, 1997.

M. P. Reynolds, A. Pellegrineschi, and B. Skovmand. Sink-limitation to yield and biomass: a summary of some investigations in spring wheat. *Annals of applied biology*, 146(1):39–49, 2005. ISSN 0003-4746. doi: 10.1111/j.1744-7348.2005.03100.x .

S. Rieben, O. Kalinina, B. Schmid, and S. L. Zeller. Gene flow in genetically modified wheat. *Plos One*, 6(12):1–7, 12 2011. doi: 10.1371/journal.pone.0029730 .

C. Robert, C. Fournier, B. Andrieu, and B. Ney. Coupling a 3D virtual wheat (Triticum aestivum) plant model with a Septoria tritici epidemic model (Septo3D): a new approach to investigate plant–pathogen interactions linked to canopy architecture. *Functional Plant Biology*, 35:997–1013, 2008. doi: 10.1071/FP08066 .

A. A. Rosielle and W. J. R. Boyd. Genetics of host-pathogen interactions to the Septoria species of wheat. Technical report, 1985.

M. C. Rousseaux, A. J. Hall, and R. A. Sánchez. Far-red enrichment and photosynthetically active radiation level influence leaf senescence in field-grown sunflower. *Physiologia Plantarum*, 96(2):217–224, 1996. ISSN 1399-3054. doi: 10.1111/j.1399-3054.1996.tb00205.x .

S. A. Ruuska, G. J. Rebetzke, A. F. van Herwaarden, R. A. Richards, N. A. Fettell, L. Tabe, and C. L. Jenkins. Genotypic variation in water-soluble carbohydrate accumulation in wheat. *Functional Plant Biology*, 33(9):799–809, 2006. doi: 10.1071/FP06062 .

S. C. Salmon and H. H. Laude. Twenty years of testing varieties and strain of winter wheat at the Kansas agricultural experiment station. Technical bulletin 80, Kansas state college of agriculture and applied science, Manhattan, Kansas, February 1932. URL `https://www.k-state.edu/historicpublications/pubs/STB030.PDF`.

R. Sanchez-Bragado, G. Molero, M. P. Reynolds, and J. L. Araus. Relative contribution of shoot and ear photosynthesis to grain filling in wheat under good agronomical conditions assessed by differential organ δ13c. *Journal of experimental botany*, 65(18):5401–5413, 2014. doi: 10.1093/jxb/eru298 .

R. Sanchez-Bragado, M. D. Serret, and J. L. Araus. The nitrogen contribution of different plant parts to wheat grains: Exploring genotype, water, and nitrogen effects. *Frontiers in Plant Science*, 7:1986, 2017. ISSN 1664-462X. doi: 10.3389/fpls.2016.01986 .

M. Sanchez-Garcia, C. Royo, N. Aparicio, J. Martin-Sanchez, and F. Alvaro. Genetic improvement of bread wheat yield and associated traits in Spain during the 20th century. *The Journal of Agricultural Science*, 151(1):105–118, 2013. doi: 10.1017/S0021859612000330 .

A. Sánchez-Vallet, M. C. McDonald, P. S. Solomon, and B. A. McDonald. Is Zymoseptoria tritici a hemibiotroph? *Fungal Genetics and Biology*, 79:29 – 32, 2015. ISSN 1087-1845. doi: 10.1016/j.fgb.2015.04.001 . Septoria tritici blotch disease of wheat: Tools and techniques to study the pathogen Zymoseptoria tritici.

S. Savary, N. P. Castilla, F. A. Elazegui, C. G. Mc Laren, M. A. Ynalvez, and P. S. Teng. Direct and indirect effects of nitrogen supply and disease source structure on rice sheath blight spread. *Phytopathology*, 85(9):959–965, Sep 1995. ISSN 0031-949X. doi: 10.1094/Phyto-85-959 .

J. Schafer. Tolerance to plant disease. *Annual review of phytopathology*, 9:235–252, 1971. ISSN 0066-4286. doi: 10.1146/annurev.py.09.090171.001315 .

A. L. Scharen and J. M. Krupkinsk. Effect of Septoria nodorum infection on CO2 absorption and yield of wheat. *Phytopathology*, 59(9):1298–&, 1969. ISSN 0031-949X.

R. A. Serrago, I. Alzueta, R. Savin, and G. A. Slafer. Understanding grain yield responses to source-sink ratios during grain filling in wheat and barley under contrasting environments. *Field Crops Research*, 150:42–51, August 2013. ISSN 0378-4290. doi: 10.1016/j.fcr.2013.05.016 .

M. W. Shaw and D. J. Royle. Factors determining the severity of epidemics of Mycosphaerella graminicola (Septoria tritici) on winter wheat in the UK. *Plant Pathology*, 42(6):882–899, 1993. ISSN 1365-3059. doi: 10.1111/j.1365-3059.1993.tb02674.x .

V. J. Shearman, R. Sylvester-Bradley, R. K. Scott, and M. J. Foulkes. Physiological processes associated with wheat yield progress in the UK. *Crop Science*, 45(1):175–185, 2005. doi: 10.2135/cropsci2005.0175 .

P. R. Shewry. Wheat. *Journal of experimental botany*, 60(6):1537–1553, 2009. doi: 10.1093/jxb/erp058 .

P. R. Shewry, R. A. C. Mitchell, P. Tosi, Y. Wan, C. Underwood, A. Lovegrove, J. Freeman, G. A. Toole, E. N. C. Mills, and J. L. Ward. An integrated study of grain development of wheat (cv. Hereward). *Journal of Cereal Science*, 56(1):21–30, 2012. ISSN 0733-5210. doi: 10.1016/j.jcs.2011.11.007 .

M. R. Simón, A. E. Perelló, C. A. Cordo, S. Larrán, P. E. van der Putten, and P. C. Struik. Association between Septoria tritici blotch, plant height, and heading date in wheat. *Agronomy Journal*, 97(4):1072–1081, 2005. doi: 10.2134/agronj2004.0126 .

T. R. Sinclair and P. D. Jamieson. Grain number, wheat yield, and bottling beer: an analysis. *Field Crops Research*, 98(1):60–67, 2006. ISSN 0378-4290. doi: 10.1016/j.fcr.2005.12.006 .

G. A. Slafer and F. H. Andrade. Changes in physiological attributes of the dry matter economy of bread wheat (Triticum aestivum) through genetic improvement of grain yield potential at different regions of the world. *Euphytica*, 58(1):37–49, 1991. URL `https://link.springer.com/article/10.1007%2FBF00035338?LI=true`.

G. A. Slafer and R. Savin. Postanthesis green area duration in a semidwarf and a standard-height wheat cultivar as affected by sink strength. *Australian Journal of Agricultural Research*, 1994a. doi: 10.1071/AR9941337 .

G. A. Slafer and R. Savin. Source-sink relationships and grain mass at different positions within the spike in wheat. *Field Crops Research*, 37:39–49, 1994b. doi: 10.1016/0378-4290(94)90080-9 .

G. A. Slafer, R. Savin, and V. O. Sadras. Coarse and fine regulation of wheat yield components in response to genotype and environment. *Field Crops Research*, 157(0): 71–83, 2014. ISSN 0378-4290. doi: 10.1016/j.fcr.2013.12.004 .

O. A. Somasco, C. O. Qualset, and D. G. Gilchrist. Single-gene resistance to Septoria tritici blotch in the spring wheat cultivar 'Tadinia'. *Plant Breeding*, 115(4):261–267, 1996. ISSN 1439-0523. doi: 10.1111/j.1439-0523.1996.tb00914.x .

G. Spano, N. Di Fonzo, C. Perrotta, C. Platani, G. Ronga, D. W. Lawlor, J. A. Napier, and P. R. Shewry. Physiological characterization of 'stay green' mutants in durum wheat. *Journal of Experimental Botany*, 54(386):1415–1420, 2003. doi: 10.1093/jxb/erg150 .

J. Spiertz and N. Devos. Agronomical and physiological-aspects of the role of nitrogen in yield formation of cereals. *Plant and soil*, 75(3):379–391, 1983. ISSN 0032-079X. doi: 10.1007/BF02369972 .

G. Steinberg. Cell biology of Zymoseptoria tritici: Pathogen cell organization and wheat infection. *Fungal Genetics and Biology*, 79:17–23, 2015. ISSN 1087-1845. doi: 10.1016/j.fgb.2015.04.002 .

S. M. Tabib Ghaffary, J. D. Faris, T. L. Friesen, R. G. F. Visser, T. A. J. van der Lee, O. Robert, and G. H. J. Kema. New broad-spectrum resistance to Septoria tritici blotch derived from synthetic hexaploid wheat. *Theoretical and Applied Genetics*, 124(1):125–142, Jan 2012. ISSN 1432-2242. doi: 10.1007/s00122-011-1692-7 .

E. A. Tambussi, J. Bort, J. Jose Guiamet, S. Nogues, and J. Luis Araus. The photosynthetic role of ears in C3 cereals: Metabolism, water use efficiency and contribution to grain yield. *Critical reviews in plant sciences*, 26(1):1–16, 2007. ISSN 0735-2689. doi: 10.1080/07352680601147901 .

H. Thomas and L. de Villiers. Gene expression in leaves of Arabidopsis thaliana induced to senesce by nutrient deprivation. *Journal of Experimental Botany*, 47(12):1845–1852, 1996. doi: 10.1093/jxb/47.12.1845 .

H. Thomas and C. J. Howarth. Five ways to stay green. *Journal of Experimental Botany*, 51 (S1):329–337, Feb 2000. ISSN 0022-0957. doi: 10.1093/jexbot/51.suppl_1.329 .

D. K. Tompkins, D. B. Fowler, and A. T. Wright. Influence of agronomic practices on canopy microclimate and Septoria development in no-till winter wheat produced in the Parkland region of Saskatchewan. *Canadian Journal of Plant Science*, 73(1):331–344, 1993. doi: 10.4141/cjps93-050 .

S. F. F. Torriani, J. P. E. Melichar, C. Mills, N. Pain, H. Sierotzki, and M. Courbot. Zymoseptoria tritici: A major threat to wheat production, integrated approaches to control. *Fungal Genetics and Biology*, 79:8–12, 2015. ISSN 1087-1845. doi: 10.1016/j.fgb.2015.04.010 .

D. A. Vansanford and C. T. MacKown. Cultivar differences in nitrogen remobilization during grain fill in soft red winter-wheat. *Crop science*, 27(2):295–300, MAr-Apr 1987. ISSN 0011-183X. doi: 10.2135/cropsci1987.0011183X002700020035x .

P. M. Vitousek. Beyond global warming: ecology and global change. *Ecology*, 75(7): 1861–1876, 1994. doi: 10.2307/1941591 .

L. Weaver and R. Amasino. Senescence is induced in individually darkened Arabidopsis leaves, but inhibited in whole darkened plants. *Plant Physiology*, 127:876–886, 2001. doi: 10.1104/pp.010312 .

R. E. Wilson. Inheritance of resistance to Septoria tritici in wheat. In *Septoria of Cereals*, 1985.

A. Wingler, S. Purdy, J. A. MacLean, and N. Pourtau. The role of sugars in integrating environmental signals during the regulation of leaf senescence. *Journal of Experimental Botany*, 57(2):391–399, Jan. 2006. ISSN 0022-0957, 1460-2431. doi: 10.1093/jxb/eri279 .

J. C. Zadoks, T. T. Chang, and C. F. Konzak. A decimal code for the growth stages of cereals. *Weed Research*, 44:415–421, 1974. doi: 10.1111/j.1365-3180.1974.tb01084.x .

J. Zhan and B. A. McDonald. The interaction among evolutionary forces in the pathogenic fungus Mycosphaerella graminicola. *Fungal Genetics and Biology*, 41(6):590–599, 2004. ISSN 1087-1845. doi: 10.1016/j.fgb.2004.01.006 .

Y.-H. Zhang, N.-N. Sun, J.-P. Hong, Q. Zhang, C. Wang, X. Qing-Wu, Z. Shun-Li, H. Qin, and W. Zhi-Min. Effect of source-sink manipulation on photosynthetic characteristics of flag leaf and the remobilization of dry mass and nitrogen in vegetative organs of wheat. *Journal of integrative agriculture*, 13(8):1680–1690, 2014. ISSN 2095-3119. doi: 10.1016/S2095-3119(13)60665-6 .

O. Ziv and Z. Eyal. Assessment of yield component losses caused in plants of spring wheat cultivars by selected isolates of *Septoria tritici*. *Phytopathology*, 68(5):791–796, 1978. ISSN 0031-949X. URL http://apsnet.org/publications/phytopathology/backissues/Documents/1978Articles/Phyto68n05_791.pdf.

E. Zuckerman, A. Eshel, and Z. Eyal. Physiological aspects related to tolerance of spring wheat cultivars to Septoria tritici blotch. *Phytopathology*, 87(1):60–65, Jan. 1997. ISSN 0031-949X. URL http://apsjournals.apsnet.org/doi/pdf/10.1094/PHYTO.1997.87.1.60.

Chapter 2

Materials and methods

2.1 Introduction

The PhD project relied on four studies (Table 2.1). The first consisted of a data mining method applied to existing data, collected from an experimental network run in France from 2006 to 2008. The dataset consisted of a subset of nine independent trials and six to nine wheat cultivars. The data analysis constituted a preliminary step to explore the genotype traits and environmental variables which can affect wheat tolerance of Septoria tritici blotch (STB), following the results highlighted by Bancal et al. (2015). The exploratory method aimed at widening the range of hypotheses to be studied in the next experiments.

The first field experiment in 2014-15 in Herefordshire focused on applying source or sink manipulations to focus on the link between STB tolerance and source/sink ratio. A glasshouse experiment was carried out in 2014-15 at the UMR ECOSYS (INRA, AgroParisTech, Grignon) and aimed at identifying more accurately physiological variations linked to STB tolerance, especially related to the nitrogen metabolism. The field experiment and the glasshouse experiment shared four common wheat doubled-haploid genotypes (C×L 14B, C×L 7A, LSP2×R 16, LSP2×R 127) and formed therefore a cross repetition/validation of observed trait behaviours. Finally, based on six commercial UK cultivars, a second field experiment was implemented in 2015-16 at the University of Nottingham farm (Leicestershire) to provide additional independent data to evaluate both hypotheses and results on STB tolerance and associated traits highlighted previously.

The methods used in the data mining task and the experimental design specifically applied in the glasshouse and field experiments are described within the respective chapters including a summary of the study design. However, the whole project relies on common methods to provide information and quantification including, but not limited to, the STB tolerance, the source/sink ratio, and the dry matter and nitrogen partitioning during the grain filling period. These methodologies are presented within the present chapter.

Table 2.1: Summary of the experiments and studies.

Experiment	Dimension	Wheat	Nitrogen	Disease	Spikelet removal
Database French network	5 locations 2 years 1/ 2006-07 2/ 2007-08 2 to 3 reps per trial	9 cultivars: Apache Charger Dinosor Koreli Paledor Rosario Royssac Sogood Toisondor	1 level: best local practices	1 level: STB-prevention (fungicide)	
Field 2014-15 Herefordshire UK	Split-split-plot 48 treatments 3 reps	6 genotypes: Cadenza x Lynx 14B CxL 7A CxL 5H LSP2 x Rialto 127 LSP2xR 20 LSP2xR 16	2 levels: additional N at heading VS Control	2 levels: STB-prevention (fungicide) VS Control	2 levels: 50% Spikelet removal VS Control
Glasshouse 2014-15 UMR Ecosys Grignon France	16 treatments 1 rep (3 sub samples)	4 genotypes: CxL 14B CxL 7A LSP2xR 16 LSP2xR 127	2 levels: Stop N nutrition at Heading VS Control	2 levels: Inoculation VS Control	
Field 2015-16 Uni. of Nottingham Leicesteshire UK	Randomised blocks 12 treatments 4 reps	6 cultivars: Sacramento Dickens Evolution Zulu Cougar Cashel		2 levels: STB-prevention (fungicide) VS Control	

2.2 Overview of the study methods

An overview of the methods used during the PhD is provided hereafter. The full details of the methods and references are provided later in corresponding chapters.

2.2.1 Data mining

Bancal et al. (2015) highlighted the senescence kinetics and the grain weight as potential STB tolerance traits. The data mining study aimed at identifying potential levers explaining these traits. Besides, based on multiple environments and genotypes, it was possible to quantify the source of variability for the traits: the genotype, the environment or the interaction. The data used were the dataset referred as "Expe.C" by Bancal et al. (2015) which included nine genotypes and two years in five locations in Northern France, focusing on treated plots. In addition to agronomic and physiologic variables, the climate description included global radiation, water balance and temperatures calculated for window panes estimated at multiple dates from the onset of the stem elongation to the end of the grain filling. The strategy for the data analysis relied on i) Random Forest models (Breiman, 2001) to classify and identify important variables, ii) multiple regression models to understand the nature of the relation with key variables, and iii) analysis of variance components to understand the levels of variation due to E, G or G×E.

2.2.2 Field experiment 2014-15

This experiment studied six genotypes (LSP2×R 127, LSP2×R 16, LSP2×R 20, C×L 14B, C×L 7A, C×L 5H) including the four studied in the glasshouse experiment in France. The six genotypes were derived from two doubled-haploid populations. The first was derived from a cross between the UK winter wheat Rialto and the Mexican CIMMYT spring wheat LSP2 of large ear-phenotype and the second from a cross between the UK spring wheat Cadenza and UK winter wheat Lynx (C×L), the target being to obtain a wide range of phenotypes to study disease tolerance. They were sown on 28 October 2014, at a density of 350 seeds $\cdot$ m^{-2}. Growth analysis was carried out from anthesis to maturity. The initial hypothesis was that the source/sink balance affects STB tolerance. To extend source/sink contrast the field experiment included an additional late nitrogen application around heading (40 kg N $\cdot$ ha^{-1}) to maintain longer post-anthesis nitrogen uptake, delay N remobilisation and senescence, and increase carbon assimilation during the grain filling period. Also, a 50% ear trimming physical treatment was applied by cutting and removing the top half of the ear at 250 °Cd after anthesis (Growth Stage, GS61, Zadoks et al., 1974) to reduce the grain sink size, and maximize the individual grain size. For a further description of the experimental design and methods, refer to Chapter 4.2 (page 107).

2.2.3 Glasshouse experiment 2014-15

Wheat plants were cultivated in pots (PVC, 7.5 cm diameter, 35 cm depth) arranged closely to obtain a field-like canopy and were grown in controlled conditions with or without nitrogen deficiency by stopping fertilisation at the heading stage. The experiment was carried out at the INRA Grignon and was sown on 16 October 2014. Four contrasting STB tolerance wheat genotypes (two tolerant: LSP2×R 127, C×L 14B; two intolerant: LSP2×R 16, C×L 7A; according to field experiment results: 2011-12 and 2013-14 at ADAS Hereford, 2011-12 at Teagasc, Carlow, Ireland) were inoculated or not at heading stage with *Zymoseptoria tritici* inoculum consisting of mixed strains of inoculum originally isolated on the genotypes (Genotypes and strain mixes provided by the ADAS, from experiments in DEFRA project IF01118). Then plants were assessed by sampling at 200 degree-days (°Cd, base 0 °C) time steps throughout the grain filling period. Plants at each sampling were characterised by their size (dry mass and dimensions of organs, grain number), and their senescence progression (humidity, chlorophyll a and b, proteins by Bradford's method, see Ben Slimane et al., 2013). Nitrogen metabolism in leaf lamina and sheaths was monitored by enzyme activity measurements (nitrate reductase and exoprotease, see Ben Slimane et al., 2013). Monitoring of total nitrogen content per organ made it possible to follow dynamic fluxes toward the grains. The experimental design consisted of semi-hydroponic wheat populations, grown in trays. Selected shoots

of the four genotypes were exposed to a combination of two nitrogen feeding and two inoculation treatments, each sample was composed of three replicates of five plants.

2.2.4 Field experiment 2015-16

The experiment relied on a post-anthesis growth analysis of six UK-grown winter wheat cultivars in a field randomized block experiment at Sutton Bonington (University of Nottingham farm, Leicestershire, UK). The cultivars were sown after a winter oilseed rape on 2 October 2015, at a rate of $325\,\text{seeds} \cdot \text{m}^{-2}$. Two disease control managements were applied to obtain either a full control of STB, or no control of STB while maintaining the non-targeted disease symptoms to low levels. The aim was to provide yield loss data with source sink quantification for validation of the highlighted potential tolerance traits and environmental effect. The cultivars were: Sacramento, Dickens, Evolution, Zulu, Cougar, Cashel. Sacramento is a very early flowering genotype, a two week variation for heading date amongst the six cultivars was observed in previous experiments. Cougar is characterised by a good resistance to STB.

2.3 Selection of genotypes or cultivars

In the data mining study, nine cultivars studied were selected within historical data. The main target was to obtain a balanced data set with comparable cultivar profiles between the 9 sites × seasons experiments. This allowed the study of genotype × environment interaction. The nine cultivars expressed a wide range of heading stage (GS55) date.

In the glasshouse experiment and the field experiment 2014-15, the studied genotypes were part of a large panel derived from two doubled-haploid populations and previously screened for STB tolerance and yield potential. The first population was derived from a cross between UK spring wheat Cadenza and UK winter wheat Lynx (C×L), the second between UK winter wheat Rialto and the Mexican CIMMYT spring wheat LSP2 of large ear-phenotype (LSP2×R); the LSP2×R lines were included in order to obtain a wider range of source/sink phenotypes to study STB tolerance in high yielding genotypes. The previous tolerance estimation results are briefly described in Chapter 4. Four and six genotypes amongst these panels were chosen in the present experiments to represent a wide range of tolerance of STB.

Finally, the last field experiment (2015-16) examined commercial cultivars contrasting for heading date stage. The cultivars were Cashel (KWS UK, first season on Recommended List (RL) 2014-15, bread-making market), Cougar (RAGT seeds UK, RL 2013-14, feed market), Dickens (Secobra France, RL 2013-14, feed market), Evolution (Sejet Denmark, RL 2014-2015, feed market), Zulu (Limagrain UK, RL 2014-15, feed/biscuit

market), Sacramento (RAGT, registration 2014, bread-making market) (HGCA, 2015; RAGT, 2016; AHDB, 2016). They were characterised by a 15 day range for heading date (GS55, Zadoks et al., 1974). Sacramento is not amongst the UK recommendation list but is a proposed cultivar in France.

2.4 Growth analysis

In the three experiments, growth analysis was performed from heading stage to maturity. It relied on samples of fertile (ear-bearing) shoots:

- Glasshouse 2014-15: 4 – 5 sampling dates; sample size: 5 ear-bearing shoots per sample.
- Field 2014-15: 4 sampling dates; sample size: 5 ear-bearing shoots per sample.
- Field 2015-16: 2 sampling dates; sample size: 10 ear-bearing shoots per sample.

1. Ear-bearing shoot selection: between heading and anthesis, ear-bearing shoot were selected and tagged to provide homogeneous material to sample over time. Different methods were applied regarding requirements of each experiment. In the field 2014-15 experiment, average ear length was determined and used ±5% to select the shoots. In the glasshouse 2014-15 experiment, the distance between the first and second ligules of the main stem on all plants was measured. Regarding this measure, lots of 15 plants equivalent in mean and standard deviation were identified. Finally, in the field 2015-16 experiment for each genotype, ear-bearing shoots reaching GS55 on the same day were tagged.
2. Shoot dissection: sampled shoots were then assessed as follows. The three upper leaf laminas (flag leaf to leaf 3) were detached at the ligule. Ears were separated at the ear collar below the lowest spikelet. The stem was cut above the node 3. The two upper stem internodes and leaf sheaths and the peduncle were referred as the stem. Lower internodes and associated organs comprised the base. Post-anthesis ear samples were manually or mechanically threshed, the grains counted (Grain Number per ear-bearing shoot, GNe) and weighed (grain yield per ear-bearing shoot, Ye). Every sample was oven dried for 48 h at 80°C and dry weighed to obtain the dry matter weight (DM). All grain yields and biomass weights in the result chapters are at 100% DM.

Noticeable experiment specificity:

- glasshouse experiment: the leaf sheath was detached from the true stem internodes and considered independently along with the other dissected organs.

- degraining treatment (Field 2014-15), the removed top half of the ear was also sampled and dry weighted to estimate the chaff and grain biomass removed when degraining.

Nitrogen concentration per organ was measured using the Dumas combustion method in the glasshouse experiment and for two genotypes (LSP2×R 16 and LSP2×R 127) at three sampling dates in the field 2014-15 experiment. The nitrogen amount was calculated as $DM \times Nc$.

Variation in DM or N is expected to be under the influence of i) the treatment applied (e.g. spikelet removal, nitrogen nutrition), ii) the sampling date and iii) random variation in the shoot dimensions between different samples (but exposed to the same treatment effects). Unlike i) and ii) corresponding to physiological responses, iii) must be limited (if not avoided). This is first achieved by the constitution of the samples themselves, as described hereafter. The data analysis can also reduce the random variations between samples exposed to the same treatment combination.

Within each treatment combination replicate (each plot in the field experiments), and because the analysis was based mainly on the post-anthesis phase it was assumed that the random shoot size variation between sampling dates was accountable for Grain Number per ear-bearing shoot (GNe) variation. Then, it was considered that the average of Grain Number per ear-bearing shoot (GNe)(t) measured at various sampling date (t) was a good estimator of the GNe of every treatment combination replicate. Further averaging GNe(t) across the replicates of a treatment combination yielded a standard grain number (sGNe) that was used to scale the dry matter or nitrogen amount actually measured at the different sampling dates. Doing so, the comparison of DM or N and fluxes was done on a comparable standard ear size across the replicates and sampling date, minimising random variation due to the shoot variability within samples. For instance, the above-ground dry matter (DMa(t)), associated with a grain count GNe(t) for one replicate at one sampling date t was scaled to the standard sGNe to obtain the standarized sDMa:

$$sDMa = DMa(t) \times \frac{sGNe}{GNe(t)}$$

2.5 The Healthy Area Duration (HAD)

Because bread wheat is a monocarpic species and STB damage occurs lately despite infecting wheat throughout the vegetative phases, the distinction between the vegetative and post-anthesis phases is relevant. Thus, the experiments focused on the grain filling period when tolerance expression occurs. As a consequence, the source quantification was mainly based on Leaf Area Index (LAI) at anthesis (GS61) or heading (GS55) which varies with pre-anthesis growth conditions and on the post heading Healthy Area Duration

(HAD) which is defined here as the area under the curve of the proportion of green leaf lamina area kinetic. The HAD was estimated in three steps: 1) the proportion of green leaf lamina area was assessed several times from GS55 to maturity, 2) then relevant equations were fitted to the kinetics of observations, 3) finally the area under the curve of the proportion of green leaf lamina area was estimated.

2.5.1 Leaf lamina area and green leaf lamina area

Leaf and green leaf area assessment was based on 5 to 8 observations during the post-heading (GS55) period: every week or two-weeks until complete senescence. Two methods were used in the experiments:

1. during the glasshouse experiment, based on destructive samples, individual leaf layers were scanned and an image analysis software (Access©, Bancal et al., 2016) was used to measure the leaf lamina area individually for each top leaf layer, along with the percentage of Green Leaf Lamina Area (%GLA). In young leaves, leaf area was linearly correlated to leaf length. The relation was used to correct data obtained from late samples where lamina shrinkage due to senescence occurred. Finally, the Leaf Lamina Area per ear-bearing shoot (LAe) for each treatment was the average of the LAe measures obtained from heading stage to maturity.

2. based on one post-anthesis destructive sample (GS65 and GS75 respectively for the experiments field 2014-15 and field 2015-2016), the LAe was measured using LiCor 3100 leaf area metre (Licor, NE, USA). The green leaf lamina area was visually estimated as a percentage (%GLA) on samples and *in vivo* during the grain filling period.

The two methods provided an estimation of the leaf lamina area per ear-bearing shoot (LAe), along with the evolution of the percentage of green leaf lamina area (%GLA) for each top leaf layer. The per-layer LAe and %GLA were aggregated to provide information at the shoot level according to the following equations:

$$LAe = \sum_{L=1}^{3} LAe_L$$

$$\%GLA = \frac{\sum_{L=1}^{3} LAe_L \times \%GLA_L}{\sum_{L=1}^{3} LAe_L}$$

with subscript L for the leaf 1 (flag-leaf) to the leaf 3 (or leaf 4 in the case of the data mining study).

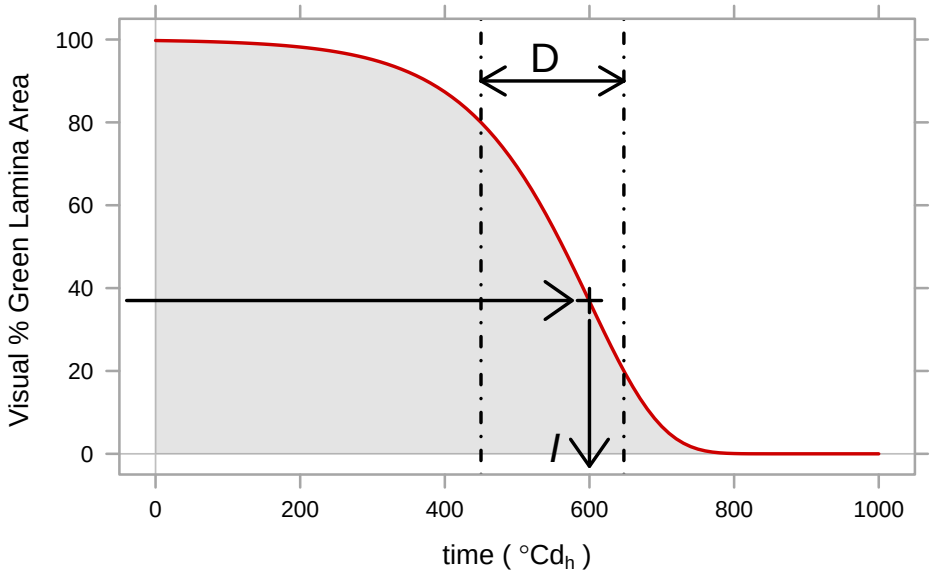


Figure 2.1: Post-anthesis green area kinetics: the Gomptertz's function. The Gompertz's function: percentage of green leaf lamina area evolution from 100% to 0%, regarding the parameters D and I. The area under the curve %GLA is the Healthy Area Duration expressed in $°Cd_H$.

2.5.2 Post-heading green leaf lamina area kinetics

The percentage Green leaf Lamina Area (%GLA) kinetics from heading stage (GS55) to maturity were fitted by Nonlinear Least Squares (R, R Core Team, 2017) to the Gompertz's function (Eq. 2.1, Fig. 2.1).

$$\%GLA(t, K = 100, D, I) = K \cdot \exp\left(-\exp\left(\frac{2 \times (I - t)}{D}\right)\right) \tag{2.1}$$

With: %GLA, the percentage of Green Leaf Lamina Area; t, the thermal time in degree-days (0 °Cd, base temp. 0 °C) since heading stage (GS55, unit $°Cd_H$); K, the maximum %GLA; D, the duration (unit: °Cd); of the senescent phase which was the time from 80%GLA to 20%GLA; I, the inflexion point.

The Gompertz's function (Eq. 2.1, Fig. 2.1) was chosen over the possible logistic function or the monomolecular equation used for instance by Gaju et al. (2011). This methodological choice relies on the parsimonious number of parameters (three parameters, two of which need to be fitted as K is set to 100%) conferring robustness to the estimations regarding the number of observations. Besides, the Gompertz's function is associated with interesting properties:

- asymmetric sigmoid function: the inflexion occurs late, when only 37%GLA remains. It minimises the decreasing-rate phase and is closer to biological observations than

the logistic function (symmetric sigmoid function).

- instead of upper and lower asymptotes the Gompertz's function starts from K (100%) and reaches 0%.

2.5.3 Healthy Area Duration

Healthy Area Duration (HAD) was the area under the %GLA curve between 0 and 1200 °Cd_H, at which point senescence or grain maturity was assumed to be fully completed. The Gompertz's function integration (Eq. 2.2) was computed using the adaptive quadrature implemented in Quadpack routines (Piessens et al., 1983). Fit quality was assessed by Root Mean Square Error of estimation (RMSE) and R^2.

$$HAD = \int_{t=0°Cd_H}^{1200°Cd_H} \%GLA(t, K = 100, D, I) \tag{2.2}$$

2.6 Source / sink ratio and tolerance

Grain source and sink parameters (C or N fluxes, yield components, HAD) were firstly considered at the shoot scale, consistent with the treatments and measurements being applied at the shoot scale inside an undisturbed canopy. The HAD ([green%] °Cd_H) shows the dimension of a time of physiological meaning, along with the intermediate parameters I and D of the senescence kinetics. By itself it is not very relevant for sink/source analysis, and it was was therefore multiplied by the LAe to obtain HADe ([green] $m^2 \cdot °\ Cd_H \cdot shoot^{-1}$): the healthy area duration per ear-bearing shoot. The HADe is a physiological descriptor quantifying the available source for the individual shoot throughout grain filling. Alternatively, it can be interesting to quantify the resource availability per grain. Thus the HADe was divided by GNe to obtain HADg ([green] $dm^2 \cdot °\ Cd_H \cdot grain^{-1}$): the healthy area duration per individual grain. It enabled the quantification of the source, regarding a unit of sink. The final target was the ground area scale as the ear population density affects the individual plant parameters through competition for the resources. The HADe was therefore multiplied by the $ears \cdot m^{-2}$ to obtain the HADm ([green] $m^2 \cdot °\ Cd_H \cdot m^{-2}$): the healthy area duration per square metre.

The tolerance is classically quantified by the ratio of yield loss (Ym) to HADm loss (Parker et al., 2004). Actually, the linear slope obtained expresses rather intolerance than tolerance: high values refer to high intolerance while low values refer to low intolerance (equivalent to tolerance).

As already used so far, the indexes "e", "g" and "m" refer to these three main scales, respectively: per ear-bearing shoot, per grain and per ground metre square. The conver-

sions to the grain or metre square scale rely on the variables GNe and EN: the quality of GNe and EN estimations therefore affects directly the source and source/sink ratio estimation.

References

AHDB. Ahdb Recommended List - winter wheat 2016/17. tables, 2016. URL https://cereals.ahdb.org.uk/media/883980/1-RLDL_2016-17_Winter_Wheat_RL-V6.pdf.

M.-O. Bancal, R. B. Slimane, and P. Bancal. Zymoseptoria tritici development induces local senescence in wheat leaves, without affecting their monocarpic senescence under two contrasted nitrogen nutrition. *Environmental and Experimental Botany*, 132:154–162, 2016. doi: 10.1016/j.envexpbot.2016.09.002 .

P. Bancal, M.-O. Bancal, F. Collin, and D. Gouache. Identifying traits leading to tolerance of wheat to Septoria tritici blotch. *Field Crops Research*, 180:176–185, 2015. doi: 10.1016/j.fcr.2015.05.006 .

R. Ben Slimane , P. Bancal, and M. Bancal. Down-regulation by stems and sheaths of grain filling with mobilized nitrogen in wheat. *Field Crops Research*, 140(0):59 – 68, 2013. ISSN 0378-4290. doi: 10.1016/j.fcr.2012.10.006 .

L. Breiman. Random forests. *Machine Learning*, 45(1):5–32, 2001. ISSN 1573-0565. doi: 10.1023/A:1010933404324 .

O. Gaju, V. Allard, P. Martre, J. W. Snape, E. Heumez, J. LeGouis, D. Moreau, M. Bogard, S. Griffiths, S. Orford, S. Hubbart, and M. J. Foulkes. Identification of traits to improve the nitrogen-use efficiency of wheat genotypes. *Field Crops Research*, 123(2):139 – 152, 2011. ISSN 0378-4290. doi: 10.1016/j.fcr.2011.05.010 .

HGCA. HGCA recommended list - winter wheat 2015/16. tables, 2015. URL https://cereals.ahdb.org.uk/media/537620/winter-wheat-2015-16.pdf. Accessed 2017-07-04.

S. R. Parker, S. Welham, N. Paveley, J. M. Foulkes, and R. K. Scott. Tolerance of Septoria leaf blotch in winter wheat. *Plant Pathology*, 53(1):1–10, 2004. doi: 10.1111/j.1365-3059.2004.00951.x .

R. Piessens, E. de Doncker-Kapenga, C. Uberhuber, and D. Kahaner. *Quadpack: a Subroutine Package for Automatic Integration*, springer verlag edition, 1983. ISBN: 978-3540125531.

R Core Team. *R: A Language and Environment for Statistical Computing*. R Foundation for Statistical Computing, Vienna, Austria, 2017. URL https://www.R-project.org/.

RAGT. Blé tendre d'hiver. Leaflet, 2016. URL http://www.ragtsemences.com/rs/pdf_fr/bth. accessed 2017-07-04.

J. C. Zadoks, T. T. Chang, and C. F. Konzak. A decimal code for the growth stages of cereals. *Weed Research*, 44:415–421, 1974. doi: 10.1111/j.1365-3180.1974.tb01084.x .

Chapter 3

Genotype and environment effect on senescence and grain weight

This chapter has been the subject of two posters which were presented at:

- *the 9th International Symposium on Septoria Diseases of Cereals, 7–9 April 2016, Paris, France, (Collin et al., 2016b).*
- *the 14th Congress of the European Society for Agronomy, 5–9 September 2016, Edinburgh, Scotland (Collin et al., 2016a).*

3.1 Introduction

- **Broad context**

The tolerance of winter wheat crops (*Triticum aestivum* L.) is defined as the ability of a crop to maintain the grain yield in presence of the expressed disease (Ney et al., 2013). The Septoria tritici blotch (STB) is a major threat of the grain yield of wheat in Europe (Cools and Fraaije, 2013; Fones and Gurr, 2015), also described as the most damaging foliar disease, for instance in the UK, where yield loss ranging 30-50% has been reported AHDB (2016). The fungicide-based strategy (Cheval et al., 2017; Fraaije et al., 2012) or the discovery of resistance genes in wheat (Fones and Gurr, 2015; AHDB, 2016) are prone to circumvention by the pathogen. At the same time, economic, environmental and sociological contexts demand the reduced use of inputs on wheat crops in Europe. Therefore, STB tolerance could be a relevant complementary approach to be studied to protect the grain yield.

- **Potential STB tolerance traits: senescence timing and TGW**

Recent study showed the tolerance of winter wheat crops to Septoria tritici blotch (STB) could be linked to monocarpic senescence parameters and yield components (Ban-

cal et al., 2015). Indeed, using the results of several experiments in France, conducted over two years for numerous cultivars, Bancal et al. (2015) linked physiological traits of non-diseased field crops to grain yield loss, considering the variable disease pressure within experiments. They proposed a multiple regression which suggested a linear relation of reduced yield loss with several variables, including: i) later senescence timing and ii) lower grain weight. More precisely, the model Bancal et al. (2015) specified that large leaf lamina area at heading could increase yield loss, while a delayed senescence increased the healthy area duration (the area under the green leaf lamina kinetic) without impairing wheat STB tolerance. For a given grain number, both leaf lamina area and senescence timing are expected to increase the grain source availability, which is believed to increase tolerance. However, the leaf lamina area may also modify the STB severity as epidemics are accelerated by dense canopies (Lovell et al., 1997). Conversely the later senescence timing is not expected to alter the STB environment which might explain the results of Bancal et al. (2015). The effect of TGW is not well understood but appeared strongly related to the yield loss. As they reported, TGW was previously linked to tolerance in the literature and further study about this trait is needed. Therefore, the senescence timing and the grain weight are candidate tolerance traits in this study.

- **The senescence function**

Senescence is an evolutionary strategy which improves nutrient economy by remobilisation for organ growth (Taiz and Zeiger, 2014). Within monocarpic species, and especially for wheat, sequential senescence is first observed for juvenile shoots: upper leaf growth is balanced by lower and older leaf senescence. Monocarpic senescence happens after heading, then senescence and ongoing remobilisation are coordinated with seed growth during grain filling period. Leaf senescence is visually characterised by the chlorophyll degradation but it may happen earlier and rely firstly on non-visible biochemical reactions leading to transdifferentiation of cells (Gregersen et al., 2013). Indeed, senescence is not a cell decay, it is a modification of cell functions for remobilisation. At first, senescence can be reversed and a yellowing leaf can become green again, until a certain limit when reversion is no longer possible, and the leaf dies (Gregersen et al., 2013).

- **Senescence: genotype response**

Senescence is a highly regulated response. Internal factors such as phyto-hormones, nutritional status and the phase transitions (e.g. vegetative to reproductive phase) initiate senescence. These factors are the inputs for signal pathways (ROS-species, receptor protein kinases, MAPK cascades, hormone signaling) which activate or repress transcription factors along with epigenetic regulation and small RNAs. Many genes are coding

for NAC and WRKY (Wingler et al., 2006) transcription factors involved in senescence signalling pathways whose end products are the senescence associated proteins directly promoting the onset of leaf senescence (Taiz and Zeiger, 2014). See Taiz and Zeiger (2014) for further description of the senescence regulatory network.

Given that brief description, senescence is a genotype response. This justifies the research for stay-green genotypes of wheat, which show extended green leaf life. According to the genetic modification involved, stay-green is sometimes referred to as "cosmetic" when not associated with maintained carbon assimilation, while other stay-green genotypes are associated with maintained photosynthesis which is expected to improve the yield. A major example is the repression of the NAM alleles expression associated with delayed senescence in the hexaploid bread wheat (*Triticum turgidum* ssp. *aestivum*) (Uauy et al., 2006). However, the yield increase expected of stay-green phenotype is more easily observed under stress conditions such as a drought which affect the source potential, when the grain growth may be limited by photosynthetic capacity rather than the grain capacity for carbon storage. Therefore, the effect of the genotype might not be equally expressed in all environments.

- **Senescence: environmental response**

It is suggested that senescence is also under environment control. Senescence is responsive to external factors that trigger senescence signaling. Light intensity (Noodén et al., 1996) and quality (Rousseaux et al., 1996; Causin et al., 2006), shading (Weaver and Amasino, 2001) nutrient and water availability (Ono et al., 1996; Thomas and de Villiers, 1996; Crafts-Brandner et al., 1998) were shown to be triggering the senescence. These external factors depend on the surrounding environment and make the senescence a highly plastic trait (Wingler et al., 2006). These environmental conditions, sometimes abiotic stress, are considered as funneled into a "classical" senescence pathway. It is not so clear for the biotic stress. The environment can therefore influence senescence expression, and the relation between surrounding environmental factors and genetic-dependent responses describes the high effect of Genotype Environment Interaction (G×E).

- **Problem: quantitative response of the senescence**

If the response between factors and "stress-induced" senescence is qualitatively partially described, the understanding of quantitative effects of G×E on leaf senescence is sparse. For example, if it is well known that water stress can trigger senescence, the rainfall regimen and stage effects on leaf senescence timing has not been well explored. As a second example, if leaf shading is affecting hormone distribution and then senescence, the effect of canopy density on senescence onset has not been quantified either. The aim of this study is to identify the main environmental effects and genotype traits which could

improve the prediction of senescence onset, thereby facilitating a better management of senescence during grain filling.

- **E, G, G×E as random effects.**

Because the environment (E) influences senescence, and differences between genotypes exist (G), and the genotype expression depends on environment (and reciprocally, the senescence observed in an environment may vary with the genotype, interaction G×E), a quantitative study of senescence may ideally involve a range of E and G that can be used to increase the range of phenotypes. Still considering a quantitative study, the main interest lies in the values that characterise the environment, or the variable(s) describing the genotypes, but the names of the genotype or the environment is of less interest. In other words, E and G are interesting for the range of variable values they can produce. In this sense, E, G and G×E are random effects that may randomly influence the link between the senescence and any explanatory variable.

- **Rationale**

The senescence timing and the Thousand Grain Weight (TGW) are potential STB-tolerance traits of wheat (Bancal et al., 2015). Given this association, it is hypothesised that if factors influencing the senescence timing or TGW were identified, they could also influence STB-tolerance.

However, in the crop conditions, the variations of senescence and TGW with genotype (G effect) are not well understood; especially, the results of a given experiment are generally difficult to extrapolate straightforwardly to others. It is presently assumed the main reasons are, on the one hand, that the environmental variation results in numerous phenotypes of senescence or TGW per genotype (E effect) and, on the other hand, that genotypes do not all respond similarly to one environment (G×E, Genotype Environment Interaction). It is presently supposed the mixture of E, G and G×E sources of variation explain the difficulty in understanding the factors which have an effect on senescence and TGW.

To address this difficulty and identify potential STB-tolerance traits — linked to the monocarpic senescence kinetics and the grain weight — this study relied on an appropriate data mining strategy applied on an appropriate dataset. The dataset, composed of nine winter-wheat cultivars and nine environments (almost balanced), made possible the study between response variables and explanatory variables, with a wide range of variations. The complex variations between environments or cultivars or their interaction made the dataset potentially very informative, but also more difficult to analyse. Thus, successive steps are proposed to:

1. Identify and order, without *a priori*, crop traits and environmental variables that may explain the senescence timing and TGW.

2. Establish the most parsimonious linear models that can estimate the senescence timing and TGW.

3. Then, these models are further applied to quantify the proportion of variance of the variables themselves, and of the model residuals, that the random effects E, G and G×E explain.

4. Finally, the study examined whether this approach resulted in traits or variables that can be verified on an independent data set.

3.2 Materials and methods

3.2.1 Dataset, response and explanatory variables

Observations came from a well balanced dataset, that is referenced as "Exp. C" in Bancal et al. (2015). In the present chapter, cultivar (G effect, for Genotype) and environment (E effect), as well as G×E effect on the determinism of the senescence timing and the Thousand Grain Weight (TGW) were characterized by both qualitative and quantitative variables.

3.2.1.1 E, G and G×E

Environment (E) was qualitatively characterised through nine site-seasons composed of two years in five locations (Fig. 3.1): Cesseville (department 51), 49.08 °N 1.02 °E; Plelo (department 22), 48.53 °N 2.85 °W; Cuperly (department 18), 48.95 °N 4.42 °E; Villiers le Bâcles (department 91), 48.73 °N 2.10 °E; only 1 year in Le Subdray (department 27), 47.07 °N 2.37 °E.

Although crops were always grown under non-limiting nitrogen fertilisation conditions, agricultural practices (dates and dose of inputs) differed from site to site but corresponded to optimal local practices. These variables were not explicitly taken into account to characterize E and were therefore included in the random environmental effect. Environment was also quantitatively characterised by the corresponding climatic data of average temperatures (T, unit: °C), water balance (W, i.e. precipitation minus evapotranspiration, unit: mm) and daily incoming radiation (R, unit: $J \cdot cm^{-2}$). The environments were chosen amongst the available experimental stations of Arvalis — Institut du végétal, located in the North of France following an East-West axis so as to be representative of the main French wheat-growing regions.

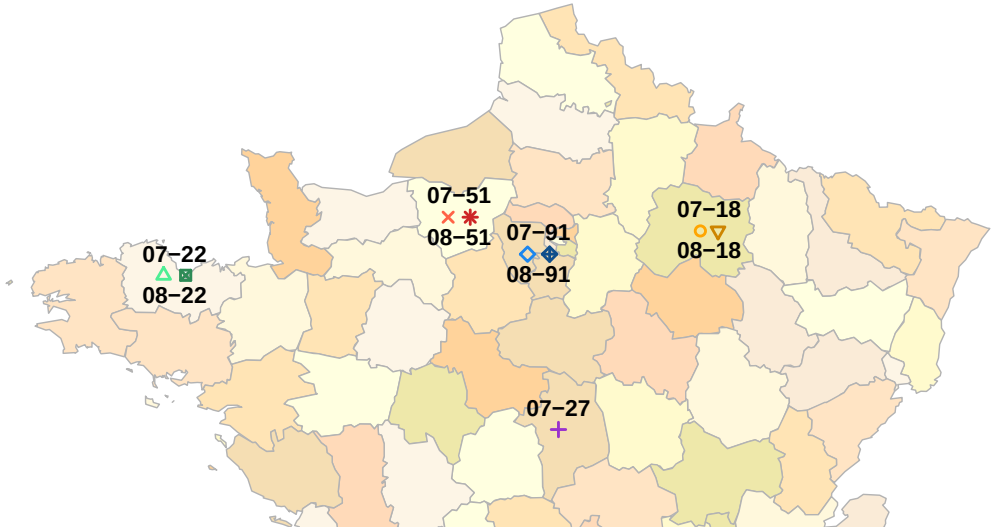


Figure 3.1: Localisation of the experiments. The numeric code associated with each site-season was composed of the year of harvest and the French department (e.g. 07-22 was the experiment harvested in 2007 in Plelo, department 22).

Genotype effect (G) was qualitatively characterized by nine winter-wheat cultivars (cv. Apache, Charger, Dinosor, Paledor, Royssac, Toisondor, Koreli, Rosario, Sogood). According to the Comité Technique Permanent de la Sélection des plantes cultivées (CTPS, permanent technical committee for plant breeding) benchmark, they were characterised by heading stage ranging from "very early" to "late". The three cultivars Koreli, Sogood and Rosario, only grown in the experiments in Villier le Bâcles (91), were "very late heading stage" types. In addition, they were characterised by variation in STB resistance and in the potential grain weight (see Appendix of Bancal et al., 2015).

The G×E was characterized by both agronomic traits and date of growth stages. Heading stage (GS55, Zadoks et al., 1974) and maturity (GS89) were precisely assessed for each cultivar within an experiment by visiting plots 3 to 4 times a week when close to GS55. During the grain filling phase, visual estimations of % green leaf lamina area per leaf layer were performed to estimate the individual senescence kinetics from leaf 1 (flag leaf) to leaf 4. As described by Bancal et al. (2015), the fertile Ear Number per m^2 (ENm) was estimated around grain maturity by counting three times the number of ears over two rows along 1 m in each plot. Other yield components were assessed at maturity. The experimental plots were combine harvested at the end the season to measure the crop grain yield (Ym, $g \cdot m^{-2}$) and the Thousand Grain Weight (TGW, g). Then, the Grain Number per m^2 (GNm) and per ear (GNe), were calculated using ENm, Ym and TGW.

3.2.1.2 The response variables: the senescence timing and the Thousand Grain Weight (TGW)

The response variables to be explained in this study were the senescence timing of the four upper leaf laminae together (canopy, I) or per leaf layer (from flag leaf, i.e. leaf 1 to leaf 4, respectively $I1$ to $I4$) and the Thousand Grain Weight (TGW) at maturity.

Senescence timing of the canopy was quantified by the inflexion point of the green fraction kinetics (parameter I, Eq. 3.1, Bancal et al. 2015) from heading stage (GS55) to maturity. Senescence timing applied either at the canopy level (I) or for each leaf layer ($I1$ to $I4$). The decline of green area fraction was fitted to a sigmoid curve defined by a Gompertz's function (Eq. 3.1, Fig. 3.2) in each individual plot. Generally, three replicates of I were computed for each G×E combination. Therefore, the study worked with 162 individual estimations of I (and corresponding $I1$ to $I4$).

$$fGLA(t,K,D,I) = K \cdot \exp\left(-\exp\left(\frac{2\times(I-t)}{D}\right)\right) \tag{3.1}$$

With: fGLA, green fraction of leaf lamina area (%); t, thermal time since heading stage (unit °Cd_H: degree-days since heading stage, base temp. 0 °C); K, left asymptote set to 1; D, the duration of rapid senescence (approximately between 80% and 20% fGLA, unit °Cd_H: degree-days base temp. 0 °C); I, the inflexion point of the kinetic which happens when 37% of the lamina area at heading is remaining green, indicating the senescence timing (unit °Cd_H).

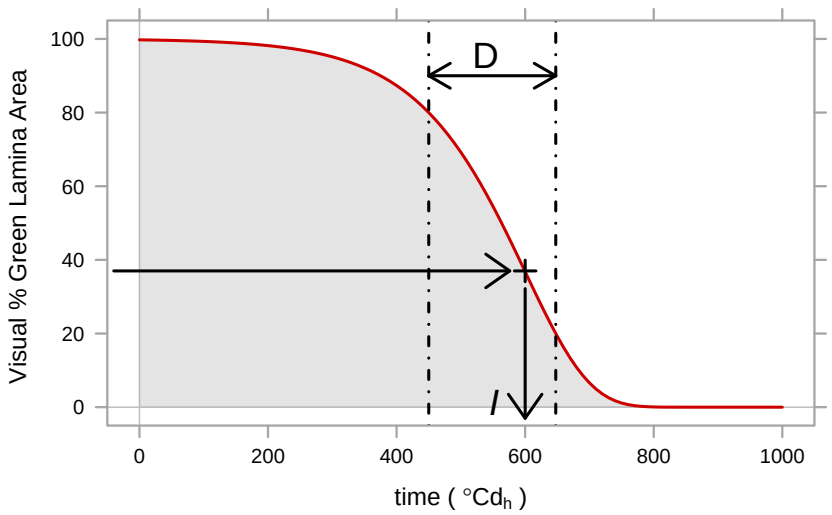


Figure 3.2: The Gompertz's function. Percentage of green leaf area evolution from 100% to 0%, regarding the parameters D and I. The area under the curve %GLA is the Healthy Area Duration expressed in thermal time from heading (°Cd_H).

The grain weight was measured. However, unlike the senescence timing (I), the block

values were not available, thus each G×E combination was associated with a unique TGW value, totalling 60 estimations of TGW.

3.2.1.3 Explanatory variables

Three kinds of explanatory variables were included in this study. Firstly, every agronomic trait recorded in Bancal et al. (2015) was accounted for. The Leaf Lamina Area per ear-bearing shoot (LAe, unit $cm^2 \cdot shoot^{-1}$) was assessed at heading stage (GS55) from 10 average shoots (in this study, *shoot* stands for individual ear-bearing shoot) per plot by measurement of length × width multiplied by a shape parameter of value 0.72. When multiplied by the number of fertile ears per m^2 (ENm), also measured in each plot, it provided an approximation of the Leaf Area Index (LAI, unit leaf lamina m^2 per ground m^2 also sometimes reported without unit). Both LAe and LAI were obtained for the canopy as well as for each leaf layer (leaf 1 to leaf 4, e.g. LAe referred to the total of the four upper leaf laminae and e.g. LAe 2 was the leaf lamina area of the leaf 2). Besides, the fraction of the canopy leaf lamina that each leaf layer represented was also estimated (e.g. fLA 1 for the fraction that the flag leaf represents). In addition to the ENm, the sink was simply described by the grain number per ear or per m^2 (GNe and GNm). Fertilisation was not taken into account as the dataset included only well fertilised crops.

The second kind of explanatory variable was the corresponding date of a set of phenological stages (a single date per G×E combination). The beginning of stem elongation (GS30) and the heading stage (GS55) dates were recorded from observations. Dates of leaf senescence onset stages (leaf 1 to leaf 4) were estimated using the model adapted by Gouache et al. (2013), with an expected accuracy of ±2 days for leaf 1 and leaf 2 (Gouache, 2009). Heading dates were expressed by their time difference (in days) to the median heading-date within the complete dataset: the 12 May of current year.

Lastly, the third kind of explanatory variable was computed from meteorological records. Climatic variables were computed over a 15-day window every 10 days starting from -66 days before to +9 days after heading stage (GS55) to cover the full range of duration between GS30 and GS55 when attempting to explain the senescence timings. The time window pane selected appears reasonable instead of a daily shift as doing so would increase considerably the number of highly correlated variables. To explain TGW, climatic variables were also computed over the grain filling period until +69 days after heading date. Later in the present chapter, every climatic variable was reported as follows: T, R or W (indicating the temperatures, incoming radiation or water balance) was followed by a number indicating the start date of the estimation, followed by an index which specified the reference date (H, for heading stage date; L1 to L4 for the leaf 1 to leaf 4 onset stage date), and followed by an exponent specifying the window-span dura-

tion: e.g. $W46_H^{s15}$ indicates a 15-day water balance which estimation started 46 days before heading stage.

3.2.2 Statistical analysis

3.2.2.1 Classification of explanatory variables by Random Forest models

The large number of variables, relative to the number of observations, and the large number of correlated variables make the research for an estimation model of I or TGW challenging. Based on these numerous variables, the first addressed question was: Without *a priori*, which are the important explanatory variables? In order to classify the variables regarding their relevance to explaining the senescence timing I (canopy and individual leaf layers) or the TGW, the data were first analysed with a machine-learning method based on classification trees: the Random Forest (RF, Breiman 2001). The Random Forest (RF) models are well suited to address variable classification questions, to face the dimension problems, and to cope with numerous correlated explanatory variables. Besides, the RF models are very easy to apply, without specific constraints other than the computing capacity, or distribution assumptions, and neither are they restricted to linear relationship. In addition, the output of the RF models was used for variable ranking regarding an evaluation of the importance of each variable. The method itself and its application are well documented, a brief description is presented hereafter (Breiman, 2001; Liaw and Wiener 2002).

- **Principle of the Random Forest models**

Unlike choosing the single best regression tree to explain a response variable, the RF regards together numerous trees (the forest). Each individual tree is computed from two random selections. Firstly, each tree is based on a different random selection of two thirds of the observations (Liaw and Wiener, 2002). Secondly, within each tree, every single binary split that the tree is composed of is based on a different random subset of one third of the variables (Liaw and Wiener, 2002); the best explanatory variable within the random subset of variables determines the binary split. These two random components enable the calculation of thousands of unique trees based on a single dataset, the sum of which increases the quality of estimations accordingly to the probability theory of the "Law of large numbers". These multiple trees and the two random components (on observations and on variables) justify the names of the method: Random Forest.

After the RF model has been fitted, the estimation of an observation is given by the averaged predictions across all the trees that compose the forest. During the computation, each individual tree that the Random Forest is composed of is tested using the spare data that was not used to compute it (i.e. a third of the observations). Therefore, the error

associated with the RF estimations (Mean Square Error, MSE) available for each tree is unbiased and that property extends to the forest estimation.

It should be noted that the whole method as described and its principles and intermediary computations was available as a package for the software R (R, version 3.3.3, R Core Team, 2017; package `randomForest` (version 4.6–12, Liaw and Wiener, 2002). The application of the Random Forest was actually straightforward after setting the parameters which were: the number of trees per forest, the proportion of observations used to build a tree and the number of variables randomly selected to find each individual best split.

The RF models were fitted to identify environmental variables and cultivar traits modifying senescence timings (I, $I1$ to $I4$) or grain weight (TGW). Up to 15 000 trees were computed, though the RF results were stabilized for 3000 trees as more trees did not reduce the MSE. Each model was first checked before being further used. The correlation between observations and predictions was calculated, as well as the root mean square error (RMSE). Additionally, the cultivar or environmental bias was checked by the comparison of observations and predictions (first graphically then confirmed by a student t test).

- **Importance of every explanatory variable**

After evaluation, the Random Forest models were used to estimate the relative importance of each potential explanatory variable. It was expected for the important variables that their absence increased sharply the model prediction error (MSE), or at least resulted in a larger increase of MSE than the absence of a non-decisive variable could cause. Practically, the variable was constantly kept within the model, but its values were randomly permuted. The importance of a variable is then based on the relative increase of the MSE that this operation induced (%IncMSE). The %IncMSEs did not represent absolute values as they were relative to a MSE that depended on the model (e.g. the MSE could vary regarding the variables included in the model, the observations, as well as regarding the settings of the RF model fit, e.g. number of trees). Consequently, the values for a model were not comparable to the values of another model. Within each model, the addition of the %IncMSE was not meaningful as obtained independently for each variable. To put it in a nutshell, the %IncMSE was uniquely used for the variable ranking regarding its relative importance in the RF models.

As the value of %IncMSE relied on random components and settings fixed by the user (e.g. the number of trees, or the number of variables and observations used to grow them) the full operation was run 50 times to test the stability of the results; the %IncMSE of each variable was then given as an average along with its standard deviation.

The advantage of RF models was that they rely on very few assumptions and previously showed good predictions compared to other methods (Genuer et al., 2010; Svetnik et al., 2004; Liaw and Wiener, 2002). Regarding a response variable, it classifies the relative importance of many variables in comparison to the number of observations, and is not restricted to linear relation between variables. However, the output lacks mechanistic interpretability. The classification is useful to justify a set of variables of interest, even though it does not provide information about the nature of the links. That is why the random forest was followed by a multiple regression.

3.2.2.2 Linear model selection

- **Multiple linear regression models**

If RF indicates the important explanatory variables, it does not explain the nature of the relation between response and explanatory variables. Therefore, multiple regression models were fitted. Because there were many explanatory variables, a forward/backward stepwise selection method was used: from an initial model based on the RF model results, variables were added or removed, one-by-one, following a selection criterion.

More specifically, the 12 most important variables designated by the RF models were used as the initial model. Because the RF is not based only on linear relationships, the procedure first removed non-significant variables. Then the stepwise selection was run, testing the addition and depletion of variables, based on the minimisation of the BIC (Bayesian Information Criterion). The BIC is a trade-off between goodness of fit and parameter number as it penalizes the addition of parameters. Besides, the maximum number of variables was restricted (<8), to avoid building very large models, which would be much more complex to interpret, and address concerns about over-parametrisation (n = 162 and n = 60 respectively for I and TGW).

Lastly, after the selection of models, the climatic variables were customized: they were initially computed over 15-day window span at a time referenced to heading date. Alternatively, the model was tentatively improved by referencing time to the closest leaf emergence stage, and by increasing or decreasing the window span considered (based on R^2 and RMSE).

- **Partial regressions**

The following rationale was rewritten from Rakotomalala (2015): once the models were fitted, partial regressions were computed to estimate how much each variable (X_p) explained the final response (Y). The partial regressions in the case of multiple linear regression with p variables (Eq. 3.2) is as follow.

$$Y = \alpha_0 + \alpha_1 \cdot X_1 + \ldots + \alpha_{p-1} \cdot X_{p-1} + \alpha_p \cdot X_p + \varepsilon \tag{3.2}$$

The partial residuals rely on two assumptions relating to the information represented by residuals:

1. The multiple regression model based on the $p-1$ variables is computed (Eq. 3.3). The residual ε_y is the information which is not explained (linearly) by the $p-1$ variables of the model.

$$Y_{(-Xp)} = \delta_0 + \delta_1 \cdot X_1 + ... + \delta_{p-1} \cdot X_{p-1} + \varepsilon_y \tag{3.3}$$

2. The multiple regression model explaining X_p by the $p-1$ variable is also computed (Eq. 3.4) as there can be redundancy between X_p and the $p-1$ other variables. The residual ε_x is the information linearly independent from the other explanatory variables included in the multiple linear regression.

$$X_p = \gamma_0 + \gamma_1 \cdot X_1 + ... + \gamma_{p-1} \cdot X_{p-1} + \varepsilon_x \tag{3.4}$$

The X_p partial-residual regression graphic represents ε_y regarding ε_x. Simple linear regressions link the two residuals: ε_y and ε_x (Eq. 3.5)

$$\hat{\varepsilon_y} = \beta_0 + \beta_1 \times \varepsilon_x + \varepsilon_r \tag{3.5}$$

It should be noted that when taking all data into account, then $beta_0 = 0$ and the estimated slope β_1 is equal to α_p (Eq. 3.2), while choosing data in a single genotype or environment will provide β_0 and β_1 to characterize it.

In addition, with complementary environment or cultivar representations, it was possible to illustrate the E or G random effects within the multiple linear regression models. It addressed the following questions:

- Was the linear relationship comparable between E or G? If not:
  - Was the slope of the relationship comparable between E or G?
  - Did the random effect of E or G affect the slope and/or the intercept?
- What range of values (x- or y- axis) did each of E or G represent?

Based on the partial residuals, the intercepts and slopes (β_0 and β_1) were calculated for each environment or cultivar. The significance of the obtained intercepts and slopes across the environments or cultivars was tested by a t test. If the validity of this approach can be discussed, it was nonetheless preferred over a mixed model multiple linear model. Indeed, the latter requires much *a priori* information about the relationship between the response and each one of the several explanatory variables. Besides, in this case, E or G could sometimes be interpreted as representative of a larger population (as it is expected

from a random effect), but for some variables, the choice of E or G was a means to obtain a specific range of observations. For instance, an extended heading date range was achieved by including early- late-heading cultivars; similarly, the cultivars were expected to express variable grain number or TGW.

3.2.2.3 Random effects: E, G and G×E

Random effect models and variance component analysis (VCA) were run to quantify the contribution of E, G and G×E to the overall observed variability of I, $I1$ to $I4$ and TGW and the selected explanatory variables (Crawley, 2007). The variance of every variable was partitioned into individual terms: σ_E, σ_G, σ_{GxE} and σ, the remainder being the residual (ε). Relative contribution of every random effect was related to the total variance (σ_{total}). For instance, the relative contribution of environment random effect to the observed variability was obtained after the random effect model was fitted by:

$$\begin{aligned} E_{\%} &= \frac{\sigma_E}{\sigma_E + \sigma_G + \sigma_{GxE} + \sigma} \times 100 \\ &= \frac{\sigma_E}{\sigma_{total}} \times 100 \end{aligned}$$

3.2.3 External validation.

The article of Bancal et al. (2015) was based on three datasets, this study relied on "Expe. C" because of its good properties. Nonetheless, the two other datasets detailed in Bancal et al. (2015) (Expe. A and B) were used in an attempt to validate the method starting from the Random Model fits.

The linear models obtained were validated using an independent dataset. It was composed of three locations and two seasons (five environments), including in total 34 cultivars, even though only 24 were cultivated per experiment. Unfortunately, the green area kinetic estimations were available at the shoot scale only and not per leaf layer. However the senescence timing of the canopy (I) could be computed at each scale. The dataset was restricted to the range of the explanatory variables used for the model fits. Then the model predictions were compared to the observed values.

3.2.4 Softwares

Statistical methods were implemented within the R environment (version 3.3.3, R Core Team, 2017). Additional packages included: the packages `DBI` (version 0.3.1, R Special Interest Group on Databases, 2014) and `RPostgreSQL` (version 0.4–1, Conway et al., 2016) for data management and variable computation; Random Forest implemented by

the pacakage `randomForest` (version 4.6–12, Liaw and Wiener, 2002); `lme4` (version 1.1-12, Bates et al., 2015) for mixed model fitting; package `lattice` (version 0.20-34, Sarkar, 2008) and `latticeExtra` (version 0.6-28 Sarkar and Andrews, 2016) for graphics drawing.

In order to avoid confusion between the methods, the target of each statistical tool used is emphasized before reporting the corresponding results.

3.3 Results

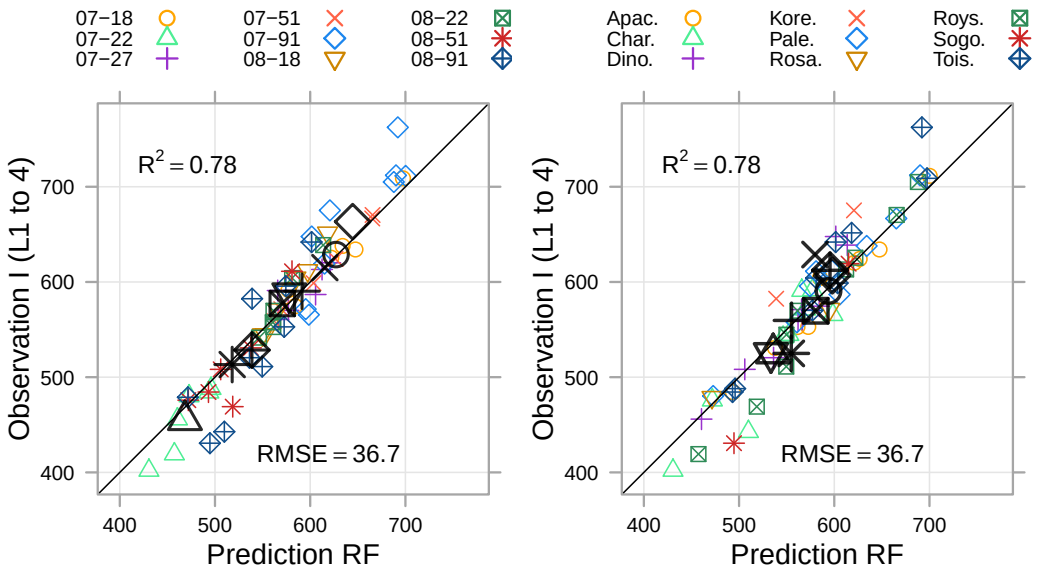
The aim in fitting models was to explain key-response variables involved in the expression of STB-tolerance of wheat using explanatory variables affected by both the cultivars and the environments. The objectives were: first to identify and classify the important explanatory variables, then to estimate relations between response variables and explanatory variables, and finally to quantify the origin and contribution of the environment (E), the cultivar (G) and their interaction (G×E), that the explanatory variables account for. The target response variables were the senescence timings of either the whole canopy (I or individual leaf layers ($I1$, $I2$, $I3$, $I4$) and the TGW.

3.3.1 Identifying the main explanatory variables using Random Forest modeling

Target: because of the large number of potentially important variables and possible correlations between them, the Random Forest models were used to rank the potential explanatory variables and select the most important ones.

3.3.1.1 Fitting the Random Forest models

A first set of 41 variables was considered to explain the senescence timings: 21 climatic variables, 7 agronomic variables (Grain Number per ear or per m^2, GNe or GNm, respectively; Thousand Grain Weight, TGW; fertile-Ear Number per m^2, ENm; heading stage date, GS55; thermal time from GS30 to GS55, equivalent to the stem elongation phase), 13 variables for canopy description (LAe, LAI and fLA). The set of variables to explain the TGW was slightly different as it included in addition 18 post-heading climatic variables and the five senescence timings (I for canopy and individual leaf layers),



(a) Symbols per environment

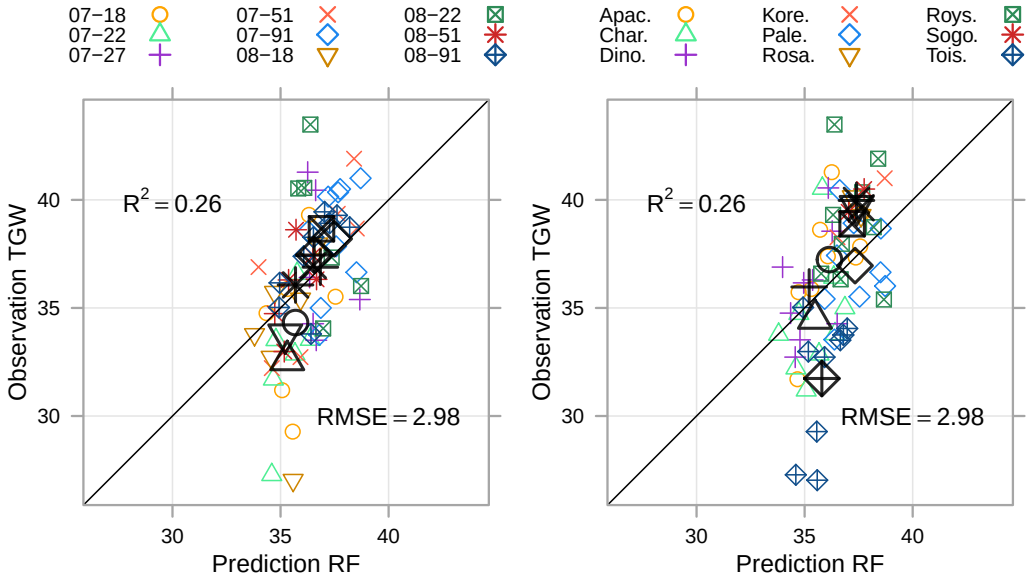
(b) Symbols per cultivar

Figure 3.3: Relationship between observations and random forest predictions of the senescence timing at the canopy level (I), expressed in degree-days since heading stage date (°Cd_H). Symbols stand either for the cultivar or for environment. The coloured symbols are aggregated data, the block repetitions are not shown to lighten the graphics, thus each point is a G×E combination. Although, the R^2 and RMSE were computed on the complete dataset, including repetitions (n = 162). The black symbols are cultivar or environment averages.

totalling 63 variables.

The obtained Random Forest (RF) models were good. For instance, Figures 3.3a and 3.3b plot predictions of I against corresponding observations. Both figures show the very same data, but the symbols represent either the environments (Fig. 3.3a) or the cultivars (Fig. 3.3b). Therefore, considering the Figure 3.3a, the small symbols represented each cultivar within an environment (colours and symbols) while the large black symbols were the average of cultivars for an environment. The R^2 = 0.78 and the RMSE of 36.7 °Cd_H (6.2% of average I) showed the good fit between observations and predictions. Moreover Figure 3.3a shows that the averages followed tightly the bisector indicating that there was no substantial bias between environments; the difference was not significant (student test, $P > 0.05$). Conversely, Figure 3.3b shows the cultivar Koréli shifted from bisector. This bias was significant, but small and restricted to Koréli, a cultivar encountered in two environments only. The senescence timings of the individual leaf layers were also fitted well (R^2 varied from 0.68 to 0.80 and the RMSE were comprised between 41 and 61 °Cd_H). Nevertheless, the $I1$ and $I4$ were the best fitted models with respectively: R^2 of 0.75 and 0.80 and RMSE of 41 and 53 °Cd_H).

By comparison, the results for the model RF describing the TGW were not as good, the R^2 was 0.26 and the RMSE was 2.98 g (Fig. 3.4). In addition, the G bias was significant and very important ($P < 0.001$), with an over-estimation for Toisondor reaching +5.15 g.



(a) Symbols per environment (b) Symbols per cultivar

Figure 3.4: Relationship between observations and random forest predictions of the Thousand Grain Weight at maturity (TGW, $g \cdot m^2$). Symbols stand either for the cultivar or for environment. The coloured symbols are aggregated data, each point is a G×E combination (single block values not available). The black symbols are cultivar or environment averages.

In that case, the E bias was also almost significant (P = 0.056), with a specific significant underestimation of -3.14 g for the 08-22 environment.

3.3.1.2 Ranking of explanatory variables according to their contribution

Explanatory variables were ranked according to their importance which was estimated by the %IncMSE (see Section 3.2.2.1 "Importance of every explanatory variable", p.62). Overall results are reported in Table 3.1. The most important variables (top ranks) included many climatic variables, which reflected their high proportion in the dataset (half the variables).

Post-heading variables were not included in RF model of senescence timings. That always emphasized the importance of the very early climatic variables of the pre-heading period. For instance, $R46_H^{s15}$, the global radiation received by the crops from 46 to 31 days before heading date, or also $W66_H^{s15}$, the water balance from 66 to 51 days before heading date, were amongst the most important variables explaining I or $I1$. If, at this very early date, the flag leaf was far from emergence, the leaf primordia were already set in the apex at the beginning of stem elongation, a phase which started even earlier. Other climatic variables were also identified in the top ranks of Table 3.1; nonetheless, the very-early climatic variables seemed rather recurrent for every leaf layer. Phenological variables were also often selected; heading date (Heading) explained the variations of I and $I1$; the duration of stem elongation (SE, thermal time for stem elongation) also explained

Table 3.1: Relative importance of 40 most important variables for each leaf layer to explain the senescence timings or the grain weight. The %IncMSE is the mean of the 50 Random Forest fits along with standard deviation. The MSE of the model is given along with the response variable in the top line. Climatic variable was a measure (R, average daily global radiation; W, water balance; T, average daily temperature) given for 15 days time pane starting a given number of days before heading date or after (in which case the number is followed by "p" for post), unlike the general chapter notation for climatic variables, time span and reference stage are not given as identical throughout the table. Other variables: heading date (Heading); grain number and ear number per m^2 (GNe, GNm), fertile ear per m^2 (ENm); thermal time from Z30 to Z55 (SE, for stem elongation), Leaf Lamina area per ear-bearing shoot (LAe), Leaf Area Index (LAI), fraction of the canopy leaf lamina that each leaf layer represent (e.g. fLA 3 for the fraction that the leaf 3 represents), senescence timing (I), and Thousand Grain Weight (TGW). When relevant, the leaf layer is indicated after the variable notation.

	I_{L1-4} (MSE: 1357)		I_{L1} (MSE: 1655)		I_{L4} (MSE: 2756)		TGW (MSE: 8.9)	
Rank	Var.	%IncMSE	Var.	%IncMSE	Var.	%IncMSE	Var.	%IncMSE
1	R46	81.6 (0.61)	R46	86.6 (0.66)	T26	88.7 (0.57)	GNm	68.7 (0.69)
2	T6	68.4 (0.58)	Heading	64.5 (0.49)	W36	75.9 (0.68)	W46	58.9 (0.53)
3	Heading	67.5 (0.59)	fLA 3	61.9 (0.68)	W66	69.1 (0.72)	W24p	52 (0.79)
4	W66	66 (0.73)	R56	61.7 (0.61)	GNm	65.9 (0.65)	fLA 2	43.4 (0.82)
5	T16	64.3 (0.53)	W66	61.3 (0.58)	fLA 1	63.3 (0.52)	T4p	43 (0.79)
6	T66	64.2 (0.63)	T66	61 (0.48)	T16	61.2 (0.64)	LAe 2	41.9 (0.93)
7	R56	62.9 (0.49)	T6	58.7 (0.69)	W56	52.9 (0.55)	T34p	34.4 (0.8)
8	W56	62.9 (0.62)	T16	58.5 (0.69)	SE	52.2 (0.62)	T36	34.1 (0.55)
9	T46	56.3 (0.46)	R66	55 (0.51)	fLA 3	50.8 (0.54)	T6	32.7 (0.75)
10	R16	55.3 (0.9)	W6	53.8 (0.49)	fLA 4	49.8 (0.59)	W16	32.5 (0.76)
11	SE	50.7 (0.7)	W26	52.1 (0.48)	R36	48.2 (0.53)	W34p	30.9 (0.83)
12	W46	49.1 (0.58)	W46	47 (0.67)	R66	46.4 (0.63)	T16	29.7 (0.82)
13	W16	48.6 (0.79)	fLA 1	46.4 (0.7)	W46	44.9 (0.68)	R66	28.6 (0.82)
14	W6	47.3 (0.54)	T46	46.4 (0.52)	T56	44.7 (0.54)	R14p	27.1 (0.67)
15	R36	44.2 (0.62)	W16	44.7 (0.52)	R6	41.8 (0.58)	I2	26.9 (0.8)
16	T56	44.1 (0.54)	LAe 3	44.5 (0.55)	LAe 1	41.6 (0.7)	R56	26 (0.88)
17	LAe 3	44 (0.48)	T56	42.3 (0.57)	T36	41.6 (0.57)	T44p	25.5 (0.87)
18	ENm	42.8 (0.78)	R26	41.8 (0.77)	TGW	41.5 (0.87)	R54p	25.4 (0.91)
19	TGW	41.2 (0.79)	R16	41.7 (0.65)	R26	40.8 (0.81)	R34p	25.2 (0.91)
20	fLA 3	40.9 (0.72)	fLA 4	41.1 (0.63)	T6	40.4 (0.51)	R46	23.3 (0.93)
21	GNm	39.6 (0.68)	SE	41 (0.82)	W26	38.6 (0.58)	T26	22.8 (0.81)
22	R66	37.6 (0.61)	W56	40.2 (0.61)	R56	38.4 (0.73)	W26	22.4 (0.97)
23	W26	37.6 (0.68)	ENm	40 (0.69)	GNe	37.6 (0.7)	R44p	21 (0.88)
24	LAe 1	36.1 (0.68)	R36	39.3 (0.74)	R16	36.8 (0.73)	ENm	20 (0.85)
25	LAI 1	35.3 (0.69)	GNm	37.2 (0.65)	LAI 3	35.5 (0.6)	Heading	19.9 (1)
26	T26	35.1 (0.82)	W36	36.7 (0.61)	W16	35.3 (0.55)	LAe 3	19.6 (0.76)
27	R6	34.7 (0.98)	LAI 4	35.1 (0.65)	W6	35.3 (0.48)	LAI 4	18.7 (0.77)
28	W36	34 (0.57)	TGW	33.4 (0.7)	LAI 4	34.7 (0.61)	I	18.4 (0.94)
29	T36	31.9 (0.53)	T26	32.6 (0.56)	T66	34.3 (0.62)	LAe 4	18.3 (0.89)
30	fLA 2	30.8 (0.76)	LAe 1	31.1 (0.69)	LAI	32.4 (0.83)	T66	18.1 (0.86)
31	fLA 1	30.7 (0.9)	T36	30.7 (0.65)	R46	32.4 (0.64)	R6	17.4 (0.75)
32	R26	30.3 (0.81)	R6	30.2 (0.72)	Heading	31.5 (0.63)	fLA 3	17.1 (0.9)
33	LAI	28.9 (0.67)	LAI 1	29.1 (0.74)	ENm	30.7 (0.68)	SE	16.2 (1.02)
34	LAI 3	26.5 (0.75)	LAI 3	26.4 (0.77)	LAI 1	29.9 (0.7)	fLA 4	16.1 (1.01)
35	LAe	25.4 (0.82)	GNe	25.8 (0.7)	LAe 4	28.7 (0.69)	W4p	16 (0.93)
36	GNe	25.3 (0.89)	LAe 4	25.5 (0.71)	LAe	26.9 (0.81)	T54p	15.7 (0.91)
37	LAI 4	24.6 (0.67)	LAe 2	24 (0.61)	LAe 3	26.4 (0.78)	W14p	15.1 (0.93)
38	LAI 2	23.8 (0.72)	LAe	23.4 (0.71)	T46	25.3 (0.68)	I1	14.9 (0.99)
39	LAe 2	23.5 (0.74)	fLA 2	19.1 (0.98)	fLA 2	25 (0.75)	W36	14 (0.91)
40	LAe 4	19.5 (0.84)	LAI	17.8 (0.67)	LAI 2	24.7 (0.79)	W44p	13.9 (0.85)

well I and $I4$. The relative proportion of individual leaf layers was also identified as a key variable for the estimation of $I1$ and $I4$, the most important being the LAI proportion in leaf 3 (fLA 3) to explain $I1$ and the LAI proportion in flag leaf (fLA 1) to explain $I4$. Finally, although the grain sink size was expected to influence the senescence timings, only $I4$ selected the number of grain per m^2 (GNm) among its main explanatory variables.

Although post-heading climate variables were also considered in the case of TGW, the RF models estimating TGW were not as good as for I (low R^2 and variable bias regarding E or G). However, the GNm was, as expected, the most important explanatory variable of TGW. Other unexpected variables were identified as fLA 2 and LAe 2. Many climatic variables were also detected, during the grain filling phase such as the temperature around anthesis (more precisely: $T4^{s15}_{post\ H}$, temperature from 4 to 19 days after heading stage), but also early-climatic variables such as the water balance from 46 to 31 days before heading ($W46^{s15}_{H}$) which was the second most important variable.

3.3.2 Multiple regression models

Target: important explanatory variables have been identified (by RF models), multiple linear models were fitted to understand the effect of the important variables on the responses. In general, the following question was investigated: what was the variation of y for a variation of x?

The RF models helped identify the most important variables to explain I or TGW, without *a priori* on the dataset. Although the variable ranking is valuable information, the nature of the relation to y remained unknown — and, reminder, was not restricted to linear relationships — and the direction of the variations was also unknown (*Does y increase or decrease with x?*). In order to have a better understanding of the link between x and y, a more classical multiple linear regression method was applied in addition to the RF. To do so, starting from the 12 most important variables according to the RF models, a backward/forward stepwise selection was applied to identify (*linearly-*) explanatory variables, but also keeping parsimonious models. These linear models were improved, when possible, by i) calculating the early-climatic variables in reference to the date of leaf onset — i.e. the date of leaf emergence — rather than heading stage, and ii) looking for the best time-window span. The selected models correspond to the equations 3.6, 3.7, 3.8 and 3.9.

Hereafter, the selected/improved multiple linear models are reported, the parameters are given along with the standard error of the estimation. As described above, the senescence-timing models were fitted on 162 observations of 41, while the TGW model was fitted on 60 observations of 63 variables. (Section 3.2.2.2, paragraph "Multiple linear regression models", p.63).

$$
\begin{aligned}
I = &-545(\pm123) - 4.8(\pm0.6)Heading + 4.9(\pm1.0)\%LAI_{L1} && (3.6)\\
&- 1.90(\pm0.32)[W56_H^{s15}] + 0.13(\pm0.03)[R46_H^{s15}] + 0.82(\pm0.16)[W16_H^{s15}] && R^2 = 0.65\\
&+ 17(\pm2.3)[T9_H^{s3}] + 38(\pm5)[T6_H^{s15}] && RMSE = 47
\end{aligned}
$$

$$
\begin{aligned}
I_1 = &748(\pm44) - 9.1(\pm0.57)Heading && (3.7)\\
&+ 13.7(\pm1.6)\cdot10^{-3}GN\cdot m^{-2} - 5.4(\pm0.8)GN\cdot ear^{-1} && R^2 = 0.63\\
&- 1.3(\pm0.3)[W18_{L4}^{s22}] - 55.2(\pm12.2)\cdot10^{-3}[R6_{L2}^{s4}] && RMSE = 49
\end{aligned}
$$

$$
\begin{aligned}
I_4 = &-429(\pm71) + 211(\pm27)LAI_{L3} - 140(\pm16)LAI_{L1} && (3.8)\\
&- 4.6(\pm0.8)Heading + 10.6(\pm1.8)\cdot10^{-3}GN\cdot m^{-2} && R^2 = 0.71\\
&- 2.2a(\pm0.3)[W7_{L4}^{s19}] + 17(\pm4)[T0_{L2}^{s21}] && RMSE = 62
\end{aligned}
$$

$$
\begin{aligned}
TGW = &48.1(\pm5.02) - 5.12(\pm1.0)\cdot10^{-4}GN\cdot m^{-2} && (3.9)\\
&- 0.10(\pm0.02)[W46_H^{s15}] + 0.081(\pm0.018)[W36_H^{s15}] + 0.99(\pm0.28)[T6_H^{s15}] && R^2 = 0.63\\
&- 0.053(\pm0.01)[W24_{post\ H}^{s15}] - 0.008(\pm0.002)[R54_{post\ H}^{s15}] && RMSE = 2.07
\end{aligned}
$$

Estimations of I relied on a model of low R^2 based on seven variables (0.65, Eq. 3.6). In comparison, $I1$ model was characterised by a comparable R^2 (0.63) but based on five variables only (I1, Eq. 3.7). The $I4$ was more accurately estimated as the R^2 was 0.71, yet relied on six variables. The senescence timings $I2$ and $I3$ were not so well estimated and are not reported here. Notwithstanding, the development and senescence timings of these leaf layers were highly correlated with the canopy, leaf 1 and leaf 4 ($r(I1,I2) = 0.74$; $r(I,I2) = 0.88$; $r(I,I3) = 0.88$); therefore, $I2$ and $I3$ could be deduced from I, $I1$ and $I4$ (not presented in the chapter).

As some very early climatic variables were identified by RF and confirmed during the selection of the multiple linear models, the reference to heading date for calculation could be a misleading choice in comparison to a reference to a closer phenological stage. The climatic variables in $I1$ and $I4$ models were thus refined in order to optimise developmental stage and span-window duration. Thereby, the senescence timing of the flag leaf ($I1$) involved an early stem-elongation water balance, the best approximation of which was $W18_{L4}^{s22}$, i.e. the 22-days water balance starting from 18 days before the emergence of leaf 4. The senescence timing $I1$ was also highly correlated with $R6_{L2}^{s4}$, the incident radiation of the crop over 4 days, starting 6 days before the onset of leaf 2. Similarly, $I4$ was correlated with the 19-days water balance starting 7 days before the onset of leaf 4

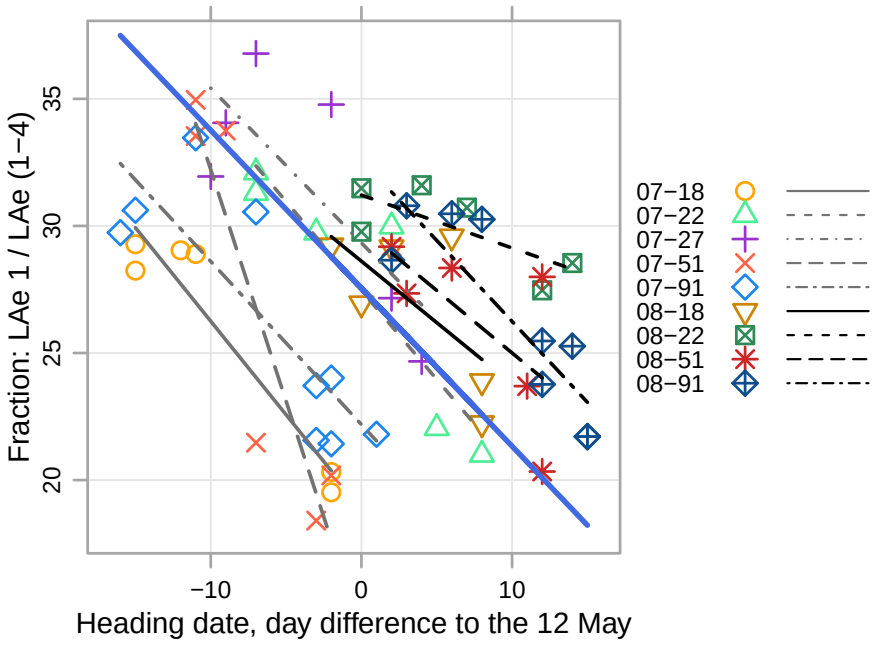
($W7_{L4}^{s19}$) and the temperature during the three weeks following leaf 2 emergence ($T0_{L2}^{s21}$).

The importance of ontogenical variables on the senescence timings was also confirmed by the multiple regressions. Indeed, heading date was negatively correlated with the senescence timings (I, $I1$ and $I4$): the later the heading date, the earlier the senescence timing (9.1 °Cd_H per day for the flag leaf). Whichever the time unit used (days or °Cd), this relation depended (only) partially on the increase of the temperatures associated with a later heading date. To investigate this specific relationship, some extra multiple linear regressions were fitted. For the flag leaf, $I1$ was fitted (R^2 = 0.45) to both heading date and the mean temperature experienced by the flag leaf over its whole life time (from onset of leaf 1 to $I1$). The mean temperature accounted for 27% of the variance explained by this model. However, as temperature also influenced heading date, $I1$ was thus fitted to the mean temperature and the flag-leaf emergence date date (instead of heading date). Then, mean temperature accounted for 37% of the variance explained by this new model. For lower leaves, the influence of temperature was much higher, accounting for 73% to 82% of $I2$ and $I4$, respectively.

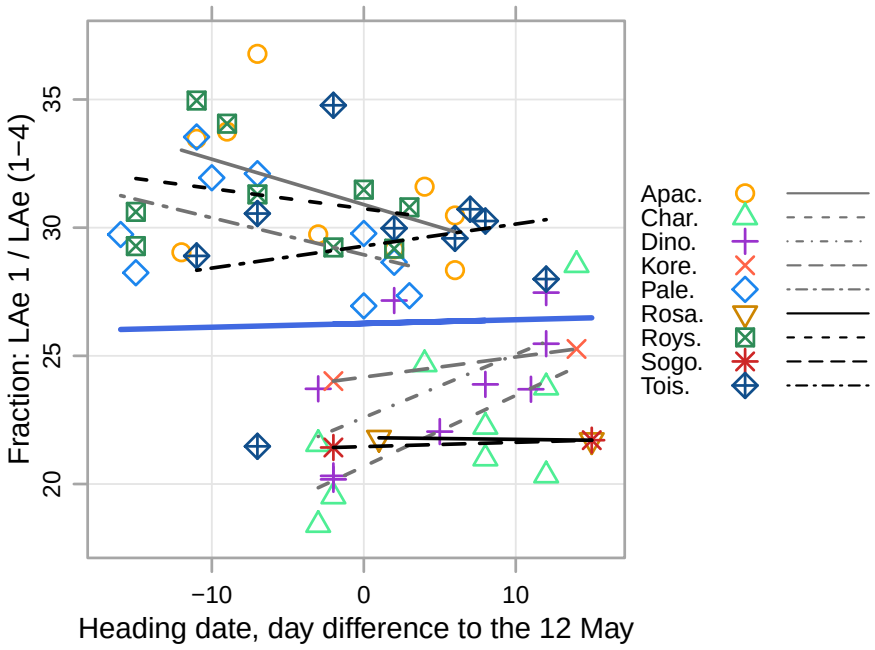
The senescence timings were also linearly dependent on the grain sink description: GNm increase was associated with a delayed $I1$ and $I4$. Conversely, $I1$ was anticipated by the increase in GNe. The combined effects of GNm and GNe according to Eq 3.7, were highly correlated with ENm (R^2 = 0.85); nevertheless, replacing GNm and GNe by ENm reduced the accuracy in $I1$ prediction as shown by the decrease in R^2 from 0.63 to 0.57.

In agreement with RF ranking, the different senescence timings did not vary with quantitative source-dependent variables, e.g. LAe or LAI. Conversely, some variables describing the leaf profile were selected in the models: fLA 1 explained I while $I4$ was explained by a combination of LAI 1 and LAI 3 that highly correlated with fLA 1 (R^2=0.86). Interestingly, fLA 1 correlated with heading date, which was an explanatory variable of the senescence timing models, but showed a large G×E interaction that is represented in the Figure 3.5a. Within each environment, the heading date was negatively related to fLA 1 (Fig. 3.5a), but with visible large variation of the intercept between experiments. A mixed model taking into account the E random effect on the intercept led to a single and highly significant slope describing the G effect within the various E. In contrast, a comparable approach did not lead to a significant slope if considering the E effect within the various G (Fig. 3.5b). In other words, the E effect was not consistent on the relationship between heading date and fLA 1, while the G effect resulted in a constant negative slope.

Unlike I, the repetitions of TGW within the experiments were not available. Therefore, it was decided to aggregate the available repetition values into the mean, which modifies the structure of the dataset: repetitions were taken into account for I, but not for TGW. Additionally, post-anthesis climatic variables were taken into account in the case of TGW, unlike in the case of senescence timings. The selected linear model describing



(a) Symbols and lines per environment



(b) Symbols and lines per genotype

Figure 3.5: Relationship between the fraction of flag leaf and heading date. The two figures were strictly based on the same data. Each point is the average value on x- and y-axis for each G×E combination. The symbols and lines represent either the different environments (in a) or cultivars (in b). Within each environment (sub-figure a) each point is a cultivar. A linear mixed model was used to estimate the average relation between x and y, assuming a random effect of E on the intercept (blue line: $y = 0.28 \pm 0.02 - 6.2(\pm 0.5) \cdot 10^{-3} \times x$, $P < 0.001$). A similar model assuming a random effect of the genotype G was fitted, the slope is not significantly different from 0.

the TGW relied on six variables and was better than the corresponding RF model (R^2 = 0.63). However, unlike the senescence timing models, attempts to refine the climatic variables (reference to leaf emergence stage, or better suited time-span) failed to improve the TGW model. The GNm was the only biological variable selected, which was negatively correlated with the TGW — as expected from the literature. The model confirmed the interest of the early-estimated water balance; two early-climatic variables were selected ($W46_H^{s15}$ and $W36_H^{s15}$) which describe overlapping water-balances from 46 to 31 days and from 36 to 21 days before heading, respectively. However, these two variables showed a similar weight affecting negatively and positively the TGW, respectively. Such opposite weights made interpretation of the direct biological meaning complex. However, the interaction of the two variables highlighted an important contrast between the two years as 2007, unlike 2008, was characterised by a spring drought (followed by high precipitation during the summer). The TGW model also highlighted climatic variables linked to the grain-filling phase, for which a biological explanation could be proposed. The daily temperatures from 6 days before to 8 days after heading ($T6_H^{s15}$) related to the climatic conditions during the anthesis. The water balance 24 to 39 days after heading ($W24_{post\ H}^{s15}$) related to the beginning of the grain watery ripe (GS71), when the grain filling reaches its maximum rate. However, the negative coefficient of $W24_{post\ H}^{s15}$ was surprising. The global incident radiation from 54 to 69 days after heading ($R54_{post\ H}^{s15}$) occurs at the end of the grain filling, and its negative effect could be related to senescence.

3.3.3 Identifying the origin of G, E or G×E

3.3.3.1 Variance component analysis

Target: the selected models involved many variables (responses and explanatory), how much does each variable depend on E or G or G×E random variations? Which random variation was explained by the selected models?

A Variance Component Analysis (VCA) was run to estimate the proportion of variance of a variable caused by the E, G or G×E effect. The VCA was applied on all the variables involved in the selected multiple regression models (Eq. 3.6 to 3.9), responses as well as explanatory variables (Fig. 3.6). The climatic variables depended on the environment which accounted for 24% to 82% of the observed variability, especially for the late climatic variables. But a genotype effect also applied to the climatic variables as they were calculated over window times that referred to growth stages which, in turn, depended substantially on the genotype. For instance, 39% of the variability in heading date was explained by the genotype range (Genotype + Genotype × Environment interaction). The sole genotype variation represented 20% to 30%. For I and $I1$ 50-55% of the variability was associated with E variations, but only 26% for $I4$ for which G×E reached 34%. G and E

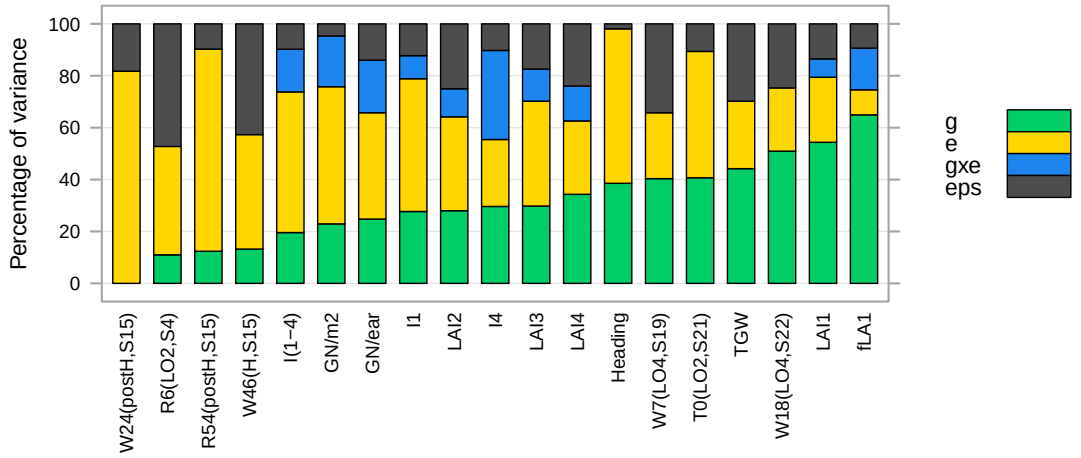


Figure 3.6: Variance component analysis of the variables included in the I_1, I_4 and TGW multiple regression models. How much variability was because of E, G, G×E (Environment, Genotype, Interaction, respectively)? How much is the residual variation of the model, i.e. epsilon ("eps")?

did not affect LAI of the different leaf layers in the same way. For lower leaves 28% to 34% of LAI variance was explained by G while the G×E effect represented 12%. Only 7% of the LAI 1 variance was due to G×E and 25% was due to E, but an important proportion was attributable to G variations (54%). This proportion increased to 65% for fLA 1, the proportion of the flag leaf, while the E effect dropped to 10%.

Consistently with the expectation, the cultivar was the main source of TGW variation, before the environment (44% and 26%, respectively); however, the absence of repetitions made the estimation of G×E impossible which was therefore confounded with the residuals (eps.) that reached 30%. It was not the case of GNe and GNm which depended moderately on the cultivar (25% and 23%, respectively), similarly on the G×E effect, and largely on the E variations (53% and 41%, respectively).

Since the models were constructed without *a priori*, some explanatory variables only fit the response variable through combinations to other explanatory variables (e.g. GNe and GNm, LAI 1 and LAI 3, $W46_H^{S15}$ and $W36_H^{S15}$). Indeed, ultimately an attempt was made to quantify which part of the variability of the response variable was explained by the different models. The Figures 3.7 and 3.8 then showed the proportion of the variance due to E or G or G×E that was explained by the RF model, or the final linear model selected as well as intermediate models. The variance component analysis was applied on the residuals of the null model (estimation by the average), and compared to the VCA applied to intermediate models for which the explanatory variables (Eq. 3.7 and 3.9) were added successively. Figure 3.7 reports the results for $I1$, for which the RF model was good (R^2, RMSE and bias). It explained 78% of the variance of $I1$, while the remaining variance, i.e. the residual (eps.), could not be attributed to the E, G or G×E random effect.

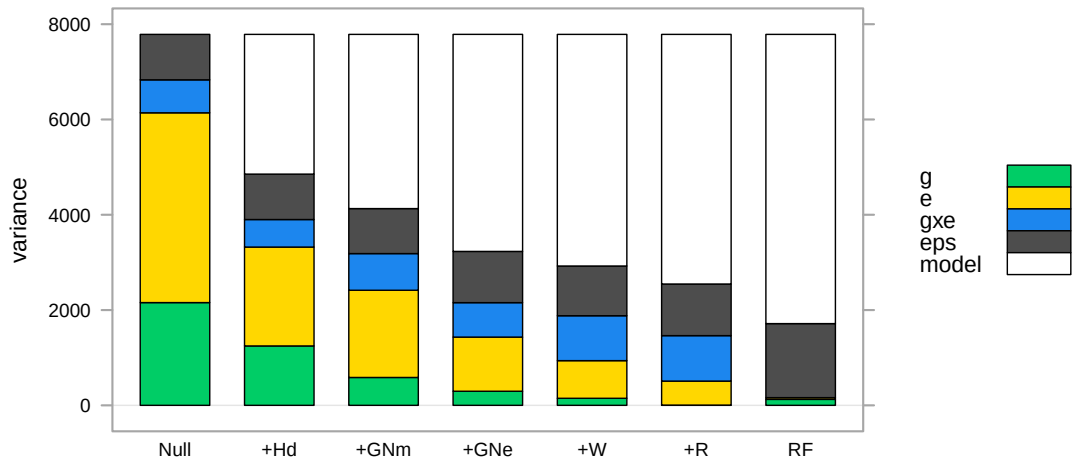


Figure 3.7: Synthesis of the response variance explained/unexplained by the models. The successive models represent the transition from the model null ("Null") to the selected model through the successive addition of heading date ("+Hg"), grains $\cdot$ m^{-2} ("GNm"), grains $\cdot$ ear^{-1} ("+GNe"), the water balance from 18 days before to 4 days after leaf-4 onset ("+W"), the global radiation from 6 to 2 days before leaf-2 emergence ("+R", = the selected model), the last model being the Random Forest ("RF"). Note: the residual of the RF model is higher as the estimation of the error is unbiased as tested on the "out-of-the-bag" data.

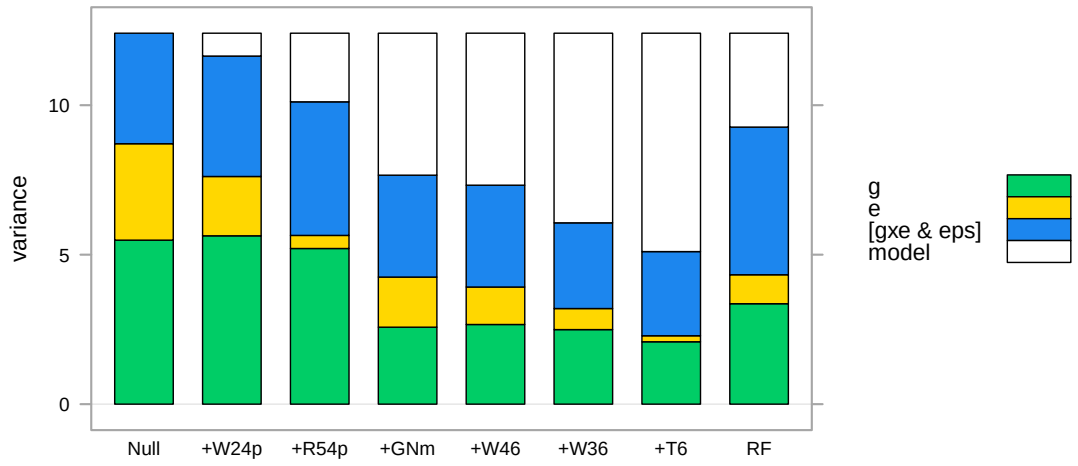


Figure 3.8: Synthesis of the variances of TGW explained/unexplained by the models. The variation due to G×E can't be dissociate from ε. The successive models represent the transition from the model null ("Null") to the selected model through the successive addition of water balance from 24 to 39 days after heading ("+W24p"), global radiation from 54 to 69 days after heading ("+R54p"), grains $\cdot$ m^{-2} ("GNm"), water balance from 46 to 31 days before heading ("+W46"), water balance from 36 to 21 days before heading ("+W46"), the daily temperature from 6 days before to 9 days after heading ("+T6" = the selected model), the last model being the Random Forest ("RF").

The various models did not affect that residual variance (eps.) which remained between 10% and 15%. The addition of the heading date explained 45% of $I1$ variations, but the repartition of the variance between G, E and G×E did not change much compared to the null model. On the other hand, up to 68% of $I1$ variance was explained by three variables, i.e. the heading date, the GNm and the GNe, and contributed to explain preferentially E and mostly G, while G×E was left unchanged. After the addition of the five top variables of the model, the variance explained by the linear model (Eq. 3.7) was relatively close to the RF model. The E- and G-variance were almost totally explained, while the interaction G×E and the residuals (eps.) were poorly affected by the addition of variables.

Likewise, the variability of TGW explained by the models was decomposed (Fig. 3.8). In this case G×E could not be estimated because of the absence of repetitions. According to simple correlations, only GNm was significantly correlated with TGW, but within the multiple regression model (Eq. 3.9) the most decisive variables were those describing the climate during the grain filling ($W24^{s15}_{post\ H}$ and $R54^{s15}_{post\ H}$). These variables, when added, decreased the E variance. Conversely, the addition of GNm was followed by a sharp decrease of the G variance. After the addition of six variables, the linear model performed much better than the RF model. The effect of E was almost totally explained; G variance was halved, but one more time G×E variance was hardly decreased.

3.3.3.2 Partial regressions

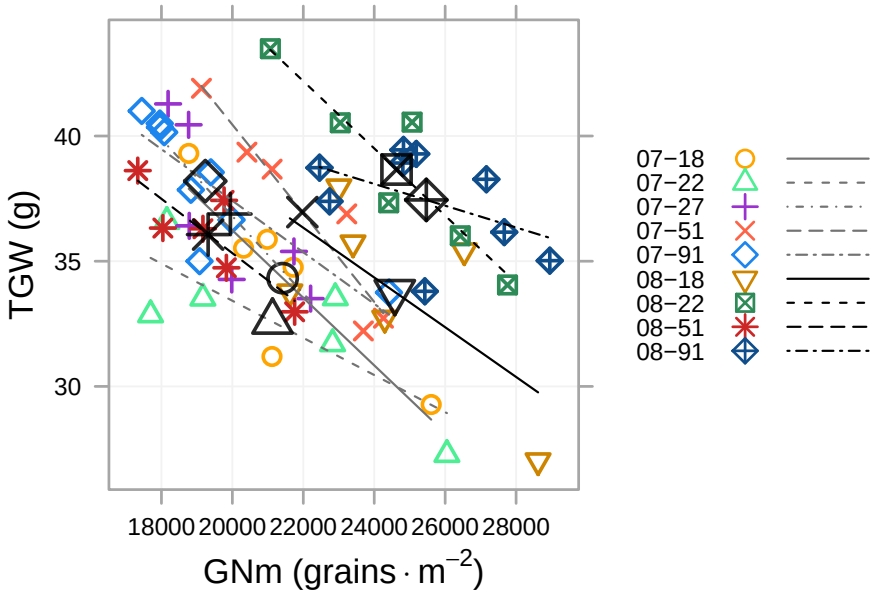
Target: within each selected multiple linear model, it was investigated how the environment E, or the genotype G, affects the relationship between the response variable and each explanatory variable — while the effects of the other variables were taken into account.

The preceding section assigned variance to G, E or G×E, but ignored the relationships between variables. In the Section 3.3.2, a simple regression described the relation between the heading date and the fLA 1; this example demonstrated the interest in including the E or G random effects, as this is required for the identification and estimation of an adequate slope; this was done with a simple mixed model regression, random effect was assigned to intercept, i.e. either E (Fig. 3.5a) or G (Fig. 3.5b). It was also suspected E or G have an effect on the multiple regression models which were fitted on the dataset (Eq. 3.6 to 3.9). Unfortunately, the mixed model can be a complex tool, difficult to apply to these multiple regression models given the number of parameters they are composed of, and the number of assumptions that would be required to assign the random effects. Indeed, the multiple regression models include several variables, some of which are likely to explain either part of the genotype-induced variability (e.g. "biological" variables), or part of the environmental-induced variability (e.g. the climatic variables). Consequently, the multiple regression models controlled, to some extent, part of the random variations due to E and G which, thus allowing for the detection of linear relations between X_p and

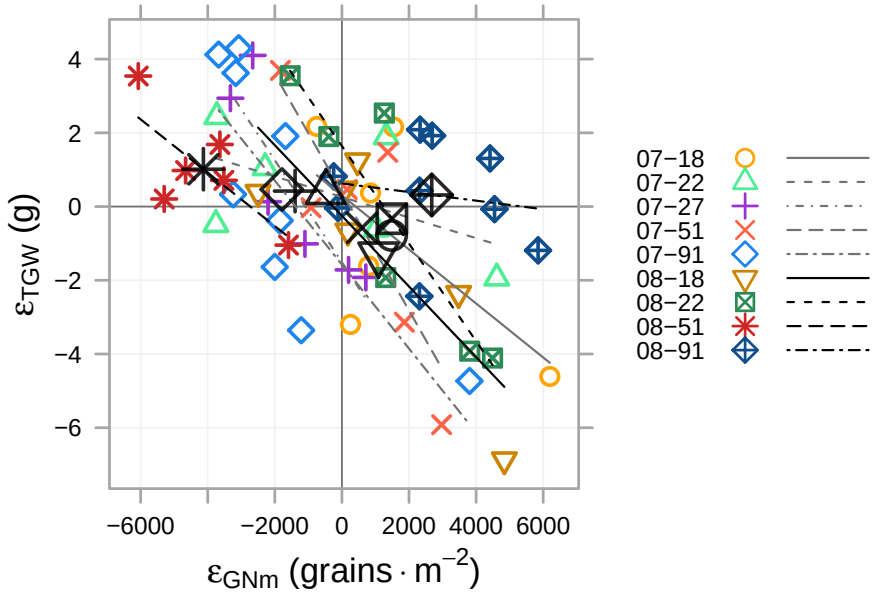
Y that could not be detected in the absence of the other $p-1$ explanatory variables. To improve the understanding of E and G variation within the selected models, a method was proposed based on the partial regressions.

The partial regression explained the association between a response variable Y and an explanatory variable Xp *taking into account the effect of the other variables of the multiple regression model* on both Y and Xp (see Section 3.2.2.2, paragraph "Partial regressions", p.63). The graphic of the partial regressions represented the residuals of the response variable regarding residuals of the explanatory variable Xp. Using symbols that emphasized either the environments or the genotypes, it helped understanding how E or G or both may have affected the relation of X_p to Y: Was the range of values obtained due to E or G? How did the slope vary according to environments or to genotypes? Were there important differences found between the various E or G for either the slope or the intercept?

The pathway for result interpretation is similar to that exemplified about Figure 3.5.For instance, Figure 3.9 represents the well-known relation between TGW and GNm. The overall correlation was r = -0.40** on raw data (Fig. 3.9a) and r = -0.58*** based on partial residuals (Fig. 3.9b). Regarding the regression on raw data within each environment, the slope did not vary ($P > 0.05$) but the intercept varied significantly ($P < 0.001$) which explained the group of (roughly) parallel segments. However, the environment averages (large black symbols), did not follow any significant relation. In this example (largely comparable to Figure 3.5a) it signifies that the relation, linked to G, was confirmed within each environment. But it was not exactly repeatable, due to an off-set from one environment to another; which may have possibly resulted from different E effects on GNm and TGW in the dataset. In this example, the best estimation of the slope between the TGW and GNm would be the slope obtained using a mixed model, considering a random variation of the intercept between environments (-9.7 ± 1.2); or *a minima*, the average of the slope obtained between the environments (-11.4 ± 1.4), was compared to the slope directly obtained between TGW and GNm (-4.4 ± 1.3). The same method was applied on partial residuals from Eq. 3.9 (Fig. 3.9b) instead of the raw data. By taking into account the covariate, the scatter of points is tighter. An overall slope can be calculated at -5.1 ± 0.9, but Figure 3.9b shows specific patterns for 07-22 and 08-91. When comparing the regressions within each environment, both slopes and intercepts significantly varied ($P < 0.05$). The slope variation suggested a G×E effect, once deducted the variability already explained by the other variables of the multiple linear regression model (Eq. 3.9) the slopes varied from -1.2 ± 3.1 (08-81) to 16.0 ± 5.5 (07-51).



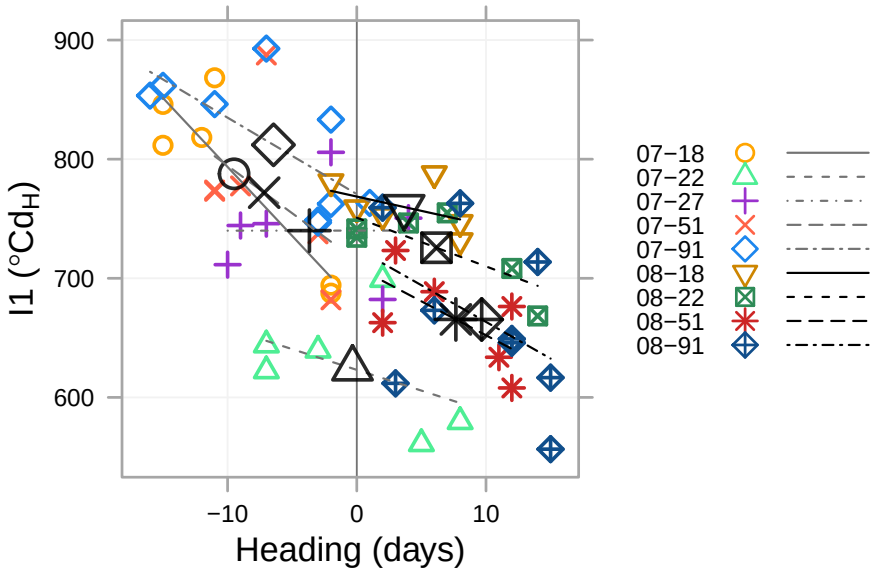
(a) Raw data



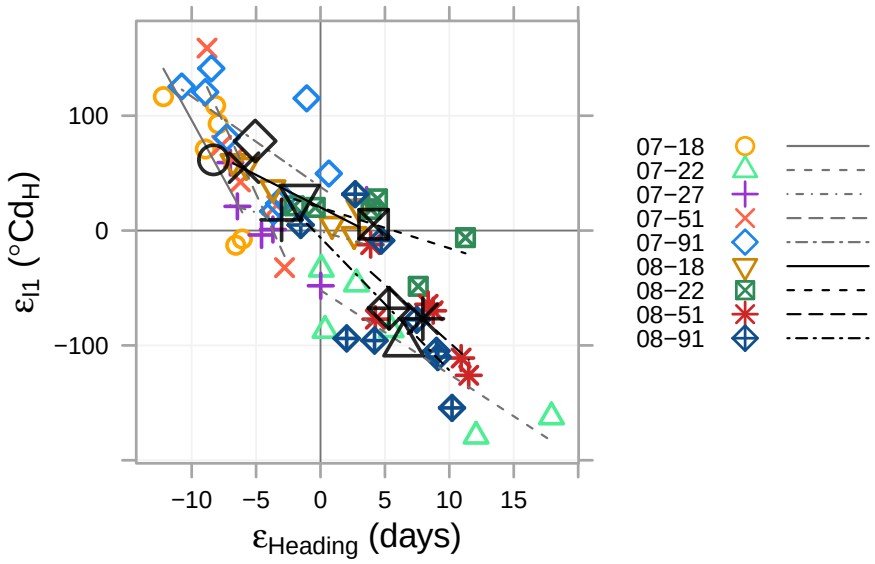
(b) Residuals (partial regression)

Figure 3.9: Relationships between TGW and grain number per m^2: raw data and residuals of partial regressions. Each point is the average of a cultivar × environment combination. The symbols and lines and colours represent the environment. The values of the residuals from the partial regressions are based on $TGW = \alpha_0 + \alpha_1 GN \cdot m^{-2} + \alpha_2[W46_H^{s15}] + \alpha_3[W36_H^{s15}] + \alpha_4[T6_H^{s15}] + \alpha_5[W24_{post\ H}^{s15}] + \alpha_6[R54_{post\ H}^{s15}] + \varepsilon$. And were therefore the partial residuals obtained by: $TGW = \delta_0 + \delta_1[W46_H^{s15}] + \delta_2[W36_H^{s15}] + \delta_3[T6_H^{s15}] + \delta_4[W24_{post\ H}^{s15}] + \delta_5[R54_{post\ H}^{s15}] + \varepsilon_{TGW}$ and $GNm = \gamma_0 + \gamma_1[W46_H^{s15}] + \gamma_2[W36_H^{s15}] + \gamma_3[T6_H^{s15}] + \gamma_4[W24_{post\ H}^{s15}] + \gamma_5[R54_{post\ H}^{s15}] + \varepsilon_{GNm}$.

A second example shows the unexpected relation between $I1$ and heading date either on raw data or on residuals from partial regressions. On raw data (Fig. 3.10a), both slopes ($P < 0.05$) and intercepts ($P < 0.001$) were significant, but the former much less than the latter, suggesting that the G effect was stronger than G×E effect. Using residuals from partial regressions (Fig. 3.10b), each environment was associated with a reduced range of $I1$ and heading date in comparison to the complete dataset. The linear relation estimated within each environment (colours and symbols and lines) was part of a larger relation which seems defined on the full range of $I1$ and heading dates of the dataset. In this example, not only the slopes were comparable (all negative) but the differences in the intercepts were small. Each regression line obtained in an individual environment followed an average relation which was represented by the average of the environmental values (the large black symbols). The E random effect was checked and found to be low (i.e. the slope did not vary significantly with E, $P = 0.10$): either because the relation of $I1$ to the heading date was well defined amongst the genotypes and poorly affected by the environment, or — as it is partial residuals — the other variables of the model accounted for most of the differences between the environments. Figure 3.10b is also interesting as it showed that the large range of responses was possible only because the range of environments has generated this variable heading date.



(a) Raw data



(b) Residuals (partial regression)

Figure 3.10: Relationships between $I1$ and heading date: raw data and residuals of partial regressions. Each point is the average of a cultivar × environment combination. The symbols and lines and colours represent the environment. The values of the residuals from the partial regressions are based on $I1 = \alpha_0 + \alpha_1 Heading + \alpha_2 GN \cdot m^{-2} + \alpha_3 GNe + \alpha_4[W18^{s22}_{L4}] + \alpha_5[R6^{s4}_{L2}] + \varepsilon$. And therefore the partial residuals were obtained by: $I1 = \delta_0 + \delta_1 GN \cdot m^{-2} + \delta_2 GNe + \delta_3[W18^{s22}_{L4}] + \delta_4[R6^{s4}_{L2}] + \varepsilon_{I1}$ and $Heading = \gamma_0 + \gamma_1 GN \cdot m^{-2} + \gamma_2 GNe + \gamma_3[W18^{s22}_{L4}] + \gamma_4[R6^{s4}_{L2}] + \varepsilon_{I1}$.

Slopes and intercepts for all partial regression pairs were then estimated, per genotype or per environment. Tables 3.2 to 3.5 report the estimations obtained from the multiple regression models explaining I (Eq.3.6, Table 3.2), $I1$ (Eq.3.7, Table 3.3), $I4$ (Eq.3.8, Table 3.4) and TGW (Eq.3.9, Table 3.5). Within each table, the nine first lines report the slopes (β_0) and the intercepts (β_1) between partial residuals estimated for each environment. The nine following lines report the slopes and intercepts estimated for each cultivar. The significance of the slope or intercept estimations is indicated for each environment or cultivar. As underlined in Tables 3.2 to 3.5, correlations of partial residuals of a response to an explanatory variable were rarely significant per genotype or per environment due to the lack of degrees of freedom. Rather, correlations may be significant when it accounted for E or G mean effects. For instance, although not significant, the slopes estimated between $I1$ and $R6^{s4}_{L2}$ were constantly negative. A t-test would conclude that the average slope across environments was significant ($P < 0.01$) -0.0495 ± 0.013. In a general way, we may conclude there was a strong E effect when the E slopes of the relationship was significantly different from 0 by the time no significant slope was found when accounting for G (e.g. in Table 3.3, $I1 = f(GNe)$, $I1 = f(W18^{s22}_{L4})$). Otherwise, both E and G mean slopes may be highly significant as in the case of the relation $I1 = f(Heading\ date)$, which suggests a comparable importance of E and G. The G×E interaction can be suspected when slopes significantly differed in various E and G.

Partial regression results clearly would need extending for a complete biological study of senescence timings and TGW determinism, but is beyond the topic of this chapter. Further observations are reported in discussion section, but now the focus will rather be on validation of procedures and the obtained results.

Table 3.2: Partial regression: individual E and G intercept (β_0) and slopes (β_1) from the relationships between partial residuals of the inflexion point of canopy senescence (I) and the explaining variables selected in the model. The average of the coefficients (β_0 and β_1) across the environment or cultivar and the standard deviation are given. The significance of the mean was tested according to a t test. Coefficient significance level ($H_0: \beta = 0$): (.), 0.1; (*), 0.05; (**), 0.01; (***),0.01; (na), non applicable.

		$I = f(Heading)$		$I = f(fLA\ 1)$		$I = f(T9_H^{s3})$		$I = f(R46_H^{s15})$		$I = f(T6_H^{s15})$		$I = f(W16_H^{s15})$		$I = f(W56_H^{s15})$	
EG	group	β_0	β_1	β_0	β_1	β_0	β_1	β_0	β_1	β_0	β_1	β_0	β_1	β_0	β_1
E	07-18	168 *	13.7 ·	-27.6	-4.5	-16.6	32.1 *	27.2	-0.252	12.3	-43.8	102 *	6.57 **	19.6	2.54
	07-22	-26.5	-21.9 ·	-29.7	3.97	3.68	34.4	10.9	0.47 *	11.6	70.7	-28.6	0.68	-56.4 *	1.04
	07-27	14 ·	-1.8	8.36	3.17	3.7	9.67	6.97	0.0868 **	-3.95	23.7 *	24.9 ·	1.71 *	10.1	-0.805
	07-51	-10.1	-6.46 ·	-4.04	4.69 ·	3.98	7.1	-2.71	0.166	-2.16	44.3 ·	-4.53	0.654	-4.34	-2.2
	07-91	-14.7	-14.9 ·	26.2	8.69	20.6	3	18.4	-0.0607	46.3	-7.91	75.6 *	-0.533	5.93	11.2
	08-18	-5.79	0.749	8.47	1.71	1.09	22.9 **	7.82	0.0445	19.6 *	15.2 ·	12.3 ·	-0.45	11.2	-2.88 ***
	08-22	13.1	-3.18	60.7	-6.01	21.3	15.4	24.4	0.0562	-1.47	-76.9 ***	36.1	-0.182	17	-3.28 *
	08-51	-41.3	-0.97	-22.7	-4.48	-14.6	6.9	-54.9	-0.382	-9.21	-11.7	-18	0.361	-14.7	-1.74
	08-91	1.25	-6.02	-9.25	11.1	-5.33	17.3	-2.63	0.32	-11.8	67.3	-3.7	1.16	-5.41	-1.71
	mean	10.9^{ns}	-4.5^{ns}	1.16^{**}	2.03^{ns}	1.99^{ns}	16.5^{ns}	3.94^{ns}	0.05^{ns}	6.81^{ns}	8.99^{ns}	21.9^{ns}	1.11^{ns}	-1.88^{ns}	0.24^{ns}
	sd	61.6	9.98	29.1	6.00	13.3	11.3	24.5	0.26	18.2	49.5	43.4	2.18	23.3	4.51
G	Apache	-19.5 ·	-4.95 ·	-40.4 ***	13.5 **	-13.1	9.98	-21.8 *	0.217 *	-19.5 ·	42.4 *	-19.5 ·	0.799 *	-18 ·	0.828
	Charger	-8.12	-5.64 ***	-18.2	2.36	-8.45	11.5	-9.03	0.121 ·	-11.8	29.8	-9.82	0.531	-6.28	-1.04
	Dinosor	16.6	-3.06 ·	26.5	9.18	19	10	19.1	0.0349	9.48	3.85	21.6	1.36 *	14	-3.28 *
	Koreli	52.1 ^{na}	-2.92 ^{na}	49.1 ^{na}	37.7 ^{na}	50.1 ^{na}	2.78 ^{na}	69.9 ^{na}	-0.198 ^{na}	107 ^{na}	-44.3 ^{na}	71.3 ^{na}	0.214 ^{na}	52.5 ^{na}	-4.79 ^{na}
	Paledor	14.1	-4.94	13	-1.48	9.94	10	11	0.0866	14.8	50.9 ·	12	0.157	9.13	-0.102
	Rosario	-38.4 ^{na}	-2.2 ^{na}	-52.1 ^{na}	-16.5 ^{na}	-78.9 ^{na}	-9 ^{na}	-21.4 ^{na}	-0.0758 ^{na}	11.4 ^{na}	-5.59 ^{na}	-8.25 ^{na}	-0.0148 ^{na}	-53 ^{na}	-8.44 ^{na}
	Royssac	-33.3	-11.3 *	-27.8	8.08	-36.5	4.06	-21.7	0.183	-25.1	50.8 ·	-23.3	0.764	-24.4	-1.62
	Sogood	-19.3 ^{na}	-8.44 ^{na}	-201 ^{na}	-65.6 ^{na}	-10.2 ^{na}	31.9 ^{na}	-22 ^{na}	0.633 ^{na}	-199 ^{na}	379 ^{na}	-54.7 ^{na}	1.87 ^{na}	-19.9 ^{na}	3.36 ^{na}
	Toisondor	19.4	-5.04 *	17.5	6 *	10.1	23.1 **	18.3	0.147	19	44.3 ·	19.3 ·	1.17 *	19.6 ·	-2.29 *
	mean	-1.82^{ns}	-5.39^{***}	-26.0^{ns}	-0.77^{ns}	-6.44^{ns}	10.48^{*}	2.50^{ns}	0.13^{ns}	-10.4^{ns}	61.2^{ns}	0.94^{ns}	0.76^{**}	-2.91^{ns}	-1.93^{ns}
	sd	29.4	2.89	73.7	28.2	36.4	11.7	30.9	0.23	80.8	123	35.6	0.62	30.6	3.40

Table 3.3: Partial regression: individual E and G intercept (β_0) and slopes (β_1) from the relationships between partial residuals of the inflexion point of flag leaf senescence (I_1) and the explaining variables selected in the model. The average of the coefficients (β_0 and β_1) across the environment or cultivar and the standard deviation are given. The significance of the mean was tested according to a t test. Coefficient significance level ($H_0 : \beta = 0$): (.), 0.1; (*), 0.05; (**), 0.01; (***),0.01; (na), non applicable.

		$I_1 = f(GNe)$		$I_1 = f(GNm)$		$I_1 = f(Heading)$		$I_1 = f(W18^{s22}_{L4})$		$I_1 = f(R6^{s4}_{L2})$	
EG	group	β_0	β_1	β_0	β_1	β_0	β_1	β_0	β_1	β_0	β_1
E	07-18	-18.3	-10.4 *	-19.4	0.0175 ·	-102	-19.7 ·	-8.31	0.483	-28.6	-0.114
	07-22	-42.4 ·	-4.77	-47.9 *	0.0084	-52.3 *	-7.27 *	-78.5 ·	0.539	-39	-0.0499
	07-27	-16.9	-5.95	-19.1	0.0105	-1.2	-3.51	-42.9	-5.16	-15.9	-0.0655
	07-51	7.39	-9.89	-6.72	0.0212 ·	-96.6 *	-25.1 ***	-0.189	-1	2.73	-0.0805
	07-91	35.3 ·	-3.47	28.9 ·	0.0125 ·	37.9	-7.92 ·	28.7	-1.46	29.6 ·	-0.0494
	08-18	13.5	-6.08 *	18.5	0.0102 ·	20.1 *	-5.62 ***	16.9	-0.849	9.34	-0.0669
	08-22	18.8	2.05	48.6 *	0.00337	19.9	-3.55	40.6 *	0.872	36.7 *	0.0118
	08-51	-11.9	-10.2	25.2	0.0261 *	4.58	-10.2 *	-8.78	0.0239	4.48	-0.03
	08-91	-16.3	-3.72	-18.5	0.015 ·	-6.5	-11.7 *	-16.1	-1.63	-19.3	-0.000173
	mean	-3.43^{ns}	-5.8**	1.07^{ns}	0.0139***	-19.6^{ns}	-10.5**	-7.62^{ns}	-0.909^{ns}	-2.22^{ns}	-0.0495**
	sd	23.9	4.03	30.8	0.0069	51.7	7.39	36.5	1.84	25.6	0.039
G	Apache	-10.4	-5.14	-6.16	0.00595	-12.9	-8.31 *	-27.8	0.163	-12.5	-0.0808
	Charger	3.18	-11.1	-8.82	0.00731	-10.1	-7.45 ***	1.93	-0.762	-2.28	-0.0482
	Dinosor	-20.3	-2.85	-17.6	0.0132	-28.2	-6.18 ·	-15	-0.712	-16.8	-0.0583
	Koreli	-191 ^{na}	138 ^{na}	58.8 ^{na}	-0.001 ^{na}	91.5 ^{na}	-21.8 ^{na}	-52.5 ^{na}	-9.73 ^{na}	120 ^{na}	0.353 ^{na}
	Paledor	25.4 ·	-9.91 ***	14	0.0232 **	11.7	-8.72 ***	6.93	-0.511	9.13	-0.0665
	Rosario	-370 ^{na}	123 ^{na}	-19.4 ^{na}	-0.0112 ^{na}	60.7 ^{na}	-18.6 ^{na}	-38.1 ^{na}	-5.55 ^{na}	-35 ^{na}	0.885 ^{na}
	Royssac	-0.337	-6.42 ·	6.76	0.0188 ·	-3	-10.8 ***	0.632	-1.71	-2.11	-0.0632
	Sogood	-18 ^{na}	-12.9 ^{na}	-276 ^{na}	-0.188 ^{na}	-12.3 ^{na}	-14.1 ^{na}	-90.1 ^{na}	-6.86 ^{na}	-36.4 ^{na}	-0.435 ^{na}
	Toisondor	15.3	-5.25	6.11	0.0158 *	3.54	-11.6 ***	13	-2.55	14.7	0.0144
	mean	-63.0^{ns}	23.1^{ns}	-26.0^{ns}	-0.0013^{ns}	11.2^{ns}	-11.4***	-22.3^{ns}	-3.14*	4.25^{ns}	0.0556^{ns}
	sd	132.3	61.1	96.4	0.066	39.2	5.29	33.7	3.44	46.7	0.369

Table 3.4: Partial regression: individual E and G intercept (β_0) and slopes (β_1) from the relationships between partial residuals of the inflexion point of leaf 4 senescence (I_4) and the explaining variables selected in the model. The average of the coefficients (β_0 and β_1) across the environment or cultivar and the standard deviation are given. The significance of the mean was tested according to a t test. Coefficient significance level ($H_0 : \beta = 0$): (.), 0.1; (*), 0.05; (**), 0.01; (***),0.01; (na), non applicable.

		$I4 = f(GNm)$		$I4 = f(Heading)$		$I4 = f(LAI\ 1)$		$I4 = f(LAI\ 3)$		$I4 = f(W7_{L4}^{s15})$		$I4 = f(T0_{L2}^{s21})$	
EG	group	β_0	β_1	β_0	β_1	β_0	β_1	β_0	β_1	β_0	β_1	β_0	β_1
E	07-18	-33.1	0.00254	-26.4	-3.41	-42.1	-153	-59.6 *	661	-42 ·	-2.3 *	-37.2	6.93
	07-22	-7.71	0.0136 *	-10.7	-7.21 ·	-12.9	-190 *	-13.3	291 *	-9.55	-1.71 ·	0.564	21.8
	07-27	-8.78	0.00174	12.1	-5.7	33.9	-229 ***	42.3	386 *	1.99	-3.12 *	13.7	-5.32
	07-51	-16.8	0.0136	-18.6	-8.33	-18.1	-176 *	-8.53	296 *	-19.4	-0.529	4.68	-18.2
	07-91	56.7 *	0.0261 *	0.647	-12.6	38.3	-115	67.5 ·	0.826	51.6 *	-0.0209	36.2	28.7
	08-18	12.3	0.0142	23.9	-0.688	18.3	-118	55.6	-169	1.66	-0.868	18.8	29 ·
	08-22	-1.44	0.00702	-29.9	0.787	-13.6	-120	-17.8	30.5	-42.7	-4.76 ·	15.5	33.4
	08-51	5.54	0.0142	53.7	-13.7	-5.16	-137	-0.15	324	18.5	-3.67	5.16	-8.76
	08-91	-35.4	0.0326 *	6.32	-8.79	-0.704	-201	-4.31	208	-9.36	0.304	24.9	-39
	mean	-3.19^{ns}	0.014**	1.23^{ns}	-6.62**	-0.22^{ns}	-160***	6.86^{ns}	226*	-5.47^{ns}	-1.85*	9.13^{ns}	5.34·
	sd	28	0.01	27	4.92	26	41.4	41	245	29	1.74	21	25
G	Apache	-20.4	0.00757	-13.6	-5.33	-28.5	-114	-14.4	289 **	-14.2	-2.35	-9.08	3.29
	Charger	-2.42	0.012	-2.61	-5.84 *	9.54	-96.6	-2.76	194 ·	-2.56	-3.06 ***	-0.201	-3.79
	Dinosor	13.8	0.0065	17.3	-1.25	28.7	-51	21.2	192	12.2	-2.61 ***	8.03	-8.36
	Koreli	-15.4 ^{na}	0.0217 ^{na}	-33.7 ^{na}	4.95 ^{na}	-30.6 ^{na}	397 ^{na}	6.64 ^{na}	-314 ^{na}	99.6 ^{na}	8.13 ^{na}	-48.5 ^{na}	126 ^{na}
	Paledor	24.4	0.00928	32.1	-0.386	21.7	-145	22	280 ·	19.5	-2.05	15.4	6.01
	Rosario	16.8 ^{na}	0.00985 ^{na}	20.6 ^{na}	-6.43 ^{na}	1.12 ^{na}	-293 ^{na}	18.3 ^{na}	272 ^{na}	14.6 ^{na}	-2.46 ^{na}	19 ^{na}	9.36 ^{na}
	Royssac	-32	-0.00519	-21.3	-12.7 ·	-14.5	-132	-14.9	163	-21.9	0.398	1.94	42.3 ·
	Sogood	-21.4 ^{na}	0.00434 ^{na}	-12.2 ^{na}	-7.4 ^{na}	-52.4 ^{na}	-342 ^{na}	-18.2 ^{na}	307 ^{na}	-29.3 ^{na}	-3.93 ^{na}	-12.1 ^{na}	-3.29 ^{na}
	Toisondor	-8.73	0.015	-0.448	-6.83 ·	-4.49	-129	2.15	278	-6.04	-0.669	-18.5	40.4
	mean	-5.02^{ns}	0.010***	-1.54^{ns}	-4.57*	-7.70^{ns}	-101^{ns}	2.21^{ns}	185*	8.01^{ns}	$-0.96ns$	-4.90	23.6^{ns}
	sd	20	0.007	21	5.04	26	209	16	194	38	3.64	21	42.6

Table 3.5: Partial regressions: individual slopes corresponding to partial correlation between the grain weight (TGW) and explaining variables selected in the model. The average of the coefficients (β_0 and β_1) across the environment or cultivar and the standard deviation are given. The significance of the mean was tested according to a t test. Coefficient significance level ($H_0: \ \beta = 0$): (.), 0.1; (*), 0.05; (**), 0.01; (***),0.01; (na), non applicable.

		$TGW = f(GNm)$		$TGW = f(R54^{s15}_{post\ H})$		$TGW = f(T6^{s15}_{H})$		$TGW = f(W24^{s15}_{post\ H})$		$TGW = f(X36^{s15}_{H})$		$TGW = f(W46^{s15}_{H})$	
EG	group	β_0	β_1	β_0	β_1	β_0	β_1	β_0	β_1	β_0	β_1	β_0	β_1
E	07-18	0.3	-0.00073	0.022	-0.011	-0.74	1.9	-2	-0.017	0.041	0.12	0.06	-0.07
	07-22	0.26	-0.00028	0.19	-0.0085 $^{\cdot}$	0.13	0.98	0.46	-0.062	-0.14	0.03	-0.89	-0.04
	07-27	-1.5	-0.0014 *	-0.51	-0.014 *	0.5	2.5	-0.56	-0.092 *	-0.55	0.021	-0.17	-0.034
	07-51	0.39	-0.0016 *	-0.047	-0.0064	-0.69	1.7	1.7	0.017	2.3	0.25	0.19	-0.16
	07-91	-1.6	-0.0011 *	0.63	0.003	0.24	-0.93	1.4	0.12	-0.65	-0.024	-1.2	-0.25 $^{\cdot}$
	08-18	-0.25	-0.00096 *	0.014	-0.012	-1.4	2.6 $^{\cdot}$	-1.6	-0.0095	-1.3	0.13 *	-0.74	-0.17 *
	08-22	1.6	-0.0013 *	1.2	-0.0038	-0.19	0.34	-0.48	-0.098	-7.3	0.36	4.2	0.11
	08-51	-2	-0.00072 $^{\cdot}$	-1.6	-0.0055	-0.49	-0.77	-0.37	-0.0027	-1.1	0.097	-0.034	-0.22 $^{\cdot}$
	08-91	0.63	-0.00012	1.8 *	-0.014	0.6	2.8	-0.015	-0.15 *	1.1 $^{\cdot}$	-0.068	2.6 **	0.27 $^{\cdot}$
	mean	-0.233^{ns}	-0.0009***	0.193^{ns}	-0.0081**	-0.231^{ns}	1.23*	-0.165^{ns}	-0.0332^{ns}	-0.837^{ns}	0.102^{ns}	0.447^{ns}	-0.062^{ns}
	sd	1.21	0.0005	0.994	0.006	0.668	1.42	1.25	0.0781	2.66	0.136	1.79	0.166
G	Apache	0.62	-0.00038	0.63	-0.0043	0.5	0.53	0.52	-0.027 *	0.56	0.036	0.33	-0.047
	Charger	-1.4 *	-0.00051 $^{\cdot}$	-0.84	-0.012 ***	-1.4 *	1	-1.3 *	-0.084 ***	-1.3 ***	0.14 **	-1.5 *	-0.13 *
	Dinosor	0.72	-5.1e-05	1.9 *	-0.017 ***	0.53	0.72	0.74	-0.074 *	0.74	0.11 *	0.44	-0.17 *
	Koreli	2.8 ^{na}	-0.00035 ^{na}	23 ^{na}	-0.68 ^{na}	2.5 ^{na}	2.5 ^{na}	1.1 ^{na}	-0.16 ^{na}	1.4 ^{na}	-0.079 ^{na}	3.4 ^{na}	0.04 ^{na}
	Paledor	-0.28	-0.00065 $^{\cdot}$	0.45	-0.003	-0.19	0.59	-0.33	-0.063 *	0.4	0.012	-0.3	-0.032
	Rosario	3 ^{na}	-0.00041 ^{na}	3.3 ^{na}	-0.011 ^{na}	2.5 ^{na}	1.9 ^{na}	2.9 ^{na}	-0.069 ^{na}	1.8 ^{na}	-0.037 ^{na}	3.3 ^{na}	-0.055 ^{na}
	Royssac	1.3	-8.1e-05	0.034	-0.012 $^{\cdot}$	0.42	1.2 $^{\cdot}$	0.56	-0.039	0.079	0.12 $^{\cdot}$	0.51	-0.14 *
	Sogood	2.7 ^{na}	-0.00028 ^{na}	4.1 ^{na}	-0.088 ^{na}	2.2 ^{na}	2.3 ^{na}	1.3 ^{na}	-0.12 ^{na}	0.92 ^{na}	-0.11 ^{na}	3.2 ^{na}	0.044 ^{na}
	Toisondor	-2.4 $^{\cdot}$	-0.00033	-1.8 *	-0.0049	-1.9 *	0.26	-1.9 *	-0.031	-1.8 $^{\cdot}$	0.079	-1.8 $^{\cdot}$	-0.097
	mean	0.788^{ns}	-0.0003***	3.41^{ns}	-0.092^{ns}	0.57^{ns}	1.22**	0.39^{ns}	-0.074***	0.311^{ns}	0.031^{ns}	0.835^{ns}	-0.065*
	sd	1.92	0.0002	7.55	2.22	1.61	0.82	1.43	0.043	1.18	0.091	2.00	0.076

3.3.4 External validation

3.3.4.1 Validation of the Random Forest models

In attempt to validate the method and the results from the Random Forest model fit, external data were used for which identical variables were available. The data considered so far came from Bancal et al. (2015). This study was based on three different datasets from which we used "Expe. C" because of its rather balanced composition in both cultivars and environments. The validation was carried out building a RF model with the datasets "Expe. A" and "Expe.B" (see Bancal et al., 2015). The fit quality of these new RF models was very comparable to the preceding ones (R^2 = 0.74, RMSE = 37.1 °Cd_H), the average bias was null, and bias per environment or per genotype was also null. However, the ranking of variables in order of importance was rather different, i.e., it is noteworthy the heading date was no longer selected. Looking more cautiously the data actually revealed that, amongst the three datasets, only "Expe. C" was characterised by a large range of heading dates (Fig. 3.11). Therefore, the other datasets were not useful to validate the ranking of the variables explaining *I* as they did not include a comparable range of explanatory variables.

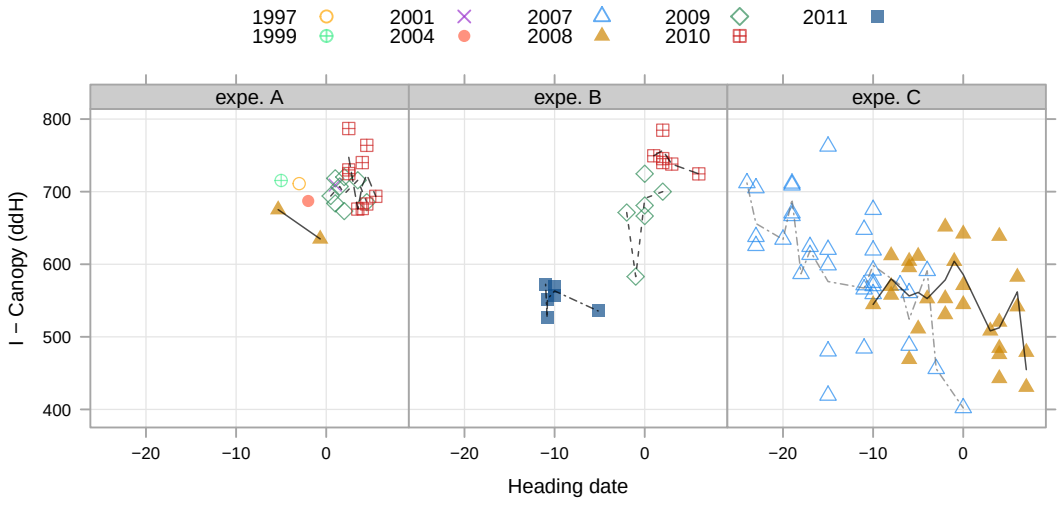


Figure 3.11: Relation between heading date and I in the three datasets (A, Grignon; B, Villiers-le-Bâcle; C, varsepto). Date are averaged per E and G. The symbols represent the year. Only the dataset C is associated with large Heading date variation every year.

3.3.4.2 Validation of the linear models

In order to also test the robustness and the limits of the results, it was checked if the selected multiple linear models were validated on independent data. Another separate dataset was used, characterised by a large number of genotypes and season-locations. However, fLA 1 data were not available despite this variable being needed for estimation of I (Eq. 3.6). Therefore, the closest model 3.10 that did not involve fLA 1 was checked, thus lowering somewhat its quality compared to Eq.3.6 as its R^2 was 0.59.

$$\begin{aligned} I = &- 178 + 0.070 \times [R46_H^{s15}] && (3.10)\\ &+ 29 \times [T6_H^{s15}] - 5 \times heading && R^2 = 0.59\\ &- 1.9 \times [W56_H^{s15}] + 0.76 \times [W16_H^{s15}] + 16 \times [T9_H^{s3}] \\ I = &1834 - 0.065 \times [R46_H^{s15}] && (3.11)\\ &- 75.7 \times [T6_H^{s15}] - 11.6 \times heading && R^2 = 0.67\\ &+ 7.14 \times [W56_H^{s15}] - 1.51 \times [W16_H^{s15}] - 5.11 \times [T9_H^{s3}] \end{aligned}$$

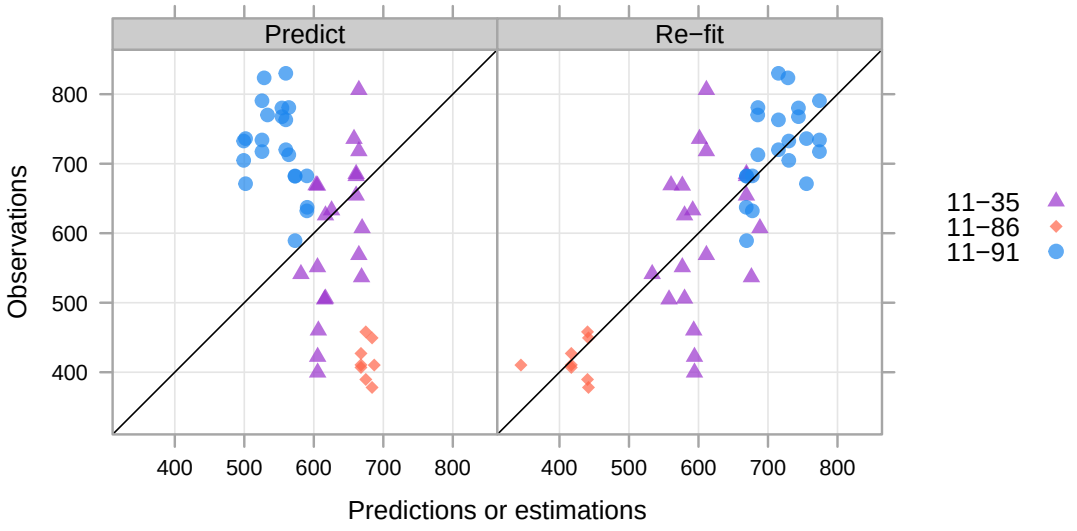


Figure 3.12: External validation: observations, predictions and estimations of I. The variable fLA 1 required in model 3.6 was not available in the validation dataset, it was fitted again without the variable (Eq. 3.10). From the external dataset, only the observations within the range of the data used to fit the model 3.10 were considered, the others were discarded, reducing substantially the number of observations for validation of the model. The left panel represents predictions of model 3.10. The right panel represents the estimation of the model once fitted to the external dataset (Eq. 3.11).

Regarding the new dataset, the predictions of this model (Eq. 3.10) were significantly

different from the observations (P < 0.001), according to both the Root Mean Square Error of Prediction (RMSEP) of 176 °Cd_H, and on a bias which varied with the environment (Fig. 3.12). Nonetheless, using the same explanatory variables, a third model can be fitted to the new dataset (Eq. 3.11). Accordingly, the differences between the observations and estimations within each experiment was null (P > 0.45) and the RMSE was then 76 °Cd_H. The early water balance ($W56_H^{s15}$) and the temperatures around heading stage ($T6_H^{s15}$) were significant (slopes: 7.1^{***}, 0.75^{**}, respectively) which highlights the importance of these variables on an independent dataset. Conversely, heading date was no longer significant whereas it was the main effect according to the Eq. 3.6. This was explained by the data obtained in the environment 11-35 and 11-86 which included only a narrow range of heading dates. Indeed, the experiment 11-91 which included 32 cultivars and genotypes maintained a high correlation between the heading date and I (r = 0.75^{***}).

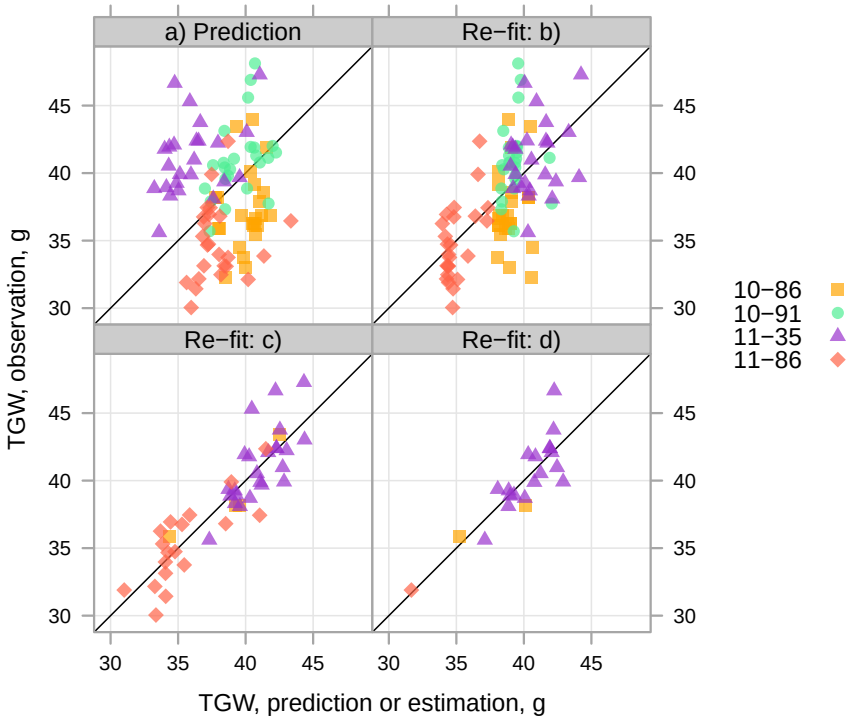


Figure 3.13: External validation: observations, predictions and estimations of TGW. a) Prediction of the TGW (Eq. 3.9) on the complete available validation dataset. The model was fitted on the complete validation dataset (b, Eq. 3.13), or alternatively restrict to the range of $W46_H^{s15}$ and $W36_H^{s15}$ studied in the learning dataset (c, Eq. 3.13), or restricted to the range of every variable from the learning dataset.

Likewise, the estimation model of TGW (Eq. 3.9) needed to be fitted again on the external dataset, as not doing so provides a prediction very different from the observations (Fig. 3.13a). A first re-fit on the complete available dataset (n=96) confirmed the significance of $W36_H^{s15}$, $T6_H^{s15}$ and $R54_{post\ H}^{s15}$ (slopes: 0.17^{***}, -0.98^{*}, -0.007^{*}, respectively)

for the TGW estimations (Eq. 3.12, Fig. 3.13b) while the GNm was no longer significant. However, the relation of TGW to GNm depends largely on the environment, the validation dataset increased largely the range of environments. To compare the performance of the model in comparable environments it was decided first to restricted the dataset to environments with an early water-balance comparable to those that were used to fit initially the TGW model (Eq. 3.13, Fig. 3.13c). As expected, controlling the environment variation the GNm variable was significantly and negatively associated with TGW in this new model, and the late radiation was no longer significant. Finally, the dataset was similarly restricted, but not only for early water-balance but for every explanatory variable of the model (Eq. 3.14, Fig. 3.13d). Therefore, the GNm and the early water balance ($W36_H^{s15}$) were very significant variables (slopes: -0.0011** and 0.29**).

$$\begin{aligned} TGW =& 74(\pm 8)^{***} - 5(\pm 14)\cdot 10^{-5} GNm^{ns} \\ &- 0.08(\pm 0.04)[W46_H^{s15}]^{ns} + 0.17(\pm 0.04)[W36_H^{s15}]^{***} - 0.98(\pm 0.49)[T6_H^{s15}]^{*} \\ &- 0.03(\pm 0.03)[W24_{post\ H}^{s15}]^{ns} - 0.007(\pm 0.003)[R54_{post\ H}^{s15}]^{*} \end{aligned} \quad \begin{aligned} &(3.12) \\ &n_{obs} = 96 \\ &R^2 = 0.40 \end{aligned}$$

$$\begin{aligned} TGW =& 115(\pm 10)^{***} - 1.1(\pm 0.2)\cdot 10^{-3} GNm^{***} \\ &+ 0.04(\pm 0.09)[W46_H^{s15}]^{ns} + 0.34(\pm 0.05)[W36_H^{s15}]^{***} - 2.0(\pm 0.7)[T6_H^{s15}]^{*} \\ &+ 0.10(\pm 0.05)[W24_{post\ H}^{s15}]^{*} - 0.005(\pm 0.003)[R54_{post\ H}^{s15}]^{ns} \end{aligned} \quad \begin{aligned} &(3.13) \\ &n_{obs} = 46 \\ &R^2 = 0.79 \end{aligned}$$

$$\begin{aligned} TGW =& 116(\pm 16)^{***} - 1.1(\pm 0.3)\cdot 10^{-3} GNm^{**} \\ &+ 0.03(\pm 0.11)[W46_H^{s15}]^{ns} + 0.29(\pm 0.09)[W36_H^{s15}]^{**} - 2.7(\pm 1.4)[T6_H^{s15}]^{\cdot} \\ &+ 0.11(\pm 0.08)[W24_{post\ H}^{s15}]^{ns} - 0.001(\pm 0.005)[R54_{post\ H}^{s15}]^{ns} \end{aligned} \quad \begin{aligned} &(3.14) \\ &n_{obs} = 21 \\ &R^2 = 0.74 \end{aligned}$$

If the models could not be directly used to predict I or TGW, the G×E interactions explained in the previous sections are probably involved. Nonetheless, after a new fit, the independent dataset confirmed the interest of some variables which were first identified by the RF models and also selected by the multiple regression model.

3.4 Discussion

Tolerance to STB aims at partly reducing the loss in yield due to non repeatable epidemics, thus making it difficult to quantify. It is, moreover, likely based upon addition of small effects contributed by multiple factors. Altogether tolerance could therefore benefit from data-mining of large datasets such as that obtained by high throughput phe-

notyping. This chapter is, to some extent, a feasibility study using the results of Bancal et al. (2015) that indicted the senescence timing of the leaves and the Thousand Grain Weight (TGW) to be the main determinants of the wheat tolerance of Septoria tritici blotch (STB). Yet determinism of senescence timings and TGW is not well understood. An important genotype (G) effect would confer high heritability required by plant breeders. Conversely, understanding environment (E) or G×E effect is required by agriculture consultants. In order to identify the main factors associated with the variations of *I* and TGW, a dataset (almost balanced) was selected gathering the results of former experiments in nine season-locations (E) and including up to nine cultivars (G) contrasting for senescence, TGW and STB resistance. The dataset was improved to obtain many climatic, phenological and agronomic variables to resemble what would be obtained from high throughput phenotyping. Then, a method was proposed, composed of three successive steps to identify the variables which are important to explain *I* or TGW, and to model the *I* or TGW response understanding the influence of E or G. To do so, the senescence timing and the TGW were first modeled by an holistic approach, without *a priori*, that applied the random forest modeling (RF). The RF results were used to identify the most important explanatory variables, as a starting point for the following stepwise multiple linear regression. Multiple linear regression thereby proposed accurate fits of response variables using five to seven explanatory variables. Variance component analysis (VCA) was used to quantify E, G or G×E variability of every response variable or important explanatory variable. Finally the E, G or G×E variability was investigated on the multiple linear regressions through the E or G simple regressions between partial residuals.

The successive methods used to analyse the data provided consistent and complementary results. They confirmed the interest of the RF models, which are associated with a very low number of constraints for application, and proposed interesting results even in the presence of highly correlated variables. Indeed, the large number of correlated variables prevented the direct use of stepwise regression as this procedure made the results highly dependent on an *a priori* hypothesis to run it. Thus, the preliminary ranking of the explanatory variables by RF regarding their importance estimated by the %IncMSE was needed to build conventional linear models. Conversely, the important variables identified by the RF method were confirmed by the linear models. In addition, the RF model results were consistent as they retained largely expected variables (e.g. the TGW depends on the GNm); but it also suggested new variables which were more unexpected that were *a posteriori* confirmed by the linear regression. This first step, without *a priori* was therefore very useful to suggest explanatory variables not previously identified by the literature and for which the link to response variables was not obvious.

3.4.1 Method

The analysis of multiple season-location and genotypes datasets is challenging. The environment (E) or the genotype (G) induce random variations which, if they are not taken into account, may reduce the relationship of y to x.

- **The Random Forest models**

The strategy applied in the present study consisted first of a large description of E and G, assuming that if much of E or G variation was explained, further interesting relationships could be revealed. However, this required a large increase in the number of variables, because, for instance, an extensive description of the climate was needed, which could also result in an increased number of correlated variables (e.g. within climate variables and also within canopy variables). Facing a relatively large number of potentially correlated variables, while the number of observations was relatively low, we decided to use a learning machine method: the Random Forest. This resulted in a valuable classification of all the variables, regarding their importance to explain the responses. Moreover, as the method worked without *a priori*, it allowed for the investigation and identification of unusual and sometimes unexpected relationships.

- **The multiple linear regression models**.

After having identified the important variables, we tried to understand how they influenced the responses (*What response y for a variation of x?*). The multiple linear regressions helped handling several quantitative explanatory variables and estimating the corresponding slopes; but unlike the RF models and by definition, these multiple regressions were restricted to linear relations to y. Starting from the most important variables (identified by the RF models), the non-significant variables (i.e. non-significant *linear* relation) were then removed; then whether the addition or removal of variables could improve the multiple linear model was tested while imposing a relatively low number of variables to facilitate later interpretation; and finally a multiple linear regression for each response was selected. The results of these models confirmed the important variables according to the RF model and gave more insights on the relation between x and y.

- **Variance component analysis**

The influence of the E and G was described on the identified explanatory variables and responses, running a variance component analysis. This helped understand what were the key determinants of each variable and provided an indirect estimation of broad sense heritability (variance proportion the G is accountable for). It also helped identify what source of variation was explained by the models, and what remained unexplained

(i.e. mostly environment induced variation of the senescence timing of the flag leaf ($I1$), and genotype induced variation of the TGW).

- **Mixed model use?**

The simple regression example between fLA 1 and heading date demonstrated (if need be) that taking into account the E and G variation was crucial to identify and estimate the relation between two variables in the case of multiple E and G datasets. In this example, using a mixed model, the E effect was taken into account as a random variable restricted to the intercept. Actually a range of models which differed in the way they take into account E or G random effect (E or G on the intercept and/or the slope) should firstly be compared, which was achieved from graphic representations and Fisher's tests suggesting in that case that the intercept was variable according to E but not the slope. Multiple regression now assumed that selected variables account partially for the E and G variations, and therefore facilitate further identification of potential explanatory variables. Yet, despite the residual variation being reduced, to assign it to E or G requires numerous hypotheses about the random effect that can not be verified. Therefore, the best use of the mixed models on multiple regression is complex.

- **E and G random effect and multiple linear regressions**.

As an easier alternative, it was decided to look at the partial residuals of the selected multiple linear models: the effect of E or G was then analysed by direct computation of the slopes and intercepts of the partial residuals of y and x. The interest of the partial regression is that they rely on the multiple regression models, and, therefore, what is already explained by the other variables of the model can account for E or G variance explanations, and allow observation of the specific effect of a considered explanatory variable itself. Computing the regressions and estimating the slopes and intercepts for each E or each G informs on which G effects were involved (if the slope across environment is different from 0) or which E effects were involved (if the slope of the genotypes exposed to several environments is significantly different from 0). If the corresponding slopes were significantly different according to G (or to E), then a G×E would be indicated and could be tentatively quantified.

3.4.2 Senescence timings

The senescence timings varied from two third with E and one third with G (the G×E was limited except for the leaf 4). The RF models followed by the linear regressions highlighted the senescence timing of the canopy depends on phenology (heading stage date), on leaf profile (fLA 1, fLA 3) and also the climate described at specific stages of

crop development. However, the main RF variables actually changed according to leaf layer, thus needing specific consideration.

- **Phenology**

First of all, the senescence timing of the canopy (I) or the flag leaf ($I1$) variations were found to be associated with the heading stage date, i.e. early heading was associated with a delayed senescence timing. Because senescence timings were computed since heading date, early canopies benefited from improved conditions for grain filling. On the other hand, senescence timings were computed in $°Cd_H$ while heading date was in days, the analysis therefore checked the reported effect was neither an unit artefact nor a simple shift of the senescence associated to a shift of heading stage. Actually the variability of the heading date was larger than the variability of the final senescence date. Some proportion, varying with the leaf layer, of the effect of heading date on senescence timings was linked to warmer days associated with later heading. In turn, the heading date varied largely because of genotype: there was generally a 10 to 15 day range in heading date in each experiment. In addition, the E effect, as estimated by the average heading date for each environment, also varied in a 15 day range. Finally, the VCA quantified that 40% of the observed variation in heading stage was due to the genotype while 60% was explained by the variation between environments.

The relationship of $I1$ to heading date was rather strong and, once the effect of other explanatory variables was deduced, it was poorly influenced by the random E- or G-effects. According to regressions of partial residuals, heading date explained the variations of both $I1$ observed between environment or between genotypes. The most significant effect of the heading date was observed on $I1$ and $I4$, but with different slopes. Heading date effect is, therefore, also probably associated with a varying contribution of the different leaf layers to grain filling.

- **Leaf profile**

Whereas neither LAI nor leaf area per shoot (LAe) were explanatory variables, the relative contribution of each leaf layer influenced the senescence timing. The senescence timing of the canopy (I) was delayed for a larger proportion of flag leaf in the canopy area (fLA 1). Nevertheless, if the effect was significant, it was strongly influenced by E or G as indicated by the variation in the slope of the partial regression of I and fLA 1 (Table 3.2). According to RF, fLA 1 was relatively important in explaining $I1$ as that variable ranked 13th, while fLA 3, negatively correlated with fLA 1, ranked third. Yet, these variables were not retained by the multiple regression $I1$ model (Eq. 3.7), pushed out by heading date. Indeed, according to mixed model, the G-variations of heading date were negatively correlated with those of fLA 1. Therefore, it is highly probable

that early heading date and/or large fLA 1 were associated with a delayed senescence timing of the flag leaf ($I1$). The relationship between heading date and fLA 1 could be confirmed/compared only to two studies. Firstly, according to Bancal (2017) (Bancal P. personal communication), manipulation of heading date by extended photoperiod did not affect fLA 1 while conversely manipulation of fLA 1 by shading during stem elongation did not change heading date. It suggests that their relationship did not rely directly on physiological process. However, in a recent study of the effects of vernalisation and photosensibility genes, Steinfort et al. (2017) found a relation between the day length at sowing of spring wheat and the surface of the flag leaf. The data reported in their study (Steinfort et al., 2017) enabled the calculation of fLA 1, and an ANOVA including a random effect of G on the average detected significantly higher fLA 1 for early sowing ($P < 0.001$). In the present study, the day length at Plelo (08-22) at GS30 ranged 10.6h to 12.2h. Similar to the well-defined relation between $I1$ and heading date, the senescence timing of leaf 4 ($I4$) was largely dependent on G and E variation of LAI 1 and LAI 3. So, genotypes described by — or environments generating — large LAI 1 or small LAI 3 are also associated with early senescence timing of the leaf 4.

Leaf senescence is known to be influenced by shade (Weaver and Amasino, 2001): a modification of quality (Causin et al., 2006; Rousseaux et al., 1996) or a diminution of the amount of light (Noodén et al., 1996) that reached the lower leaves increases their senescence rate. Importantly, greater LAI 1 (or the fLA 1 selected in the RF model $I4$) may, thus, increase the self-shading on the lower leaves and therefore lead to earlier senescence of leaf 4, decreasing $I4$. According to the RF model, the fLA 3 and fLA 4 were also amongst the most important explanatory variables of $I4$. It is noteworthy fLA 1 and fLA 3 were negatively correlated ($r = -0.92^{***}$), so when the contribution of the flag-leaf increased, the proportion of the leaf 3 decreased. Conversely, fLA 3 and fLA 4 were positively correlated ($r = 0.72^{***}$) which suggest an increase of the leaf 3 was also generally associated with an increase of leaf 4. Consequently, it is likely that an increase in LAI 3, as identified in the linear model, is actually associated with a decrease in fLA 1, and an increase in fLA 4, reducing the self-shading on the lower leaves.

Interestingly, VCA results suggested that the LAI 1 variations were mainly governed by genotype differences, while the LAI variations of lower leaves were mostly governed by E variations. It can be assumed the lower leaves are responsive to E variations as they are exposed to large E variations. Which is not the case of the flag leaf, which is not as much affected by the competition for the light as the lower leaves. Therefore, the flag-leaf LAI is a trait for which G variation is more repeatable between environments than the lower leaf LAIs.

- **Sink effects**

The wheat grain growth is assumed to be sink limited in high productivity environments (Borrás et al., 2004; Cartelle et al., 2006); therefore, it was assumed that the G×E combinations, grown according to the optimal local practices, that composed the dataset resulted mainly in sink limited grain yield. Although sink limited, the source/sink ratio varies and may affect the source availability for the grain carbohydrate accumulation in source organs. According to the literature, the carbohydrate accumulation could potentially lead to photosynthesis inhibition (Lemoine et al., 2013), despite long term demonstration it is not available by plants that store fructan in the vacuole instead of starch in chloroplasts. Besides, the accumulation of carbohydrates (review of Gregersen et al., 2008; Crafts-Brandner et al., 1984) or the increased C/N ratio during the grain filling period (barley study, Parrott et al., 2010) may also trigger senescence. Therefore, a large sink size may limit the accumulation of carbohydrate in the leaves (which is rapidly assimilated by the grain), and promote a delayed senescence. This could explain that a sink size index such as GNm was positively correlated with both I4 and I1, although not with I. The relation was better defined for I4, where the average G slope or average E slope of $I4$ to GNm were very significant. In $I1$ multiple regression model (Eq. 3.7), GNm was actually combined with GNe and their coefficients made them close to ENm, the variable preferentially selected by RF models of both $I1$ and I.

- **Climate**

Several climatic variables were found associated with the senescence timings. Many early climatic variables were identified. Some of them are probably linked to large contrasts between the environments. Indeed, the year 2007, unlike 2008, was generally associated with early heading date. Therefore, the early radiation detected as an explanation of I (46 days before heading) refers to the spring period, when the daily variation of global radiation due to the photoperiod are the largest, especially when comparing the early-heading year 2007 to 2008.

However, biological explanation may not be systematically relevant, even if associated with very early climatic variables. For instance, the water balance associated with $I4$ refers to the period of the leaf-4 emergence. In the French agronomic practices, the fungicide strategies generally do not target the infection prevention of leaf 4. Therefore, the water balance could be associated with the epidemic pressure on the leaf 4 which does not benefit from targeted fungicide protection.

3.4.3 The TGW

Although the RF model explaining the TGW proposed consistently the GNm as the most important variable, the low correspondence between observations and prediction in addition to the bias depending on the environment or on the genotype, suggested that the classification of the variables could be misleading. However, the multiple linear regression seemed better performing, and the only selected biological variable was the GNm negatively correlated with the TGW. The analysis of the E random variation was also consistent with the expectation: within a trial, there was generally a negative association between TGW and GNm, but the relation was hardly repeatable across different environments; the GNm and consequently the TGW accommodate with the environment resource availability.

The two early water-balance overlapping variables, if not of biological significance, were still interesting to support the assumption made when the methods were decided. Indeed, the two variables indicated the contrasting spring conditions between the two years during which the experiment were run. The year 2007, unlike 2008, was characterised by a spring drought, taking into account these variables in a multiple linear model was appropriate to control part of the random variation between environments. This partial control of E random variation probably helped a better estimation of the other variables included in the model, among which was GNm. However, when tested on an independent dataset (different set of genotypes and site-seasons), the 15-day water balance from 36 to 21 days before heading stage was highly significant. The physiological basis of this relation remains therefore unclear.

3.4.4 Hypotheses to improve tolerance of STB

Heading date appeared to be a major determinant of the leaf senescence timing; it is also probable that late senescence timing was associated with large fLA 1. The heading-date precocity could increase availability of the grain sources and tolerance, directly linked to an increase in the upper-leaf lifetime during the grain filling phase. Indeed, if part of the early heading date effect on senescence time was linked to the general increase in daily temperature, part of it also resulted in a direct extension of the green leaf lifetime during the grain-filling phase, increasing substantially source availability. However, heading date was also associated with fLA 1.

The upward propagation of STB infections makes large symptoms less likely on the flag leaf. Therefore, the increase in contribution of the flag leaf to canopy-photosynthesis is believed to increase wheat tolerance of STB. Foulkes et al. (2006) found a positive correlation between tolerance of STB and the surface of the flag leaf in pairs of Near Isogenic Lines. In addition, Parker et al. (2004) assumed higher extinction coefficient could be a

tolerance traits, Bingham et al. (2009) suggested prostrate flag-leaf was associated with barley tolerance of *Rhynchosporium* leaf scald (although they also signified a wider range of extinction coefficient in barley than in wheat), increasing the contribution of the flag-leaf, and they also emphasize the potential for tolerance in increasing upper-leaf contribution. However, Bancal et al. (2015) reported an increase in the yield loss associated with the large flag-leaf lamina area while the delayed senescence timing reduced the yield loss. Therefore, the promotion of STB tolerance by higher contribution of the flag leaf should not rely on its lamina area but rather on its senescence timing. This chapter emphasized that the manipulation of the canopy trait fLA 1 is associated with senescence timings which could in turn explain tolerance of STB.

The direct effect of senescence timings on tolerance or the indirect effect of heading date and proportion of flag leaf (fLA 1) were studied and identified in healthy crops. However, it should be noted that heading stage and canopy description are also susceptible to modify epidemics. Indeed, early heading stage is a known factor which increases disease severity. Murray et al. (1990) explained that late sowing date of winter wheat (resulting in late heading) would reduce primary infections because of low temperatures. Shaw and Royle (1993) signified also that the early sowing favours a development of upper leaves — whose contribution to the grain filling can be very high — which is slower and better synchronized with the susceptible phase of the infection cycle. In addition, it was also demonstrated that the lush canopy promotes the STB epidemics (Lovell et al., 1997), when in the present study, the increase in EN quantified by the combination of the GNe and GNm effects, also delayed the senescence of the flag leaf. These mechanisms relating to source of avoidance of STB were also demonstrated in the Septo3D model (Robert et al., 2008, 2009). Therefore, it would be interesting to use such a model to quantify the yield protection which is lost by lowering avoidance in regard to the potential yield protection offered by improved tolerance through the putative tolerance traits: heading date, fLA 1 and ear density.

Foulkes et al. (2006) identified the grain sink capacity negatively correlated with tolerance in historic wheat UK cultivars; they proposed that the increase in GNm — being the main factor of improvement of the UK cultivar (Shearman et al., 2005) — induced an decrease in the sink growth limitation resulting in cultivar more susceptible to source shortage as STB can produce. In the present chapter, the role of GNm was complex as it seemed to increase the senescence timings of the leaf 1 and 4, although for the leaf 1, because in association with GNe, seems rather an indication of the ear density per m^2. In addition, the GNm was negatively associated with the TGW, but the effect of TGW on tolerance is rather difficult to predict for now as Bancal et al. (2015) suggested a general negative correlation but in dataset where nitrogen fertilisation level could vary substantially, the association between tolerance and TGW was no longer visible when restricted

to standard fertilisation treatment.

STB tolerance will be considered by breeders if it depends on traits which are easily accessible, easy to measure, and with low effect of the environment, i.e. highly heritable. From this standpoint, heading stage is interesting as well as the LAI 1 which were observed to be mainly dependent on the genotype, moderately affected by the environment, and highly linked to the leaf senescence timing. Finally, the grain sink effect is more challenging. If it is assumed that carbohydrate accumulation can occur when the sink is saturated and trigger senescence; then the large sink size, relative to the source availability, might decrease the accumulation of carbohydrates (which are rapidly assimilated by the grain) and therefore promote long leaf life as observed for the leaf 1 and 4. In addition, a lower accumulation in the non-sink organs might also avoid inhibition of the photosynthesis. A reduced Source/Sink ratio is not expected to confer tolerance, but extended leaf life is.

References

AHDB. *Wheat disease maagement guide*. AHDB, 2016. URL https://cereals.ahdb.org.uk/media/176167/g63-wheat-disease-management-guide-february-2016.pdf.

P. Bancal. Data: Précocité et surface de feuille étendard. Personal communication, project CP2P2, Aug 2017.

P. Bancal, M.-O. Bancal, F. Collin, and D. Gouache. Identifying traits leading to tolerance of wheat to Septoria tritici blotch. *Field Crops Research*, 180:176–185, 2015. doi: 10.1016/j.fcr.2015.05.006 .

D. Bates, M. Mächler, B. Bolker, and S. Walker. Fitting linear mixed-effects models using lme4. *Journal of Statistical Software*, 67(1):1–48, 2015. doi: 10.18637/jss.v067.i01 .

I. J. Bingham, D. R. Walters, M. J. Foulkes, and N. D. Paveley. Crop traits and tolerance of wheat and barley to foliar disease. *Annals of Applied Biology*, 154:159–173, 2009. doi: 10.1111/j.1744-7348.2008.00291.x .

L. Borrás, G. A. Slafer, and M. E. Otegui. Seed dry weight response to source sink manipulations in wheat, maize and soybean: a quantitative reappraisal. *Field Crops Research*, 86(23):131–146, 2004. ISSN 0378-4290. doi: 10.1016/j.fcr.2003.08.002 .

L. Breiman. *Manual On Setting Up, Using, And Understanding Random Forests*. URL https://www.stat.berkeley.edu/~breiman/Using_random_forests_V3.1.pdf. V3.1.

L. Breiman. Random forests. *Machine Learning*, 45(1):5–32, 2001. ISSN 1573-0565. doi: 10.1023/A:1010933404324 .

J. Cartelle, A. Pedró, R. Savin, and G. A. Slafer. Grain weight responses to post-anthesis spikelet-trimming in an old and a modern wheat under mediterranean conditions. *European Journal of Agronomy*, 25(4):365–371, 2006. ISSN 1161-0301. doi: 10.1016/j.eja.2006.07.004 .

H. F. Causin, R. N. Jauregui, and A. J. Barneix. The effect of light spectral quality on leaf senescence and oxidative stress in wheat. *Plant Science*, 171(1):24–33, Jul 2006. ISSN 0168-9452. doi: 10.1016/j.plantsci.2006.02.009 .

P. Cheval, A. Siah, M. Bomble, A. D. Popper, P. Reignault, and P. Halama. Evolution of QoI resistance of the wheat pathogen *Zymoseptoria tritici* in Northern France. *Crop protection*, 92:131–133, Feb 2017. ISSN 0261-2194. doi: 10.1016/j.cropro.2016.10.017 .

F. Collin, P. Bancal, J. Foulkes, and M. O. Bancal. A statistical analysis of gxe contribution to leaf senescence during grain filling in wheat. In *ESA 14 - Growing landscapes - Cultivating innovative agricultural systems*, pages 13–14, Edinburgh, Scotland, September 2016a. ESA. Poster presentation - session 12.

F. Collin, D. Gouache, M.-O. Bancal, and P. Bancal. Tolerance of wheat to Septoria tritici blotch; genetic vs environmental variations of key traits. In *9th International Symposium on Septoria Diseases of Cereals*, page 76, Paris, France, April 2016b. ISSDC. Poster presentation.

J. Conway, D. Eddelbuettel, T. Nishiyama, S. K. Prayaga, and N. Tiffin. *RPostgreSQL: R interface to the PostgreSQL database system*, 2016. URL https://CRAN.R-project.org/package=RPostgreSQL. R package version 0.4-1.

H. J. Cools and B. A. Fraaije. Update on mechanisms of azole resistance in Mycosphaerella graminicola and implications for future control. *Pest management science*, 69(2):150–155, 2013. doi: 10.1002/ps.3348 .

S. J. Crafts-Brandner, F. E. Below, V. A. Wittenbach, J. E. Harper, and R. H. Hageman. Differential senescence of maize hybrids following ear removal II. Selected leaf. *Plant Physiology*, 74(2):368–373, 1984. doi: 10.1104/pp.74.2.368 .

S. J. Crafts-Brandner, R. Hölzer, and U. Feller. Influence of nitrogen deficiency on senescence and the amounts of RNA and proteins in wheat leaves. *Physiologia Plantarum*, 102(2):192–200, 1998. ISSN 1399-3054. doi: 10.1034/j.1399-3054.1998.1020206.x .

M. Crawley. *Statistics: an introduction using R*, chapter Mixed-effects models, pages 627–660. Wiley, 2007.

H. Fones and S. Gurr. The impact of Septoria tritici blotch disease on wheat: An EU perspective. *Fungal Genetics and Biology*, 79:3 – 7, 2015. ISSN 1087-1845. doi: 10.1016/j.fgb.2015.04.004 . Septoria tritici blotch disease of wheat: Tools and techniques to study the pathogen Zymoseptoria tritici.

M. J. Foulkes, N. D. Paveley, A. Worland, S. J. Welham, J. Thomas, and J. W. Snape. Major genetic changes in wheat with potential to affect disease tolerance. *Phytopathology*, 96:680–688, 2006. URL http://apsjournals.apsnet.org/doi/pdf/10.1094/PHYTO-96-0680.

B. A. Fraaije, C. Bayon, S. Atkins, H. J. Cools, J. A. Lucas, and M. W. Fraaije. Risk assessment studies on succinate dehydrogenase inhibitors, the new weapons in the battle to control Septoria leaf blotch in wheat. *Molecular Plant Pathology*, 13(3):263–275, 2012. ISSN 1364-3703. doi: 10.1111/j.1364-3703.2011.00746.x . URL http://dx.doi.org/10.1111/j.1364-3703.2011.00746.x.

R. Genuer, J.-M. Poggi, and C. Tuleau-Malot. Variable selection using random forests. *Pattern Recogn. Lett.*, 31(14):2225–2236, Oct. 2010. ISSN 0167-8655. doi: 10.1016/j.patrec.2010.03.014 . URL http://dx.doi.org/10.1016/j.patrec.2010.03.014.

D. Gouache. Toward a new indicator of cultivar resistance to Septoria tritici blotch accounting for cultivar phenology. *unpublished*, 2009.

D. Gouache, A. Bensadoun, F. Brun, C. Pagé, D. Makowski, and D. Wallach. Modelling climate change impact on Septoria tritici blotch (STB) in France: accounting for climate model and disease model uncertainty. *Agricultural and Forest Meteorology*, 170:242–252, 2013. doi: 10.1016/j.agrformet.2012.04.019 .

P. Gregersen, P. Holm, and K. Krupinska. Leaf senescence and nutrient remobilisation in barley and wheat. *Plant Biology*, 10(s1):37–49, 2008. doi: 10.1111/j.1438-8677.2008.00114.x .

P. L. Gregersen, A. Culetic, L. Boschian, and K. Krupinska. Plant senescence and crop productivity. *Plant Molecular Biology*, 82(6):603–622, Aug 2013. ISSN 0167-4412. doi: 10.1007/s11103-013-0013-8 .

R. Lemoine, S. La Camera, R. Atanassova, F. Dédaldéchamp, T. Allario, N. Pourtau, J.-L. Bonnemain, M. Laloi, P. Coutos-Thévenot, L. Maurousset, et al. Source-to-sink transport of sugar and regulation by environmental factors. *Frontiers in Plant Science*, 4: 1–21, 2013. doi: 10.3389/fpls.2013.00272 .

A. Liaw and M. Wiener. Classification and regression by Rrandom Forest. *R News*, 2(3): 18–22, 2002. URL http://CRAN.R-project.org/doc/Rnews/.

D. J. Lovell, S. R. Parker, T. Hunter, D. J. Royle, and R. R. Coker. Influence of crop growth and structure on the risk of epidemics by Mycosphaerella graminicola (Septoria tritici) in winter wheat. *Plant Pathology*, 46(1):126–138, Feb 1997. ISSN 0032-0862. doi: 10.1046/j.1365-3059.1997.d01-206.x .

G. M. Murray, R. H. Martin, and B. R. Cullis. Relationship of the severity of Septoria tritici blotch of wheat to sowing time, rainfall at heading and average susceptibility of wheat cultivars in the area. *Australian journal of agricultural research*, 41(2):307–315, 1990. doi: 10.1071/AR9900307 .

B. Ney, M.-O. Bancal, P. Bancal, I. J. Bingham, J. M. Foulkes, D. Gouache, N. D. Paveley, and J. Smith. Crop architecture and crop tolerance to fungal diseases and insect herbivory. Mechanisms to limit crop losses. *European Journal of Plant Pathology*, 135(3): 561–580, 2013. ISSN 0929-1873. doi: 10.1007/s10658-012-0125-z .

L. D. Noodén, J. W. Hillsberg, and M. J. Schneider. Induction of leaf senescence in Arabidopsis thaliana by long days through a light-dosage effect. *Physiologia Plantarum*, 96(3):491–495, 1996. ISSN 1399-3054. doi: 10.1111/j.1399-3054.1996.tb00463.x .

K. Ono, I. Terashima, and A. Watanabe. Interaction between nitrogen deficit of a plant and nitrogen content in the old leaves. *Plant and Cell Physiology*, 37(8):1083–1089, 1996. doi: 10.1093/oxfordjournals.pcp.a029057 .

S. R. Parker, S. Welham, N. Paveley, J. M. Foulkes, and R. K. Scott. Tolerance of Septoria leaf blotch in winter wheat. *Plant Pathology*, 53(1):1–10, 2004. doi: 10.1111/j.1365-3059.2004.00951.x .

D. L. Parrott, J. M. Martin, and A. M. Fischer. Analysis of barley (Hordeum vulgare) leaf senescence and protease gene expression: a family C1A cysteine protease is specifically induced under conditions characterized by high carbohydrate, but low to moderate nitrogen levels. *New Phytologist*, 187(2):313–331, 2010. ISSN 0028-646X. doi: 10.1111/j.1469-8137.2010.03278.x .

R Core Team. *R: A Language and Environment for Statistical Computing*. R Foundation for Statistical Computing, Vienna, Austria, 2017. URL https://www.R-project.org/.

R Special Interest Group on Databases. *DBI: R Database Interface*, 2014. URL https://CRAN.R-project.org/package=DBI. R package version 0.3.1.

R. Rakotomalala. Pratique de la régression linéaire multiple — Diagnostic et sélection de variables. Version 2.1, May 2015. URL https://eric.univ-lyon2.fr/~ricco/cours/cours/La_regression_dans_la_pratique.pdf.

C. Robert, C. Fournier, B. Andrieu, and B. Ney. Coupling a 3D virtual wheat (Triticum aestivum) plant model with a Septoria tritici epidemic model (Septo3D): a new approach to investigate plant–pathogen interactions linked to canopy architecture. *Functional Plant Biology*, 35:997–1013, 2008. doi: 10.1071/FP08066 .

C. Robert, B. Andrieu, C. Fournier, D. Gouache, P. Gate, and B. Ney. Septo3D: un modèle pour analyser les effets de la structure des couverts de blé sur les épidémies de septoriose. In *9. Conférence internationale*, page np, Tours, France, Dec. 2009. Association Française de Protection des Plantes. URL https://hal.archives-ouvertes.fr/hal-01192172. Actes sous forme de cédérom + tome résumés.

M. C. Rousseaux, A. J. Hall, and R. A. Sánchez. Far-red enrichment and photosynthetically active radiation level influence leaf senescence in field-grown sunflower. *Physiologia Plantarum*, 96(2):217–224, 1996. ISSN 1399-3054. doi: 10.1111/j.1399-3054.1996.tb00205.x .

D. Sarkar. *Lattice: Multivariate Data Visualization with R*. Springer, New York, 2008. URL http://lmdvr.r-forge.r-project.org. ISBN 978-0-387-75968-5.

D. Sarkar and F. Andrews. *latticeExtra: Extra Graphical Utilities Based on Lattice*, 2016. URL https://CRAN.R-project.org/package=latticeExtra. R package version 0.6-28.

M. W. Shaw and D. J. Royle. Factors determining the severity of epidemics of Mycosphaerella graminicola (Septoria tritici) on winter wheat in the UK. *Plant Pathology*, 42(6):882–899, 1993. ISSN 1365-3059. doi: 10.1111/j.1365-3059.1993.tb02674.x .

V. J. Shearman, R. Sylvester-Bradley, R. K. Scott, and M. J. Foulkes. Physiological processes associated with wheat yield progress in the UK. *Crop Science*, 45(1):175–185, 2005. doi: 10.2135/cropsci2005.0175 .

U. Steinfort, B. Trevaskis, S. Fukai, K. L. Bell, and M. F. Dreccer. Vernalisation and photoperiod sensitivity in wheat: Impact on canopy development and yield components. *Field Crops Research*, 201:108–121, 2017. doi: 10.1016/j.fcr.2016.10.012 .

V. Svetnik, A. Liaw, C. Tong, and T. Wang. *Multiple Classifier Systems: 5th International Workshop, MCS 2004, Cagliari, Italy, June 9-11, 2004. Proceedings*, chapter Application of Breiman's Random Forest to Modeling Structure-Activity Relationships of Pharmaceutical Molecules, pages 334–343. Springer Berlin Heidelberg, Berlin, Heidelberg, 2004. ISBN 978-3-540-25966-4. doi: 10.1007/978-3-540-25966-4_33 .

L. Taiz and E. Zeiger. *Plant physiology and development*, chapter Plant senescence and cell death, pages 665–692. Sinauer Associates, Inc., 6th edition edition, 2014.

H. Thomas and L. de Villiers. Gene expression in leaves of Arabidopsis thaliana induced to senesce by nutrient deprivation. *Journal of Experimental Botany*, 47(12):1845–1852, 1996. doi: 10.1093/jxb/47.12.1845 .

C. Uauy, J. C. Brevis, and J. Dubcovsky. The high grain protein content gene Gpc-B1 accelerates senescence and has pleiotropic effects on protein content in wheat. *Journal of Experimental Botany*, 57(11):2785–2794, Aug 2006. ISSN 0022-0957. doi: 10.1093/jxb/erl047 .

L. Weaver and R. Amasino. Senescence is induced in individually darkened Arabidopsis leaves, but inhibited in whole darkened plants. *Plant Physiology*, 127:876–886, 2001. doi: 10.1104/pp.010312 .

A. Wingler, S. Purdy, J. A. MacLean, and N. Pourtau. The role of sugars in integrating environmental signals during the regulation of leaf senescence. *Journal of Experimental Botany*, 57(2):391–399, Jan. 2006. ISSN 0022-0957, 1460-2431. doi: 10.1093/jxb/eri279 .

J. C. Zadoks, T. T. Chang, and C. F. Konzak. A decimal code for the growth stages of cereals. *Weed Research*, 44:415–421, 1974. doi: 10.1111/j.1365-3180.1974.tb01084.x .

Chapter 4

Field experiment at Hereford, 2014-15

This chapter is the subject of a peer-review article. It has been submitted to Field Crop research. Lastly, the editor has invited a revised version of the paper to be submitted (revision requested 7 September, due to 6 November 2017). Finally, the article has been accepted and published (Collin et al., 2018).

Title: Wheat lines exhibiting variation in tolerance of Septoria tritici blotch differentiated by grain source limitation

Abstract

Septoria tritici blotch (STB) is the most damaging disease of wheat crops in Europe. Because of the partial nature of genotypic resistance or the increasing resistance against fungicides, the tolerance, i.e. maintaining yield in the presence of expressed disease, is a relevant alternative. Tolerance is generally estimated through the yield loss per unit of source reduction, contrasts of tolerance between genotypes have been observed previously suggesting that either increasing the source availability or improving the use of stored assimilate could improve tolerance. This paper aims at developing a source/sink approach to understand the tolerance mechanism and identifying potential traits to increase tolerance of STB. A field experiment was designed to explore the relation between tolerance of STB and source/sink balance. Based on six wheat genotypes contrasting for tolerance exposed to natural STB epidemics, late nitrogen fertilisation and a 50% spikelet removal were applied to change the source/sink balance. The tolerance of genotypes was quantitatively estimated over three additional field experiments. We found that STB tolerance was correlated with traits of healthy crops (high individual grain weight and

high third last leaf lamina area as a proportion of the three upper leaves). The spikelet removal revealed a highly variable degree of source limitation for grain filling amongst the six genotypes. Thus, we proposed an easily calculated index that highly correlated positively with the labor intensive estimation of STB tolerance. Finally, potential yield and tolerance were not correlated, which suggests that breeding for yield performance and tolerance could be possible.

Highlights

- Tolerance of STB in six wheat genotypes was correlated with traits of healthy crops.
- Low source limitation for grain filling is a genotype-specific tolerance trait.
- The grain weight in healthy crops was colimited by source and sink.
- Sink manipulation by late degraining can help screening for STB tolerance traits.

4.1 Introduction

The Septoria tritici blotch (*Zymoseptoria tritici*, STB) is responsible for substantial grain yield loss of wheat crops in Europe (Burke and Dunne, 2006). Genotype resistances to the disease in wheat are partially effective, and fungicide-based strategies are marked by a sharp increase in pathogen resistance (e.g. northern France, Cheval et al. 2017, the UK, Fraaije et al. 2003). At the same time, economic, environmental and sociological contexts demand reduced use of inputs on wheat crops in Europe. Given these pressures and pathogen potential to circumvent genotype resistances or fungicide activity, disease tolerance - the maintenance of crop grain yield in the presence of expressed disease (Ney et al., 2013) - is a relevant approach to protect grain yield.

There is a genetic potential for tolerance of foliar diseases in wheat (e.g. hard wheat × leaf rust (*Puccinia recondita*), Kansas, USA, Salmon and Laude 1932; spring wheat × STB, Israel, Ziv and Eyal 1978). Formerly, Schafer (1971) considered tolerance as a relative property, evident by comparison of crops exposed to comparable severity disease (Bingham et al., 2009). Attempts to quantify tolerance have considered the effect of STB on the healthy area duration (HAD, the area under the green leaf lamina area progress curve) that summarises the variability of the canopy size across genotypes and sites and seasons (Parker et al., 2004). The STB symptoms on the upper leaves reduce the HAD, and therefore the grain yield loss per unit of HAD reduction was used as a quantitative trait of the wheat crops for STB intolerance in tolerance studies (Parker et al., 2004; Foulkes et al., 2006; Castro and Simón, 2016). Because of poor repeatability of STB epidemics,

however, the traits of healthy crops have been screened in an attempt to improve tolerance and understand underlying mechanisms (Bancal et al., 2015). Given the tolerance estimation method grain source or sink traits are potential candidate traits.

The grain yields of wheat crops in Europe are mostly sink limited or co-limited under favourable conditions (Acreche and Slafer, 2009; Slafer and Savin, 1994; Cartelle et al., 2006), but disease, through decreasing HAD, could modify this pattern. The source/sink balance in healthy crops might therefore be related to tolerance of foliar disease. Thus, when HAD per grain is high in healthy crops, yield loss is low when disease decreases HAD, resulting in high tolerance.

This was supported by Foulkes et al. (2006) who, studying three pairs of near isogenic lines (NILs), detected a negative correlation between STB tolerance and grains $\cdot$ m^{-2} indicative of crop sink size. It was assumed that the UK breeding trends led to the increase in grains $\cdot$ m^{-2} observed in modern cultivars in the study while maintaining equivalent potential grain size (Shearman et al., 2005); this increased grains $\cdot$ m^{-2} but also decreased the sink limitation conferring higher susceptibility to yield loss when exposed to source limitation because of STB. While studying wheat yield losses due to STB in France, Bancal et al. (2015) pooled the results of three field-experiments (seven sites, at least two seasons, and 18 varieties). They identified a highly significant negative correlation amongst cultivars between HAD per grain in healthy crops and intolerance. In other words high source/sink balance increased tolerance.

Source traits have also been found to be correlated with STB tolerance in wheat. Parker et al. (2004) hypothesised that increased radiation-use efficiency (above-ground dry matter per unit of radiation interception; RUE) associated with the 1BL/1RS chromosome translocation reduced tolerance: the loss of green area and light interception may cause larger source reduction in genotypes with higher RUE. The green canopy area, light extinction coefficient and leaf photosynthetic traits were proposed to be candidate traits for tolerance of STB (Parker et al., 2004; Bingham et al., 2009). Foulkes et al. (2006) identified on wheat near-isogenic lines (NILs) that the flag-leaf area was positively correlated with tolerance of STB, which could be related to the upward movement of the pathogen through the canopy leaf layers by rain-splash events with an advantage for those genotypes with relatively more light interception in the flag-leaf layer. Bancal et al. (2015) did not observe a significant effect of flag-leaf area, but they confirmed its interest through the timing of senescence: crops with later flag-leaf senescence exhibited greater tolerance.

It is possible that up-regulation of photosynthesis in remaining healthy tissues may compensate partially for source reduction caused by STB. The tolerant spring wheat cv. Miriam (Ziv and Eyal, 1978) showed an enhanced carbon fixation by the healthy tissues (Zuckerman et al., 1997). Furthermore, Reynolds et al. (2005) identified a positive correlation of post-anthesis RUE with sink demand in spring wheat, where grains $\cdot$ m^{-2} was

increased by row opening during booting, compared to a control treatment. Although not validated yet, tolerance could rely on post-anthesis RUE increase in response to lower assimilate availability relative to sink strength. More recently, Zhang et al. (2014) suggested a positive feedback from the sink strength on sources: an altered source/sink balance, decreased by ear shading or increased by spikelet removal treatments in wheat, led to either up-regulation or down-regulation of flag-leaf photosynthetic rate.

Several hypothesis were tested in the present study. Firstly, a high source/sink balance is a STB tolerance trait. Secondly, wheat is mainly sink limited, so manipulations that extend source or decrease sink would increase tolerance. Finally, genotype would impact similarly source:sink balance during grain filling and STB tolerance

The link between tolerance of STB and source/sink balance is important but remains largely unclear. Our aim was to investigate further this link using six wheat genotypes contrasting for tolerance of STB that were source/sink manipulated during a field experiment. The literature reports that source/sink manipulations after grain setting (e.g. shading, defoliation, ear trimming) have been used previously by other authors to understand the source/sink balance effect on grain growth and direct strategies to increase the yield of wheat (Serrago et al., 2013; Slafer and Savin, 1994; Ma et al., 1996) or barley (Cartelle et al., 2006) or soybean (Egli and Bruening, 2001). In this study, fungicide treatment was applied to induce differences in HAD reduction and yield loss linked to STB epidemic at the crop scale. In addition, a late nitrogen fertilizer treatment was applied at booting to delay leaf senescence thus increase source during grain filling. Lastly, a spikelet removal treatment was applied at anthesis plus 13 days, removing the upper half of ear. The HAD, yield and tolerance were calculated to test the preceding hypotheses.

4.2 Materials and methods

4.2.1 Genotypes screened for tolerance

The studied genotypes were part of a large panel derived from two doubled-haploid populations which were screened for STB tolerance and yield potential. The first population was derived from a cross between UK spring wheat Cadenza and UK winter wheat Lynx (C×L), the second from a cross between UK winter wheat Rialto and the Mexican CIMMYT spring wheat LSP2 of large ear-phenotype (LSP2×R). The LSP2×R lines were included in order to obtain a wider range of source/sink phenotypes to study STB tolerance in high yielding genotypes. The full details of this preliminary STB tolerance screening in three field experiments are out of the scope of this paper for which six genotypes were selected, that are contrasted for STB tolerance.

Briefly, these three experiments were sown: i) 8 October 2013 at ADAS (Herefordshire, United Kingdom, 52.2627 °N 2.8477 °W) following a crop of winter oats, ii) 10

October 2011 at ADAS (Herefordshire, United Kingdom, 52.1403 °N 2.8315 °W), and iii) 1 November 2011 at Teagasc Oak Park (Carlow, Ireland, 52.8637 °N 6.9136 °W) following a crop of winter oilseed rape. The crops were exposed to natural STB epidemics and fungicides were used to provide STB protection to contrast with control plots. Intolerance i_{eg} of each genotype (g) was calculated in each experiment (e) as $[\Delta Yield/\Delta HAD]_{eg}$ (grain yield loss per unit of healthy area duration reduction) as described by Foulkes et al. (2006). A genotype crop tolerance grade T (without unit) was then calculated as $-1\times$ the genotype average of i_{eg} standardized beforehand by environment (Eq. 4.1).

$$T = \frac{-1}{n_e} \sum_{e=1}^{3} \frac{i_{eg} - \mu_e}{sd_e} \tag{4.1}$$

With: μ_e, sd_e, n_e the environment average, standard deviation and number.

4.2.2 Experimental design and treatments

The main field experiment of our study was grown in 2014-5 on a silty clay loam soil in Herefordshire United Kingdom, 52.1403 °N 2.8315 °W). Air temperature (1 m above ground surface) was recorded hourly by a weather station at Weobley located 3 km from the site. Using a split plot design, the combinations of 6 genotypes (G) and 2 fungicide treatments (F) were allocated in 3 replicates, 36 main plots in total, according to a fully randomized design. The 36 main plots (2×14 m, 14 cm inter-row space, 12 rows) were sown on 28 October 2014, at a density of 350 seeds $\cdot$ m^{-2} and managed according to the local best practice, with the exception of fungicide and nitrogen management. Each plot was split into two zones for the application of the late nitrogen treatment (N). In addition, a direct sink manipulation treatment (S) was applied within each split plot, on ear-bearing shoots of average ear length (± 5%) which were identified at GS65 and tagged.

Two disease control treatments were applied (F) to obtain either a full control of STB (F1) or no control of STB (F0) while maintaining the non-targeted disease symptoms at low levels. This was based on three fungicide applications targeting growth stages (Zadoks et al., 1974) stem extension (GS32, 13 May), flag-leaf emergence (GS39, 30 May) and ear emergence (GS59, 10 June). Pyraclostrobin, proquinazid, cyflufenamid were used for F0 (to control rusts and mildew) and epoxiconazole, metconazole, chlorothalonil were added for F1 to control STB. Each combination of G and F was repeated in three replicates.

The general nitrogen fertilisation of the experimental area consisted of 220 kg N $\cdot$ ha^{-1}, split into 3 applications before GS51 on 21 March, 18 April and 9 May). In order to study the effect of nitrogen content at anthesis for a given canopy structure and grain number per ear, a late Nitrogen treatment (N) was applied at GS51 and consisted of an additional nitrogen fertilisation input (N1, +40 kg $\cdot$ ha^{-1}) versus a control (N0, +0 kg $\cdot$ ha^{-1}). The N1 treatment was applied on a 3 m plot length at the end of each plot. Using a backpack

sprayer equipped with a single 1 m length lance with a regular nozzle, 54 g of ammonium nitrate (34.4% of Nitrogen content) was applied under the canopy. An adjacent zone of 3 m length zone was dedicated to the control N0.

Genotype anthesis date (GS65) was precisely estimated for each genotype. Spikelet removal manipulation (S) was applied on average 13 days after anthesis (daa), which corresponded to a range of 163 – 271 °Cd after anthesis (degree-days, base temperature 0 °C). This timing prevented any effect on endosperm cell division potential grain weight and grain sink size (Dupont and Altenbach, 2003), while increasing assimilate availability per grain. Within each N treatment, the top-half of 10 randomly selected ears was removed (S1, the spikelets count divided by two, rounded up if odd number) while 20 other ears remained intact as a control (S0). This method reduced the wound stress and transpiration stream perturbations in the ear in comparison to spikelet removal from one side of the ear. No interaction has been found between genotype and the horizontal or vertical spikelet removal methods in spring wheat (Reynolds et al., 2012). The upper part of the ear was collected, oven dried and weighed. At this stage, three replicates of 6G × 2F × 2N × 2S = 48 treatment combinations were identified.

4.2.3 Crop measurements

Shortly before GS65, the length of 75 ears in total per genotype was measured randomly across all the plots in the experiment. Then 60 ear-bearing shoots representative of the average (±5%) of the genotype population were identified per plot and tagged. Five tagged shoots were cut at ground level in each nitrogen treatment within each plot at mid-anthesis (GS65, A) and at A+13 daa (day after anthesis, i.e. the day of spikelet removal treatment). Similarly, five-shoot samples were collected in each nitrogen × spikelet removal treatment combination at A+26 daa (387 – 483 °Cd after anthesis) and at maturity (i.e. after spikelet removal treatment).

The five-shoot samples were dissected. The lamina of leaf 1 (flag leaf), leaf 2 and leaf 3 was detached at the ligule. Green, diseased and senescent leaf lamina areas were visually scored for each leaf layer as a percentage of total leaf lamina area. Ears were cut at the ear collar and the stem and leaf sheath was separated into the upper internodes (peduncle, internode 2, internode 3) by cutting above the nodes and the remaining basal internodes. Each component was oven dried for 48 h at 80°C and weighed. Additionally, green and senescent and diseased percentage areas were scored *in situ* using the same methodology on a weekly basis in the weeks when no sampling was scheduled, totalling eight leaf lamina assessments from mid-anthesis to physiological maturity.

The width and length of the top three leaf layers were measured in each plot on four randomly selected ear-bearing shoots at two stages (GS59 and GS59 +20 days in each plot). Leaf lamina area per ear-bearing shoot (LAe) was estimated per leaf layer:

$width \times length \times 0.83$ (Bryson et al., 1997).

The number of fertile ears was counted at GS75 in four randomly selected 0.5 m row lengths per plot, to estimate the density of ear-bearing shoots (ENm, unit: shoots $\cdot$ m^{-2}). Grain number per ear (GNe) and thousand grain weight (TGW) were measured on the five-shoot samples at A+13 daa and at A+26 daa and at maturity. The two last assessments were averaged to provide GNe estimation. The yield per ear (Ye) was calculated from GNe and TGW. The ear density assessed at plot scale (ENm) was used to estimate the grains $\cdot$ m^{-2} (GNm) and the grain yield $\cdot$ m^{-2} at A+13 daa, at A+26 daa and at maturity (Ym, $Ym = ENm \cdot GNe \cdot TGW \cdot 1000^{-1}$).

4.2.4 Data analysis

In every replicate of G $\times$ F $\times$ N $\times$ S combination, percentage of Green Leaf Lamina Area (%GLA) kinetics were fitted to Eq. 6.1 (Bancal et al., 2015) for each leaf layer and for the cumulated three upper leaves (uppermost leaf being the flag leaf). For the whole dataset, R^2 was 0.98, and root mean square error of estimations was 5%GLA.

$$\%GLA(t,K,D,I) = K \cdot \exp\left(-\exp\left(\frac{2\times(I-t)}{D}\right)\right) \tag{4.2}$$

With: %GLA, percentage of green leaf lamina area; t, thermal time since heading stage (unit °Cd$_H$: degree-days since heading stage, base temp. 0 °C); K, left asymptote set to 100%; D, the duration of rapid senescence (approximately between 80% and 20% GLA; unit °Cd: degree-days base temp. 0 °C); I, inflexion point of the kinetic which occurs when 37% of the lamina area is green, indicating the time of the senescence (unit °Cd$_H$).

The area under the %GLA fitted curve was calculated and then scaled to the individual shoot using the leaf lamina areas to obtain the Healthy Area Duration per ear-bearing shoot (HADe, unit m^2 $\cdot^\circ$ Cd$_H$ $\cdot$ shoot^{-1}). Also, the HADe was converted to the single grain scale (HADg, unit: dm^2 $\cdot^\circ$ Cd$_H$ $\cdot$ grain^{-1}) or the crop scale (HADm, unit: m^2 $\cdot^\circ$ Cd$_H$ $\cdot$ m^{-2}).

Dry matter fluxes (ΔDM) were estimated during the grain filling period. They were scaled to a standard grain number estimation (sGNe) which was the average GNe observed per G $\times$ F $\times$ N $\times$ S combination, multiplying the observed dry matter biomass - associated with an observed GNe - by the ratio $sGNe/GNe$. Dry matter flux analyses were applied for above-ground biomass, vegetative parts and grains.

The percentage increase assimilate availability per grain in the spikelet removal treatment was calculated, either based on GNe reduction (Eq. 4.3, Slafer and Savin 1994; Borrás et al. 2004) or on HADg increase (Eq. 4.4).

$$100 \times \left(\frac{GNe_{S0}}{GNe_{S1}} - 1 \right) \tag{4.3}$$

$$100 \times \left(\frac{HADg_{S1}}{HADg_{S0}} - 1 \right) \tag{4.4}$$

The experiment was a factorial experiment with three spatial scales (P main plot, N split-plot, S spikelet removal) and thus three different error variances. The analysis of responses (e.g. yield components) to treatments was based on split-plot ANOVAs, based on mixed models (Crawley 2012, Eq. 6.3).

$$y_{ijklm} = \mu + f_i + g_j + P_{ijk} + N_{l(ijk)} + S_{m(lijk)} + \varepsilon_{ijklm} \tag{4.5}$$

With: y_{ijklm}, an observed value of a response variable; μ, the population mean for the reference; f_i, the fungicide fixed effect; g_j, the genotype fixed effect; P_{ijk}, the main plot random effect (k plots for each $[F \times G]_{ij}$ combination); $N_{l(ijk)}$, the nitrogen fixed effect nested within a plot (sub-plot); $S_{m(lijk)}$, the spikelet removal fixed effect nested within the nitrogen split-plot.

Fixed effects were tested with the Wald chi-square including up to 3-way interactions between fixed effects, removing non-significant effects. Effect size was then calculated and least square means were plotted along with the 95% confidence interval (CI) when relevant. Eventually, post-hoc tests were performed to obtain least means square comparison between levels of factors, relying on Tukey's Honest Significant Difference test (Tukey HSD).

Statistical analysis was carried out using R (R Core Team, 2017). Supplementary packages included: `DBI` (R Special Interest Group on Databases, 2014) and `RPostgreSQL` (Conway et al., 2016) for data management and variable calculations, `nlme` (Pinheiro et al., 2017) for mixed models fitting, `lsmeans` (Lenth, 2016) for Tukey HSD based post-hoc tests, package `lattice` (Sarkar, 2008) for graphics.

4.3 Results

4.3.1 The tolerance grade of the genotypes

The three preliminary experiments were exposed to severe natural STB epidemics, as the maximum yield loss in comparison to the control reached -69% (Table 4.1). The intolerance (i_{eg}) for the six genotypes was generally consistent across the three site-seasons with C×L 7A showing the lowest and LSP2×R 20 the highest tolerance in each environment, although there were some interactions with environment. For example, C×L 5H was the 1st equal most tolerant genotype at ADAS Hereford 2012 but only the 5th most

tolerant genotype at ADAS Hereford 2014 and Teagasc Carlow 2014. The intolerance (i_{eg}) of the six genotypes was estimated in each experiment and then a tolerance grade (T) was calculated (Eq. 4.1). Therefore, according to the dimensionless T, the genotypes LSP2×R 127, C×L 14B and LSP2×R 20 were expected to be tolerant, and LSP2×R 16, C×L 7A, C×L 5H to be intolerant in the main experiment at ADAS Hereford 2015, which explored the relation between STB tolerance and source/sink balance.

Table 4.1: Estimation of the genotype tolerance. Intolerance (i_{eg} of the six doubled-haploid genotypes (g) was calculated in the three field experiments (e; 2011-2012 and 2013-2014 at ADAS Hereford, and 2011-2012 at Teagasc, Carlow, Ireland; respectively ADAS 2012, ADAS2014, Teagasc 2012) as $[\Delta grain\ yield/\Delta HAD]_{eg}$ (unit:kg $\cdot$ ha^{-1}, 85% DM per HAD in days since GS59). The genotype tolerance grade (T) was calculated as $-1\times$ the genotype average of i_{eg}, beforehand standardized by environment (without unit). The last line is the maximum grain yield loss as a percentage of the STB-prevented crops.

	Intolerance (i_{eg}, kg $\cdot$ ha^{-1})			T
Genotype	ADAS 2012	ADAS 2014	Teagasc 2012	
C×L 14B	57	21	7	0.23
C×L 5H	11	32	31	-0.02
C×L 7A	73	49	43	-1.45
LSP2×R 127	22	18	2	0.81
LSP2×R 16	68	28	27	-0.48
LSP2×R 20	11	19	2	0.91
max. yield loss	-69%	-42%	-40%	na

4.3.2 Variability of grain filling source traits

In the experiment at ADAS Hereford 2015, leaf area per ear-bearing shoot (LAe) varied by 10% between the lowest LSP2×R 127 and the highest LSP2×R 16 genotypes ($P < 0.001$; Table 4.2). In intact ears (S0) the LAe and GNe were positively correlated ($r = 0.37^{**}$); therefore in comparison to the LAe, the range of Leaf Area per grain (LAg) was reduced varying only by 6%. The spikelet removal (S1) not only increased LAg, but also increased the variability between genotypes and modified the ranking of the genotypes for LAg. Neither fungicide nor N fertilisation affected LAg. In plots where no fungicide STB control was applied (F0), the timing of canopy senescence (I) varied according to genotype ($P < 0.001$); it was significantly, although marginally, delayed following both N fertilisation and spikelet removal treatments by about 20 °Cd, that is, approximatively one day ($P < 0.05$). The STB disease severity was generally low with maximum values (expressed as proportion of leaf area with symptoms cumulated for the upper three leaves) ranging from 0.04–0.11 amongst the six lines in F0 plots (Fig. 4.1). There was also a small amount of yellow rust (YR) observed in some lines with maximum YR severity ranging from 0.00–0.05 amongst the six lines in F0 plots, affecting mainly LSP2×R 127 (Fig. 4.1). Therefore, the disease severity was confounded with senescence progression during the mid grain filling stage, explaining the apparent decrease in sever-

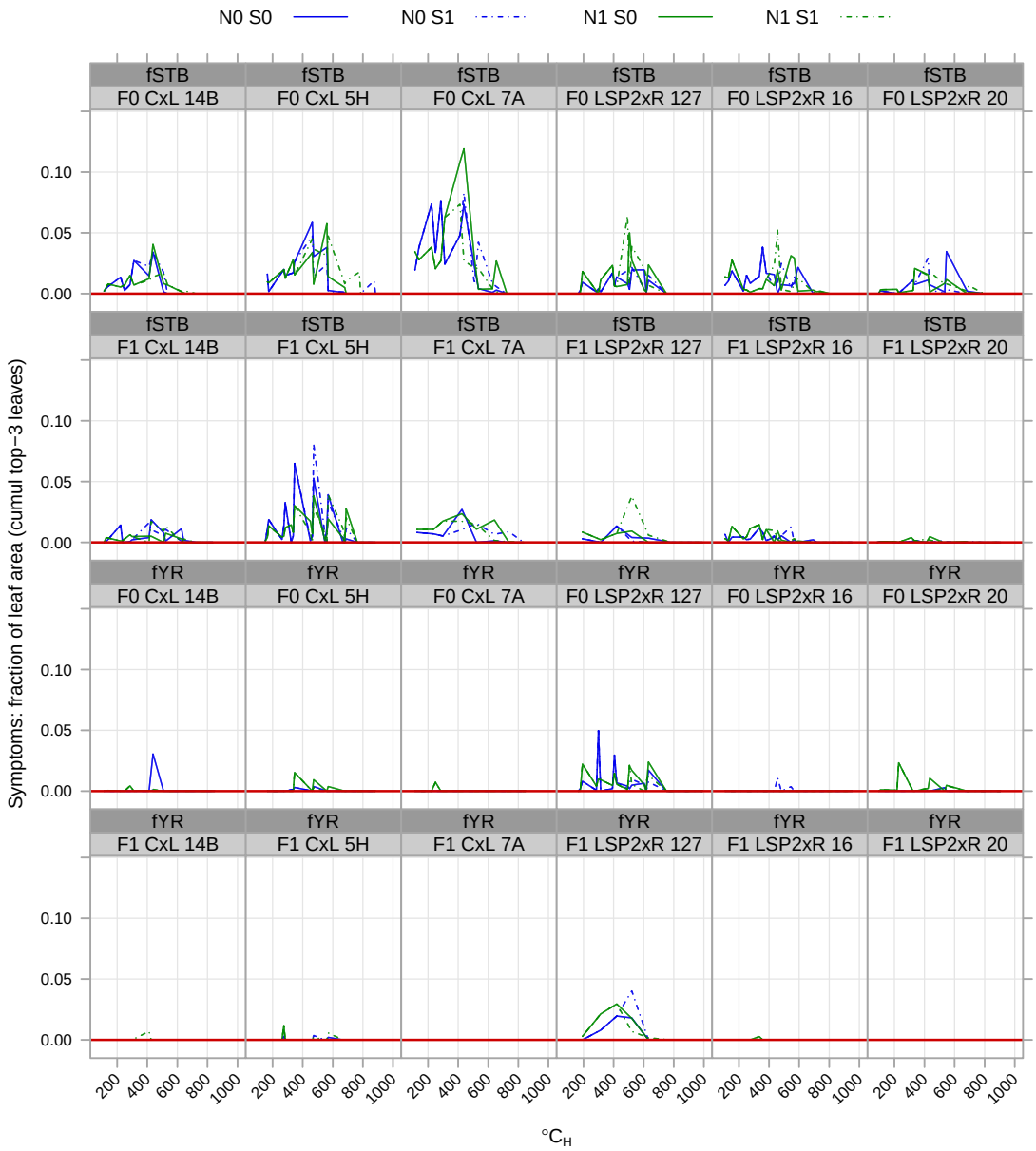


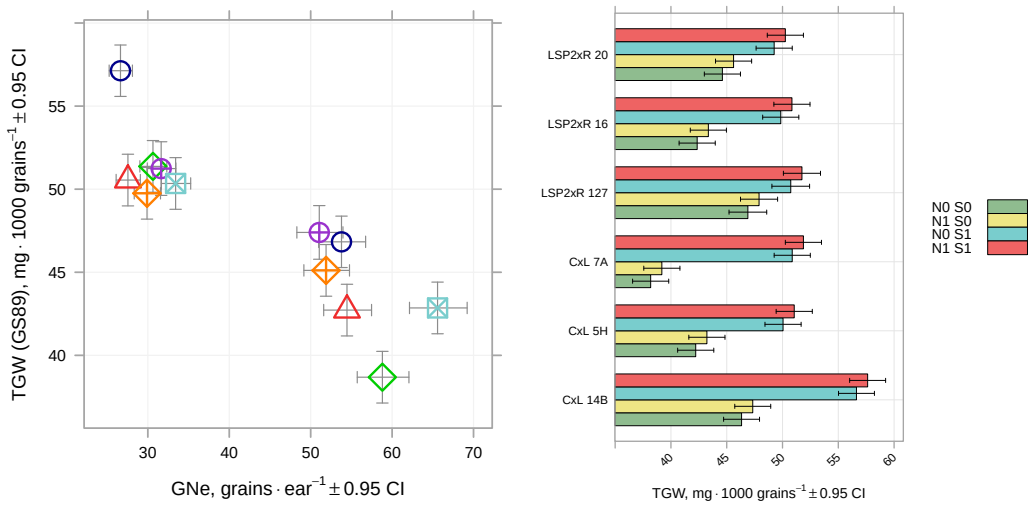
Figure 4.1: Disease severity (fraction of leaf area with symptoms) at each date for each combination of Genotype, Fungicide, Nitrogen and Spikelet removal treatment. Values are average symptoms assessment (cumulated for the three upper leaves). The x-axis is thermal time since heading stage (GS55). The two upper rows of panels correspond to the STB disease assessment (fSTB), the two bottom rows are the yellow rust assessment (fYR). The F1 treatment is the full fungicide treatment, F0 no control of STB. The lines and colours correspond to the Nitrogen × Spikelet removal treatment.

Table 4.2: Analysis of variance of different grain source traits in the field experiment at Herefordshire 2014-15. Response of leaf area per ear-bearing shoot (LAe), fraction of leaf 3 on total leaf area (fLA3), leaf area per grain in (LAg), canopy senescence time (I) and duration (D), stem DM per grain variation during late grain filling (after spikelet removal, ΔDMst) to the genotype, the fungicide treatment, the nitrogen treatment, the spikelet removal treatment. Letters after the means indicate Tukey's HSD comparisons between levels of factors. The symbol $ indicates that results were obtained by paired comparison because of deviation from ANOVA hypotheses. When not significant or non-applicable, 'ns' and 'na' are reported.

	LAe cm^2/e	fLA3	LAg(S0) cm^2/gr	LAg(S1) cm^2/gr	I(F0) $°Cd_H$	I(F1) $°Cd_H$	D§ °Cd	ΔDMst(S0) mg/e	ΔDMst(S1) mg/e
Genotype	***	***	**	***	***	***	***	***	ns
C×L 14B	70.9b	0.289b	1.32ab	2.67d	594a	649bc	205b	13.6b	25.9
C×L 5H	66.2ab	0.292b	1.22ab	2.41bcd	645bc	676c	264c	9.4a	18.8
C×L 7A	68.7b	0.275a	1.18a	2.25b	609a	685c	248c	12.0ab	21.5
LSP2×R 127	63.1a	0.321c	1.24ab	2.01a	610a	557a	163a	17.4c	24.7
LSP2×R 16	84.5c	0.274a	1.29ab	2.55cd	616ab	635b	329d§	13.6b	21.4
LSP2×R 20	70.9b	0.327c	1.37b	2.37cd	659c	629b	167a	13.7b	23.5
Fungicide	ns	ns	ns	ns		**$	***§	ns	ns
F0	71.1	0.297	1.27	2.43	622		225a	13.8	22.1
F1	70.4	0.296	1.27	2.33		639	194b	12.8	23.1
Fertilization			ns	ns	**	ns	ns§	ns	ns
N0	na	na	1.28	2.41	614a	637	208	13.4	22.8
N1	na	na	1.26	2.35	633b	640	211	13.2	22.5
Spklt remov.				***$	**	ns	ns§		***$
S0	na	na	1.27		596a	620	209	13.3	
S1	na	na		2.38	614b	623	210		22.6

ity; consistently, senescence was hardly affected in plots where full fungicide STB control was applied (F1). It is noteworthy that LSP2×R 127 exhibited earlier senescence in F1 than in F0. Finally, the fungicide effect was not significant on flag-leaf senescence; but it was highly significant on leaf 3 senescence time. So the resulting effect on canopy senescence occurred through the proportional contribution of leaf 3 to canopy lamina area (fLA3) which also varied according to the genotype ($P < 0.001$), and was especially high in LSP2×R 127 and LSP2×R 20. Overall, a delay of the canopy senescence time (*I*) following fungicide application was observed, although with low significance ($P < 0.05$). Unlike the senescence time, the leaf senescence duration (D) did not significantly vary with either the N fertilisation or spikelet removal treatments but did vary with the genotype ($P < 0.001$). Conversely, fungicide treatment led to shorter senescence duration and large variations in duration were observed between genotypes so that LSP2×R 16 had to be removed from the analysis to allow ANOVA for this trait. In addition to canopy traits, the stem dry mass after A+13 daa (the time of spikelet removal) was regarded as a secondary source of grain nutrition by carbohydrate remobilisation. In Table 4.2 data are expressed as carbohydrate remobilisation per grain. In shoots with unmanipulated ears (S0), the genotype effect was highly significant on carbohydrate remobilisation per grain ($P < 0.001$), while no significant effect of fungicide or fertilisation was observed. Spikelet removal (S1) largely increased carbohydrate remobilisation per grain, yet the genotype effect was no longer significant, nor was it for fungicide or fertilisation.

4.3.3 Variability of grain sink traits



(a) TGW versus grain number per ear (b) TGW of each genotype

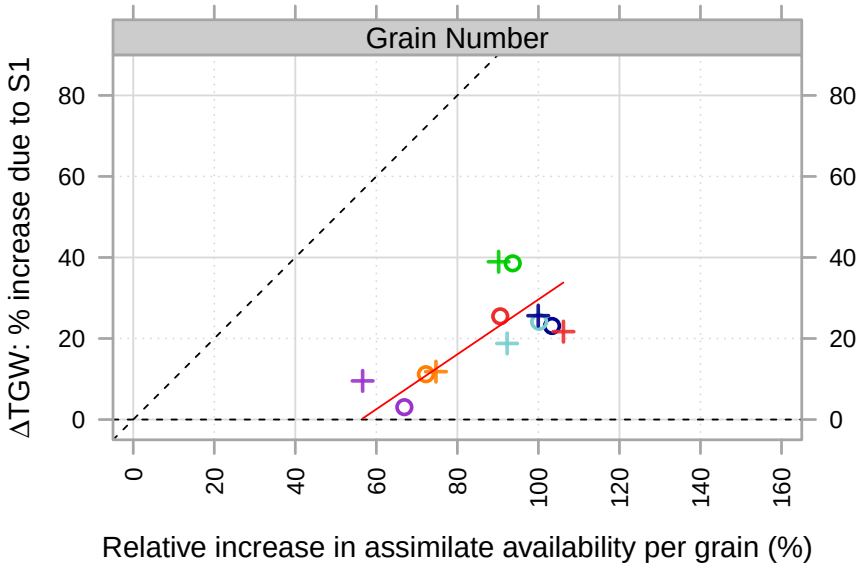
Figure 4.2: a) Relationship of the TGW at maturity (GS89) to the grain number per ear, according to the genotype (C×L 14B, dark blue empty circles; C×L 5H, red triangles; C×L 7A, green empty diamonds; LSP2×R 127, purple crossed circles; LSP2×R 16, light blue squares; LSP2×R 20, orange crossed diamonds) and to the spikelet removal treatment. b) TGW measured at maturity for the genotypes (x-axis, ordered according to their maximum TGW estimation), the nitrogen (N) and spikelet (S) removal treatments. The values are the least mean square estimations from the ANOVA models along with the 95% confidence interval. Effects and significance: TGW at maturity, G and S and G×S, $P < 0.001$ and N $P = 0.024$; GNe, G and S and G×S, $P < 0.001$ (tested on log-transformed values for homoscedasticity).

As shown in Fig. 4.2a grain number per intact ear (S0) varied among genotypes ($P < 0.01$) from 50 to 66 (LSP2×R 16), without significant effect of fungicide or N fertilisation. Removing half the spikelets reduced grain number by 40% in LSP2×R 127 and LSP2×R 20 versus 50% in other genotypes ($P < 0.001$). No compensation in grain number per ear occurred following spikelet removal, as the grain counts on the day of treatment (A+13 daa) were consistent with those obtained later. Mean grain weight (TGW) varied at maturity (GS89) in intact ears according to genotype ($P < 0.001$) and fertilisation ($P < 0.05$, Fig. 4.2b). The post-heading N application (N1) significantly increased TGW (+0.9 g) without interaction with genotype. However, the fungicide treatment did not modify TGW. Removing spikelets led to a grain yield loss per ear ranging from 32% to 40%; thus, the grain number reduction was not compensated by a corresponding TGW increase. The increase in final TGW of S1-ears compared to S0-ears ranged from +9% (LSP2×R 127) to +33% (C×L 7A, $P < 0.001$). Among S1-ears, only C×L 14B had significantly heavier grains compared to the other genotypes. Overall, there was a negative correlation between the TGW response to spikelet removal and the TGW in the control S0 ($r = -0.74$, $P < 0.001$). TGW was also measured at A+13 daa, the time of spikelet removal. LSP2×R 127 had then a higher TGW (16.9 g) than the other genotypes which ranged

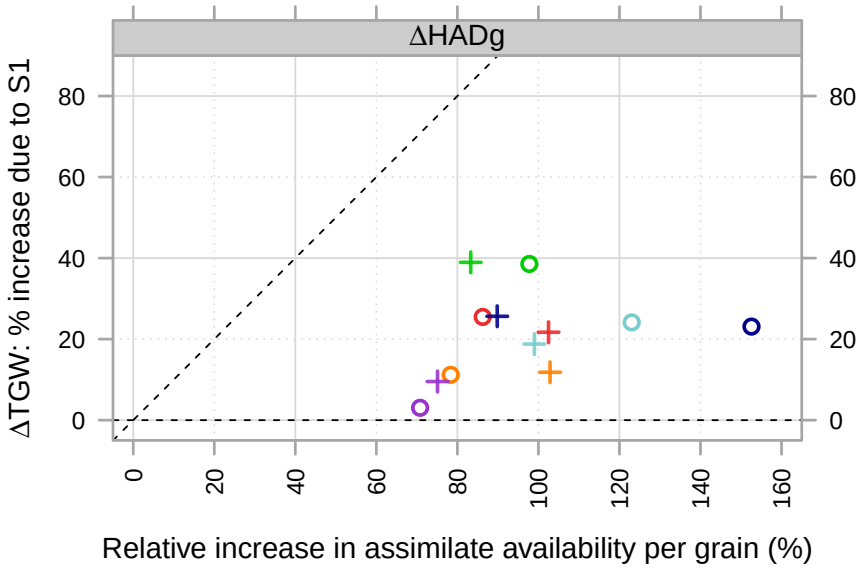
from 7.6 g (C×L 7A) to 10.3 g (C×L 5H). Spikelet removal thus occurred when 15-20% of final TGW_{S1} had been achieved, except for LSP2×R 127, for which it occurred later in its development (about 35% of final TGW_{S1}). Furthermore, TGW was higher by 6% in S1 than in S0 ($P < 0.001$) as soon as the day of spikelet removal; probably because the treatment removed grains from the upper part of the ear, which were apparently lighter than those from the lower part of the ear.

4.3.4 Source-sink balance

The source/sink balance mostly varied with both genotype and spikelet removal, N fertilisation or fungicide treatments showing a lesser effect. We thus examined if the observed variation could be interpreted by a single rule. In the literature, the relative increase in assimilate availability following spikelet removal is commonly assessed by the reduction in grain number, such as shown in Fig. 4.3a. A grain number reduction of 50% then leads to an increase in assimilate availability of 100%, and so on according to Eq. 4.3. In the present study, spikelet reduction thus created a potential increase of assimilate availability ranging from +61% to +106% depending on genotype and N fertilisation. It resulted in an increase in TGW, through enhanced late grain filling (that is after A+13 daa), ranging from 3 to 39% depending on the genotype, that was significantly correlated with the increase in assimilate availability. Regardless of genotype and treatments, ΔTGW was therefore determined by assimilate availability, although with a slope less than 1. Furthermore, the different genotypes did not exactly follow the common regression; spikelet removal in C×L 7A apparently generated a larger ΔTGW than in other genotypes (Fig. 4.3a). In addition, as indicated by Table 4.2, not only sinks, but also sources were affected by the removal of spikelets. Therefore, Fig. 4.3b represents the relative increase in assimilate availability based on HAD per grain during the late grain filling (ΔHADg) according to Eq. 4.4. Following spikelet removal, ΔHADg increased from 70% to 152%, yet without significant correlation with the relative increase in ΔTGW. We suspected it was linked to error accumulation by using relative ratios. Therefore, ΔTGW was then directly correlated with ΔHADg (Fig. 4.4), calculated from the time of spikelet removal. Fig. 4.4 shows a linear regression of late HADg on ΔTGW that is highly significant ($y = 0.025(\pm 0.003)x + 26(\pm 1.0)$; $P < 0.001$). The relationship of grain yield loss to HAD that is commonly used at the m^2 scale can also be used at the grain scale. A crop tolerance index (T) was previously derived from the slope of grain yield to HAD at the m^2 scale between control and stressed crops in the three preliminary experiments (Table 4.1), and using the same rationale tolerance indices at the grain scale (Tg) were built in the present source/sink experiment. As tolerance applies to any stress, indices could be built regarding each of the applied treatments (fungicide, fertilisation and spikelet removal). However, because spikelet removal showed the largest effects, attention is fo-



(a) Grain Number per ear



(b) HAD per grain

Figure 4.3: Relationship between relative increase in grain dry weight and relative increase in assimilate availability from the time of spikelet removal (A+13 daa) to maturity. Relative assimilate availability increase was calculated according to methods: left, the grain number reduction per ear; right, the ΔHADg increase (HAD per grain estimated since the time of spikelet removal). The dashed lines represents full source or sink limitation (slopes 1 and 0). The colours represents the genotypes (C×L 14B, dark blue; C×L 5H, red; C×L 7A, green; LSP2×R 127, purple; LSP2×R 16, light blue; LSP2×R 20, orange) and nitrogen treatment (control, circles; additional nitrogen at heading stage, crosses). The red line is the reduced major axis regression line (Smith, 2009), preferred in this case to least mean square estimation which underestimates variations along with x-axis values; equation is $y = 0.677(\pm 0.22)x - 38(\pm 45)$ ($P < 0.001$).

cused on it hereafter. Therefore, Tg was defined as the grain weight variation per unit of HADg variation because of (and since the time of) the spikelet removal treatment: $\Delta TGW/\Delta HADg$.

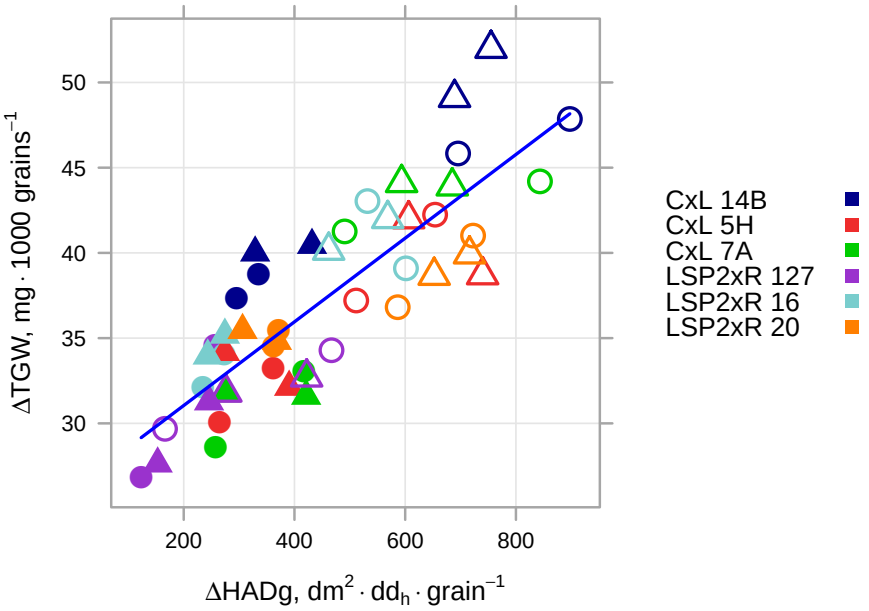


Figure 4.4: From the time of spikelet removal, relationship of TGW growth (ΔTGW) to HADg ($\Delta HADg$). Each point is the average for each genotype (colours: C×L 14B, dark blue; C×L 5H, red; C×L 7A, green; LSP2×R 127, purple; LSP2×R 16, light blue; LSP2×R 20, orange) and nitrogen treatment (control, circles; additional nitrogen at heading stage, triangles) and spikelet removal (control, full; spikelets removed, empty). The blue line is the least square mean regression fit on the cloud ($y = 0.025(\pm 0.002) \cdot x + 26(\pm 1.1)$, $R^2 = 0.71$).

4.3.5 Tolerance prediction using source and sink traits

From our results, we tried to obtain a prediction of STB tolerance at the m^2 scale using the various source and sink traits measured. Unfortunately, the low STB pressure combined with minor yellow rust symptoms prevented estimating STB tolerance from our assay. However, the six genotypes had been previously characterized for their STB tolerance in three independent field experiments as described above (Table 4.1). Hypothesizing tolerance was at least partly genetically determined, a single tolerance grade T was then calculated according to Eq. 4.1 yielding a value that extended from 1.45 ± 0.35 (C×L 7A, intolerant) to 0.91 ± 0.14 (LSP2×R 20, tolerant). T was further correlated with various traits observed during the present experiment (Table 4.3). Some of these traits were recorded using only the control treatment (S0), while others combined observations on S0 and S1 plants. In each case the reported values pooled all the data from F0/F1 and N0/N1 treatments.

Among the traits observed on S0 crops, TGW was correlated with T ($P < 0.05$), as

Table 4.3: Correlation between tolerance (T) and grain tolerance (Tg) and grain source or grain sink traits. The genotype tolerance grade (T) was calculated as $-1\times$ the genotype average of x_{eg}, beforehand standardized by environment (without unit). For each treatment combination (S×F×N) the correlation was calculated on the 6 genotype values. The traits included the TGW (g), the grain yield per ear (Ye, $g \cdot m^{-2}$) or per square metre (Ym, $g \cdot m^{-2}$), the grain number per ear (GNe), HADg or HADe ($dm^2 \cdot^\circ Cd \cdot grain^{-1}$ or $m^2 \cdot^\circ Cd \cdot m^{-2}$), Δ indicates variable estimated after the time of the spikelet-removal treatment, 1 and 3 indicate the leaf layer when relevant, the last 3 lines are based on the difference between spikelet removal treatment and control.

	C×L 14B	C×L 5H	C×L 7A	LSP2×R 127	LSP2×R 16	LSP2×R 20	Cor. T	Cor. Tg
Tolerance								
T	0.23	-0.02	-1.45	0.81	-0.48	0.91	1	0.98***
Tg	0.977	0.975	0.961	0.987	0.975	0.987	0.98***	1
Complete ears (S0)								
TGW	46.8	42.7	38.7	47.4	42.9	45.1	0.90*	0.86*
Ym	1070	911	824	868	1082	756	-0.16	-0.17
Ye	2.5	2.3	2.3	2.4	2.8	2.3	-0.04	0.06
GNe	54	55	59	51	66	52	-0.71	-0.59
ΔTGW	39	32	31	30	34	35	0.24	0.15
ΔHADg	348	323	343	201	256	352	-0.24	-0.35
HADe 1	163	170	169	122	197	148	-0.65	-0.61
HADe 3	90	83	76	94	96	118	0.74	0.80
HADg 3	167	154	130	187	147	22.8	0.89*	0.89***
%LA 1	0.36	0.36	0.36	0.32	0.37	0.32	-0.68	-0.69
%LA 3	0.29	0.29	0.28	0.32	0.27	0.33	0.88*	0.88*
Comparison (S1-S0)								
ΔTGW	9.6	7.6	12.1	2.0	7.2	4.0	-0.85*	-0.92**
ΔHADg	411	305	310	147	284	317	-0.24	-0.35
ΔHADg 3	76	42	36	36	30	87	0.55	0.45

well as several traits related to leaf 3. On the other hand, traits linked to the flag leaf or the whole canopy did not correlate with T, neither did stem DM mobilisation nor late grain filling ΔTGW. However, the difference in late grain filling ΔTGW between S1 and S0 was negatively correlated with T. No other combined S1 and S0 traits were significantly correlated with T, even those traits related to canopy or leaf 3. Interestingly Tg correlated very tightly with T ($P < 0.001$).

4.4 Discussion

The experiment provided large source/sink balance variations that could be related to the tolerance T of the six genotypes, assessed during three preceding experiments. The low STB disease severity could not provide an additional tolerance evaluation, but the T could be connected to traits of healthy crops similarly to the study of Bancal et al. (2015).

4.4.1 Tolerance and yield

Foulkes et al. (2006) found that tolerance of STB might be negatively correlated with yield of healthy crops. They pointed out, however, it may indirectly result from a breeding strategy mainly focused on yield instead of tolerance. Tolerance indeed decreased with the year of release of the cultivar backgrounds of their studied NILs. The present experiment

was based on doubled-haploid genotypes derived from crosses between modern cultivars and no correlation was found between tolerance and grain yield, either at the crop scale or shoot scale. This is in agreement with Bancal et al. (2015) who did not find a correlation between yield and tolerance and the recent work of Castro and Simón (2016).

4.4.2 TGW was co-limited by source and sink

The six genotypes, contrasting for STB tolerance, showed a large range of TGW in the control S0. The spikelet removal treatment induced large variations in grain growth (TGW) reaching a maximum relative grain weight increase of 33% (39% considering the grain weight increment since spikelet removal); this effect is large in comparison to similar studies of grain reduction impact on grain growth in wheat crops (Zhang et al. 2014, +12%; Serrago et al. 2013, +32%) or barley (Cartelle et al. 2006, +15%; Serrago et al. 2013, +7%). With respect to the results of Borrás et al. (2004) and Slafer and Savin (1994), a relationship between the relative grain weight increment since spikelet removal (ΔTGW, %) and the relative grain source availability ($dGNe$ or $\Delta HADg$, %) far below the 1:1 slope in our results denotes the genotypes were not only source limited. Nonetheless, as the relative TGW increase after the spikelet removal was significant and substantial, so the grain filling was not sink limited but rather co-limited by source and sink (Acreche and Slafer, 2009). The genotype difference in TGW increase following spikelet removal could result from uncontrolled variations in treatment application, such as spikelet removal intensity or stage. However, as four among the six genotypes experienced similar sink reduction, their contrasting response to spikelet removal likely reflects their contrasting degree of source limitation (Zhang et al., 2014; Ma et al., 1996). Therefore, genotypes selected for their contrasting tolerance of STB also contrasted highly for TGW source limitation.

4.4.3 Low source limitation is a genotype tolerance trait

In the control treatment S0 (intact ears) TGW was positively correlated with the STB-tolerance grade (T). Conversely, Bancal et al. (2015) suggested the tolerance of STB was negatively correlated with TGW. However, their results were based on a multiple field-experiment data and the correlation was driven by large variation in N fertilisation level. When restricting the analysis to assays receiving a standard N fertilisation, they no longer observed any TGW effect on tolerance.

The tolerant genotypes also showed the lowest response in grain weight increment following spikelet removal (ΔTGW_{S1-S0}). As a low response to spikelet removal suggests a low degree of source limitation in the control, then tolerance would be linked to low degree of source limitation during grain filling. Grain growth caused by the spikelet removal (ΔTGW_{S1-S0}) was negatively correlated with the control grain weight at maturity

(TGW_{S0}). This suggests that the genotypes exhibiting the heaviest control TGW were closer to their potential grain weight (Aisawi et al., 2015). The present results are consistent with those of Voltas et al. (1997) which also showed a larger increase in grain weight increment following sink reduction for smaller TGW genotypes (14.6% to 25.1% grain weight increase) for three barley genotypes; but the spikelet removal treatment was applied early at anthesis and might have altered the sink potential size (Dupont and Altenbach, 2003; Calderini et al., 2001; Cartelle et al., 2006). Furthermore, Zhang et al. (2014) found that eight out of the nine wheat genotypes in a field experiment in China showed a similar negative relation between control grain weight and TGW increase following spikelet removal, although low TGW increases were observed (< 12%). Similarly, Serrago et al. (2011) using three contrasted cultivars found the TGW increase following fungicide treatment was highly correlated to healthy area absorption per grain (HAA_G), a unique relationship being observed when HAA_G was related to TGW of healthy crops. Overall, these results indicate that a low source limitation to grain, which depends on source-sink balance, is a genotype tolerant trait.

4.4.4 The grain source?

Although the present experiment did not produce a wide range of canopy green area, STB-tolerance T was found to be correlated with some of the traits describing the canopy, especially those related to the leaf 3. Thus, the leaf 3 proportion of the canopy area and the HADg3 positively correlated with T, while HADe3 and $I3$ were not far from being significant. Conversely no trait linked to flag leaf was found to be significant. The importance of leaf 3 was unexpected and may be explained by the low disease intensity, limiting most of the STB symptoms to the lower leaves which may have emphasized the link between tolerance and leaf 3 traits. According to Carretero et al. (2010), the leaf 3 relevance depends both on the extinction coefficient of leaf-layers and the vertical position of the disease in the canopy. We have not measured these parameters, but our study confirms that the leaf profile composition, the canopy leaf area and the senescence parameters could influence genotype tolerance by increasing the resource availability, despite more attention having been placed to date on the flag leaf (Foulkes et al., 2006; Bingham et al., 2009; Bancal et al., 2015).

Other traits of tolerance were also previously proposed related to an increased radiation-use efficiency of remaining healthy area (Bingham et al., 2009; Ney et al., 2013) or the use of stored carbohydrates in the stem (Foulkes et al., 2006). Schierenbeck et al. (2016) stated that the biotroph *P. triticina* (leaf rust) reduced the RUE, while *Py. tritici-repentis* (tan spot) reduced the light interception. For a latent necrotoph pathogen such as *Z. tritici* (Sánchez-Vallet et al., 2015), the compensation could arise from an increased RUE of remaining green area (Ziv and Eyal, 1978; Zuckerman et al., 1997) or an increased remo-

bilisation of stored carbohydrate (Ney et al., 2013). Indeed some studies suggested the mobilisation of stem water soluble carbohydrates (WSC) somewhat compensated losses in HAD (Cornish et al., 1990; Gaunt and Wright, 1992); but although Serrago et al. (2011) showed cultivars modified differently their WSC utilisation rates when diseased, they also concluded that in their experiments losses in HAA_G were not compensated by observed increases in WSC mobilisation. As STB severity was low in the present study, it was therefore beyond the scope of this experiment to check for the physiological modifications of WSC remobilisation linked to the disease expression. Tolerance (T) was not correlated with dry matter remobilisation from the stem or more generally from the above-ground biomass, but the present study was not designed to follow WSC dynamics over time and remobilisation was roughly estimated. Tolerance is generally thought to be associated either with higher grain source availability strategies or plant compensation mechanisms (such as the increase of the RUE, increased remobilisation, Ney et al., 2013). The present study gives more weight to the higher grain source availability by a predominant effect of low degree of source limitation.

4.4.5 Tolerance estimation in healthy crops

The degree of source-limitation at the grain level was the most consistent trait linked to the range of genotype tolerance observed in this experiment. The tolerance (T), that was estimated from Ym and HADm, can also be similarly calculated at the grain scale (Tg) using the TGW and HADg. The T index, established in the independent field STB-trials, was highly correlated with our healthy-trait based Tg; thus, it suggests STB tolerance was highly related to a higher degree of TGW source saturation. It is not surprising source-limited crops would be less tolerant to foliar damage by STB. Despite Tg being quite sensitive to imprecision in HADg estimation, our results show it could provide an alternative to usual tolerance assessments that are highly dependent on random epidemics. However, this relation at the grain scale has not been reported previously and needs to be explored on a larger range of genotypes and environmental conditions.

Similar to the study of Bancal et al. (2015), tolerance of STB assessed on our three independent trials was positively correlated with the traits observed in healthy crops of a fourth experiment. This is encouraging given the difficulty to ensure the STB epidemics in real crop conditions. Finally, if it is confirmed that the genotype crop tolerance of STB is correlated with tolerance at the grain scale (i.e. degree of TGW source limitation) then the spikelet removal treatment would be an adequate method to study tolerance of STB in disease free crops. Confirmation of the results requires a larger dataset with a greater number of genotypes to avoid possible uncertainty in trait correlations. The application of non-destructive proxy measurements of green area kinetics could also increase the availability and accuracy of HAD per grain estimations.

4.5 Conclusion

The source-sink traits observed in crops in the absence of STB damage to grain yield correlated with the STB tolerance estimated in three independent site-season experiments. The degree of TGW source limitation at the grain scale (Tg) is highly and negatively correlated with the STB tolerance estimated at the crop scale (T). The leaf area profile was shown to be linked to tolerance expression but the mechanism is still uncertain. Finally, the tolerance grade was not found to be correlated with the potential yield of the genotypes, suggesting breeding for tolerance traits is possible in high-yielding genotypes.

4.6 Acknowledgements

The authors thank Arvalis Institut du Vegetal, France, UK government Department of Environment, Food and Rural Affairs (DEFRA) Project IF01118, Teagasc, Ireland and University of Nottingham, UK for funding.

References

M. M. Acreche and G. A. Slafer. Variation of grain nitrogen content in relation with grain yield in old and modern Spanish wheats grown under a wide range of agronomic conditions in a Mediterranean region. *The Journal of Agricultural Science*, 147(6):657–667, 2009. doi: 10.1017/S0021859609990190 .

K. A. B. Aisawi, M. P. Reynolds, R. P. Singh, and M. J. Foulkes. The physiological basis of the genetic progress in yield potential of CIMMYT spring wheat cultivars from 1966 to 2009. *Crop Science*, 55:1749–1764, 2015. doi: 10.2135/cropsci2014.09.0601 .

P. Bancal, M.-O. Bancal, F. Collin, and D. Gouache. Identifying traits leading to tolerance of wheat to Septoria tritici blotch. *Field Crops Research*, 180:176–185, 2015. doi: 10.1016/j.fcr.2015.05.006 .

I. J. Bingham, D. R. Walters, M. J. Foulkes, and N. D. Paveley. Crop traits and tolerance of wheat and barley to foliar disease. *Annals of Applied Biology*, 154:159–173, 2009. doi: 10.1111/j.1744-7348.2008.00291.x .

L. Borrás, G. A. Slafer, and M. E. Otegui. Seed dry weight response to source sink manipulations in wheat, maize and soybean: a quantitative reappraisal. *Field Crops Research*, 86(23):131–146, 2004. ISSN 0378-4290. doi: 10.1016/j.fcr.2003.08.002 .

R. J. Bryson, N. D. Paveley, W. S. Clark, R. Sylvester-Bradley, and R. K. Scott. Use of in-field measurements of green leaf area and incident radiation to estimate the effects of yellow rust epidemics on the yield of winter wheat. *European Journal of Agronomy*, 7: 53–62, 1997. doi: 10.1016/S1161-0301(97)00025-7 .

J. Burke and B. Dunne. Septoria tritici in winter wheat – to spray or not to spray? *Irish farmer*, pages 14–18, April 2006.

D. F. Calderini, R. Savin, L. G. Abeledo, M. P. Reynolds, and G. A. Slafer. The importance of the period immediately preceding anthesis for grain weight determination in wheat. *Euphytica*, 119(1–2):199–204, 2001. ISSN 0014-2336. doi: 10.1023/A:1017597923568 .

R. Carretero, R. A. Serrago, M. O. Bancal, A. E. Perelló, and D. J. Miralles. Absorbed radiation and radiation use efficiency as affected by foliar diseases in relation to their vertical position into the canopy in wheat. *Field Crops Research*, 116(1):184–195, 2010. doi: 10.1016/j.fcr.2009.12.009 .

J. Cartelle, A. Pedró, R. Savin, and G. A. Slafer. Grain weight responses to post-anthesis spikelet-trimming in an old and a modern wheat under mediterranean conditions. *European Journal of Agronomy*, 25(4):365–371, 2006. ISSN 1161-0301. doi: 10.1016/j.eja.2006.07.004 .

A. C. Castro and M. R. Simón. Effect of tolerance to Septoria tritici blotch on grain yield, yield components and grain quality in Argentinean wheat cultivars. *Crop Protection*, 90: 66–76, 2016. ISSN 0261-2194. doi: 10.1016/j.cropro.2016.08.015 .

P. Cheval, A. Siah, M. Bomble, A. D. Popper, P. Reignault, and P. Halama. Evolution of QoI resistance of the wheat pathogen *Zymoseptoria tritici* in Northern France. *Crop protection*, 92:131–133, Feb 2017. ISSN 0261-2194. doi: 10.1016/j.cropro.2016.10.017 .

F. Collin, P. Bancal, J. Spink, P. Kock Appelgren, J. Smith, N. D. Paveley, M.-O. Bancal, and M. J. Foulkes. Wheat lines exhibiting variation in tolerance of Septoria tritici blotch differentiated by grain source limitation. *Field Crops Research*, 217:1– 10, March 2018. ISSN 0378-4290. doi: 10.1016/j.fcr.2017.11.022 . URL https://www.sciencedirect.com/science/article/pii/S0378429017312078.

J. Conway, D. Eddelbuettel, T. Nishiyama, S. K. Prayaga, and N. Tiffin. *RPostgreSQL: R interface to the PostgreSQL database system*, 2016. URL https://CRAN.R-project.org/package=RPostgreSQL. R package version 0.4-1.

P. S. Cornish, G. R. Baker, and G. M. Murray. Physiological responses of wheat (triticum aestivum) to infection with Mycosphaerella graminicola causing Septoria tritici blotch. *Australian Journal of Agricultural Research*, 41(2):317–327, 1990. doi: 10.1071/AR9900317 .

M. J. Crawley. *The R Book, 2nd Edition*, chapter Mixed-Effects Models, pages 681–714. Wiley, 2012. ISBN 978-0-470-97392-9.

F. M. Dupont and S. B. Altenbach. Molecular and biochemical impacts of environmental factors on wheat grain development and protein synthesis. *Journal of Cereal Science*, 38 (2):133–146, September 2003. ISSN 0733-5210. doi: 10.1016/S0733-5210(03)00030-4 .

D. B. Egli and W. P. Bruening. Source-sink relationships, seed sucrose levels and seed growth rates in soybean. *Annals of botany*, 88(2):235–242, Aug 2001. ISSN 0305-7364. doi: 10.1006/anbo.2001.1449 .

M. J. Foulkes, N. D. Paveley, A. Worland, S. J. Welham, J. Thomas, and J. W. Snape. Major genetic changes in wheat with potential to affect disease tolerance. *Phytopathology*, 96:680–688, 2006. URL http://apsjournals.apsnet.org/doi/pdf/10.1094/PHYTO-96-0680.

B. A. Fraaije, J. A. Lucas, W. S. Clark, and F. J. Burnett. QoI resistance development in populations of cereal pathogens in the UK. In *Proceedings of the BCPC International Congress, Crop Science and Technology*, 689–694, Alton, Hampshire, UK, 2003. The British Crop Protection Council.

R. E. Gaunt and A. C. Wright. Disease-yield relationship in barley. II. Contribution of stored stem reserves to grain filling. *Plant Pathology*, 41(6):688–701, 1992. ISSN 1365-3059. doi: 10.1111/j.1365-3059.1992.tb02552.x .

R. V. Lenth. Least-squares means: The R package lsmeans. *Journal of Statistical Software*, 69(1):1–33, 2016. doi: 10.18637/jss.v069.i01 .

Y.-Z. Ma, C. T. MacKown, and D. A. van Sanford. Differential effects of partial spikelet removal and defoliation on kernel growth and assimilate partitioning among wheat cultivars. *Field Crops Research*, 47:201–209, 1996. ISSN 0378-4290. doi: 10.1016/0378-4290(96)00016-0 .

B. Ney, M.-O. Bancal, P. Bancal, I. J. Bingham, J. M. Foulkes, D. Gouache, N. D. Paveley, and J. Smith. Crop architecture and crop tolerance to fungal diseases and insect herbivory. Mechanisms to limit crop losses. *European Journal of Plant Pathology*, 135(3): 561–580, 2013. ISSN 0929-1873. doi: 10.1007/s10658-012-0125-z .

S. R. Parker, S. Welham, N. Paveley, J. M. Foulkes, and R. K. Scott. Tolerance of Septoria leaf blotch in winter wheat. *Plant Pathology*, 53(1):1–10, 2004. doi: 10.1111/j.1365-3059.2004.00951.x .

J. Pinheiro, D. Bates, S. DebRoy, D. Sarkar, and R Core Team. *nlme: Linear and Nonlinear Mixed Effects Models*, 2017. URL `https://CRAN.R-project.org/package=nlme`. R package version 3.1-131.

R Core Team. *R: A Language and Environment for Statistical Computing*. R Foundation for Statistical Computing, Vienna, Austria, 2017. URL `https://www.R-project.org/`.

R Special Interest Group on Databases. *DBI: R Database Interface*, 2014. URL `https://CRAN.R-project.org/package=DBI`. R package version 0.3.1.

M. Reynolds, A. Pask, and D. Mullan. *Physiological breeding I: interdisciplinary approaches to improve crop adaptation*. CIMMYT, Mexico, Mexico, DF (Mexico), 2012. URL `http://repository.cimmyt.org/xmlui/bitstream/handle/10883/1288/96144.pdf`.

M. P. Reynolds, A. Pellegrineschi, and B. Skovmand. Sink-limitation to yield and biomass: a summary of some investigations in spring wheat. *Annals of applied biology*, 146(1):39–49, 2005. ISSN 0003-4746. doi: 10.1111/j.1744-7348.2005.03100.x .

S. C. Salmon and H. H. Laude. Twenty years of testing varieties and strain of winter wheat at the Kansas agricultural experiment station. Technical bulletin 80, Kansas state college of agriculture and applied science, Manhattan, Kansas, February 1932. URL `https://www.k-state.edu/historicpublications/pubs/STB030.PDF`.

A. Sánchez-Vallet, M. C. McDonald, P. S. Solomon, and B. A. McDonald. Is Zymoseptoria tritici a hemibiotroph? *Fungal Genetics and Biology*, 79:29 – 32, 2015. ISSN 1087-1845. doi: 10.1016/j.fgb.2015.04.001 . Septoria tritici blotch disease of wheat: Tools and techniques to study the pathogen Zymoseptoria tritici.

D. Sarkar. *Lattice: Multivariate Data Visualization with R*. Springer, New York, 2008. URL http://lmdvr.r-forge.r-project.org. ISBN 978-0-387-75968-5.

J. Schafer. Tolerance to plant disease. *Annual review of phytopathology*, 9:235–252, 1971. ISSN 0066-4286. doi: 10.1146/annurev.py.09.090171.001315 .

M. Schierenbeck, M. C. Fleitas, D. J. Miralles, and M. R. Simón. Does radiation interception or radiation use efficiency limit the growth of wheat inoculated with tan spot or leaf rust? *Field Crops Research*, 199:65–76, 2016. doi: 10.1016/j.fcr.2016.09.017 .

R. A. Serrago, R. Carretero, M. O. Bancal, and D. J. Miralles. Grain weight response to foliar diseases control in wheat (triticum aestivum l.). *Field Crops Research*, 120(3):352 – 359, 2011. ISSN 0378-4290. doi: 10.1016/j.fcr.2010.11.004 .

R. A. Serrago, I. Alzueta, R. Savin, and G. A. Slafer. Understanding grain yield responses to source-sink ratios during grain filling in wheat and barley under contrasting environments. *Field Crops Research*, 150:42–51, August 2013. ISSN 0378-4290. doi: 10.1016/j.fcr.2013.05.016 .

V. J. Shearman, R. Sylvester-Bradley, R. K. Scott, and M. J. Foulkes. Physiological processes associated with wheat yield progress in the UK. *Crop Science*, 45(1):175–185, 2005. doi: 10.2135/cropsci2005.0175 .

G. A. Slafer and R. Savin. Source-sink relationships and grain mass at different positions within the spike in wheat. *Field Crops Research*, 37:39–49, 1994. doi: 10.1016/0378-4290(94)90080-9 .

R. J. Smith. Use and misuse of the reduced major axis for line-fitting. *American Journal of Physical Anthropology*, 140(3):476–486, 2009. ISSN 1096-8644. doi: 10.1002/ajpa.21090 .

J. Voltas, I. Romagosa, and J. L. Araus. Grain size and nitrogen accumulation in sink-reduced barley under Mediterranean conditions. *Field Crops Research*, 52:117–126, 1997. ISSN 0378-4290. doi: 10.1016/S0378-4290(96)01067-2 .

J. C. Zadoks, T. T. Chang, and C. F. Konzak. A decimal code for the growth stages of cereals. *Weed Research*, 44:415–421, 1974. doi: 10.1111/j.1365-3180.1974.tb01084.x .

Y.-H. Zhang, N.-N. Sun, J.-P. Hong, Q. Zhang, C. Wang, X. Qing-Wu, Z. Shun-Li, H. Qin, and W. Zhi-Min. Effect of source-sink manipulation on photosynthetic characteristics of flag leaf and the remobilization of dry mass and nitrogen in vegetative organs of wheat. *Journal of integrative agriculture*, 13(8):1680–1690, 2014. ISSN 2095-3119. doi: 10.1016/S2095-3119(13)60665-6 .

O. Ziv and Z. Eyal. Assessment of yield component losses caused in plants of spring wheat cultivars by selected isolates of *Septoria tritici*. *Phytopathology*, 68(5):791–796, 1978. ISSN 0031-949X. URL http://apsnet.org/publications/phytopathology/backissues/Documents/1978Articles/Phyto68n05_791.pdf.

E. Zuckerman, A. Eshel, and Z. Eyal. Physiological aspects related to tolerance of spring wheat cultivars to Septoria tritici blotch. *Phytopathology*, 87(1):60–65, Jan. 1997. ISSN 0031-949X. URL http://apsjournals.apsnet.org/doi/pdf/10.1094/PHYTO.1997.87.1.60.

Chapter 5

Glasshouse experiment at Grignon, 2014-15

5.1 Introduction

- **Rationale**

Wheat tolerance of STB relies on source/sink balance during the grain filling phase; large source availability relative to the grain was shown to be a tolerance trait in the previous Chapter 4. Nitrogen metabolism is associated with source availability during the grain filling phase as is it involved in the photosynthesis of the plant, and is also remobilised to the grain. Genetic variability of the nitrogen metabolism exists, so it is relevant to investigate the tolerance of STB in regard to contrasting nitrogen treatments. Nitrogen treatment and STB-symptoms contrasts are usually more accurately monitored in the controlled conditions of a glasshouse experiment.

To study association between genotype tolerance and nitrogen metabolism, the present study relied on the following hypotheses:

- STB tolerance depends on source/sink balance, it is possible to produce field-like canopies in a glasshouse, with consistent shoot, ear and grain number densities.
- the genotype variation observed in the field can be translated to variation in a glasshouse experiment.
- the traits associated with a low source limitation of the grain filling are potential STB tolerance traits.
- STB tolerance variation is genotype dependent and linked to nitrogen metabolism.

The experiment relied on semi-hydroponic "field-like" wheat populations, grown in trays, in a glasshouse. Two doubled-haploid (DH) populations were screened for STB tolerance and yield potential in three season×locations experiments (details, cf. Chapter 4).

The six selected genotypes were included in the Field 2014-15 experiment, and four of these were the genetic material of the present experiment, chosen according to their tolerance potential. Selected shoots of the four tolerance-contrasting genotypes were exposed to a combination of two post-heading (GS55) nitrogen feeding and two Septoria tritici blotch (STB) inoculation treatments. A growth analysis was carried out to investigate the traits which might influence tolerance of STB.

5.2 Materials and methods

5.2.1 Experimental design

5.2.1.1 Genotype materials

Four genotypes were selected based on three years of field experiments, screening for grain yield and STB tolerance in populations of doubled-haploid lines (Chapter "Material and Methods", section 2.3, p.46). The method for the estimation of tolerance/intolerance is detailed in the Chapter 3 "Field experiment at Hereford 2014-15" (section **??** "Genotypes screened for tolerance", p.**??**):

> *"Intolerance i_{eg} of each genotype (g) was calculated in each experiment (e) as $[\Delta Yield/\Delta HAD]_{eg}$ (grain yield loss per unit of healthy area duration reduction) as described by Foulkes et al. (2006). A genotype crop tolerance grade T (without unit) was then calculated as $-1\times$ the genotype average of i_{eg} beforehand standardized by environment (Eq. 5.1).*
>
> $$T = \frac{-1}{n_e} \sum_{e=1}^{3} \frac{i_{eg} - \mu_e}{sd_e} \tag{5.1}$$
>
> *With: μ_e, sd_e, n_e the environment average, standard deviation and number."*

The Figure 5.1 illustrates the numerical values reported in the Chapter 4 paragraph "3.1 The tolerance grade of the genotypes". The genotypes LSP2×R 127 and C×L 14B were expected to be STB tolerant, while LSP2×R 16 and C×L 7A were expected to be intolerant.

5.2.1.2 Obtaining a field-like crop in the glasshouse

A thousand seeds per genotype were placed in trays to imbibe water on 13 October 2014. When the radicle and coleoptile appeared, 780 plants per genotype were planted in trays filled with peat and transferred to a controlled environment room at 5 °C. Fluorescent lighting (12h photoperiod) provided a Photosynthetic Photon Flux Density (PPFD) of $30 \pm 4\ \mu\text{mol} \cdot \text{s}^{-1} \cdot \text{m}^{-2}$. In early December, after a vernalisation period of

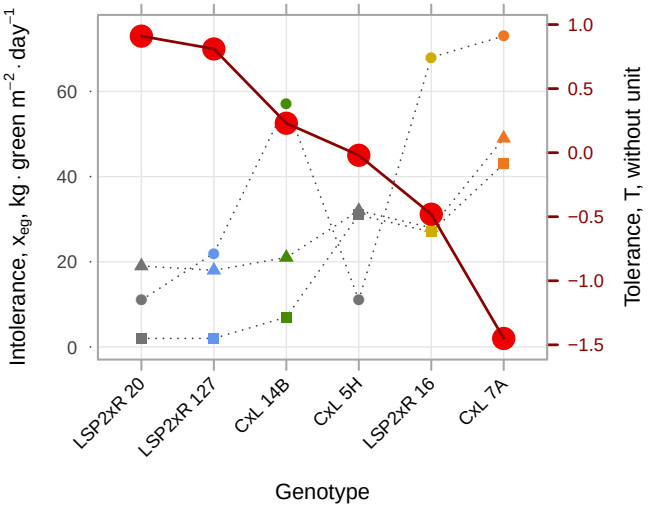


Figure 5.1: Intolerance (x_{eg}, small symbols, dotted lines, left y-axis) of the six doubled-haploid genotypes (g, C×L 14B, green; C×L 7A, orange; LSP2×R 127, blue; LSP2×R 16, yellow; others, gray) calculated in three field experiments (e; 2011-2012 and 2013-2014 at ADAS Hereford, and 2011-2012 at Teagasc, Carlow, Ireland; respectively circles, triangles and squares) as $[\Delta grain\ yield/\Delta HAD]_{eg}$ (unit: kg · ha^{-1}, 85% DM per HAD in days since GS59). The genotype tolerance grade (T, red dots and plain line, right y-axis) was calculated as −1× the genotype average of x_{eg}, beforehand standardized by environment (without unit).

6 weeks, 770 plants per genotype (total 3080 plants) were transplanted into 1540 pots (PVC, 7.5 cm diameter, 35 cm depth; two plants per pot) filled with moistened perlite (neutral substrate) distributed in 44 trays (0.24 m^2, 25 cm depth), resulting in a crop density of 292 plants · m^{-2}. In a glasshouse, the trays were positioned in four rows of 11 trays (one row per genotype) under two HQI-T™ lamp (Metal halide lamps with quartz technology OSRAM®, Munich, Germany) ramps providing 275 μmol · s^{-1} · m^{-2} PPFD (200 μmol · s^{-1} · m^{-2} measured at the plant level, solar radiations were negligible at this time of the year). Plants grew, exposed to increasing photoperiod, +1h daylight per week from 12h to 16h, and exposed to average daily temperature of 12 °C varying from 10 °C to 20 °C (daily maximum temperature <25 °C, Fig. 5.4). Each tray was filled with nutrient solution, the lower 10 cm of each pot remaining constantly immersed. The nutrient solution (see appendix 5.A.1) was changed once a week. Preventive treatment against eyespot and mildew (cyprodinil) was applied one week after the start of growth in glasshouse. The trays were swapped every week and at start of stem elongation the trays were surrounded by side shading net to prevent an edge effect. These conditions were maintained until the application of the experimental treatments.

5.2.1.3 Experimental treatments

Illustration of obtaining the field-like canopy is provided Figure 5.2 (p.130).

At mid booting (GS44, mid to end of February), the distance between the ligules

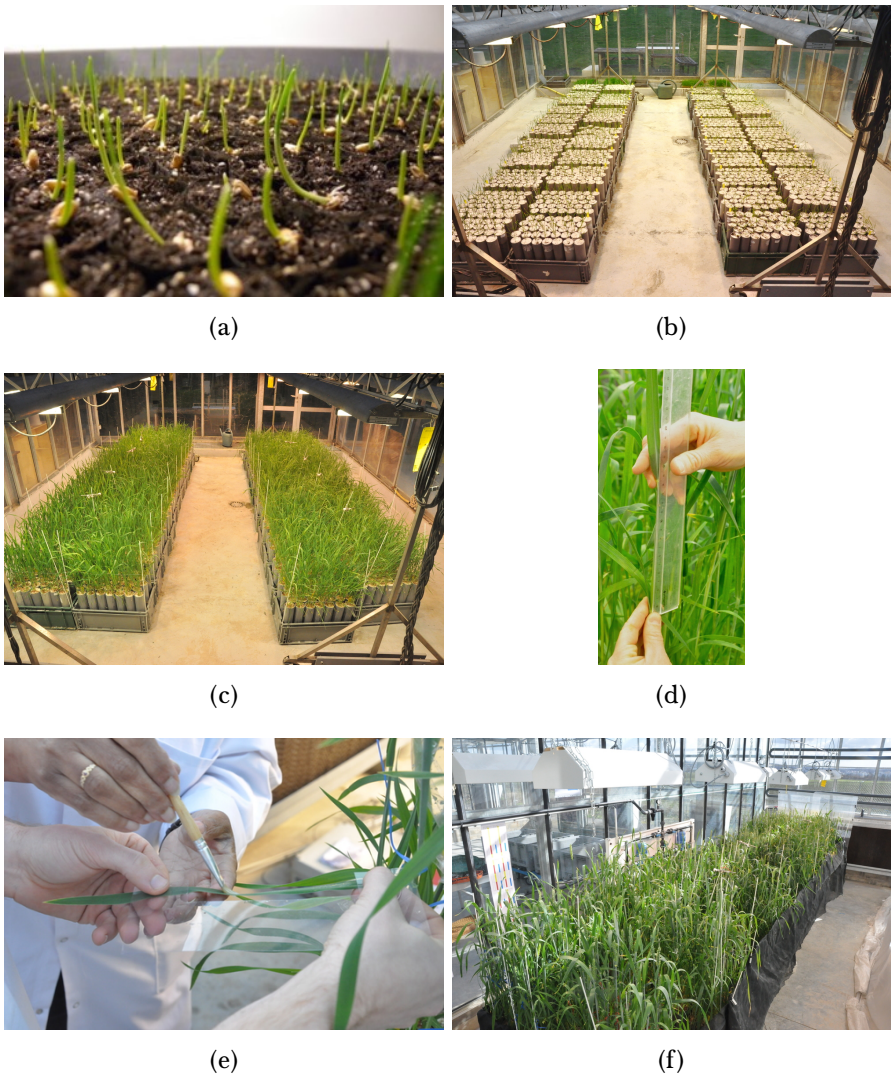


Figure 5.2: Illustration of the phases of the glasshouse experiment. a) Vernalisation of the plants. b) Transfer to the glasshouse. c) Early stem extension stage. d) Inter-ligule space measurements. e) Paintbrush inoculation. f) Grain-filling phase.

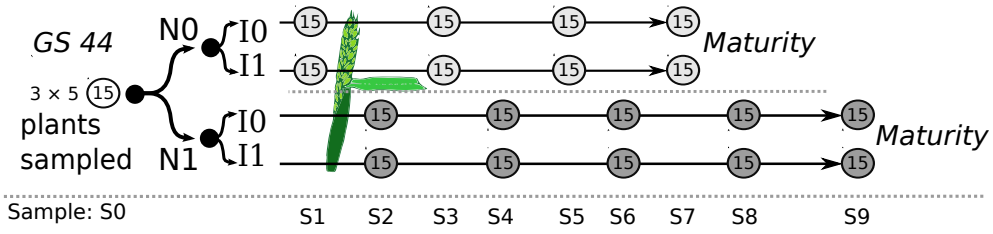


Figure 5.3: Sampling schedule of greenhouse experiment applied to each genotype. The arrows represent the timeline. The circled "15" represents the three sub-samples of five shoots collected and dissected at every sampling date, the corresponding sampling date identifier is given below the bottom line. At GS44, an initial sample was collected, then the nitrogen treatment and the inoculation treatment were applied before further sampling. The N0 (discontinued nitrogen nutrition) induced an earlier maturity and is therefore based on four sampling dates, while N1 (maintained nitrogen nutrition) was associated with a later maturity and five sampling dates. Heading stage (GS55) occurred between S1 and S2.

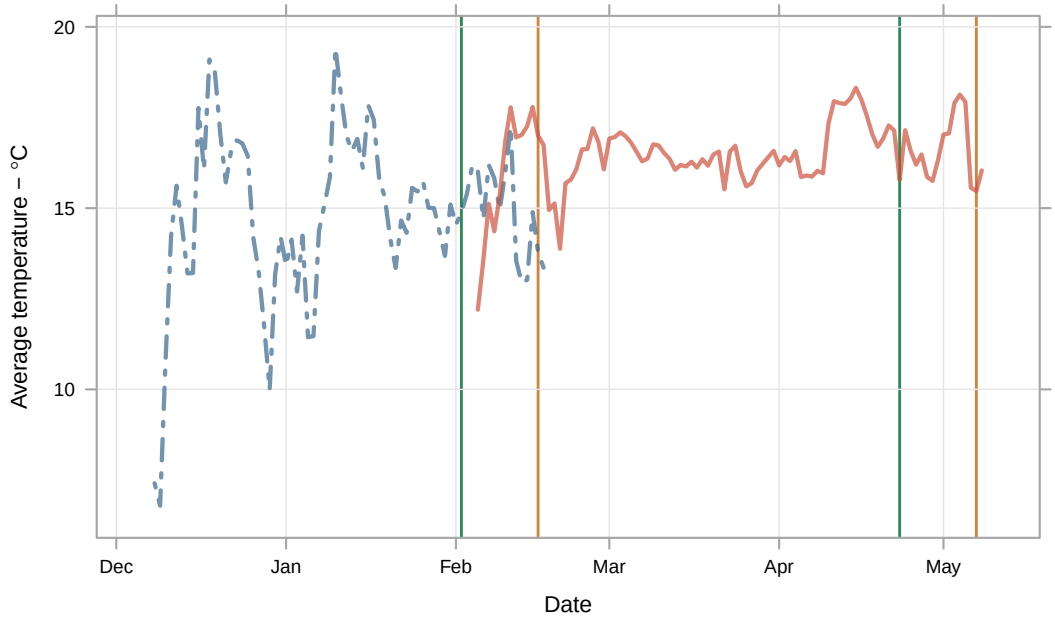
of the first leaf (flag leaf) and second leaf of the main shoot on all plants was measured. Regarding this measurement, 19 lots of 15 plants equivalent in mean and standard deviation were formed. The selected plants were tagged and the first lot was sampled (sample S0, Fig. 5.3). The remaining plants were then transferred to a thermo-regulated glasshouse (±1 °C): 16 h photoperiod, temperature 17 °C and 10 °C at day and night, respectively. At this time of the year, solar radiation became substantial affecting daily radiation exposition which tended to increase with the time, from 250 μmol $\cdot$ s^{-1} $\cdot$ m^{-2} to 450 μmol $\cdot$ s^{-1} $\cdot$ m^{-2} (Fig. 5.4).

Per genotype, 10 lots of 15 plants were grouped in trays with maintained nitrogen nutrition (treatment modality N1) and 8 lots of 15 plants were grouped in trays where nitrogen nutrition was halted after the pots were drained of their nutrient solution (treatment modality N0). In the same week, four and five lots of 15 plants per genotype were inoculated/non-inoculated (I1, control I0), respectively in N0 and N1 trays. To ensure appropriate disease pressure, an inoculum solution 10^6 spores $\cdot$ ml^{-1} was prepared and spread using a paintbrush over 10 cm at 1 cm above ligule of leaf 1 and leaf 2. Leaves were incubated for 48 h in individual plastic bags to maintain relative humidity saturation and lamps were turned off preventing scorching.

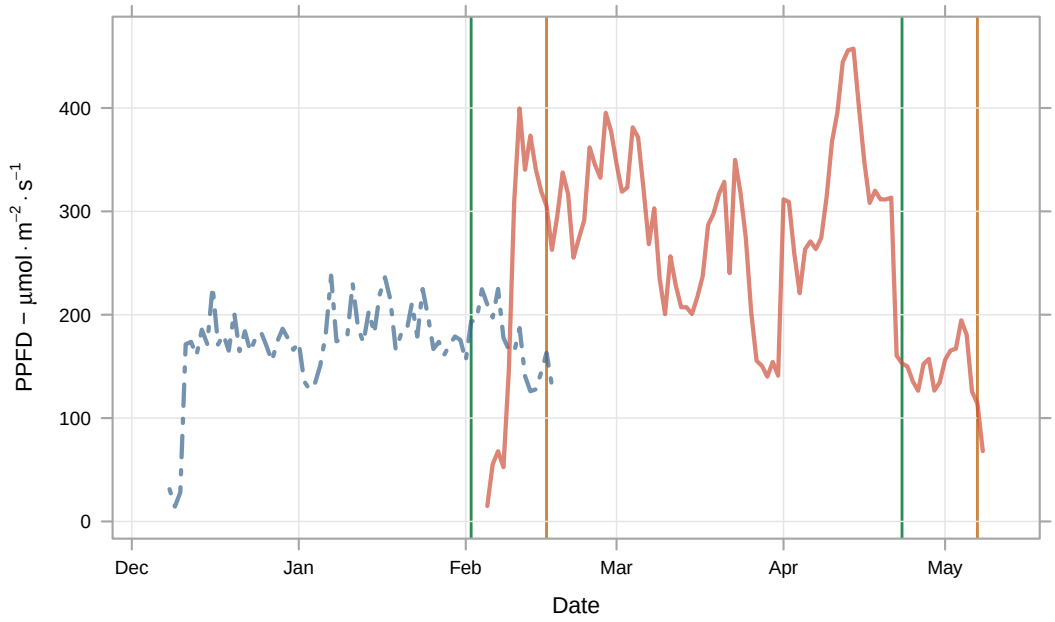
5.2.1.4 Growth analysis

Firstly, samples were collected just before the N treatment was applied. Then, every week, 15 inoculated and 15 control plants were sampled alternatively in N0 one week and N1 trays the following week, for each genotype (four and five sampling dates respectively, Fig. 5.3). The latest samples were collected during the first week of May.

Each sample of 15 plants was divided randomly into three repetitions of five plants. In each repetition, the main shoot was separated from tillers. The top three leaves were precisely cut at the ligule and scanned to measure the leaf lamina area and green leaf lamina area per leaf rank. The stem was cut above node 3 and the leaf sheath was peeled off the stem. The fresh weight of leaf lamina and sheath was recorded, the material was chopped to prepare aliquots 225±25 mg that were frozen at −80 °C. Non-selected plants remaining in the pots were collected. The pots were emptied to obtain the roots which were thoroughly rinsed to remove perlite and collected. The remaining material of the leaf sample (apart of aliquots stored at −80 °C) was freeze dried as were the internodes above the third leaf (later designated as stem), the base of plant (combined internodes and lower leaves) and the ears. Tillers, non-selected plants and roots were oven dried. All the samples were then weighed separately. Starting from sampling-date S3 (Fig. 5.3) ears were threshed, the grain separated from chaff and the number of grains counted. Dried samples were finely milled and their nitrogen content was estimated by the Dumas combustion method. Frozen aliquots were used for metabolic assays according to Ben



(a) Temperature



(b) Global radiation

Figure 5.4: Daily temperature (top, °C) and global radiation exposition (bottom, μmol $\cdot$ s^{-1} $\cdot$ m^{-2}). The dotted blue / plain red lines represent the first/second glasshouse environments. The vertical lines represent successively: transfert of the LSP2×R genotypes to the second glasshouse, transfert of the C×L genotypes to the second glasshouse, final samples for the LSP2×R genotypes, final samples for the C×L genotypes.

Slimane et al. (2013). Total water-soluble carbohydrate content was also measured on stem extracts of LSP2×R genotypes using an enzymatic procedure (Bancal, 2008). As part of the experiment here described, gas exchange of the flag leaf was also recorded in young N1 plants using Licor 6400 XT at 25 °C under 400 μmol · mol^{-1} external CO_2 concentration and vapor pressure deficit below 1 kPa. Pmax was the observed gas exchange rate under 2000 μmol · s^{-1} · m^{-2} irradiance.

5.2.2 Data analysis

5.2.2.1 Population settings

- **Ear number**

The plant density (d) was 292 plants · m^{-2}. The measurements were applied on main shoots. The tillers and main shoot dry matter ($DM_{tillers}$ and $DM_{main\ shoot}$, respectively) were converted into the equivalent number of main shoots per square metre (ENeq) to allow for estimation of the crop parameters at the square metre scale:

$$ENeq = \frac{d}{n_S \cdot n_r} \sum_{S=3}^{9} \sum_{r=1}^{3} \left(1 + \frac{dm_{tillers}}{dm_{main\ shoot}}\right)_{Sr} \tag{5.2}$$

With: S = { 3, 5, 7} for N0 estimations, and S = { 4, 6, 8, 9 } for N1 estimations, thus ENeq was, respectively, based on 9 and 12 sub-samples estimations.

- **Grain number per ear**

The grains · ear^{-1} (GNe) was the average of the counts from S3 to S9. The GNe was based on 9 and 12 sub-samples in the N0 and N1 treatments, respectively, see above paragraph.

- **Leaf lamina area**

The leaf size was stabilized from sample S1. The leaf lamina area per ear-bearing shoot (LAe) was the average of the sum of the three upper leaf lamina areas over the various sampling dates for each treatment combination (therefore based on 12 and 15 sub-samples for N0 and N1, respectively). The LAe was used to calculate the Leaf Area Index (LAI, leaf area per square metre, $LAI = LAe \times ENeq$) or the leaf area per grain (LAg, $LAg = LAe \times GNe^{-1}$). The LAe, LAI and LAg were computed for the overall upper canopy (cumulation leaf 1 to leaf 3) or per single leaf layer (then signified by number of leaf layer, e.g. LAe 1 for the leaf 1). Finally the fraction of upper leaf lamina area that represented each leaf layer was also computed (e.g. $fLA2 = LAe2 \times LAe^{-1}$).

5.2.2.2 The grain yield

The Thousand Grain Weight (TGW) was estimated on three sub-samples for each treatment combination from S3 to S9. The grain yield per ear (Ye) was estimated using average estimation of GNe and TGW available per G × N × I combination ($Ye = TGW \times GNe$) and the grain yield per square metre was then estimated using the average estimation of ENeq (Ym, $Ym = TGW \times GNe \times ENeq$).

Grain maturity was not fully reached in every treatment at harvest. The TGW and Ye and Ym at maturity were therefore estimated. To do so, for each treatment combination, TGW and Ye and Ym evolution from samples S3 to S9, including an additional theoretical null value at GS55 (thus n = 4 and n = 5 respectively for N0 and N1) were fitted to a logistic function (Eq. 5.3; $R^2 > 0.998$; RMSE: $0.8\,mg \cdot grain^{-1}$ and $0.03\,g \cdot ear^{-1}$ and $13\,g \cdot m^{-2}$, for TGW, Ye, Ym, respectively). Grain yield (TGW, Ye, Ym) was reported at 100% DM.

For extrapolation at maturity of TGW and Ye and Ym, the observations from S3 to S9 were fitted to a 3-parameter logistic curve for each repetition of the final sample. Each final observation of TGW and Ye and Ym could therefore be extrapolated at maturity (1130 °Cd_H, five degree-days after the latest sampling date), and estimated at any time from heading stage (GS55) to maturity. Each logistic fit was therefore actually based on 7 and 10 true observations for N0 and N1, respectively.

$$y(t) = K \cdot \frac{1}{1 + a \cdot e^{-r \cdot t}} \tag{5.3}$$

where: $y(t)$ is the response variable (TGW or Ye or Ym) at the time t (thermal time since heading stage, GS55, unit °Cd_H); and K and a and r are the logistic parameters.

5.2.2.3 The Healthy Area Duration (HAD)

Fraction of Green Leaf Lamina Area per shoot (fGLA, % green leaf area) observations were fitted to the Gompertz's function (Bancal et al., 2015) for each G×N×I (Eq. 5.4, $R^2 > 0.99$; RMSE: 2.5 green % ·° Cd_H, Chapter 2 - Section 2.5 "The Healthy Area Duration" p.48).

$$fGLA(t, K = 100, D, I) = K \cdot \exp\left(-\exp\left(\frac{2 \times (I - t)}{D}\right)\right) \tag{5.4}$$

$$HAD = \int_{t=0°Cd_H}^{1130°Cd_H} fGLA(t, K = 100, D, I) \tag{5.5}$$

The area under the fGLA curve in the range 0 – 1 130 °Cd_H was referred to the Healthy (= green) Area Duration (HAD, Eq. 5.5, unit: % ·° Cd_H). The amount of healthy tissue

and hence the potential source for a single shoot was obtained by $HAD \times LAe$ and referred to as the HAD per ear-bearing shoot (HADe, unit $m^2 \cdot^\circ Cd \cdot shoot^{-1}$). Source was also scaled to ground area m^2 (HADm = $HADe \times ENeq$, unit: $m^2 \cdot^\circ Cd \cdot m^{-2}$) or a single grain (HADg =$HADe \cdot GNe^{-1}$, unit: $dm^2 \cdot^\circ Cd \cdot grain^{-1}$).

5.2.2.4 Dry matter weight and Nitrogen amounts

The dry matter per shoot was measured at each sampling date (M). The nitrogen amount per shoot was calculated per sampling date and per organ as the product $M \times \%N/100$ and expressed in mg per shoot.

Similarly to the grain yield per ear Ye was estimated during the grain filling phase as the measured TGW multiplied by the average GNe of the G × N × I combination at each sampling date, the Thousand Grain Nitrogen amount was estimated (TGN, $mg \cdot [1000\,grains]^{-1}$) at each sampling date when the nitrogen analysis was run. The grain nitrogen amount per ear was then obtained by $GNe \times TGN$. This reduced the variability associated with the random variation in sampled shoot size within treatment combinations.

The nitrogen and dry-matter fluxes were estimated from S0 to S7 or S9, according to the nitrogen treatment N. The dry matter fluxes and nitrogen fluxes are referred to as ΔDM and ΔN, respectively. The fluxes ΔDM and ΔN were first estimated at the ear-bearing shoot scale as the difference between the last sampling date (S7 or S9) and S0 for each G × N × I treatment combination. A positive value of ΔDM and ΔN was, therefore, associated with a net assimilation (DM fixation or N uptake), while a negative value was associated with a net mobilisation flux. The fluxes were estimated for: total above-ground biomass (ag, i.e. without the roots), vegetative above-ground biomass (v, i.e. without the roots or the grains), and grain biomass. Hence, the fluxes estimated were: ΔDMt, ΔDMv, ΔDMg, ΔNt, ΔNv, ΔNg. The fluxes, initially calculated per ear-bearing shoot (/ear), were then multiplied by ENeq to estimate the flux at the crop scale ($/m^2$) or divided by GNe to estimate the flux at the grain scale (/grain). The different scales were explicitly specified in the text, for instance dMt/grain indicated the total (dry-) mass flux per single grain.

The dMg/grain dMg/ear dMg/m^2 flux notations were equivalent to the grain mass observed at harvest expressed per grain, ear or m^2, respectively. Unless specified otherwise, the TGW, Ye and Ym were assigned to the extrapolation of the grain yield at $1130\,^\circ Cd_H$.

5.2.2.5 Tolerance estimation

The tolerance of STB study relied on the relationship between the grain yield and the source availability. Firstly, intolerance was estimated as the Ym loss per unit of HADm reduction. The intolerance was also estimated at the grain scale as $\Delta TGW/\Delta HADg$. This method is straightforward but doesn't take into account the asymptotic relationship

between grain sink and source. Therefore, an alternative method was applied, comparing the actual grain yield loss to the potential yield loss. The potential yield loss relationship was estimated by a monomolecular equation which joins a potential yield with a given HADm available: $Ypot = K \cdot \left(-\exp\left(-1 \cdot r \cdot HADm/K\right)\right)$, with the proposed values K = 1090 and r = 1.33 (Gouache et al. 2012, based on 560 plots, multiple environments × seasons × cultivars). Therefore, a second expression of tolerance was given by the ratio $\Delta Ym/\Delta Ypot$.

5.2.3 Statistics

The experiment was not divided into replicate or block, but each sampling date was composed of three subsamples. The different sampling date could be used for analysis of the population settings (ENeq, GNe, LAe). The healthy area duration accuracy was estimated by a bootstrap strategy as the green area kinetics were estimated by 50 random association of subsamples and dates. However, no repetition of the HAD (or kinetics-related parameters) were available for analysis. More details about the analysis are presented hereafter.

- **Population settings**: **ENeq**, **GNe**, **LAe**

For population settings, the data were first averaged per sampling date (necessary for ANOVA hypotheses). There were eight observations per sampling date (4G × 2I × 1N, remainder: nitrogen treatments were sampled in alternate weeks), so for GNe, ENeq and LAe, the number of observations (n) was: 56, 72 and 72, respectively. The LAg and LAI were estimated using the "per sampling date" LAe, either divided by the GNe estimated for each G × N × I combination, or multiplied by ENeq. The sampling date (S) was included as a random effect in a mixed model of ANOVA. Effects G, N and I, including up to three-way interaction were tested by the Wald chi-square.

- **Healthy area duration**, **grain yield**, **dry matter and nitrogen flux**

Although each individual observation was based on three sub-samples, there was no repetition in blocks of the treatment combinations. Therefore, the three sub-samples at each sampling date were averaged resulting in single estimation for each G × N × I combination, therefore n = 16. A three-way ANOVA model was fitted including up to 2-ways interactions, through a Fisher's test. In the absence of G × N × I repetition, the 3-way interaction could not be tested.

- **Model simplification and post-hoc test**

Given the low number of observations, non-significant effects were removed for parsimonious use of the degrees of freedom. A stepwise ANOVA model selection was op-

erated, removing the least significant effects, to restrict the model to the sole significant effects. The differences between level of factors were tested based on the Tukey's Honest Significant Difference test (Tukey HSD).

5.3 Results

5.3.1 From source:sink characterisation to tolerance

5.3.1.1 Development rate

Heading stage for the genotypes C×L was synchronous (1 March), being reached 15 days (243 °Cd) later than LSP2×R genotypes. There was a 2 days difference (35 °Cd) between LSP2×R genotypes as heading occurred on 13 and 15 February, respectively, for LSP2×R 127 and LSP2×R 16. Therefore, there was no significant difference of heading date within tolerance/intolerance pairs, but a large difference between the two crosses. This could in part be due to a difference in vernalisation requirements as plants were vernalized for 50 days, which is enough for France-adapted genotypes, but could be limiting for UK-selected genotypes; the differences in photoperiod insensitivity between the DH crosses could also explain earliness variation. As evoked later, the Nitrogen treatment induced a very large extension of the senescence, especially for the genotype C×L 7A for which senescence was not totally achieved at the time of the last sampling date, though maturity time was very close. Later in the results, the estimation for maturity variables is considered at the time 1130 $°Cd_H$.

5.3.1.2 The source traits for grain filling

- **Canopy characterisation**

Ear and equivalent fertile-ear numbers per m^2 Tiller number randomly fluctuated from one sampling date to another, which was partly taken into account by plant random variation of above-ground DM. Consequently, ENeq fluctuated less than EN, while it mostly exhibited the same time course. The ENeq was significantly lower for LSP2×R 127 (393 shoots $\cdot m^{-2}$) in comparison to the other genotypes (444 to 455 shoot $\cdot m^{-2}$, $P < 0.001$, Table 5.1). Both EN and ENeq did not change during the experiment in N0 crops, whereas they significantly increased with time in N1 crops, due to post-heading tillering. Averaged over experiment, ENeq in N1 was therefore higher by 67 shoots $\cdot m^{-2}$ without interaction with genotype. Lastly, unlike EN, ENeq increased by 33 shoots $\cdot m^{-2}$ in I1, with no significant interaction with either G or N. The discrepancy between EN and ENeq indicated above-ground DM was less rapidly increased in inoculated main shoots than in the tillers. These time effects were not further considered, instead ENeq was regarded as constant with time in each treatment which could challenge data interpolation at the crop scale.

Table 5.1: Analysis of variance of the grain source trait responses: the Equivalent Number of shoot per square metre (ENeq), the Leaf Lamina Area per ear-bearing shoot (canopy, LAe; flag leaf, LAe 1), the fraction of flag leaf (fLA 1), the senescence time (I) and duration (D), the healthy area duration (HADe, $m^2 \cdot^\circ Cd \cdot shoot^{-1}$; HADm, $m^2 \cdot^\circ Cd \cdot m^{-2}$), variation in vegetative dry matter mobilisation per ear-bearing shoot (ΔMv/ear, Z89 - Z55, > 0 if net accumulation). Significance of genotype, nitrogen or inoculation treatments and interactions on ENeq, LAe, LAe 1, fLA 1 responses were tested using Wald Chi-square (mixed model, random variation caused by the sampling date); the other responses were tested by F test (significance marked by usual star code and "ns" for non-significant). When based on n=16 observations, the three-way interaction could not be tested ("na", non applicable). The non significant effects were removed for parsimonious use of degree of freedom. The values provided were the least square mean estimations of the simple effects (averaged over the levels of the other effects). The symbol & refers to a test on differences between I0 and I1 as an alternative because of a homoscedasticity problem.

	ENeq $ears \cdot m^{-2}$	LAe cm^2	LAe 1 cm^2	LAI	fLA 1	I $^\circ Cd_H$	D $^\circ Cd$	HADe $^\circ Cd \frac{m^2}{shoot^{-1}}$	HADm $^\circ Cd \frac{m^2}{m^{-2}}$	ΔMv/ear $mg \cdot ear^{-1}$
Genotype (G)	***	***	***	***	***	**	**	***	***	***
C×L 14B	455b	98.3d	36.8b	4.47d	0.37a	648a	346b	5.42a	2519b	0.354b
C×L 7A	444b	93.9c	36.8b	4.17c	0.39b	855b	332b	6.99b	3145c	-0.047a
LSP2×R 127	393a	77.8a	34.9a	3.06a	0.45c	629a	218a	4.41a	1780a	0.177ab
LSP2×R 16	451b	81.9b	39.2c	3.69b	0.48d	684a	336b	4.80a	2233ab	0.634c
Nitrogen (N)	**	ns	*	***	ns	***	***	***	***	***
N0	403a	88.7	37.4a	3.58a	0.43	493a	227a	3.85a	1555a	0.495b
N1	470b	87.4	36.5b	4.12b	0.42	915b	389b	6.96b	3283b	0.064a
Inoculation (I)	***&	ns	ns	***	ns	ns	ns	ns	ns	ns
I0	424a	88.5	37.1	3.37a	0.42	717	322	5.49	2363	0.344
I1	457b	87.5	36.7	3.97b	0.42	692	294	5.32	2476	0.215
G × N	ns&	ns	ns	ns	ns	ns	ns	ns	ns	*
G × I	ns&	ns	ns	ns	ns	ns	ns	ns	ns	ns
N × I	ns&	ns	ns	ns	ns	ns	ns	ns	ns	ns
G×N×I	ns&	ns	ns	ns	ns	na	na	na	na	ns

Table 5.2: Values for grain source traits, for column description see Table 5.1.

Nitro. Inoc. Genotype	ENeq $ears \cdot m^{-2}$	LAe cm^2	LAe 1 cm^2	LAI	fLA 1	I $^\circ Cd_H$	D $^\circ Cd \frac{m^2}{shoot^{-1}}$	HADe $^\circ Cd \frac{m^2}{\cdot m^{-2}}$	HADm $mg \cdot ear^{-1}$	ΔMv/ear
N0 I0										
C×L 14B	407	98.0	37.5	3.99	0.38	416	236	3.45	1403	0.670
C×L 7A	399	96.5	37.6	3.85	0.39	652	272	5.54	2212	0.398
LSP2×R 127	342	78.7	35.0	2.69	0.45	465	155	3.31	1130	0.350
LSP2×R 16	408	83.1	40.4	3.39	0.49	481	310	3.31	1351	0.736
N0 I1										
C×L 14B	429	99.4	37.0	4.26	0.37	508	232	4.40	1887	0.807
C×L 7A	432	94.2	37.5	4.08	0.40	628	234	5.28	2285	0.138
LSP2×R 127	377	76.7	35.2	2.89	0.46	449	156	3.11	1171	0.145
LSP2×R 16	421	82.6	39.1	3.48	0.47	349	221	2.39	1006	0.721
N1 I0										
C×L 14B	478	97.2	35.9	4.65	0.37	832	447	6.87	3287	0.128
C×L 7A	451	93.8	36.4	4.23	0.39	1151	431	9.12	4113	-0.387
LSP2×R 127	400	78.7	35.1	3.15	0.45	774	340	5.33	2133	0.182
LSP2×R 16	471	82.1	39.1	3.86	0.48	962	381	6.96	3276	0.672
N1 I1										
C×L 14B	503	98.6	36.8	4.95	0.37	836	468	6.96	3498	-0.189
C×L 7A	497	91.7	35.9	4.55	0.39	993	390	8.00	3972	-0.339
LSP2×R 127	455	77.2	34.3	3.51	0.44	829	222	5.91	2686	0.029
LSP2×R 16	505	80.2	38.3	4.05	0.48	944	432	6.54	3301	0.417

Leaf lamina area The leaf area per ear-bearing main-shoot (LAe) of every leaf layer strongly discriminated the genotypes ($P < 0.001$). The plants selected for early cut off of nitrogen nutrition (N0) showed an unexpected increment of +0.9 cm^2 of the flag-leaf compared to N1 (LAe 1, $P = 0.031$). At the crop scale, the LAI estimation was the result of ENeq and LAe product. Both ENeq and LAe varied with the genotype, but only ENeq varied with I or N, consequently LAI varied also with I and N in the same direction as ENeq: N1 and I1 increased the LAI (13% and 7%, respectively). The G variations were relatively more important for the LAI (3.0 to 4.5) than for the LAe (78 to 98 cm^2).

The leaf profile fLA 1 The contribution of leaf layers to canopy leaf area varied significantly with the genotype. Indeed, the genotypes were characterised by contrasting flag-leaf contributions ($P < 0.001$); the two crosses were highly different with a 10% higher contribution of the flag leaf (fLA 1) for early-heading LSP2×R than C×L. Within cross, difference was also significant (2%); the two putative tolerant crosses exhibited smaller fLA 1. The flag-leaf contribution was negatively correlated with that of the leaf 2 or the leaf 3 ($r = -0.86^{***}$ and $r = -0.96^{***}$, respectively). Finally, leaf contribution to canopy leaf area was not altered by either N or I treatments.

- **Senescence parameters *I* and D**

The Figure 5.5 represents the percentage green leaf lamina area kinetics from heading stage to maturity. Inoculation did not significantly change green area, and actual STB symptoms were only recorded on flag-leaf of LSP2×R 16 under N0 treatment (Fig. 5.5). Conversely, the nitrogen deficiency (N0) resulted in a sharp advance in the senescence timings (I, $-422\,°Cd_H$, $P < 0.001$, Table 5.1). Genotype differences relied mainly on the genotype C×L 7A that showed a very late senescence timing (G effect $P = 0.002$, Table 5.1); under N1I0, C×L 7A senescence timing I was 24% later than the other genotypes. Actually, the genotypes under N1 achieved total leaf senescence just before the last sampling except for C×L 7A genotype which still showed stay-green of the two upper leaves even though ear chaff was completely dry at this time. The senescence phase duration (D) was shorter for the genotype LSP2×R 127 (Table 5.1, G effect $P = 0.004$). Moreover, the Nitrogen treatment N0 resulted in a 40% faster senescence ($P < 0.001$), while inoculation showed no significant effect on D.

- **The healthy area duration**

Leaf lamina area and senescence timing and duration shaped the area under the senescence progress curve, resulting in different Healthy Area Duration (HAD) with treatments. Associated with a large LAe, late senescence timing (I) and long senescence duration (D), the genotype C×L 7A showed the largest HADe (HAD per ear-bearing shoot),

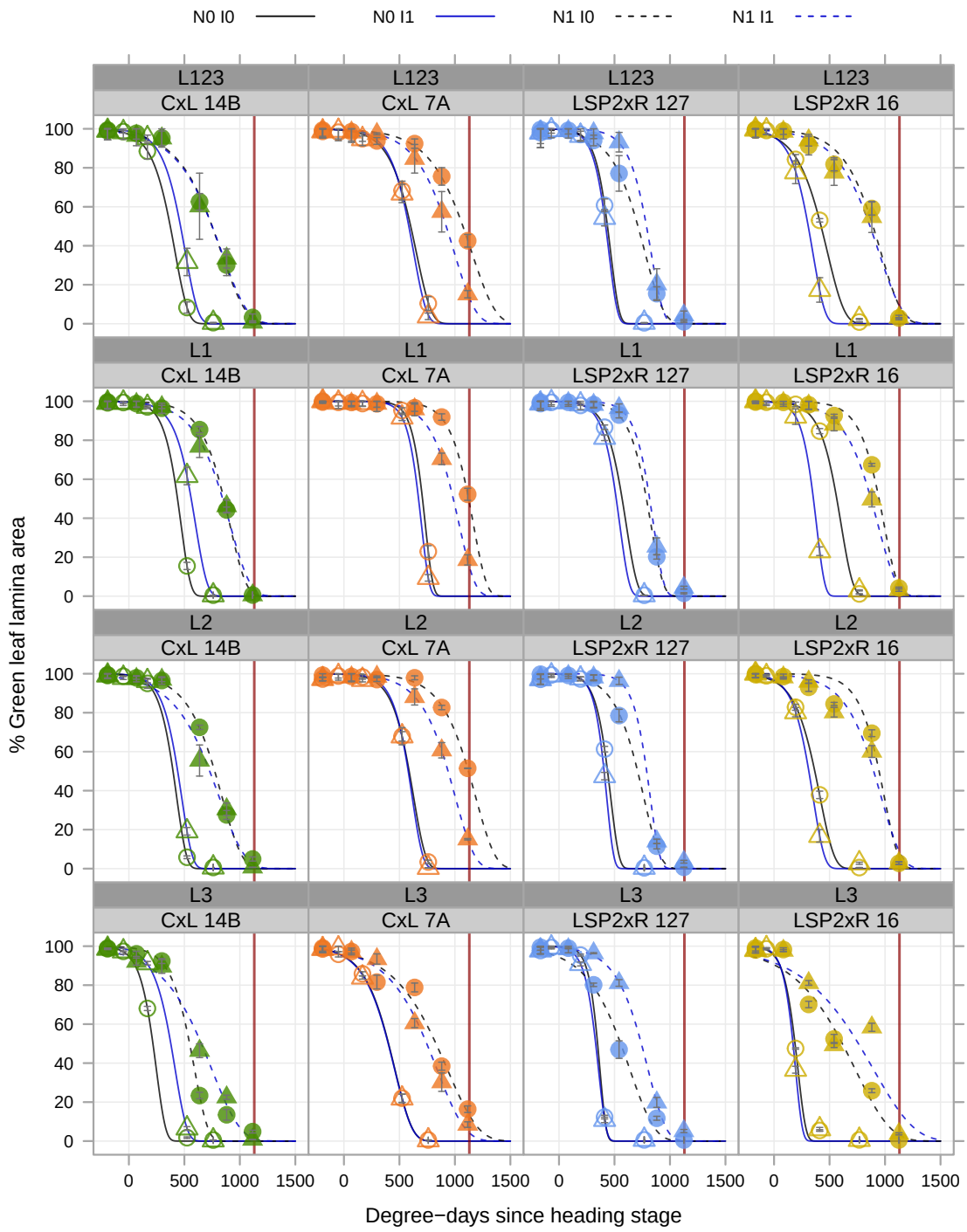


Figure 5.5: Kinetics of fraction of Green leaf lamina area. The y-axis represents the %GLA for the cumulated 3 upper leaves (± standard error). The x-axis represents the thermal time since heading stage (GS55). Each column of panels and colour corresponds to a genotype (C×L 14B, green; C×L 7A, orange; LSP2×R 127, blue; LSP2×R 16, yellow), each row corresponds to a leaf layer (L123 for the cumulated three upper leaf layers. The empty/closed symbols and plain/dotted lines represent the N0/N1 treatments. The circle/triangle symbols and black/blue lines represent the I0/I1 treatments. The last samples were collected at 1125 degree-days post heading stage. A red vertical line was added at 1130 degree-days.

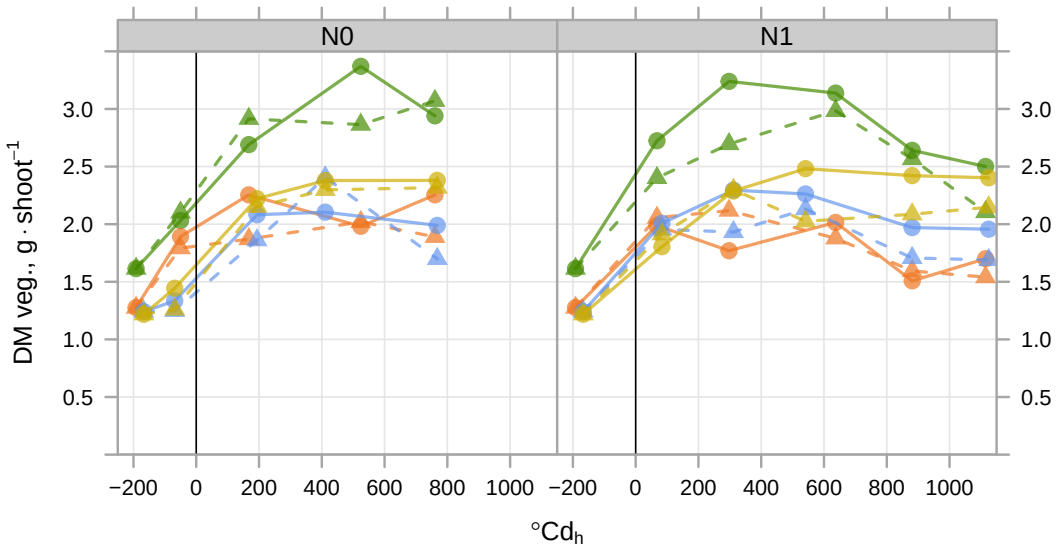


Figure 5.6: Evolution of the vegetative dry-matter (root, leaves, stem and chaff). The y-axis represents the vegetative dry-matter per ear-bearing shoot ($g \cdot shoot^{-1}$). The x-axis represents the thermal time since heading stage (GS55). The colours represent the genotypes (CxL 14B, green; CxL 7A, orange; LSP2xR 127, blue; LSP2xR 16, yellow). The left/right panels represent the N0/N1 treatment. The circles and plain lines represent I0, while the triangles and dotted lines represent I1.

the other genotypes had significantly lower HADe (by 22% to 37%). Severity of STB was very low as stated before, inoculation did not significantly modify HADe and HADm. The Nitrogen deprivation N0 did not alter the canopy leaf area per shoot, thus, the sharp reduction of senescence timing *I* was directly translated into a large reduction of HADe (-45%). Nitrogen fertilisation (N1) promoted lush canopy as the ENeq was positively correlated with HADe of the canopy or each individual leaf layer ($r = 0.69^{**}$ to $r = 0.74^{**}$ for the individual leaf layers or the canopy). Consequently, the genotype contrast revealed for HADe was emphasized at the crop scale HADm, from 1780 to $3145\,m^2 \cdot ^\circ Cd \cdot m^{-2}$ for LSP2×R 127 and C×L 7A, respectively (averaged across I and N treatment levels); HADm varied with the N treatment as, on average, the HADm under N0 represented only 53% of the N1 HADm ($P < 0.001$; actually from 35 to 56% of N1 HADm for LSP2×R 127 to C×L 7A, respectively). The genotype and nitrogen effect on canopy HADm were comparable for the individual leaf-layer HADm, with the addition of a significant G×N interaction ($P = 0.015$): the HADm of LSP2×R 127 and LSP2×R 16 were comparable under N0 but under N1 LSP2×R 127 HADm was significantly lower than LSP2×R 16 HADm.

- **Alternative source: Dry-matter remobilisation**

Surprisingly, DM accumulated in vegetative organs (including roots, Fig. 5.6) until very late during grain filling: approximately 250 °Cd_H in C×L 7A and 500 °Cd_H in other genotypes. Because samplings were achieved at different dates in the N0 and N1 treatments, the kinetics of vegetative DM could not be adequately compared, but visual examination indicated a similar pattern and peaks. The balance in vegetative dry matter (ΔDMv) was then calculated from GS55 to GS89 at both the shoot and the crop scale, which were found to be highly correlated ($r > 0.99^{***}$). Most of the balances indicated that a DM accumulation (ΔDMv > 0) in the vegetative organs had occurred. The inoculation did not influence significantly ΔDMv, but there was variation between genotypes and nitrogen treatments ($P < 0.001$) including an interaction ($P < 0.05$). Under N1, the two C×L genotypes showed a net remobilisation of dry matter (ΔMv < 0) while the two LSP2×R genotypes accumulated dry matter (ΔM > 0). Under the N0 stress, the two crosses behaved differently as N0 induced a significant ΔDMv increase for C×L genotypes (therefore leading to net accumulation) while it was not significantly changed for LSP2×R genotypes. Surprisingly, ΔDMv at the shoot scale was negatively correlated with the HADe ($r = -0.69^{**}$) indicating higher HADe increased the remobilisation from the vegetative organs. A very similar correlation was observed between ΔDMv and either the senescence time (I) or the HADm. No other source variable (i.e. LAe, LAe 1, fLA 1, D) was correlated with dry mass remobilisation during grain filling.

5.3.1.3 The grain sink traits

- **Grain Number**

The Grain Number per ear (GNe) varied significantly regarding the three way interaction G × N × I (Table 5.3, $P < 0.001$). In the most favourable conditions for grain filling (high N nutrition without inoculation, N1 I0, Table 5.4) two groups of significantly different genotypes were identified: the LSP2×R 127 and C×L 7A (33.6 and 35.5 grains per ear, respectively) versus LSP2×R 16 and C×L 14B (46.6 and 46.2 grains per ear). Thus, GNe was not linked to putative tolerance. The inoculation (I1) generally resulted in a significant GNe reduction (-17% on average), while the single nitrogen treatment did not affect GNe significantly. However, a significant interaction between inoculation and nitrogen treatments was observed: in the case of C×L 7A for which the inoculation I1 was not associated with a GNe decrease under N1. Altogether, G × N × I combinations resulted in GNe variation with I1 ranging from $+3.7\%^{ns}$ to $-28\%^{***}$ (average: $-15.1\%^{***}$). This GNe decrease was not linked to STB as it did not correlate with HAD 1 variation in inoculated flag leaves.

Table 5.3: Analysis of variance of the grain yield component responses: the Grain Number per ear (GNe), the Equivalent Number of shoot per square metre (ENeq), the grain dry-matter observed at last sampling expressed per grain (DMg/grain) and per ear-bearing shoot (DMg/ear) and per m^2 (DMg/m^2), the estimated Thousand Grain Weight (TGW), grain yield per ear (Ye) and per m^2 (Ym). Estimated TGW, Ye and Ym were obtained by extrapolating at 1130 °Cd_H a logistic fit of grain DM. The fraction fTGW ($(dMgrain \cdot grain^{-1})/(TGW)$) quantified the grain filling level at the time of last sampling. Significance of genotype, nitrogen or inoculation treatments and interactions were tested by F test, and GNe and ENeq were tested using Wald Chi-square (significance marked by usual star code and "•" for P < 0.10 and "ns" for non-significant). When based on n=16 observations, the three-way interaction could not be tested ("na", non applicable). The non significant effects were removed for parsimonious use of degree of freedom. The values provided were the least square mean estimations of the simple effects (averaged over the levels of the other effects). The symbol & refers to a test on differences between I0 and I1 as an alternative because of homoscedasticity problem. The symbol $ was used for suspected three-way interactions (based on graphics representation). For the corresponding data see Table 5.4.

	Observed or measured					fTGW		Maturity (1130 °Cd_H, extr.)		
	GNe	ENeq	DMg/grain	DMg/ear	DMg/m^2	N0	N1	TGW	Ye	Ym
Genotype (G)	***	***	***	**	***	ns	ns	***	*	***
C×L 14B	43.5c	455b	47.8b	2.06b	950b	0.96	0.99	48.6b	2.10b	956b
C×L 7A	36.7b	444b	43.9ab	1.59a	713a	0.87	1.02	46.5b	1.70ab	751a
LSP2×R 127	29.2a	393a	59.2c	1.73ab	689a	0.97	0.98	60.2c	1.76ab	694a
LSP2×R 16	39.0b	451b	41.6a	1.62a	746a	0.94	1.02	42.3a	1.64a	749a
Nitrogen (N)	ns	**	***	***	***	**		***	*	***
N0	37.6	403a	42.9a	1.57a	637a	0.93	-	45.8a	1.68a	678a
N1	36.6	470b	53.4b	1.93b	912b	-	1.01	53.0	1.91b	896b
Inoculation (I)	***	***&	**	*	ns	ns	•	***	ns	ns
I0	40.6b	424a	46.0a	1.84b	785	0.93	0.99	47.0a	1.88	794
I1	33.5a	457b	50.2b	1.65a	764	0.94	1.02	51.8b	1.72	781
G × N	*	ns	ns	ns	*	na	na	*	ns	*
G × I	•	ns&	ns	ns	ns	na	na	ns	ns	ns
N × I	ns	ns&	ns	ns	ns	na	na	ns	ns	ns
G×N×I	***	ns&	na	na	na	na	na	na	na$	na$

Table 5.4: Values for grain sink traits, for column description see Table 5.3.

Nitro. Inoc.	Observed or measured					obs./extr.	Maturity (1130 °Cd_H, extr.)		
Genotype	GNe	ENeq	DMg/grain	DMg/ear	DMg/m^2	fTGW	TGW	Ye	Ym
N0 I0									
CxL 14B	47.6	407	39.8	1.89	776	0.98	40.8	1.94	791
CxL 7A	44.7	399	35.3	1.58	634	0.81	43.4	1.94	774
LSP2xR 127	31.1	342	53.0	1.65	565	0.96	55.1	1.71	585
LSP2xR 16	39.6	408	33.4	1.32	543	0.97	34.4	1.36	555
N0 I1									
CxL 14B	41.9	429	46.4	1.95	842	0.95	49.0	2.06	882
CxL 7A	33.6	432	43.9	1.47	644	0.93	47.2	1.59	686
LSP2xR 127	25.9	377	55.8	1.45	550	0.97	57.4	1.49	561
LSP2xR 16	36.1	421	35.3	1.28	541	0.90	39.1	1.41	594
N1 I0									
CxL 14B	46.2	478	49.7	2.30	1106	1.00	49.4	2.28	1092
CxL 7A	35.5	451	48.5	1.72	784	1.06	45.9	1.63	735
LSP2xR 127	33.6	400	63.0	2.12	854	0.98	62.6	2.10	842
LSP2xR 16	46.6	471	46.1	2.15	1020	1.03	44.6	2.08	978
N1 I1									
CxL 14B	38.1	503	55.5	2.11	1075	0.98	55.4	2.11	1059
CxL 7A	32.9	497	47.8	1.57	792	0.97	49.5	1.63	810
LSP2xR 127	26.3	455	65.0	1.71	786	0.98	65.8	1.73	786
LSP2xR 16	33.6	505	51.4	1.73	881	1.00	51.2	1.72	868

- **The grain yield at maturity**

Only three samplings were achieved on N0 plants, making it uncertain if grain maturity was achieved at the time of the last sampling despite visual appearance of full senescence (Fig. 5.7). Logistic fits were used to provide estimations of the grain yield (TGW, Ye and Ym) at 1130 °Cd_H that was 5 °Cd after the last sampling on N1 plants (Eq. 5.3; $R^2 > 0.998$; RMSE: 0.8 mg · $grain^{-1}$ and 0.03 g · ear^{-1} and 13 g · m^{-2}, for TGW, Ye, Ym, respectively). The observed yield was 93% of the estimated yield under N0, and 100% under N1 (Table 5.3, P = 0.006). However, the combination C×L 7A × N0 × I1 was particularly low as observed yield was 87% only of estimated yield while the 15 other treatment combinations of G × N × I were sampled between 94% and 102% of the estimated yield. As the asymptote was not reached for C×L 7A × N0, extrapolation at 1130 °Cd_H was relatively uncertain and must be treated cautiously. Unlike that specific case, the other genotypes were visibly close to maturity, adding to the confidence in the grain yield estimations.

When ANOVAs were first applied on estimated TGW, Ye and Ym the residual distribution did not comply strictly with required hypotheses of normality and homoscedasticity of the residuals. No transformation could help. However, averaging across G × N × I combinations further to work on aggregated data resolved the problem, although the three-way interactions could not therefore be tested (Table 5.3). In N1 I0, the estimated TGW varied amongst genotypes (P < 0.001) from 44.6 g (LSP2×R 16) to 62.6 g (LSP2×R 127). The inoculated shoots were associated with heavier grains (P < 0.001). While the nitrogen N0 was generally associated with a reduction in estimated TGW (P < 0.001) comparable across inoculation treatments. However, the reduction was not significant for the genotype C×L 7A (thus generating a significant G×N interaction).The grain yield per ear (Ye) varied significantly with the genotypes and nitrogen treatment (P < 0.05). Under N1, estimation of Ye ranged from 1.77 g (LSP2×R 16) to 2.22 g (C×L 14B). Under N0, estimated Ye was 0.24 g lower than in N1 (no significant G×N interaction). Although the inoculation increased TGW, it also reduced GNe. GNe and TGW were negatively correlated (r = -0.65**). Because of its balanced effects on GNe and TGW, the inoculation did not significantly reduced the estimated Ye. The two-way interactions were never significant, but although the three-way interaction could not be tested with averaged data, a graphic representation (not shown) suggested that C×L 7A, under I0, was not affected by N0.

The crop grain yield (Ym) varied with the genotype (P < 0.001). Under N1, Ym ranged from 801 g · m^{-2} (LSP2×R 127) to 1057 g · m^{-2} (C×L 14B). Under N0, Ym was generally strongly and significantly reduced in comparison to N1 by -20%** to -36%***, with the exception of C×L 7A (-8%^{ns}). The graphic representation (not-shown) indicated a possible three-way interaction as the effect of N0 on C×L 7A depended on the inoculation treatment. The N0 treatment reduced C×L 7A Ym under I0 only.

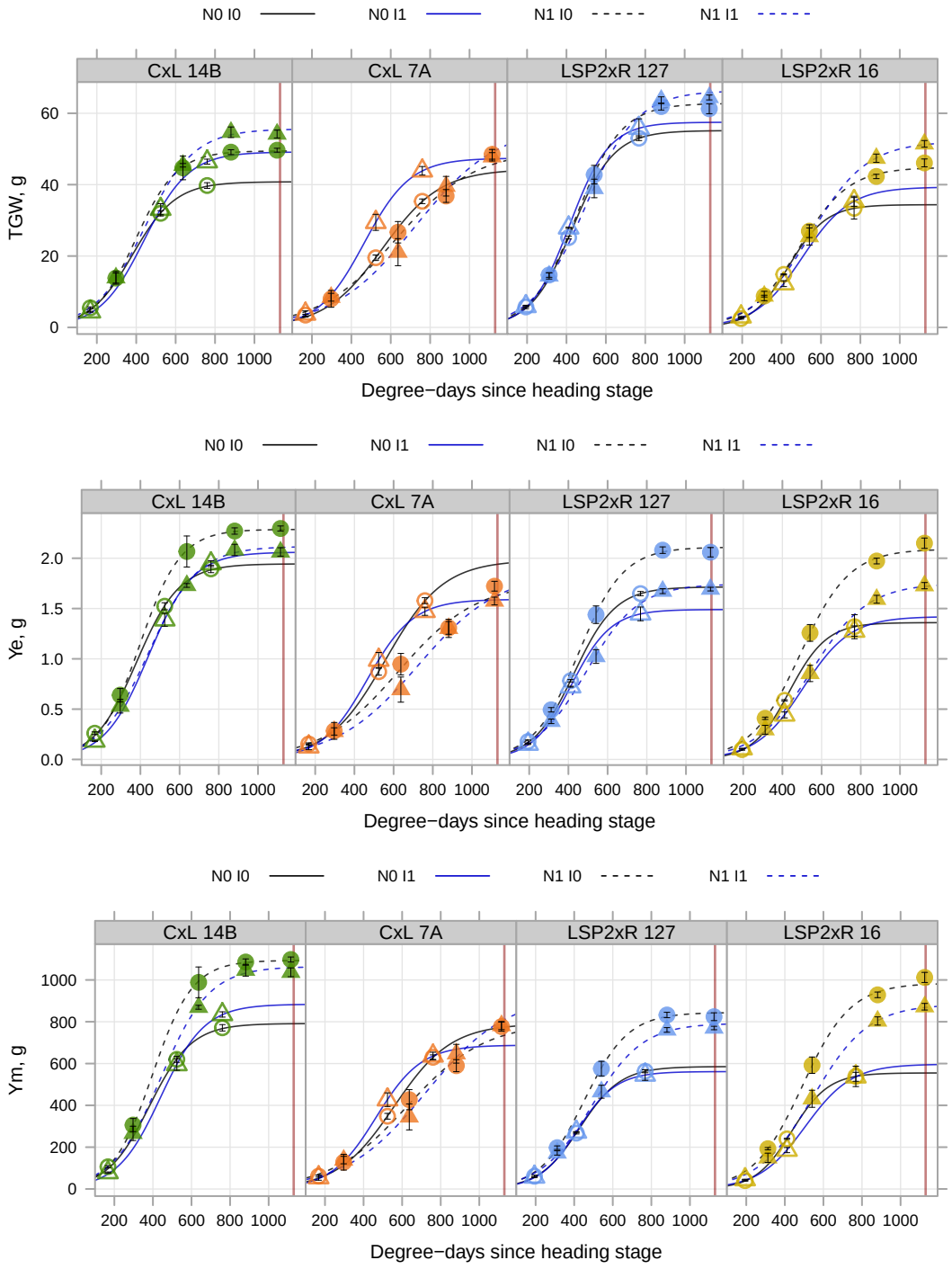


Figure 5.7: Grain filling kinetics. The y-axis represents the Thousand Grain Yield (g), the grain yield per ear-bearing shoot (Ye, g·shoot^{-1}), the grain yield per m^2 (Ym), along with an error interval (± standard error). Measurements were applied on main shoots only, GNe and ENeq were used for conversion to different scales (TGW, Ye, Ym). The x-axis represents the thermal time since heading stage (GS55). The colours represent the genotypes (C×L 14B, green; C×L 7A, orange; LSP2×R 127, blue; LSP2×R 16, yellow). The empty/closed symbols represent the N0/N1 treatment. The circles represent I0, while the triangles represent I1. Regression lines are reported for logistic fit per nitrogen treatment, dotted/plain line represents N0/N1 treatment, black/blue line represents I0/I1 treatments. Fits suggested grain filling was not achieved by the time of last sampling, noteworthy in C×L 7A; thus TGW, Ye and Ym were estimated at 1130 degree-days (right vertical line).

5.3.1.4 Relation between the grain yield and HAD

- **The relationship between Ym and HADm**

Figure 5.8 represents the estimated Ym and TGW in relation to the HADm and HADg, respectively. Estimated Ym was not proportional to HADm, increasing with HADm for N0 crops (from 1000 to 2500 $m^2 \cdot^\circ Cd \cdot m^{-2}$), but showing a trend to saturation for N1 crops (beyond 3000 $m^2 \cdot^\circ Cd \cdot m^{-2}$). Yet genotype differences also appeared: C×L 14B showed both high HADm and high Ym, while C×L 7A showed high HADm and low Ym. LSP2×R 16 and LSP2×R 127 were in the same ranges under the N0 treatment, but LSP2×R 16 gained more benefit from N1 treatment, both for Ym and HADm. Yet data were quite sparse and comparison of linear correlations from HADm with Ym indicated significant variation with genotype variation for the intercept (C×L < LSP2×R; $P < 0.05$) but not for the slope ($P > 0.05$). Data of HADg and TGW were more tightly linked within genotypes and comparison of linear correlation detected a significant genotype effect not only for the intercept ($P < 0.001$), but also for the slope ($P < 0.05$). Intercept differences (LSP2×R 16 < C×L 7 = C×L 14 < LSP2×R 127) suggested genetic variation in TGW potential, while slope differences indicated LSP2×R 127 and C×L 14 were more affected by HADg loss than C×L 7 and LSP2×R 16. Such a ranking was unexpected, as LSP2×R 127 and C×L 14 were putative tolerant genotypes.

Both grain yield and green area were fitted against time from heading stage to maturity. Consequently, either Ym and HADm accumulating during the grain filling phase could be drawn for every G × N × I treatment combination (Fig. 5.9), indicating progress of the source/sink balance. On Figure 5.9 the HADm accumulated until senescence was achieved, while Ym increased until grain maturity. The rapid phase of grain filling did not exactly start at anthesis (at the time when green leaf area was maximal); therefore, HADm initially accumulated despite not being associated with Ym increase. The rate of grain filling generally increased while the source availability (HADm) accumulated between 500 and 1000 [green]$m^2 \cdot^\circ Cdm^{-2}$. Under the N0 treatment (plain lines) the marginal Ym gain with HADm kept increasing and HADm did not accumulate beyond 1000 to 2000 $m^2 \cdot^\circ Cd \cdot m^{-2}$, depending on genotype. Under the N1 treatment (dotted lines), the marginal Ym gain with HADm progressively declined. Grain filling eventually ended up with high HADm but very low marginal gain to Ym. The N1 Ym was therefore associated with a late sink limitation, while N0 Ym was clearly limited by source availability. Genotype led to changes in both HADm and Ym kinetics, but it can be regarded using an empirical curve released from literature (Gouache et al., 2012), that proposed a maximum, potential yield for each obtained HADm ($Ypot = K \cdot \left(-\exp\left(-1 \cdot r \cdot HADm/K\right)\right)$, with K = 1090 and r = 1.33). The ratio of observed Ym to potential Ym, according to Gouache et al. (2012) was then regarded as HADm efficiency. Accordingly, C×L 14B

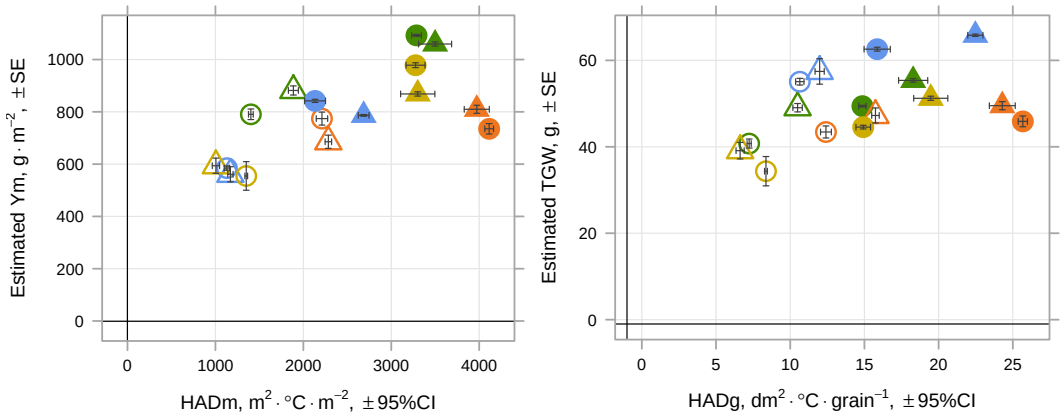


Figure 5.8: The crop grain yield (Ym, $g \cdot m^{-2}$) in relation to HADm ($m^2 \cdot {}^\circ Cd_H \cdot m^{-2}$). The colours represent the genotypes (C×L 14B, green; C×L 7A, orange; LSP2×R 127, blue; LSP2×R 16, yellow). The empty/closed symbols represent the N0/N1 treatments. The circles represent I0, while the triangles represent I1. The 95% confidence interval of HADm and HADg was computed following a bootstrap method, involving the calculation of 50 green area kinetics based on random selection of repetitions at the sampling date level.

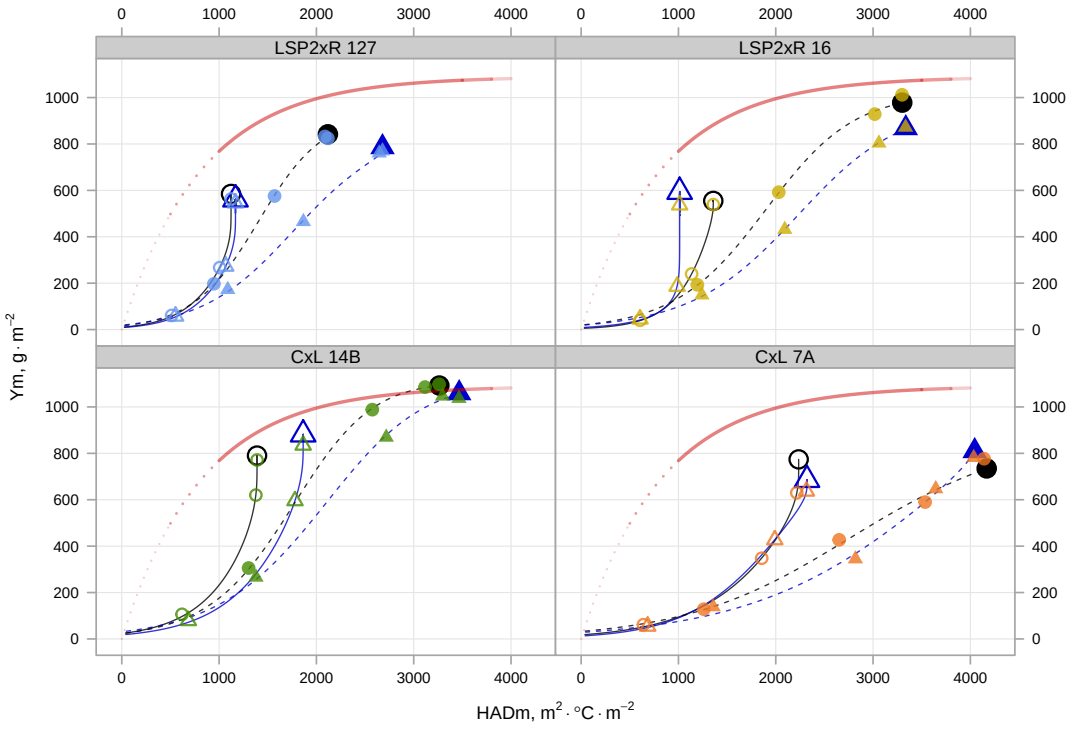


Figure 5.9: Relationship between the grain yield and the Healthy Area Duration at the crop scale. The colours represent the genotypes (C×L 14B, green; C×L 7A, orange; LSP2×R 127, blue; LSP2×R 16, yellow). The empty/closed symbols represent the N0/N1 treatment. The circles represent I0, while the triangles represent I1. The plain/dotted (N0/N1) blue/black (I1/I0) lines represent the estimations of HADm (Gompertz's function) and Ym (logistic function) throughout the grain filling phase, finally extrapolated at 1130 $^\circ Cd_H$ and ended by large symbols. The potential curve (red curve) was defined (independently from the present experiment) as follow: $Ym = K \cdot (-\exp(-1 \cdot r \cdot HADm/K))$ with values K = 1090 and r = 1.33 (Gouache et al., 2012).

Table 5.5: Tolerance estimations: Tolerance to GNe reduction ($1 - dYm_{I1-I0}/dHADm_{I1-I0}$, within N0 or N1 treatment), tolerance to Nitrogen deficiency ($1 - dYm_{N1-N0}/dHADm_{N1-N0}$, within I0 or I1 treatment). The two last lines refer to the tolerance grade estimation either based on three independent experiments (Eq. 5.1), or the tolerance of the spikelet removal treatment according to Chapter 4 results.

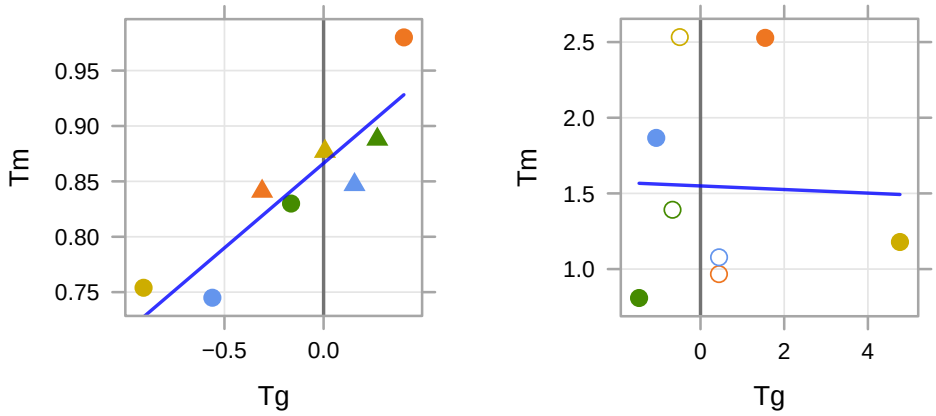
Genotype:	C×L 14B	C×L 7A	LSP2×R 16	LSP2×R 127
Tol. inoculation (GNe reduction effect)				
Within N treatment:	N1	N1	N1	N1
Tg, mg · dm^{-2} ·° Cd^{-1}	-0.669	0.441	-0.495	0.443
Tm, g · m^{-2} ·° Cd^{-1}	1.392	0.967	2.533	1.078
Within N treatment:	N0	N0	N0	N0
Tg, mg · dm^{-2} ·° Cd^{-1}	-1.468	1.546	4.766	-1.058
Tm, g · m^{-2} ·° Cd^{-1}	0.809	2.528	1.179	1.867
Tol. fertilisation				
Within I treatment:	I0	I0	I0	I0
Tg, mg · dm^{-2} ·° Cd^{-1}	-0.164	0.405	-0.908	-0.561
Tm, g · m^{-2} ·° Cd^{-1}	0.830	0.980	0.754	0.745
Within I treatment:	I1	I1	I1	I1
Tg, mg · dm^{-2} ·° Cd^{-1}	0.271	-0.310	0.007	0.156
Tm, g · m^{-2} ·° Cd^{-1}	0.888	0.841	0.877	0.847
Tol. literature				
T	0.226	-1.447	-0.484	0.812
T spik. remov., mg · dm^{-2} ·° Cd^{-1}	-1.322	-2.904	-1.545	-0.285

exhibited a high efficiency, as compared to C×L 7A while the LSP2×R genotypes showed intermediate efficiencies when compared to the C×L genotypes.

- **Tolerance**

The pairwise comparison between I0/I1 indicated a very low effect of the inoculation treatment: the resulting Ym loss was not substantial. Most of Ym loss was due to the contrasting nitrogen treatment. Moreover, the inoculation failed to trigger substantial infections and did not significantly affect HADm. Nonetheless, the inoculation treatment decreased grain number. Therefore, despite being not possible to study the tolerance of STB because of its low severity, inoculation treatment could be regarded as a degraining treatment, although to a much less extent and more variable than that encountered for the field 2014-15 experiment (Chapter 4). On the other hand, apart from its Ym effect, nitrogen treatment also produced a large variation of HADm. Therefore, indices for tolerance of Nitrogen deficiency were calculated to be compared to both putative STB-tolerance of genotype and their degraining tolerance. The aim was to study if the tolerance to biotic stress is linked to the tolerance of abiotic stress.

Tolerance was then calculated, as $1 - dY/dHAD$, either at the crop or the grain scale, using estimated Ym and TGW at 1130 °Cd$_H$. Calculations were obtained pooling repetitions, either for degraining by I treatment, or for fertilisation by N treatment. Tolerance for degraining (Eq. 5.6) was thus calculated within each N0 or N1 treatment while, using



(a) Nitrogen deficiency (b) STB inoculation

Figure 5.10: Comparison of tolerance estimations at the grain (Tg) and the crop scale (Tm). a) Tolerance for fertilisation. b) Tolerance for inoculation, i.e. GNe reduction. Relationship between estimated grain yield and HAD. The colours represent the genotypes (C×L 14B, green; C×L 7A, orange; LSP2×R 127, blue; LSP2×R 16, yellow). The empty/closed symbols represent the N0/N1 treatment. The circles represent I0, while the triangles represent I1. A regression line was fitted by ordinary least square regression.

the same data, tolerance for fertilisation (Eq. 5.7) was calculated within each I0 or for I1 treatment (Table 5.5).

$$Tol.\ Inoc. = 1 - dYm_{I1-I0}/dHADm_{I1-I0} \tag{5.6}$$

$$Tol.\ ferti. = 1 - dYm_{N1-N0}/dHADm_{N1-N0} \tag{5.7}$$

Unfortunately, given the low freedom degrees, no significant correlation could be obtained with either putative tolerance value or with results of spikelet-removal experiment reported in Chapter 4. Moreover, neither degraining tolerance obtained by I0/I1 contrast for N0 and N1 plants, nor fertilisation tolerance obtained by N0/N1 contrast for I0 and I1 plants correlated. Data might not be pooled together. On the other hand, the eight values obtained for N fertilisation tolerance at the grain scale correlated with those obtained at the crop scale (Figure 5.10a; r = 0.90**), suggesting the experiment could have provided valuable information if involving more genotypes. Conversely the eight values obtained for degraining tolerance at the grain scale did not correlate with those obtained at the crop scale (r = 0.00; P > 0.05). Degraining obtained through inoculation treatment was too small and too variable to provide valuable tolerance information.

5.3.2 Analysis of dry-matter and nitrogen balance behaviour of cultivars

Results reported in other chapters in this thesis suggest tolerance might be linked to source/sink balance. The dry matter and nitrogen balances were estimated as the difference between an initial date and the last sampling date, positive values therefore represent accumulation while negative values represent remobilisation. This section mostly focuses on the shoot scale, while view points on grain and crop scales are also considered.

5.3.2.1 Dry-matter fluxes

The fluxes were estimated from GS55 to the last sampling date (Fig. 5.11). Data at GS55 were estimated by interpolation using several sampling dates and therefore several N treatments. It was hypothesised that fertilisation treatment had not yet affected DM per shoot at this early stage. When data were regarded at the crop scale, an artefact occurred because ENeq was considered constant over time. Indeed, for the N1 treatment, for which average ENeq was higher, a higher DM per m^2 was calculated as soon as the heading stage. Conversely, the I1 treatment, which reduced GNe, also led to higher DM per grain than I0.

- **Initial state: GS*55***

The total dry-matter (including roots) varied significantly amongst the genotypes ($P < 0.001$, Fig. 5.11), C×L 14B ($2.3\,g \cdot shoot^{-1}$) being heavier than the other genotypes ($1.7\,g \cdot shoot^{-1}$in average). Initial shoot DM was unaffected by both N fertilisation and inoculation treatments that occurred later. It correlated with GNe (Table 5.3).

- **DM yield: ΔDMgrain**

The grain dry-matter accumulation was estimated from heading stage to maturity (the last sampling date): ΔDMgrain per ear (Tables 5.3 and 5.4; Fig. 5.11). However, the observed Ye at the last sampling date was presently used, while the estimated Ye at $1130\,°Cd_H$ was presented in the Section 5.3.1.3 "The grain sink traits". Of course, the results were very similar to that of the estimated Ye. Briefly, within each DH cross ΔDMgrain/ear was higher in the putative tolerant genotypes (within LSP2×R: LSP2×R 127 vs LSP2×R 16; within C×L: C×L 14B vs C×L 7A, $P < 0.001$). ΔDMgrain/ear was largely increased by the fertilisation treatment N1 (+0.35 g, $P < 0.001$), and reduced to a lesser extent by the inoculation treatment I1 (-0.18 g, $P < 0.001$), yet with interactions with nitrogen treatment. Genotype C×L 14B exhibiting a large biomass per grain at GS55 also developed a large ΔDMgrain.

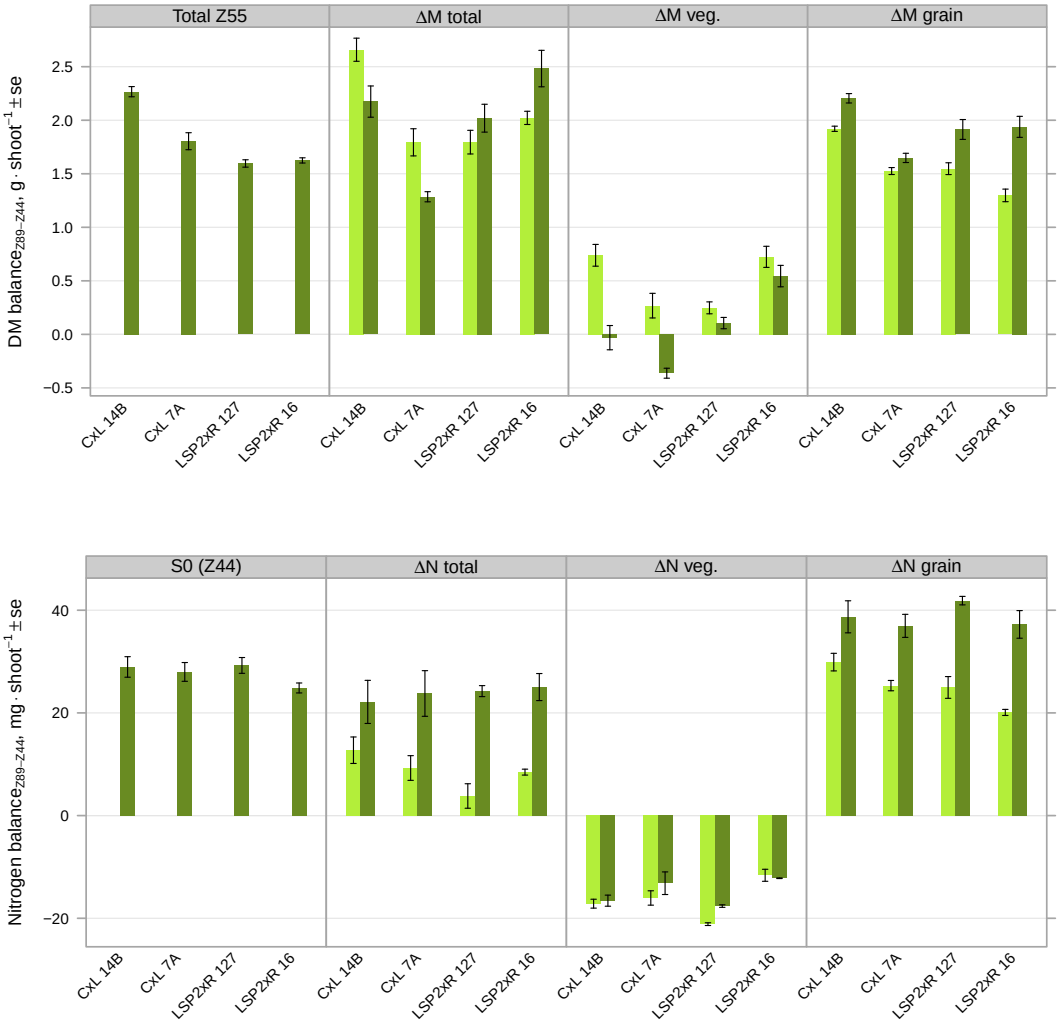


Figure 5.11: Dry matter or Nitrogen balance per shoot. The four upper panels report DM balances from GS55 to the last sampling date, while the four lower panels report the Nitrogen balance from GS44 to the last sampling date. The balance values are indicated on the y-axis, the genotypes are indicated on the x-axis, light/dark green bars represent N0/N1 treatment averaged over inoculation treatments. Within DM and N panels, the first represent the total amount at initial date (therefore not *strictly* a balance), the second is the total variation, the third is the variation of the vegetative dry matter (these three panels include root), the fourth panel is the grain balance.

- **Net assimilation**: **Pmax and ΔDMt**

Gas exchange measurements were achieved on N1 I0 flag leaves at three occasions during the two first weeks after heading. The overall correlation of Pmax to STB tolerance was significant and positive, but despite tolerant C×L 14B had greater Pmax than intolerant C×L 7A, tolerant LSP2×R 127 had lower Pmax than intolerant LSP2×R 16. Alternatively, net assimilation balance over the whole grain filling was estimated in each treatment by the total DM net accumulation in plants (total DM including the roots, ΔDMt; Fig. 5.11). At the grain scale, the genotypes under N0 were ordered according to putative tolerance from the least tolerant C×L 7A to the most tolerant LSP2×R 127 (46 to 63 $mg \cdot grain^{-1}$, respectively). Under N1, putative tolerant genotypes still showed higher performance within each DH cross. The ranking was, however, lost at the shoot scale: although C×L 7A showed the lowest assimilation (1.5 $g \cdot shoot^{-1}$), LSP2×R 127 (1.9 $g \cdot shoot^{-1}$) net assimilation ΔDMt was much lower than LSP2×R 16 and C×L 14 (2.3 $g \cdot shoot^{-1}$). Moreover, ΔDMt was increased by the N1 treatment in LSP2×R genotypes, unlike amongst C×L genotypes. Under the N1 treatment, net assimilation did not correlate with initial DM (r = 0.04), whereas it did correlate under N0 treatment (r = 0.77). In turn, net assimilation ΔDMt correlated with ΔDMgrain in a linear regression (R^2 = 0.65) suggesting a difference in the intercept between N0 and N1 ($P < 0.001$) but an equivalent slope ($P > 0.05$).

- **Remobilisation, balance of vegetative dry matter**: **ΔDMv**

The remobilisation from the vegetative parts (ΔDMv; Fig. 5.11, 5.12 and 5.6) has already been described as part of the source availability (Section 5.3.1.2 "The source traits for grain filling"). Briefly, a net accumulation rather than remobilisation was generally observed from heading date to the last sampling. Accumulation was lower under N1, so that a net remobilisation was even observed in most of the G×N treatments. Surprisingly, however, ΔDMv did not correlate with ΔDMgrain neither in N0 and in N1 treatments, suggesting that growth of vegetative parts was not fully achieved at this time, heading could be a wrong initial point. Thus, dry-matter fluxes were also calculated starting not from heading but from the time of maximum DMv before the last sampling. These fluxes were negative (-1.0 to +0.0 $g \cdot shoot^{-1}$) indicating remobilisation had indeed occurred. Overall remobilisation did not differ differ visibly between N0 and N1 treatments, although fluxes could not be accurately compared because sampling dates were not the same. Fluxes correlated negatively but weakly with ΔDMgrain (r = -0.33), and therefore higher remobilisation only marginally sustained yield. Interestingly, at the grain scale fluxes did not correlate with ΔDMgrain in the N1 treatment, while a negative correlation was observed under N0 treatment (r = -0.58).

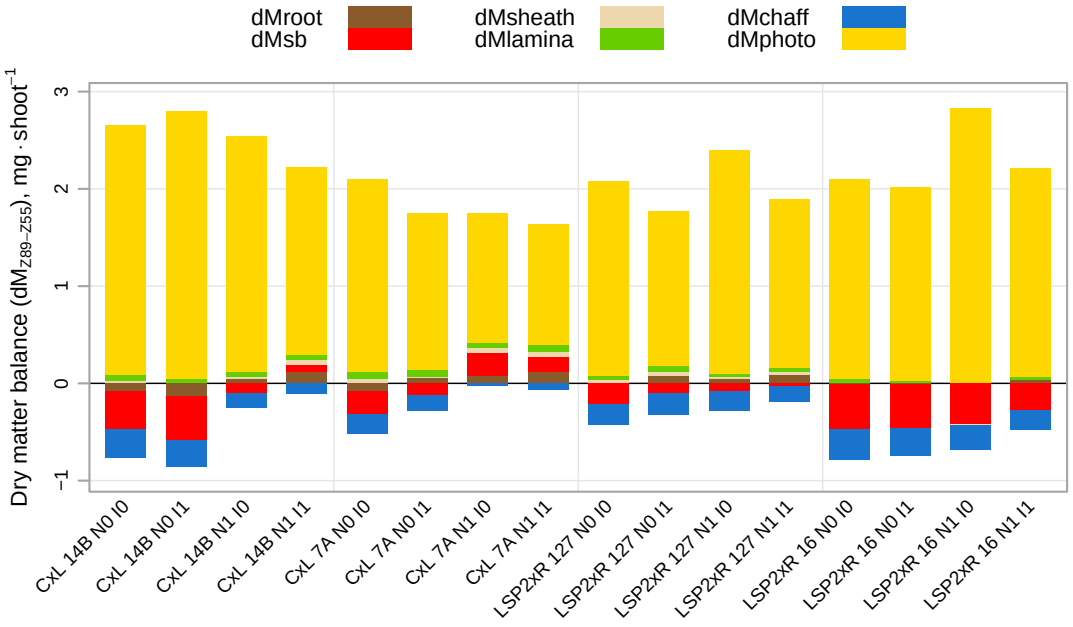


Figure 5.12: Origin of grain dry-matter per ear-bearing shoot. (dM, DM balance from GS55 to GS89; sb, stem and base; photo, photosynthesis). An organ reduction in DM from GS55 to GS89 was supposed to contribute to the grain dry matter accumulation and was represented as a positive bar (colour according to the organ). The difference between the grain weight at GS89 and the organ DM remobilisation was assumed due to photosynthesis. Each stacked bar is the addition of the different organs as sources of remobilisation. Negatives values represent net accumulation, i.e. vegetative organs which grew between GS55 and GS89.

5.3.2.2 Nitrogen fluxes

Table 5.6: Analysis of variance of the nitrogen balances (from S0 to S7 or S9) expressed per single shoot ($mg \cdot shoot^{-1}$). Responses were: the total nitrogen content at GS44 (Nt GS44), the nitrogen content balance of the grain (ΔNgrain), the nitrogen content balance of the whole plants (including roots, ΔNt), the nitrogen content balance of the vegetative organs (including roots, ΔNv). Each ANOVA model was fitted on n=16.

	Nt GS44	ΔNgrain	ΔNt	ΔNv	ΔNstem and base	ΔNroot	ΔNlamina
Genotype (G)	ns	**	ns	***	***	***	*
C×L 14B	28.9	34.3b	18.6	-16.9ab	-3.35b	-0.75c	-10.4ab
C×L 7A	28.0	31.1ab	16.0	-14.6bc	-2.17c	-0.66c	-10.7a
LSP2×R 127	29.2	33.4ab	14.6	-19.4a	-3.97a	-3.15a	-9.3ab
LSP2×R 16	24.9	28.7a	17.0	-11.9c	-1.40d	-1.65b	-8.81b
Nitrogen (N)	na	**	***	.	ns	ns	*
N0	-	25.1a	7.2	-16.5	-2.74	-1.66	-10.3a
N1	-	38.7b	25.8	-14.9	-2.70	-1.44	-9.3ba
Inoculation (I)	na	**	ns	ns	*	ns	ns
I0	-	33.2b	17.8	-15.3	-2.58b	-1.49	-9.7
I1	-	30.5a	15.3	-17.1	-2.86a	-1.61	-9.9
G × N	na	.	ns	ns	ns	ns	ns
G × I	na	ns	ns	ns	ns	ns	ns
N × I	na	ns	*	ns	ns	ns	ns

- **Initial stage: GS44**

Unlike DM, N measurements were not available throughout the grain filling phase. Consequently, N balances were calculated from the first sampling date, at GS44 (at the same time as N supply was withdrawn in N0), despite growth of vegetative parts being far from fully achieved at this time (Fig. 5.11). The initial N content of the plant (including the roots) at GS44 was 28 $mg \cdot shoot^{-1}$ and showed no variation according to the genotype (Table 5.6). As the initial N content per shoot was constant, the initial N content per grain was negatively correlated with the number of grains per ear (r = -0.87***). Lastly, the initial partitioning of N per organ indicated more N was found in lower leaves of C×L genotypes, and more in roots of LSP2×R genotypes.

- **Nitrogen yield: ΔNgrain**

The nitrogen balance in the grain (ΔNgrain, Fig. 5.11), i.e. nitrogen content per grain at last sampling, varied from 29 to 34 $mg \cdot shoot^{-1}$ with genotype ($P < 0.001$, Table 5.6). Despite being weakly significant, the genotype ranking suggested the putative tolerant genotypes might yield more nitrogen than the others. N fertilisation showed a highly significant effect ($P < 0.001$) and more substantial than that of genotypes as the N1 treatment increased the nitrogen content of the grain by 55%, up to 39 $mg \cdot shoot^{-1}$ on average. Inoculation decreased ΔNgrain by only 9% ($P < 0.001$). At the grain scale, only LSP2×R 127 exhibited higher nitrogen content (1.01 $mg \cdot grain^{-1}$, averaged over N and I levels) that the other genotypes (0.74 to 0.86 $mg \cdot grain^{-1}$). The inoculation, which

decreased also GNe, was associated with a significant ΔNgrain increase of 14% ($P < 0.001$).

The nitrogen content per ear was not correlated with GNe ($r = 0.02$, $P = 0.89$), but was positively with the initial N content. Comparison of regressions showed a large and expected intercept due to the fertilisation treatment ($P < 0.001$), but a common slope at $1.2 \pm 0.4\,mg \cdot mg^{-1}$ ($P < 0.01$): each mg of N already absorbed at GS44 led to 1.2 mg in grains at maturity.

- **Nitrogen uptakes**: **ΔNt and ΔNag**

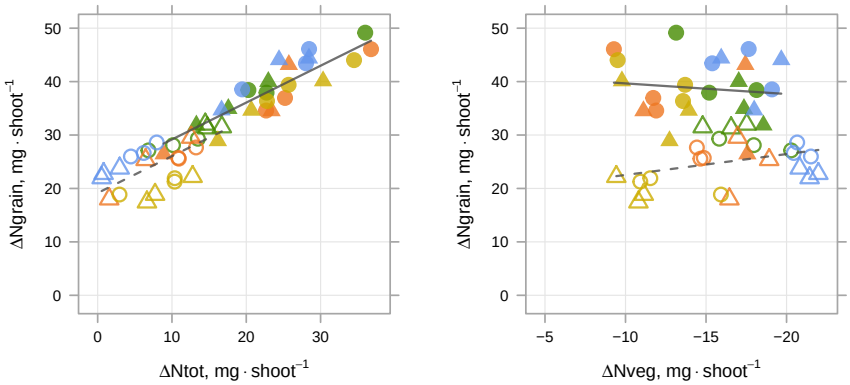
The plant nitrogen content increased after GS44 until GS89, and ΔNt was the estimation of the true nitrogen uptake taking into account the roots (Fig. 5.11), while ΔNag which did not regard roots was the apparent N uptake, most commonly cited in the literature. The N true uptake did not vary with the genotype, and was reduced by $3.5\,mg \cdot shoot^{-1}$ following inoculation ($P < 0.05$, Table 5.6). The main variation occurred with fertilisation treatment. Although N fertilisation was stopped after GS44, ΔNt increased in N0 plants by $8.6\,mg \cdot shoot^{-1}$, probably due to a contaminant fertilisation, that led to large variation from $1.4\,mg \cdot shoot^{-1}$ by inoculated LSP2×R 127 to $15.3\,mg \cdot shoot^{-1}$ by inoculated C×L 14B. However, N0 contrasted very strongly with N1 as ΔNt was 2.8 fold higher in N1 ($P < 0.001$). Nevertheless, the weight of N uptake as compared to N yield was much higher than commonly observed in the fields: ΔNt was in average 34% of ΔNgrain in N0 treatment, and as much as 62% of ΔNgrain in N1 treatment.

The N true uptake was not correlated with initial N content, but was positively with GNe. A regressions ($R^2 = 0.69$) again suggested a large intercept due to the fertilisation treatment (N1: $+15.6\,mg \cdot grain^{-1}$; $P < 0.001$), but a common slope at $0.34 \pm 0.12\,mg \cdot grain^{-1}$ ($P < 0.01$). In turn, the N true uptake correlated with ΔNgrain (Fig. 5.13a) with an intercept due to the fertilisation treatment ($P < 0.001$), but a common slope at $0.7 \pm 0.1\,mg \cdot mg^{-1}$ ($P < 0.05$): each mg of N absorbed by plants since GS44 led to further 0.7 mg in grains at maturity.

The N apparent uptake (ΔNag) was highly correlated with true N uptake ($R^2 = 0.99$), yet with both intercept and slope varying with fertilisation ($P < 0.01$). Under N0 treatment the intercept due to remobilisation from the roots was $4\,mg \cdot shoot^{-1}$, not negligible where low N true uptakes were observed.

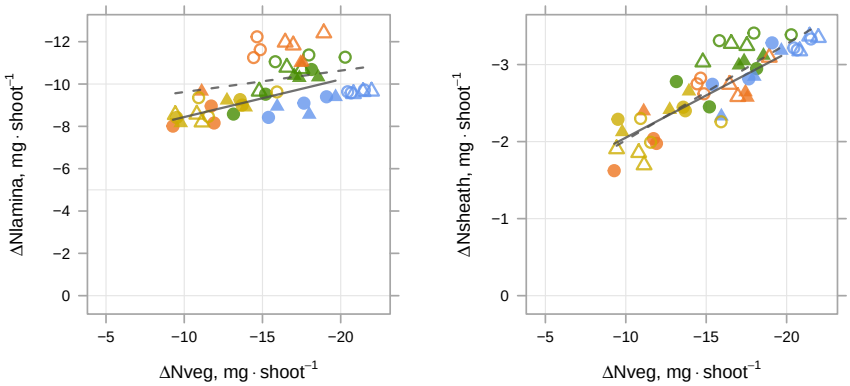
- **Nitrogen remobilisation**: **ΔNv**

Despite an early initial point at GS44, the nitrogen balance of vegetative organs (including roots) was largely negative indicating remobilisation of nitrogen (Fig. 5.11 and 5.15). A highly significant genotype effect was observed with tolerant genotypes remobilising more than the intolerant genotypes (Table 5.6); LSP2×R 127 remobilised more ($-19\,mg \cdot shoot^{-1}$) than LSP2×R 16 ($-12\,mg \cdot shoot^{-1}$), and C×L 14 ($-17\,mg \cdot shoot^{-1}$)

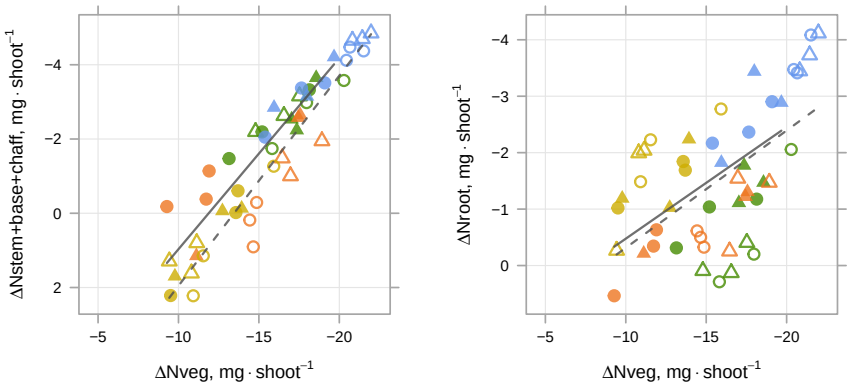


(a) (b)

Figure 5.13: Nitrogen yield (ΔNgrain per shoot) in relation to: a) true N uptake (ΔNt per shoot) and b) remobilisation (ΔNv per shoot). By convention x-axis is in reverse direction in b).



(a) Lamina (b) Sheath



(c) Stem + base+ chaff (d) Root

Figure 5.14: Nitrogen balance of vegetative organs since GS44 (A laminas, B, sheaths, C stem+bases+chaff, D roots). The colours represent the genotypes (C×L 14B, green; C×L 7A, orange; LSP2×R 127, blue; LSP2×R 16, yellow). The empty/closed symbols represent the N0/N1 treatment. The circles represent I0, while the triangles represent I1. Regression lines are fitted per nitrogen treatment, dotted/plain line represents N0/N1 treatment.

more than C×L 7A ($-15\,\mathrm{mg}\cdot\mathrm{shoot}^{-1}$). Remobilisation was not affected by inoculation while it was as expected higher under N0 treatment than under N1 treatment (-17 and $-15\,\mathrm{mg}\cdot\mathrm{shoot}^{-1}$, respectively).

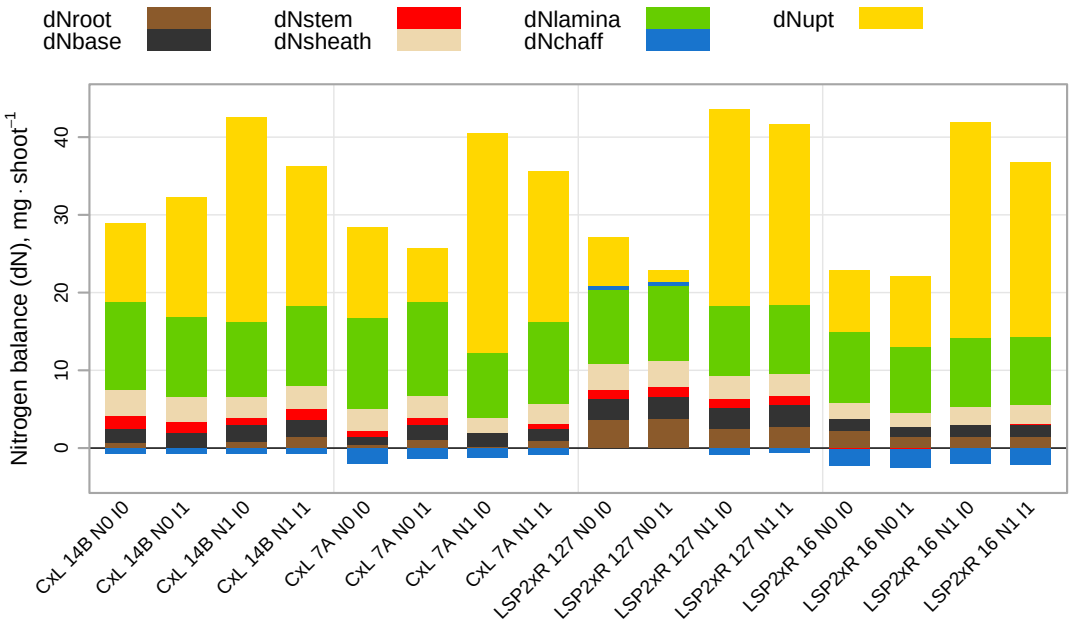


Figure 5.15: Origin of grain dry-matter and nitrogen per ear-bearing shoot. (dN, nitrogen balance from GS44 to GS89; upt, Nitrogen uptake). The reduction in N content of every vegetative organ from GS44 to GS89 was supposed to contribute to the grain N accumulation and was represented by a positive bar (colour according to the organ). The difference between the N grain content at GS89 and N remobilisation from the vegetative organs was assumed due to nitrogen uptake. Each stacked bar is the addition of the different organs as sources of remobilisation. Negatives bars represent net accumulation; i.e. organs where accumulation of N has been measured from GS44 to GS89 (mainly chaff).

Nitrogen was not remobilised equally from organs; instead when plotting remobilisation from each organ versus that from whole shoot (Fig. 5.14), very significant intercepts were observed. In other words, their relative contribution to the whole N remobilisation changed with the amount of the whole N remobilisation. Leaf laminas and sheaths exhibited both negative intercepts and low slopes for organ versus whole shoot remobilisation ($0.12\,\mathrm{mg}\cdot\mathrm{mg}^{-1}$ and $0.16\,\mathrm{mg}\cdot\mathrm{mg}^{-1}$, respectively; Fig. 5.14a and 5.14b). Remobilisation from these organs was relatively little affected by amount of N remobilisation from whole shoots. The relative contribution of leaves, thus, decreased when whole remobilisation increased, such as observed in tolerant genotypes. Conversely, these genotypes showed a relatively greater contribution of their base+stem+chaff to remobilisation (Fig. 5.14c). Results about origin of remobilised N (Fig. 5.15) should, however, be cautiously regarded because of the very early starting point. At GS44, both stem and chaff accumulation were far from complete, and actually N balance of chaff was positive (net N accumulation) in

intolerant genotypes. A slight shift in development could had led to such pattern as well.

Nitrogen remobilisation was weakly correlated with GNe, and more substantially with initial N content, with a slope -1.5 ± 0.2 $mg \cdot mg^{-1}$ ($P < 0.001$): each mg of N already absorbed at GS44 led to 1.5 mg decrease in vegetative parts at maturity. Lastly, remobilized N did not correlate with ΔNgrain either in N0 or in N1 (Fig. 5.13b). At the grain scale correlations were much more significant. Hence, ΔNv was highly correlated with Nt at GS44 (N0, r = -0.96***; N1, r = -0.91***), while remobilised N correlated with ΔNgrain when N treatments were examined separately (N0, r = -0.96; N1, r = -0.80).

5.4 Discussion

The glasshouse experiment aimed at exploring detailed traits characterising genotypes contrasting for STB-tolerance, related to nitrogen metabolism. The monitoring of nitrogen nutrition conditions was conducted through a glasshouse semi-hydroponic experiment. Yet, to obtain field-like crops in artificial conditions was somewhat challenging. Both inoculation and fertilisation treatments induced a large contrast in grain-source availability and the genotypes expressed a large range of traits. Unfortunately, the inoculation method did not trigger an infection but resulted in a moderate grain sink reduction. Association of recorded traits with putative STB tolerance was nevertheless carried out. Then the effect of grain number reduction was considered. Lastly the effect of nitrogen on tolerance was further explored.

5.4.1 Obtaining a field-like canopy in the glasshouse.

The controlled-environment experiment can be useful because epidemics are not always reproducible in field conditions. However, because STB tolerance is assumed to be linked to source/sink balance, working on isolated plants in pots could be misleading. Therefore, the experiment was designed to simulate a field-like canopy in controlled conditions, but involved nevertheless a short vegetative period under relatively high temperature and low irradiance, compared to crops grown outdoors. The resulting grain density was quite low for genotype LSP2×R 127 (below 15,000 grains per m^2), while more usual for other genotypes (15,000 to 22,000 grains per m^2). In field conditions, tillers are produced during early spring and decline during stem elongation. In contrast, in short cycle mini-crops, only 0.5 tiller per plant was produced by heading date and tillering was maintained throughout the grain filling phase under the N1 treatment. Even in the N1 treatment, however, the plant density precluded tillers production beyond 1.0 tiller per plant, unlike observed in space isolated plants (Zuckerman et al., 1997). The nitrogen treatment, applied from GS44, marginally changed the sink components (grain number of sampled main stems), but induced a large response of source availability (HAD) be-

cause of extended leaf-life during the grain filling phase. The genotype C×L 7A even showed a stay-green phenotype with mature dry ears observed on green culms. On the other hand, measurement of the Nitrogen Nutrition Index (Justes et al., 1994) showed NNI was rather low (0.8) at GS44, then declining under N0 treatment until 0.6 at the end of grain filling, while NNI reached 1.0 under the N1 treatment, indicating the plants were generally not over-fertilised. Regarding the grain yield components and source availability (HAD), the range of data in the glasshouse experiment was actually consistent with expected field data. As a comparison, the Chapter 4 "Field experiment at Hereford 2014-15" also included the four genotypes reported in the present chapter. By comparison to that field study, the DM source quantified by the HADm (Fig. 5.16a) represented a wider range of values in the glasshouse experiment: similar ranges were found in the case of N0 treatment only, while N1 treatment also induced very large values for HADm. In contrast, only crops grown under the N1 treatment showed grain yields (Ym) in the range obtained in the field (Fig. 5.16b). The ratio Ym to HADm was thus quite low in the glasshouse experiment, which might have resulted from the low irradiance level (crops were grown in winter), leading to a low photothermal ratio. However, as plants were also exposed to these conditions during their vegetative growth, they also initiated quite a low grain number, which can explain that the individual grain weight (TGW) was consistent with the field data (Fig. 5.16c). The grains of N0-plants had TGW similar to that of the field experiment, while those of N1-plants were heavier.

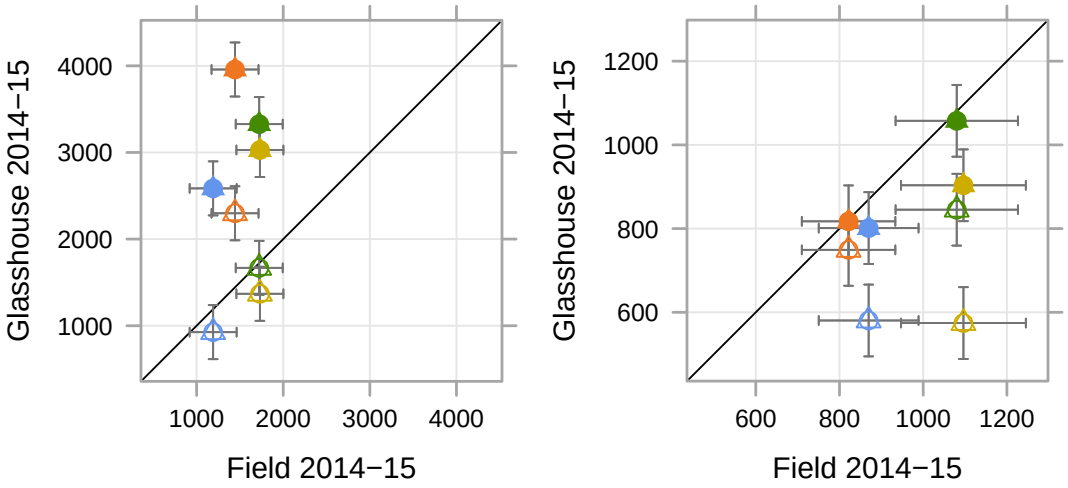
5.4.2 Traits associated with the putative tolerance of the genotypes.

The glasshouse experiment failed to generate disease following STB inoculation; therefore, STB-tolerance could not be estimated. However, the genotypes can be ranked according to their putative grade of STB-tolerance. This grade was based on the results at the crop scale of three independent experiments varying HADm and Ym through STB epidemics (Section 5.2.1.1, "Materials and methods"). In line with that STB-tolerance grade, it was expected that, within DH crosses, C×L 14B would be more tolerant than C×L 7A, and LSP2×R 127 more tolerant than LSP2×R 16; more generally, the genotypes were ranked, starting with the most tolerant, as follow: LSP2×R 127 > C×L 14B > LSP2×R 16 > C×L 7A. Correlation between putative STB tolerance and traits was then assessed.

Parker et al. (2004) identified a negative association between the potential yield and STB-tolerance of UK winter wheat cultivars, but Foulkes et al. (2006) suggested that it might be an indirect consequence of the breeding strategy, implying the need of further results. Indeed, neither Bancal et al. (2015) nor Castro and Simón (2016) did find an association between potential yield and STB-tolerance of cultivars. In the present experiment, no N×I treatment combination showed evidence for an association between Ym

(a) HADm, $m^2 \cdot ^\circ Cd \cdot m^{-2}$

(b) Ym, g



(c) TGW, g

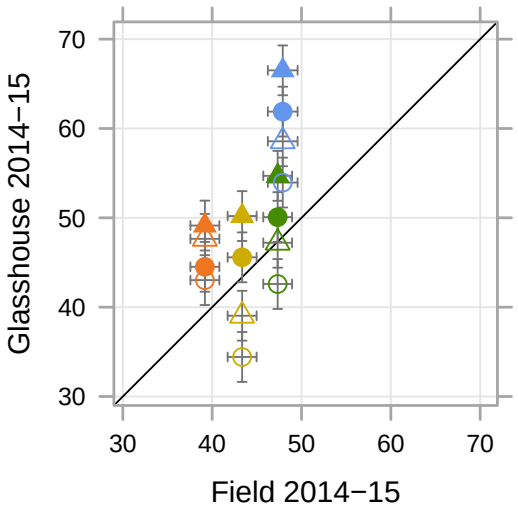


Figure 5.16: Comparison of glasshouse TGW, Ym and HADm with field observations for the same genotypes. The glasshouse values (1130 $^\circ Cd_H$) are reported on the y-axis, and compared to the field observations on the x-axis. Glasshouse values are least mean square estimations (linear models including only significant effect). The field observations come from the experiment reported in Chapter 4 "Field experiment at Hereford 2014-15" (section 4, p.104); they are least square mean estimations for fungicide-treated plots (F1), untrimmed ears (S0), addition of 40 kg N $\cdot$ ha^{-1}(N1). The colours represent the genotypes (C×L 14B, green; C×L 7A, orange; LSP2×R 127, blue; LSP2×R 16, yellow). The empty/closed symbols represent the N0/N1 treatment. The circles represent I0, while the triangles represent I1. Bars represent the 95% confidence interval.

and the putative genotype tolerance of STB.

A relationship between heading date and STB tolerance was identified in Chapter 3. Under artificial conditions the development rate was largely accelerated. However, in LSP2×R genotypes as well as in C×L genotypes, the STB tolerant genotype reached heading date some days earlier than the intolerant line. Foulkes et al. (2006) suggested the large flag leaf area as a potential tolerant trait, while Bingham et al. (2009) emphasized the canopy leaf lamina vertical distribution (a large extinction coefficient being a tolerant trait) and more recently Bancal et al. (2015) proposed large HADm rather than the large leaf area as a potential tolerant traits. The results reported in Chapter 3 also emphasized that the large proportion of flag-leaf (fLA 1) delays the senescence timings (I) and therefore HADm. Surprisingly, however, senescence timing negatively correlated with the putative tolerance in N1 crops, as also did HADm, both in N0 and in N1 crops. Besides, glasshouse growth conditions are known to modify leaf shape and canopy pattern. Indeed, the genotypes expressed larger flag leaf area and proportion (fLA 1) in the canopy in the glasshouse experiment than in the field 2014-15. However, the fLA 1 was not associated with the putative tolerance of the genotypes included in this glasshouse experiment. An other estimate of photosynthetic performance was obtained through ΔDMtot, which was positively but not significantly related to STB tolerance.

Dry matter and nitrogen balances were also estimated. Some traits were linked to the putative tolerance of the genotypes (positive correlation: ΔDMgrain/ear, ΔDMt under N0, ΔNv). The remobilisation of dry matter from the vegetative organ was generally proposed as a STB-tolerance trait by (Foulkes et al., 2006; Bingham et al., 2009). In the present experiment, the N0 plants were strongly source limited and large dry-matter remobilisation was expected. However, the N0 treatment was associated with an increased accumulation of dry-matter in the vegetative biomass. According to direct measurement in LSP2×R genotypes, stem WSC accumulated in comparable amounts in N0 and N1 plants during early grain filling, and possibly remobilised a little earlier in N0 treated plants, but at a lower rate. Thus WSC remobilisation was not achieved by the time grains reached maturity. Investigation in the literature did not help to explain this pattern, but ΔDMv was clearly not associated with tolerance in the present experiment.

5.4.3 GNe tolerance of the genotypes

Apart from LSP2×R 16, the inoculation was not followed by significant STB symptoms, but it was always associated with a significant reduction of the GNe. Regarding 322 field plots, Bancal et al. (2015) only detected GNe reduction following the worst epidemics, and always to a low extent compared to STB symptoms. Thus, the reason for the GNe reduction in glasshouse experiment was probably not the result of disease development; instead it may have resulted from the inoculation method which required the

lamps to be switched-off for 48 h. As cloudy weather also occurred at this time, inoculated plants actually suffered from very low irradiance around GS44. That time probably coincided with meiosis, a stage sensitive to low levels of radiations that could lead to male sterility (Demotes-Mainard et al., 1995, 1996) and consequently to a reduced fertilisation and grain number (Fischer and Stockman, 1980). The inoculation was therefore unexpectedly associated with an uncontrolled reduction of the grain sink (ranging 0 to -28% grain number per ear) rather than a reduction of the grain source (no leaf symptoms). The generated range of source/sink balance influenced the grain yield. Noteworthily, the grain number reduction (I1) induced an increase in source availability per grain that led to a significant compensatory growth increment of the single grain (TGW, +10% on average). This effect was substantial, and was furthermore consistent with the results of the 50% spikelet-removal treatment applied in the field experiment in 2014-15 (Chapter 4) which caused a +33% increment of the TGW. It confirms therefore that grain growth of these genotypes was rather co-limited by the sink capacity and the source availability (Acreche and Slafer, 2009). Results in Chapter 4 showed a high correlation of putative STB tolerance with the tolerance estimated at the grain scale, varying HADg and TGW though spikelet removal. Tolerance of GNe reduction following inoculation was therefore calculated. However, GNe reduction by inoculation varied according to the G×N combination, the sampling time, and even the individual plants. It was not possible due to this inconsistency in GNe reduction to explore further the link between GNe and STB tolerance as reported in Chapter 4.

5.4.4 Nitrogen and tolerance of the genotypes

The N fertilisation management being the main HADm variation driver, the contrast N0/N1 was used to focus on tolerance of N deficiency instead of the tolerance of STB. The nitrogen treatment resulted in a large contrasted source availability as N0 induced an early senescence, contrary to the continuous nitrogen nutrition N1 extending the green-leaf life of the canopy. Consequently, the source availability under N0 represented only 53% of N1 (HADm or HADg). The N0 treatment resulted in variable grain yield loss ranging from -5% to -25% of TGW in comparison to N1, or -8% to -36% when considering the crop scale (Ym). The nitrogen treatment could thus be interpreted as a stress modifying source/sink balance, and possibly leading to tolerance. The slopes of the Ym to HADm relationship were estimated per genotype as well as those of TGW to HADg. Both indices were tightly and positively correlated, supporting the hypothesis of Chapter 4 that tolerance could be estimated indifferently at either the crop or grain scale. Surprisingly, however, N-tolerance was negatively correlated with putative STB tolerance, in a trend at the crop scale, and significantly at the grain scale. The expected STB-tolerant genotypes were the most affected by the nitrogen stress. Despite being only based on two

pairs of tolerant/intolerant genotypes such a result might suggest that STB-tolerance and N-tolerance relied on different mechanisms.

In addition, traits that the literature reports related to tolerance were observed and compared to N-tolerance estimates. As mentioned above, Ym did not correlate with tolerance estimate at the crop or grain scale. Conversely, tolerance positively correlated with HADm, HADe, HADg, as well as senescence timing in N1 crops. However, the observed correlations could be challenged, as they were based on only four genotypes and clearly linked to the stay green C×L 7A. Nevertheless, within both LSP2×R genotypes and C×L genotypes the tolerant line showed greater HADm, HADe and HADg, as well as later senescence timing. Additionally, they also shower smaller flag leaf area and fLA 1.

Nitrogen metabolism may also explain some STB-tolerance mechanisms. In comparison to the other genotypes, LSP2×R 127 (tolerant) was characterised by a very large pool of vegetative nitrogen at GS44, associated later with a very large remobilisation per grain and large nitrogen content in the grains. By comparison, LSP2×R 127 was also characterised by a large remobilisation from the stem, the roots and the leaf laminae. The inoculation treatment also increased the N remobilisation, presumably from an effect on GNe rather than STB: the increased GNe would increase the N remobilisation. However, as LSP2×R 127 was the lowest GNe genotype, the nitrogen-remobilisation capacity of that genotype remains unclear from data at the grain scale. At the shoot scale a clear association was observed between ΔNv and tolerance as the STB-tolerant lines showed higher N-remobilisation. Interestingly, in N1 plants, ΔNv correlated positively with the senescence timing: the higher the N-remobilisation, the later senescence occured. The correlation did not result from remobilisation by leaf-laminas, but from remobilisation from sheaths, stem and chaff. Actually, the higher N-remobilisation by tolerant lines was linked to higher N content in sheaths, stem and chaff. Yet N balance started from GS44 at a time where both stem and chaff had just started their exponential growth, thus a slight shift in development between genotypes, such as suggested by heading delay, could explain the higher N content observed in the earliest genotypes.

5.5 Conclusion

To conclude, even if grown in mini-crops, glasshouse conditions led to development and growth very different from those observed in the field. Despite these differences, tolerance of nitrogen deficiency was characterized, and associated traits did not fully correspond to those associated with tolerance to STB. Thus further determining common and distinct traits as well as trade-off among tolerances traits would help managing overall tolerance to stresses.

References

M. M. Acreche and G. A. Slafer. Variation of grain nitrogen content in relation with grain yield in old and modern Spanish wheats grown under a wide range of agronomic conditions in a Mediterranean region. *The Journal of Agricultural Science*, 147(6):657–667, 2009. doi: 10.1017/S0021859609990190 .

P. Bancal. Positive contribution of stem growth to grain number per spike in wheat. *Field Crops Research*, 105(1–2):27–39, 2008. doi: 10.1016/j.fcr.2007.06.008 .

P. Bancal, M.-O. Bancal, F. Collin, and D. Gouache. Identifying traits leading to tolerance of wheat to Septoria tritici blotch. *Field Crops Research*, 180:176–185, 2015. doi: 10.1016/j.fcr.2015.05.006 .

R. Ben Slimane , P. Bancal, and M. Bancal. Down-regulation by stems and sheaths of grain filling with mobilized nitrogen in wheat. *Field Crops Research*, 140(0):59 – 68, 2013. ISSN 0378-4290. doi: 10.1016/j.fcr.2012.10.006 .

I. J. Bingham, D. R. Walters, M. J. Foulkes, and N. D. Paveley. Crop traits and tolerance of wheat and barley to foliar disease. *Annals of Applied Biology*, 154:159–173, 2009. doi: 10.1111/j.1744-7348.2008.00291.x .

A. C. Castro and M. R. Simón. Effect of tolerance to Septoria tritici blotch on grain yield, yield components and grain quality in Argentinean wheat cultivars. *Crop Protection*, 90: 66–76, 2016. ISSN 0261-2194. doi: 10.1016/j.cropro.2016.08.015 .

S. Demotes-Mainard, G. Doussinault, and J. M. Meynard. Effects of low radiation and low temperature at meiosis on pollen viability and grain set in wheat. *Agronomie*, 15:357–365, 1995. URL https://hal.archives-ouvertes.fr/hal-00885691/document.

S. Demotes-Mainard, G. Doussinault, and J. M. Meynard. Abnormalities in the male developmental programme of winter wheat induced by climatic stess at meiosis. *Agronomie*, 15:357–365, 1996. URL https://hal.archives-ouvertes.fr/hal-00885813/document.

R. A. Fischer and Y. M. Stockman. Kernel number per spike in wheat (*Triticum aestivum* l.): responses to preanthesis shading. *Australian Journal of Plant Physiology*, 7(2):169–180, 1980. doi: 10.1071/PP9800169 .

M. J. Foulkes, N. D. Paveley, A. Worland, S. J. Welham, J. Thomas, and J. W. Snape. Major genetic changes in wheat with potential to affect disease tolerance. *Phytopathology*, 96:680–688, 2006. URL http://apsjournals.apsnet.org/doi/pdf/10.1094/PHYTO-96-0680.

D. Gouache, M. Bancal, and P. Bancal. Projet contrat de branche "Tolérance du blé tendre aux stress biotiques et abiotiques" C2008-02 blé tendre, october 2012. URL https://hal.archives-ouvertes.fr/hal-01192469/. Rapport final.

E. Justes, B. Mary, J. M. Meynard, J. M. Machet, and L. Thelierhuche. Determination of a critical nitrogen dilution curve for winter-wheat crops. *Annals of Botany*, 74(4):397–407, Oct 1994. ISSN 0305-7364. doi: 10.1006/anbo.1994.1133 .

S. R. Parker, S. Welham, N. Paveley, J. M. Foulkes, and R. K. Scott. Tolerance of Septoria leaf blotch in winter wheat. *Plant Pathology*, 53(1):1–10, 2004. doi: 10.1111/j.1365-3059.2004.00951.x .

E. Zuckerman, A. Eshel, and Z. Eyal. Physiological aspects related to tolerance of spring wheat cultivars to Septoria tritici blotch. *Phytopathology*, 87(1):60–65, Jan. 1997. ISSN 0031-949X. URL http://apsjournals.apsnet.org/doi/pdf/10.1094/PHYTO.1997.87.1.60.

5.A Appendix

5.A.1 Composition of nutrient solution

Table 5.7: Composition of the stock solution (i).

Element	MW ($g \cdot mol^{-1}$)	Stock solution ($g \cdot l^{-}1$)
Nitrates		
$Ca(NO_3)_2$,$4H_2O$	236.2	243.2
KNO_3	101.1	51.7
Sulfate K		
K_2SO_4	174.3	74.3
Phosphates		
K_2HPO_4	174.2	13.1
KH_2PO_4	136.1	92.3
Oligoelements		
$MgSO_4$,$7H_2O$	246.5	237.6
NaCl	58.5	22.5
$ZnSO_4$,$7H_2O$	287.5	4.7
$MnSO_4$,H_2O	169.0	1.845
H_3BO_3	61.8	1.000
$CuSO_4$,$5H_2O$	249.7	0.410
KI	166.0	0.049
$Mo_7O_{24}(NH_4)6$,$4H_2O$	1235.0	0.035
$CoCl_2$,$6H_2O$	237.9	0.011
Séquestrène		
Iron/Basafer (commercial)	55.8	6%

Table 5.8: Composition of the stock solutions (ii).

	N1	N0	unit
Water	5000	5000	ml per tray
Nitrate	15	0	ml per tray
SulfateK	0	9	ml per tray
Phosphate	6	6	ml per tray
Oligoelement	6	6	ml per tray
Sequestrène	0.2	0.2	g per tray

Table 5.9: N P K balance of the nutrient solutions. The nitrate concentration was optimal for 5 liters per tray.

	N1	N0
mg		
N	539.7	0.0
P	140.0	140.0
K	492.7	492.9
mM		
N	7.7	0.0
P	0.9	0.9
K	2.5	2.5

Chapter 6

Field experiment at Sutton Bonington, 2015-16

6.1 Introduction

The tolerance of Septoria tritici blotch (STB) was addressed in three studies reported in Chapters 3 to 5. A high grain source availability, traditionally quantified by the Healthy Area Duration, per crop m^2 (HADm), is hypothesised to characterise STB-tolerant cultivars.

The HAD is mostly the result (or product) of maximum leaf lamina area expansion (LAe, Leaf Lamina Area per ear-bearing shoot), and senescence timing (*I*, expressed since heading stage), secondarily influenced by the duration of the rapid phase of senescence (D). Bancal et al. (2015) found that the yield loss because of STB epidemics was reduced in late senescing treatment combinations (cultivar × site × season), where senescence was assessed as *I*. However, their results also highlighted that yield loss might be increased by larger leaf lamina, likely through an increase of rate of disease epidemics (Lovell et al., 1997). For this reason, the senescence timing appeared to be the main tolerance trait in the Chapter 3 (p.53) intended to understand the underlying traits that influence senescence timing. It appeared that heading date was negatively correlated with the senescence timing, early heading date being associated with a later senescence timing (*I*, in days, or degree-days since heading stage). Thus, early heading date could enhance directly the grain source availability, and therefore tolerance of STB. It is noteworthy that earlier heading date has also been associated with higher severity of STB epidemics (Murray et al., 1990; Shaw and Royle, 1993).

The grain source availability was further investigated in the field experiment 2014-15 (Chapter 4, p.104). Indeed, it was hypothesised that if low grain source limitation is a tolerance trait, therefore cultivars contrasted for tolerance should also be contrasted for grain source limitation. Based on six doubled-haploid cultivars and a half-spikelet

removal treatment, the Thousand Grain Weight (TGW) increment in response to the treatment (positively associated with source limitation) was positively associated with the tolerance grade of the cultivars estimated independently in three field experiments. It could therefore be concluded that low grain source limitation is a STB-tolerance trait, and that the quantification of tolerance based on source/sink balance estimated at the crop scale was also correlated with source/sink balance estimated at the single grain scale.

In addition to low grain source limitations, strategies to improve STB tolerance based on compensation mechanisms have been proposed. The most investigated was probably the stem carbohydrate reserve remobilisation during the grain filling time. It was proposed that an increase in stem reserve remobilisation could be a STB-tolerance trait of wheat (Parker et al., 2004), but this could not be demonstrated in a field STB tolerance study (Foulkes et al., 2006), even though cultivar variation of this trait has been proven (Foulkes et al., 2006; Shearman et al., 2005).

In the present study, it is proposed to focus on the identified/hypothesised tolerance of STB traits in a set of commercial winter wheat cultivars. The rationale for the cultivar choice was mainly to provide heading date variation, in order to induce variations in senescence timing of the yield-forming leaves and consequently in grain source availability during the grain filling period. The hypotheses were:

- STB tolerance is associated with low degree of grain source limitation.
- Low grain source limitation is achieved by high HAD per grain
- Early heading stage is a trait to increase grain resource availability during grain filling.
- If STB is mainly a late stage disease and doesn't change grain density, therefore, studying tolerance at the crop or the average single grain scale is equivalent.

6.2 Materials and methods

6.2.1 Experimental design and treatment

The experimental design comprised six winter wheat cultivars exposed to two fungicide treatments in a randomised block design of four replicates.

Each experimental plot was 1.625 m × 12 m, 12 rows per plot with a 13.2 cm row spacing. The six cultivars were chosen to provide a strong contrast for STB resistance and development rate. The cultivars were Cashel (KWS UK, first season on Recommended List (RL) 2014-15, bread-making market, STB resistance grade 5/9), Cougar (RAGT seeds UK, RL 2013-14, feed market, STB resist. 5/9), Dickens (Secobra France, RL 2013-14, feed

market, STB resist. 5/9), Evolution (Sejet Denmark, RL 2014-2015, feed market, STB resist. 6/9), Zulu (Limagrain UK, RL 2014-15, feed/biscuit market, STB resist. 5/9), Sacramento (RAGT, registration 2014, bread-making market, STB resist. 5.5/9) (HGCA, 2015; RAGT, 2016; AHDB, 2016b). They were characterised by a 15-day range for heading date (GS55, Zadoks et al., 1974). Sacramento is not on the UK Recommended List but is proposed and was registered in France to the CTPS list in 2015 (*Comité Technique Permanent de la Sélection des plantes cultivées*, permanent technical committee for plant breeding). The cultivars were sown after winter oilseed rape at Sutton Bonington — University of Nottingham farm (Leicestershire, UK, 52.8355 °N 1.2501 °W) on 2 October 2015 on a sandy loam to 80 cm over Keuper Marl clay (Dunnington Heath soil series). The cultivars were sown at a seed rate of 325 seeds $\cdot$ m^{-2} and managed following the best local practices (Table. 6.1). Nitrogen fertilisation was split into three applications of ammonium nitrate prill (total: 180 kg N $\cdot$ ha^{-1}, Table. 6.1).

Two disease control managements were applied (F, fungicide) to the plots to obtain either a full control of Septoria tritici Blotch (STB, F1) or no control of STB (F0) while maintaining the non-targeted disease symptoms to low levels (Table. 6.1). The cultivars×fungicide combinations were applied randomly within each block (randomised block design, four blocks).

The growth analysis was carried out at the shoot scale on 20 randomly selected ear-bearing shoots per plot during the grain filling period (hereafter in the chapter, *shoot* refers to ear-bearing shoot). To do so, ear emergence (GS51) and heading date (GS55) were estimated in all the plots (growth stage assessment every 2-3 days). Within each cultivar, 20 ear-bearing shoots reaching GS55 on the same day were tagged, keeping at least 1 m between each tagged shoot.

6.2.2 Measurements

At mid-anthesis (GS65), 10 shoots were cut at ground level and dissected. Leaf 1 (flag-leaf), leaf 2 and leaf 3 were detached at the ligule. Green, diseased and senescent areas were visually scored for each leaf layer as percentage of total leaf lamina area. Percentage of Green Leaf Lamina Area (%GLA) was used to fit senescence kinetic functions. The individual Leaf Lamina Area per ear-bearing shoot (LAe) was measured using a leaf area metre (Licor 3100 Leaf Area Meter, Licor, Lincoln NE, USA). Ears were cut at the ear collar below the lowest spikelet. The stem was cut above the node of leaf 3. The two highest internodes, the peduncle and the three leaf sheaths surrounding them were referred as the stem. Lower internodes and associated organs comprised the base (Chapter 2 "Material and methods", section 2.4 p.47). Every sample was oven-dried for 48 h at 80°C and weighed. The total biomass was referred to as the total above-ground biomass, while the total upper shoot biomass did not take bases into account.

Table 6.1: Inputs applied on the Field 2015-16 experiment. The "Full" and "Non-target" indications refers to the respective fungicide treatments: STB-prevention versus the control.

Operation	Date	Details
Previous crop		Winter OSR
Soil Indices		P:4, K:3, Mg:3, pH:7.1
Cultivations	07/09/2015	Plough, Press, and roll after drilling
Sowing	02/10/2015	Sowing, 325 seeds/m2 (Wintersteiger) and roll after drilling
Herbicide	02/10/2015	Movon @ 1l/ha + Defy @ 2l/ha + Backrow @ 200ml/ha
Herbicide	01/04/2016	Chekker @ 180g/ha
Herbicide	26/05/2016	Cleancrop Gallifrey 3 @ 0.6l/ha
Insecticide	03/02/2016	Cleancrop Corsair, 0.1l/ha
Fertiliser	03/02/2016	Hu-man extra @ 1l/ha
Fertiliser	16/03/2016	116 kg/ha 34.5% Nitram (40kg/ha N)
Fertiliser	17/03/2016	Hu-man extra @ 1l/ha
Fertiliser	08/04/2016	Hu-man extra @ 1l/ha
Fertiliser	12/04/2016	232 kg/ha 34.5% Nitram (80kg/ha N)
Fertiliser	09/05/2016	174 kg/ha 34.5% Nitram (60kg/ha N)
Fertiliser	26/05/2016	Magnor @ 1l/ha
Fungicide	03/02/2016	Corbel @ 0.75l/ha
Fungicide (Full)	11/04/2016	0.4l/ha Toledo + 1.0l/ha Bravo
Fungicide (Non-target)	11/04/2016	0.75l/ha Corbel
Fungicide (Full)	05/05/2016	0.75l/ha Kestrel + 0.75l/ha Imtrex + 1.5l/ha Phoenix
Fungicide (Non-target)	05/05/2016	1l/ha Kayak
Fungicide (Full)		1.0l/ha Bravo
Fungicide (Full)	02/06/2016	1.5l/ha Brutus + 1.5l/ha Imtrex + 1.5l/ha Phoenix
Fungicide (Full)	21/06/2016	0.6l/ha Kestrel
PGR	08/04/2016	Meteor @ 1.5l/ha
Misc	12/10/2015	Meterex @ 5kg/ha
Misc	13/11/2015	Meterex @ 5kg/ha
Harvest	15/08/2016	Harvest combine

After mid-anthesis (GS65), the remaining 10 shoots per plot were assessed on a weekly basis. Percentage of green, diseased and senesced area of each leaf layer was assessed until the complete senescence of the three upper leaf layers. The Ear Number per m^2 (EN) was the average of two assessments carried out at GS61 and GS75 by counting the number of fertile ears within a sampled area of 0.48 m^2 (6 rows $\times$ 0.6 m) per plot.

After physiological maturity (GS89), the remaining 10 ear-bearing shoots were sampled. Organs were separated as for anthesis samples and oven dried and weighed. The ears were mechanically threshed (Haldrup LT-20 thresher, Haldrup, Ilshofen, Germany) and the grains were weighed after drying for 48 h at 80°C (grain yield per ear, Ye) and counted to calculate the Grain Number per ear-bearing shoot (GNe); then the grain weight was calculated ($TGW = \frac{Ye}{GNe} \times 1000$).

In addition, the plots were combine-harvested, providing the grain yield per crop m^2 (Ym) along with an additional TGW estimation. TGW from both methods (shoot samples and combine samples) were equivalent (r = 0.89***, Fig. 6.1), with a very small underestimation of 1.04 g (approx. -2% of the average TGW, P = 0.037). This correlation

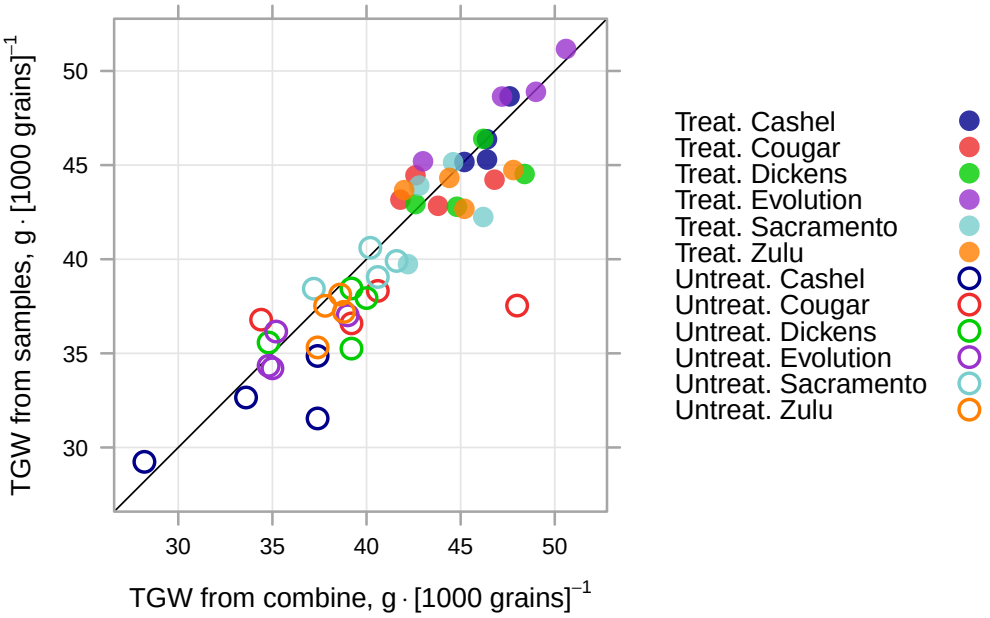


Figure 6.1: TGW from hand-harvested versus combine grain samples. The colours represent the cultivars (dark blue, Cashel; red, Cougar; green, Dickens; purple, Evolution; light blue, Sacramento; orange, Zulu). The open/closed symbol represent the fungicide untreated/treated. The plain line is the y=x bisector. The Pearson's correlation coefficient between combine and 10-shoot sample based estimations of TGW was r = 0.89*** (n = 48).

supported the scaling of the Ye to the combine yield Ym through the determination of ENeq: $ENeq = \frac{Ym}{Ye}$. The equivalent Ear Number per m^2 (ENeq) was used later for conversion of shoot scale variables to the crop scale, e.g. grain number per unit area (GNm = $GNe \times ENeq$), the Healthy Area Duration, per crop m^2 (HADm = $HADe \times ENeq$), the Leaf Area Index (LAI = $LAe \times ENeq$). Grain yield (TGW, Ye, Ym) was reported at 100% DM.

6.2.3 Data analysis

6.2.3.1 Senescence kinetics and healthy area duration

Percentage Green leaf Lamina Area (%GLA) kinetics were fitted by Nonlinear Least Squares to a Gompertz's function (Eq. 6.1) to thermal time (base temp. 0 °C) since heading stage (GS55, unit: degree days since heading °Cd$_H$). Fit quality was generally very good (R^2 > 0.95).

$$\%GLA(t, K = 100, D, I) = K \cdot \exp\left(-\exp\left(\frac{2 \times (I - t)}{D}\right)\right) \tag{6.1}$$

$$HAD = \int_{t=0°\mathrm{Cd}_H}^{1200°\mathrm{Cd}_H} \%GLA(t, K = 100, D, I) \tag{6.2}$$

The I parameter is the inflexion point reached for 37%GLA (i.e. 37% of the total leaf lamina area at GS55), D is the duration from 80%GLA to 20%GLA. Healthy Area Duration (HAD) is the area under the %GLA curve (defined by the fitted parameters I and D) between 0 and 1200 °Cd_H, and equation 6.2 integration was computed using the adaptive quadrature (Piessens et al., 1983).

The fitted equations were used to estimate the HAD (HAD, Eq. 6.2, unit: °Cd_H) scaled to the ear-bearing shoot (HADe, unit $m^2 \cdot ^\circ Cd_H \cdot shoot^{-1}$), to the single grain (HADg, unit: $dm^2 \cdot ^\circ Cd_H \cdot grain^{-1}$) or the ground area (HADm, unit: $m^2 \cdot ^\circ Cd_H \cdot m^{-2}$). The ENeq was used as an estimation of EN to estimate Ye scaled to the observed grain yield per unit area (Ym, Chapter 2 "Material and methods", section 2.6 p.51).

6.2.3.2 Tolerance/intolerance

Tolerance is defined by the ratio of grain yield reduction to HAD reduction between treated and untreated plots. It was estimated at the crop level (per square metre, $\Delta HADm/\Delta Ym$) and referred as Tm; it was also assessed at the grain level ($\Delta HADg/\Delta TGW$) and referred as Tg. In both cases, however, the uncertainty of the tolerance value largely increases when the yield denominator is low, i.e. when the crop exhibits tolerance. The alternative estimation of intolerance (ΔY to ΔHAD, as calculated by Parker et al., 2004; Foulkes et al., 2006; Castro and Simón, 2016) prevents this difficulty — referred as inTm and inTg respectively for intolerance per m^2 and per grain — but in both cases (tolerance T and intolerance inT) the variance homogeneity between cultivars is difficult to obtain. Three different methods were thus applied to: estimate the (in-) tolerance of the cultivars as well as to ensure the stability of cultivar estimated tolerance ranking.

1. The first method compared the ratios obtained in each block to estimate tolerance and intolerance at the crop and the grain scale (method 1: Tm1, Tg1, inTm1, inTg1).

2. In the second method, the four repetitions of control treated plots were averaged per cultivar (method 2: Tm2, Tg2, inTm2, inTg2).

3. The intolerance was also estimated through the linear regression: $Ym_{ij} = \beta_0 + g_i + \beta_1 HADm + \gamma_i HADm + B_j + \varepsilon_{ij}$, with Ym_{ij} the HADm for the cultivar i in the block j, β_0 the intercept, g_i the effect of the cultivar (offset), β_1 the slope, γ_i the effect of the cultivar on the slope, B_j the random effect of the block j and ε the residual of the model, assumed to follow a Normal law and homogeneity of variance between groups. Therefore, for the cultivar g_i, the intercept is given by $\beta_0 + g_i$ and the intolerance slope was given by $\beta_1 + \gamma_i$. Similarly, the intolerance slopes were estimated at the grain scale. Method 3: inTm3 and inTg3.

The notation of tolerance estimation reports the intolerance or tolerance ratio (inT or T), the scale (m and g for crop and grain scale), the method use (1 to 3): Tm1, Tg1, inTm1, inTg1, Tm2, Tg2, inTm2, inTg2, inTm3 and inTg3.

The methods based on ratios provide an (in-)tolerance value per cultivar and per plot. They allow calculation of correlations between traits measured in each block, therefore taking into account the cultivar trait values and their variations across the blocks (n = 24).

6.2.3.3 Statistics

- **Linear models**

The experiment was a factorial experiment with 2 spacial scales (Block B, Plot P) and thus 2 different error variances. The analysis of variables (*e.g.* yields components) to test the differences between the applied treatments was based on ANOVA models (Eq. 6.3). ANOVAs were performed through mixed models (Crawley, 2012).

$$y_{ijkl} = \mu + f_i + g_j + fg_{ij} + B_{ijk} + \varepsilon_{ijkl} \tag{6.3}$$

where: y_{ijkl} = an observed value of a response variable, μ = the population mean for the reference, f_i = the fungicide fixed effect, g_j = the cultivar fixed effect (g for cultivar), B_{ijk} = the block random effect.

Effects were tested with the Fisher's test, degrees of freedom estimated using Kenward-Roger's approximation. The F test was applied to the model including the 2-way interactions between fixed effects. Then non-significant effects were removed. Effect size was then computed and least square means were plotted along with the 95% confidence interval (CI) when relevant. Eventually, post-hoc tests were performed to obtain least means square comparison between levels of factors, relying on Tukey's Honestly Significant Difference test (Tukey HSD).

- **Correlation**

Correlation was used to quantify association between target traits. In the case of growth stage, the data were unique across cultivar (no intra-cultivar variation), and the correlation was computed with least means square estimation according to the models described above. The tolerance was available per block × cultivar and correlation was computed with values of fungicide-treated traits or untreated values.

- **Aberrant data**

The maturity measurement of the block 1 for the treatment combination "Treated" × Cashel was largely inconsistent with the other blocks and out of the allometric relations

between organs. As it was the only aberrant data, and in order to preserve the balance dataset, it was substituted by the average of the 3 other blocks. The substitution concerns the dry matter and grain number data at maturity only.

- **Software**

Statistical analysis was carried out using R (R Core Team, 2016). Additional packages included: `DBI` (R Special Interest Group on Databases, 2014) and `RPostgreSQL` (Conway et al., 2016) for data management and variable computations, `lme4` (Bates et al., 2015) for mixed models fitting, `lsmeans` (Lenth, 2016) for post-hoc tests, and `lattice` (Sarkar, 2008) for graphics.

6.3 Results

6.3.1 Development rate

The range of heading stage (GS55) amongst cultivars was 15 days. Sacramento was the earliest (24 May), followed by Dickens (1 June, +102 °Cd from Sacramento) and finally the other cultivars (4-8 June, +140 to 193 °Cd from Sacramento). The range for the GS51 to GS61 phase amongst cultivars was 8.8±0.2 days (117±2.3 °Cd, Fig. 6.2) and no effect of the fungicide treatment on heading date was observed.

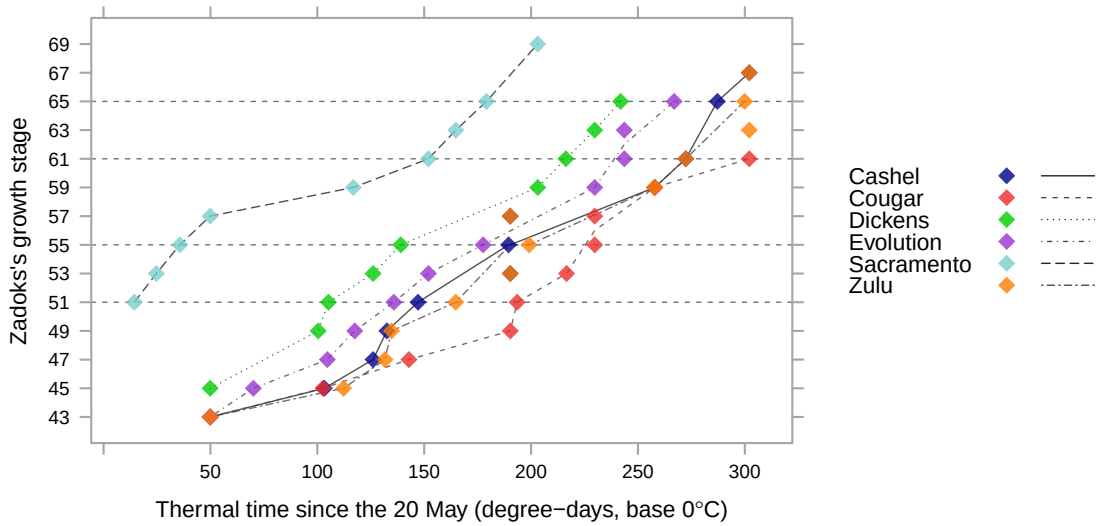


Figure 6.2: Growth stage assessment (Zadoks et al., 1974) versus thermal time since 20 May. The point colours represent the cultivars (dark blue, Cashel; red, Cougar; green, Dickens; purple, Evolution; light blue, Sacramento; orange, Zulu). Each cultivar is also associated with a line joining average values.

In fungicide-protected plots, correlations were calculated between heading date (in days since the 15 May) and cultivar traits that will be referred to later, except the very

significant positive correlation with dry matter weight of lower internodes at anthesis (AM) or maturity (MM) (r = −0.80 *** at anthesis; r = -0.83*** at maturity).

6.3.2 The sources for grain filling

6.3.2.1 Leaf area characterisation

The number of ears per m^2 (ENeq) was not different in treated and untreated plots (Table 6.2), but was affected by the cultivar ($P < 0.001$), with Evolution and Cashel showing a higher ear density ($466 - 500\,eq \cdot ears \cdot m^{-2}$) than the other cultivars ($348 - 393\,eq \cdot ears \cdot m^{-2}$). Conversely, the cultivars Cashel and Evolution had the smallest total Leaf Lamina Area per shoot (LAe, 62.9 cm^2 and 74.8 cm^2, respectively; Table 6.2), while the other cultivars had comparable lamina area (83 cm^2 to 90 cm^2). The LAe and ENeq were significantly and negatively correlated (r = -0.57***), which suggested a trade-off resulting in comparable LAI between cultivars and fungicides (LAI±se = 3.2±0.1).

However, the cultivars showed significant differences in leaf profile, i.e. the contribution of individual leaf layer to the total leaf lamina area. As commonly observed, the fraction of total leaf lamina (leaves 1 to 3) represented by the second leaf was quite constant (0.347 to 0.387, depending on the cultivar). Conversely that in the flag leaf (fLA 1, Table 6.2) was much more variable: Dickens, Cashel and Evolution were characterised by a small proportion of flag leaf (0.280) while it reached 0.352 for Sacramento ($P < 0.001$). Nevertheless flag-leaf lamina area per shoot (LAe 1) was highly correlated with total leaf lamina area per shoot (LAe, r = 0.87***). Late heading cultivars exhibited lower fLA 1 (r = -0.71***) and higher fLA 3 (r = 0.54, $P < 0.01$). However, it relied on the early heading cultivar Sacramento that also exhibited a large fLA 1. Otherwise, the correlation of heading date with fLA1 was not significant. Lastly, the fungicide did not affect the leaf lamina areas nor the fraction of total leaf lamina area.

6.3.2.2 The senescence parameters

Figure 6.3 shows the evolution of total green leaf area after heading in both fungicide-treated and untreated plots. Around heading, the green leaf lamina area was maximum, at a LAe level that differed according to the cultivar. In protected plots, the senescence timing (I) varied with the cultivar ($P < 0.001$, Table 6.2) from 679 °Cd_H (Cashel) to 881 °Cd_H (Sacramento). The earliest cultivar, Sacramento, showed the latest senescence timing. Otherwise, however, the correlation of heading date with I was not significant. Without the full fungicide treatment, I occurred earlier because of STB, on average by −244 °Cd_H (-32%) in comparison to fully treated plots ($P < 0.001$). An interaction between cultivar and fungicide effects on I suggested that the cultivars have different sensitivity to epidemics. Indeed, the advance in I induced by STB varied between cultivars (P <0.001)

Table 6.2: Analysis of variance of different grain source traits. Response of equivalent Ear Number per m^2 (ENeq), leaf Lamina Area per ear-bearing shoot (LAe), fraction of total leaf area for flag leaf (fLA 1) flag leaf Lamina Area per ear-bearing shoot (fLAe 1), senescence time (I), senescence duration (D), Healthy Area Duration (HAD) per ear-bearing shoot / square metre / grain (HADe, HADm, HADg), and dry matter reserve mobilisation between anthesis and maturity per shoot (RMe), to the effects of the cultivar (G) and the fungicide (F) including two-way interaction (G×F) were analysed. Significance of the effects is reported following the standard star code (*, **, ***), for significance, plus "$\cdot$" when $P < 0.1$ and "^{ns}" when non significant. Non significant effects were removed. The symbol \$ represents the ANOVA applied on log-transformed values to comply with ANOVA assumptions. The number of observations *n* is given. The G and G×F estimations are compared based on Tukey HSD post-hoc test, significance of effect comparison is reported by compact letter display.

	ENeq ears $\cdot$ m^{-2}	LAe cm^2	fLA 1	LAe 1 cm^2	I $^{\circ}Cd_H$	D $^{\circ}Cd$	HADe $m^2 \cdot ^{\circ}$ Cd	HADm $m^2 \cdot ^{\circ}$ Cd	RMe g $\cdot$ ear^{-1}
F	ns	ns	ns	ns	***	***	***	***\$	**
G	***	***	***	***	***	***	***	**\$	***
F×G	ns	ns	ns	ns	***	***	*	ns\$	ns
n	48	48	48	48	48	48	48	48	48
Treated									
Cashel	500 b	62.9 a	0.280 a	17.7 a	679 c	175 abcd	3.96 b	1900 bcd	-0.63 d
Cougar	371 a	89.7 c	0.300 c	29.9 cd	776 de	197 bcde	6.54 de	2352 de	-0.79 bcd
Dickens	348 a	88.3 c	0.277 a	24.6 c	790 e	121 ab	6.79 e	2248 cde	-1.06 ab
Evolution	466 b	74.8 b	0.283 ab	21.2 b	772 de	202 cde	5.31 c	2243 cde	-0.72 cd
Sacramento	348 a	83.9 c	0.352 d	29.5 d	881 f	113 a	7.01 e	2610 e	-0.90 abcd
Zulu	393 a	84.2 c	0.297 bc	25.1 c	721 cd	154 abc	5.63 cd	2279 de	-0.73 cd
Untreated									
Cashel	-	-	-	-	436 a	210 cde	2.38 a	1207 a	-0.75 bcd
Cougar	-	-	-	-	546 b	350 g	4.03 b	1495 ab	-0.91 abcd
Dickens	-	-	-	-	519 b	209 cde	4.01 b	1429 ab	-1.18 a
Evolution	-	-	-	-	441 a	253 def	2.81 a	1426 ab	-0.85 bcd
Sacramento	-	-	-	-	690 c	296 fg	5.16 c	1658 bc	-1.02 abc
Zulu	-	-	-	-	524 b	264 ef	3.86 b	1449 ab	-0.85 bcd

Table 6.3: Grain source traits observations, averaged per cultivar and fungicide treatment combinations (four blocks): equivalent Ear Number per m^2 (ENeq), leaf Lamina Area per ear-bearing shoot (LAe), fraction of total leaf area for flag leaf (fLA 1) flag leaf Lamina Area per ear-bearing shoot (fLAe 1), senescence timing (I), senescence duration (D), Healthy Area Duration (HAD) per ear-bearing shoot / square metre / grain (HADe, HADm, HADg), and dry matter remobilisation between anthesis and maturity per shoot (RMe).

		ENeq ears $\cdot$ m^{-2}	LAe cm^2	fLA 1	LAe 1 cm^2	I $^{\circ}Cd_H$	D $^{\circ}Cd$	HADe $m^2 \cdot ^{\circ}$ Cd	HADm $m^2 \cdot ^{\circ}$ Cd	RMe g $\cdot$ ear^{-1}
Treat.	Cashel	503	62.8	0.285	17.9	679	175	3.96	2008	−0.67
	Cougar	358	90.9	0.293	26.7	776	197	6.54	2329	−0.85
	Dickens	356	89.7	0.281	25.3	790	121	6.79	2452	−1.07
	Evolution	439	74.3	0.283	21.0	772	202	5.31	2337	−0.73
	Sacramento	350	82.6	0.348	28.8	881	113	7.01	2462	−0.85
	Zulu	391	83.1	0.299	24.9	721	154	5.63	2210	−0.66
	All	399	80.6	0.298	24.1	770	160	5.87	2300	−0.80
Untreat.	Cashel	498	63.1	0.276	17.4	436	210	2.38	1191	−0.71
	Cougar	384	88.4	0.306	27.1	546	350	4.03	1539	−0.84
	Dickens	340	86.9	0.273	23.8	519	209	4.01	1353	−1.17
	Evolution	494	75.3	0.284	21.4	441	253	2.81	1387	−0.84
	Sacramento	346	85.1	0.356	30.3	690	296	5.16	1787	−1.07
	Zulu	395	85.4	0.295	25.2	524	264	3.86	1528	−0.92
	All	409	80.7	0.298	24.2	526	264	3.71	1464	−0.93

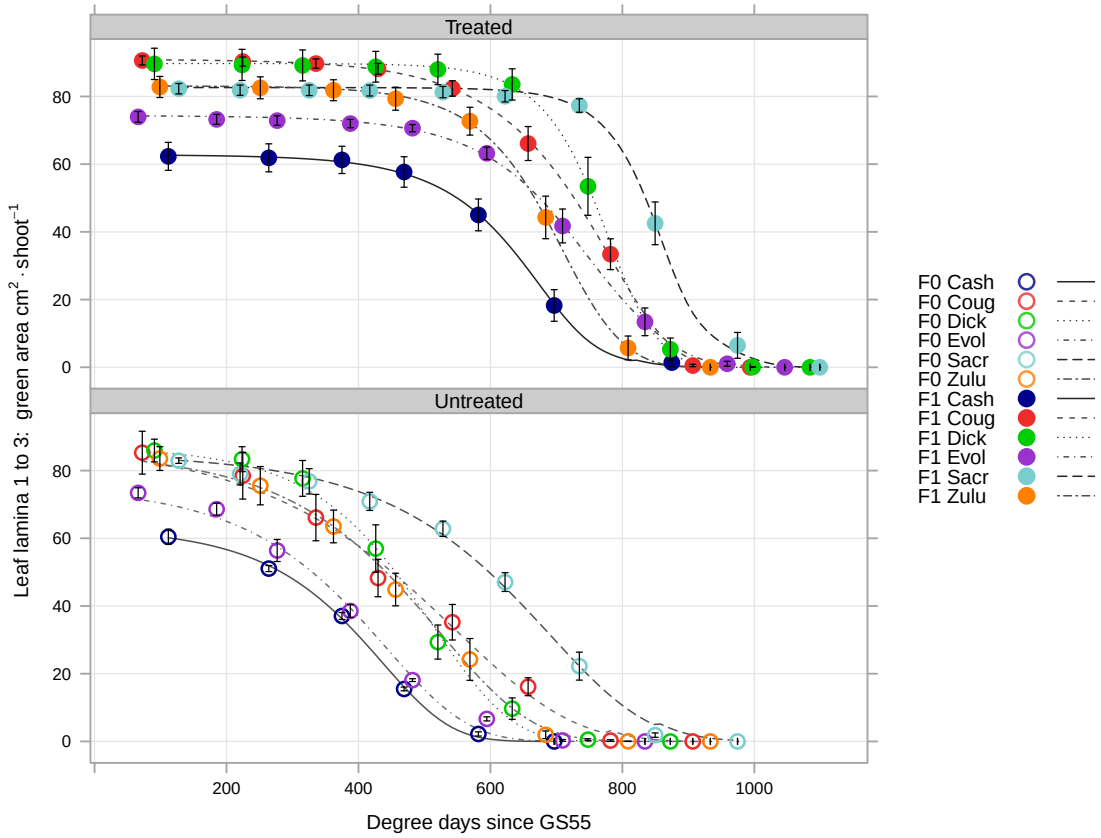


Figure 6.3: Evolution of post-heading green leaf lamina area. The y-axis is the cumulated green area per shoot of the three top leaves (green cm^2 · shoot^{-1}). The x-axis is the time in degree-days (base temp. 0 °C) since heading stage (GS55). The lines and symbol colours represent the cultivars (dark blue, Cashel; red, Cougar; green, Dickens; purple, Evolution; light blue, Sacramento; orange, Zulu). The open/closed symbols represent the fungicide treatment (untreated/treated). At each assessment date, the points represent the cultivar×fungicide combination average ± standard error (error bar).

from Evolution (−331 °Cd; -43%) to Sacramento (−191 °Cd; -22%). Lastly, the senescence time estimated for the different leaf layers (*I1* to *I3*) indicated that in both treated and untreated plots, senescence occurred later and with less variability for the flag leaf than in for the leaf 2 — and for leaf 2 than for leaf 3. However, the senescence across different leaf layers was highly correlated amongst cultivars (e.g. r = 0.87*** was the lowest correlation, calculated between leaf 1 and leaf 3, *I1* and *I3*). Senescence timing *I* was negatively correlated (r = -0.54***) with senescence duration D (duration from 80% to 20% green leaf lamina area remaining): late senescence was therefore also associated with rapid senescence. In STB-protected plots, D ranged from 113 °Cd (Sacramento) to 202 °Cd (Evolution) ($P < 0.001$). In non-treated plots, D was extended with an interaction with the cultivars ($P < 0.001$); senescence duration then ranged from 209 °Cd (Dickens) to 350 °Cd (Cougar). In STB-protected plots, late heading cultivars exhibited shorter D (r = -0.70***). Correlation was not significant for D1 and D2, but unlike in the case of *I*,

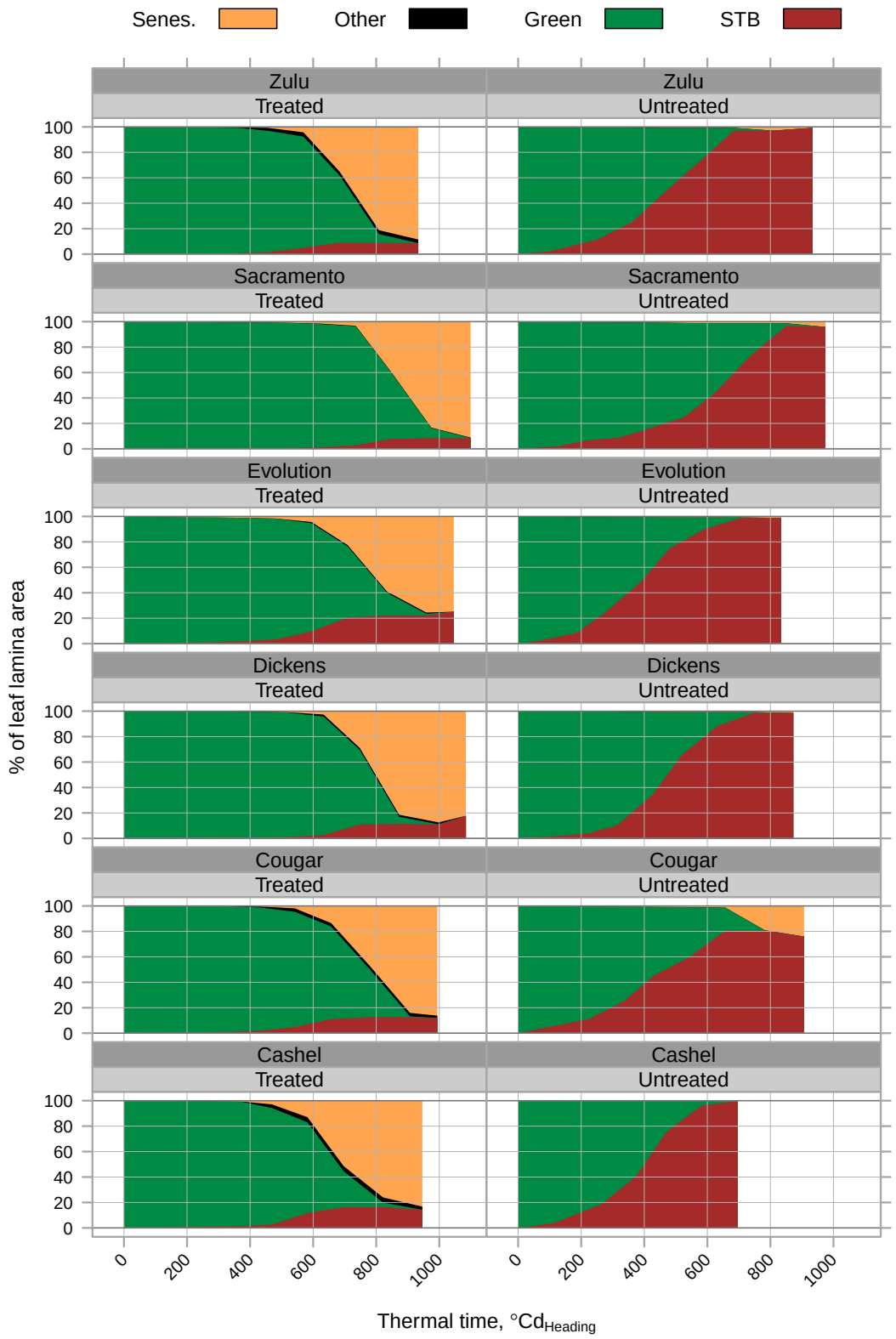


Figure 6.4: Relative senescence and disease evolution since heading stage. Each column of graphics corresponds to a cultivar. Each row of graphics corresponds to the STB-treated/untreated treatment. Each graphic is the evolution (thermal time since heading stage) of the green (green), senescent (orange), disease (red) areas as a percentage of the cumulated area of three upper leaves.

correlation with D did not rely on a single cultivar. Thus, when heading date was 100 °Cd later, D was reduced by 43 °Cd.

6.3.2.3 The healthy area duration

The green leaf lamina area kinetics were integrated over time to obtain Healthy Area Durations that characterized source potential either at the ear-bearing shoot (HADe) or at the square metre level (HADm). In treated plots, the HADe varied significantly with the cultivar and was lower for Cashel (3.96 $m^2 \cdot °$ Cd) and higher for Sacramento (7.01 $m^2 \cdot °$ Cd). HADe was reduced in untreated plots, but the magnitude depended on the cultivar ($P < 0.05$). The average reduction was 2.17 $cm^2 \cdot °$ Cd ranging from 1.58 $cm^2 \cdot °$ Cd (Cashel) to 2.51 $cm^2 \cdot °$ Cd (Cougar). Variation in HADe amongst cultivars was significant ($P < 0.01$), but less than that of HADm since compensated by ear density. In treated plots, only Sacramento was associated with significantly higher HADm in comparison to Cashel. The other cultivars had intermediate HADm. The absence of fungicide protection caused a reduction of HADm ($P < 0.001$, tested and estimated on log-transformed values). No significant interaction between cultivar and fungicide was observed on HADm that was proportionally reduced by 34%, to the same extent as *I*.

6.3.2.4 Alternative sources: the dry matter remobilisation

As expected, grain filling mainly resulted from net assimilation rate from anthesis, as shown by the significant correlation of Ye to Net dry matter Assimilation per ear-bearing shoot (NAe, the gain of above-ground dry matter after anthesis, $r = 0.93^{***}$, Table 6.4). Nevertheless, the dry matter in vegetative parts at anthesis, as well as its variation to maturity RMe (the reserve mobilisation per ear-bearing shoot from anthesis to maturity), showed variation with the cultivars ($P < 0.001$, Table 6.4) that suggested RMe was an alternative source to leaf photosynthesis for grain filling that could also affect tolerance. The above-ground dry matter at anthesis (AMe) primarily was an indicator for the plant size, and thus it was positively correlated with both HADe ($r = 0.58^{***}$, Table 6.4) and yield per ear (Ye, $r = 0.80^{***}$). Although fungicide treatment did not significantly affect AMe ($P > 0.05$, Table 6.4), both HADe and Ye decreased in untreated plots. The slope of the linear regression of AMe on HADe and Ye was thus significantly decreased in untreated plots. Plant biomass at anthesis also affected the amount of remobilisation, thus AMe positively correlated with RMe ($r = 0.58^{***}$). However RMe did not correlate with Ye in treated plots suggesting reserve remobilisation was not at a key point for yield set in healthy plants. On the other hand, RMe was significantly increased in the absence of fungicide. Moreover variation in reserve mobilisation sustained grain yield in unprotected plants, as RMe positively correlated with Ye ($r = 0.50^{*}$).

Table 6.4: Analysis of variance of Dry Matter fluxes per shoot (g per shoot). Response of above-ground dry matter at anthesis or maturity per shoot (AMe, MMe), net above-ground dry matter increase from anthesis to maturity per shoot and per m^2 (NAe, NAm), the vegetative Dry Matter reserve mobilisation per ear-bearing shoot from anthesis to maturity per shoot and per m^2 (RMe, RMm) to the effects of the cultivar (G) and the fungicide (F) including two-way interaction (G×F) were analysed. Significance of the effects is reported following the standard star code (*, **, ***), for significance, plus "·" when P < 0.1 and "^{ns}" when non significant. Non significant effects were removed. The number of observations *n* is given. The G estimations are compared based on Tukey HSD post-hoc test, significance of effect comparison is reported by compact letter display. The fungicide treatment "untreated" effect is reported in comparison to the "treated" estimation. The Pearson's correlation coefficient between responses and with sink traits are reported at the bottom of the table.

	AMe	MMe	NAe	RMe	NAm	RMm
	$g \cdot ear - bearing\ shoot^{-1}$				$g \cdot m^{-2}$	
F	ns	***	***	**	***	*
G	***	***	***	***	***	ns
F×G	ns	ns	ns	ns	ns	ns
n	48	48	48	48	48	48
Treated						-316 b
Cashel	2.61 a	3.69 a	1.07 a	-0.63 c	483 a	-
Cougar	3.25 b	5.12 b	1.85 bc	-0.79 bc	665 b	-
Dickens	3.90 c	5.81 c	1.89 bc	-1.06 a	662 b	-
Evolution	2.99 b	4.62 b	1.61 b	-0.72 bc	710 b	-
Sacramento	3.91 c	6.21 c	2.28 c	-0.90 ab	796 b	-
Zulu	3.19 b	5.11 b	1.90 bc	-0.73 bc	737 b	-
Untreated						
Effect	-	-0.64	-0.60	-0.12	-227	-373 a
Ye	0.80***	0.99***	0.93***	-0.19^{ns}	0.80***	0.35*
MMe	0.84***	-	0.91***	-0.21^{ns}	0.76***	0.34*
HADe	0.58***	0.81***	0.81***	-0.08^{ns}	0.80***	0.25·

To summarize, the range of cultivars and the fungicide treatments altogether generated — as expected — a large range of source availability to fill the grains at the crop and the ear level by combining different complementary traits. Thereby, contrasting HAD resulted in treated plots ranging from low LAe and early I (e.g. Cashel) to medium LAe and late I (e.g. Sacramento) in interaction in untreated plots with relative HADe losses ranging from 26% (cv. Sacramento) to 47% (cv. Evolution), depending on cultivar susceptibility to STB. Furthermore the cultivars also showed a different ability to partially compensate the HADe losses through the remobilisation of vegetative dry matter reserves.

6.3.3 The grain sink

6.3.3.1 Yield and yield losses

Figure 6.5 shows crop grain yield per unit area (Ym) in both treated and untreated plots. Sink traits ANOVA results are reported in Table 6.5, and average observations can be found in Table 6.6. In STB-protected plots, Ym ranged from $816\,g \cdot m^{-2}$ (Cashel) to $1089\,g \cdot m^{-2}$ (Evolution, P < 0.001). The yield was positively correlated with the grain

yield reported in the UK cultivar Recommended List (r = 0.97**, n = 5, HGCA, 2015, data not available for Sacramento), it was generally higher in the present experiment (+0 $g \cdot m^{-2}$ for Cashel to +220 $g \cdot m^{-2}$ for Evolution). The cultivars experienced significant grain yield reduction in untreated plots. The yield ranged then from 633 $g \cdot m^{-2}$ (Cashel) to 972 $g \cdot m^{-2}$ (Sacramento) in untreated plots. The interaction Cultivar × Fungicide was nearly significant (P = 0.054), suggesting STB unequally affected the cultivars in the absence of fungicide; thus, the relative yield loss due to STB ranged from -8.7% (Sacramento) to -23.0% (Evolution).

The Ym was highly positively correlated with the Ye (r = 0.75***). In disease-free plots, Ye varied amongst the cultivars (P < 0.001) from 1.70 $g \cdot ear^{-1}$ (Cashel) to 3.18 $g \cdot ear^{-1}$ (Sacramento). It was reduced by 0.48 $g \cdot ear^{-1}$ in untreated plots (P < 0.001) independently from the cultivar (non-significant interaction G×F), so Ye loss ranged from -15% to -28%.

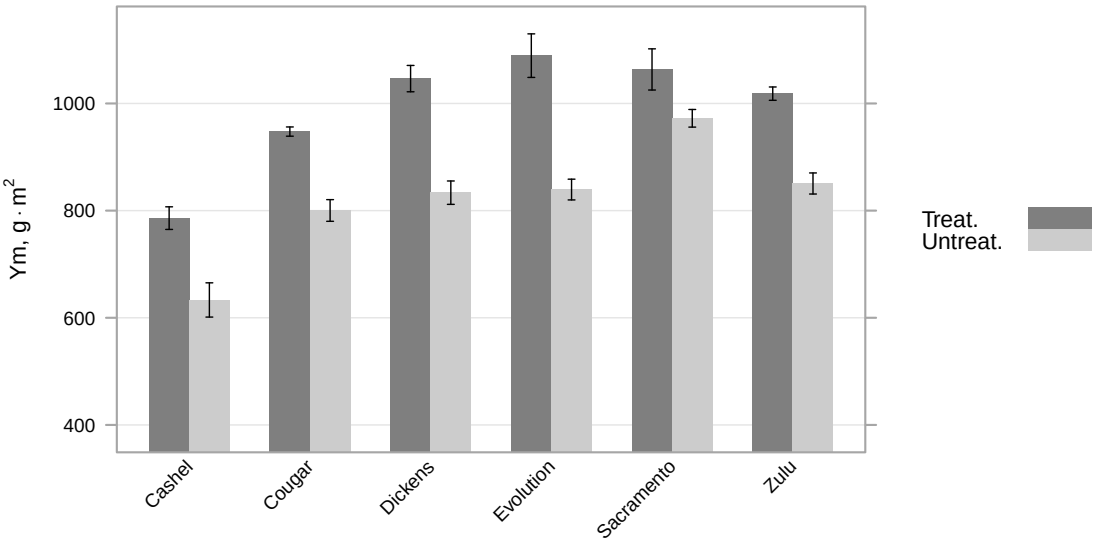


Figure 6.5: Average grain yield ($g \cdot m^{-2}$) per treatment along with the standard error of the mean. The grain yield was obtained by harvest-combining of the plot. The yield is given for each cultivar, the colours stand for the fungicide treatments.

6.3.3.2 Yield and grain number

The grain number per ear (GNe) exhibited strong variations between cultivars (P < 0.001) from 39 (Cashel) to 71 grains per ear (Sacramento) but it was not affected by the fungicide treatment (F and G×F non-significant). A trade-off between GNe and ear density (ENeq) amongst cultivars was evident with a highly negative correlation (r = -0.84***), a lower ear density was therefore associated with more grains per ear (GNe). Lastly, more grains per ear led to higher ear grain yield (Fig. 6.6a) and GNe was highly correlated with Ye (r = 0.90***), with a significantly negative offset in the absence of fungicide.

Table 6.5: Analysis of variance and correlation of different grain sink traits. Response of equivalent ear per m^2 (ENeq), grain number per ear (GNe), grain number per m^2 (GNm), individual grain weight (TGW), grain yield per ear (Ye), grain yield per m^{-2} (Ym) and harvest index (HI) to the effects of the cultivar (G) and the fungicide (F) including two-way interaction (G×F) were analysed. Significance of the effects is reported following the standard star code (*, **, ***), for significance, plus "$^{\cdot}$" when P < 0.1 and "^{ns}" when non significant. Non significant effects were removed. The symbol $ is used when the results come from individual ANOVA for observations either in treated or either untreated plots; the symbol § represents ANOVA results based on average observation between treated and untreated plots (applied because fungicide effect not significant). The number of observations *n* is given, exclamation mark "!" stands for the removal of aberrant value. The G and G×F estimations are compared based on Tukey HSD post-hoc test, significance of effect comparison is reported by compact letter display. In the absence of significant G×F interaction, the simple effect of "untreated" treatment is estimated in comparison to the "treated" effect. The Pearson's correlation coefficients between responses are reported at the bottom of the table.

	Ym $g \cdot m^{-2}$	GNm grains $\cdot m^{-2}$	HI	Ye $g \cdot ear^{-1}$	ENeq ears $\cdot m^{-2}$	GNe grains $\cdot ear^{-2}$	TGW g
F	***	ns,$	***	***	ns	ns	***
G	***	***,§	***	***	***	***	**
F×G	.	ns,§	**	ns	ns	ns	***
n	48	24	48	48	48	48	47!
Treated							
Cashel	816 b	19,500 a	0.454 b	1.70 a	500 b	39.1 a	46.2 ef
Cougar	948 cde	21,600 ab	0.514 e	2.64 bc	371 a	58.9 c	43.7 e
Dickens	1046 ef	23,200 bc	0.511 de	2.95 cd	348 a	67.0 d	44.2 e
Evolution	1089 f	23,100 bc	0.527 e	2.34 b	466 b	49.8 b	48.5 f
Sacramento	1064 ef	24,800 c	0.503 cde	3.18 d	348 a	71.5 d	42.8 de
Zulu	1018 ef	23,100 bc	0.511 de	2.63 b	393 a	58.9 c	43.9 a
Untreated				-0.48			
Cashel	633 a	-	0.400 a	-	-	-	32.1 a
Cougar	800 b	-	0.472 bc	-	-	-	37.3 bc
Dickens	833 bc	-	0.475 bcd	-	-	-	36.8 bc
Evolution	839 bc	-	0.450 b	-	-	-	35.4 ab
Sacramento	972 def	-	0.495 cde	-	-	-	39.5 cd
Zulu	851 bcd	-	0.483 bcde	-	-	-	37.0 bc

Table 6.6: Grain sink traits observations, averaged per cultivar and fungicide treatment combinations (four blocks).

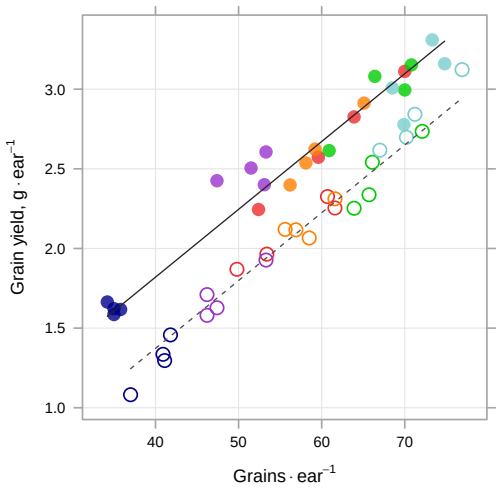
F	G	Ym $g \cdot m^{-2}$	GNm grains $\cdot m^{-2}$	HI	Ye $g \cdot ear^{-1}$	ENeq ears $\cdot m^{-2}$	GNe grains $\cdot ear^{-1}$	TGW g
Treat.	Cashel	816	17,597	0.460	1.62	503	35.0	46.4
	Cougar	948	21,705	0.514	2.69	358	61.5	43.7
	Dickens	1046	23,741	0.511	2.96	356	67.0	44.2
	Evolution	1089	22,484	0.517	2.48	439	51.3	48.5
	Sacramento	1064	24,984	0.503	3.06	350	71.6	42.8
	Zulu	1018	23,226	0.511	2.62	391	59.6	43.9
	All	997	22,290	0.503	2.57	399	57.7	44.9
Untreat.	Cashel	633	19,875	0.400	1.29	498	40.2	32.1
	Cougar	800	21,465	0.481	2.10	384	56.4	37.3
	Dickens	833	22,685	0.475	2.47	340	67.0	36.8
	Evolution	839	23,705	0.450	1.71	494	48.3	35.4
	Sacramento	972	24,623	0.495	2.82	346	71.3	39.5
	Zulu	851	22,972	0.483	2.15	395	58.1	37.0
	All	822	22,554	0.464	2.09	409	56.9	36.4

The crop grain number per unit area (GNm) was mainly associated with GNe variation amongst cultivars. Indeed, GNm was not correlated with ENeq but it was positively correlated with GNe. As a consequence, the cultivar rank of GNe and GNm was similar, but the GNe×ENeq trade-off tended to reduce the differences in grain number between cultivars that was observed at the shoot scale (GNe) compared to the crop scale (GNm). Lastly GNm was correlated with Ym, but with a lower coefficient ($r = 0.64^{***}$) than for the GNe versus Ye correlation.

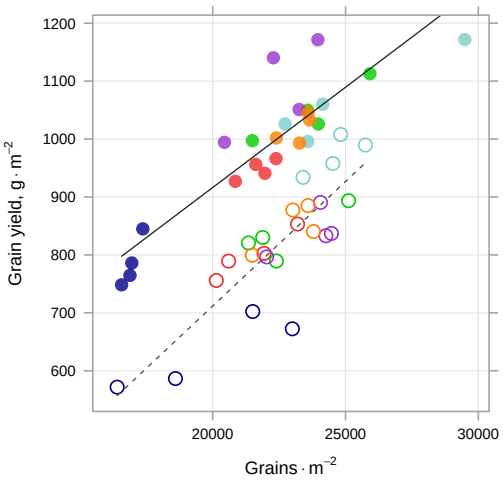
6.3.3.3 Grain weight

In treated plots TGW variation depended closely on cultivar ($P < 0.01$), with Evolution (48.5 g) being significantly heavier than Cougar, Dickens, Sacramento and Zulu (43.6 g). Untreated plots showed a significantly reduced TGW and the decrease ranged from -7.6% (Sacramento) to -30.5% (Evolution) ($P < 0.001$). The grain number at the crop (GNm) and at the ear level (GNe), correlated significantly with TGW (Fig. 6.6c). However, opposite relationships were observed with and without fungicide. In treated plots the correlations were as expected negative ($r = -0.53$ and -0.52 from GNe and GNm, respectively), whereas they were positive in unprotected plots ($r = 0.81$ and 0.27 from GNe and GNm, respectively). Finally, in treated plots TGW was not correlated with yield, either Ye or Ym. By contrast, in unprotected plots, TGW was positively correlated with yield at both the ear or the crop level ($r = 0.88$ and 0.74 to Ye and Ym respectively).

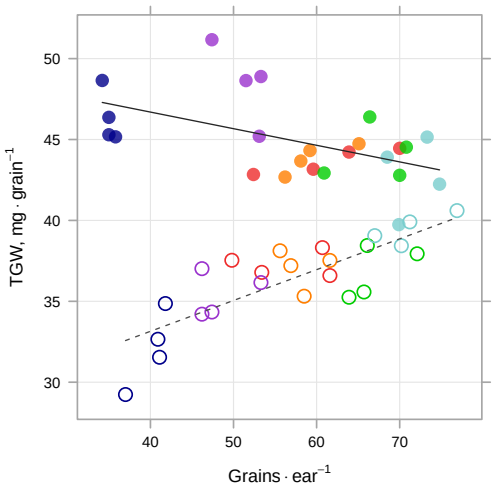
The cultivar choice generated a large range of yields in treated plots, with a 25% variation between the extreme yields of Cashel ($819\,g \cdot m^{-2}$) and Evolution ($1089\,g \cdot m^{-2}$). Furthermore, cultivars also showed different associations of yield components, which may affect their response to treatments. For example, a 12% variation in TGW of treated plots between Zulu and Evolution related to the same GNm and an overall 21% variation in GNm between Cashel and Sacramento, resulted from many small ears and fewer big ears, respectively. Interestingly, the cultivars showed different ways to reach either similar GNm or similar TGW. Finally, fungicide treatments only decreased TGW according to the susceptibility grade of each cultivar to STB, TGW loss ranging from 8% (Sacramento) to 31% (Evolution). Together with the variation in source availability, this experiment succeeded in generating a large variability in source-sink traits potentially important for tolerance of STB.



(a) Ye and GNe



(b) Ym and GNm



(c) TGW and GNe

Figure 6.6: Linear relationship between grain yield and grain number, per ear or per square metre. The colours represent the cultivars (dark blue, Cashel; red, Cougar; green, Dickens; purple, Evolution; light blue, Sacramento; orange, Zulu). The open/closed symbols stand for treated and untreated plots. Linear regression was fit in treated and untreated plots by ordinary least square means.
a) Ye and GNe: relationship at ear level, treated (plain line) $y = 0.117(\pm0.083)+0.043(\pm0.001)GNe$; untreated (dotted line) $y = 0.117(\pm0.083) - 0.447(\pm0.033) + 0.043(\pm0.001)GNe$ ($R^2 = 0.98$).
b) Ym and GNm: relationship at the square metre level, treated (plain line) $y = 244(\pm85) + 0.034(\pm0.004)x$ ($R^2 = 0.78$); untreated (dotted line) $y = -148(\pm13) + 0.043(\pm0.006)x$ ($R^2 = 0.72$).
c) TGW and GNe: relationship at single grain level, treated (plain line) $y = 50.8(\pm2.12) - 0.103(\pm0.036)x$ ($R^2 = 0.27$); untreated (dotted line) $y = 25.5(\pm1.71) + 0.191(\pm0.030)x$ ($R^2 = 0.65$).

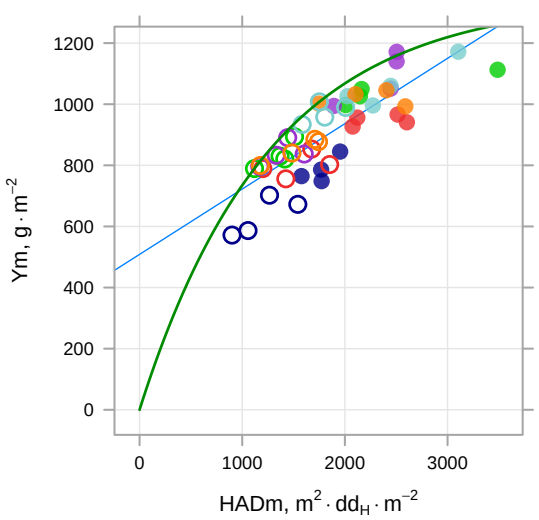
6.3.4 Source-sink relationship, HAD and yield

As yield finally results from source and sink relationships, the ratio of the source trait (LAe) to the sink trait (GNe) was chosen to better understand the yield variation. This ratio, (leaf lamina area per grain, LAg), contrasted amongst cultivars ($P < 0.001$) ranging from 1.18 (Sacramento) to 1.58 cm^2 per grain (Cougar, Cashel). By contrast, no significant difference of the healthy area per grain (HADg) was shown amongst cultivars. The HADg was on average 10.2 $dm^2 \cdot °Cd_H$ per grain in treated plots while a similar reduction averaging -36% was found in untreated plots, furthermore, equivalent reductions were observed for the HADm (tested and estimated on log-transformed values). As the cultivars were characterised by differences in the leaf profile composition (fractional contribution of each leaf layer to the cumulated canopy leaf lamina area), significant differences in HADg were therefore observed for the flag leaf; in untreated plots, the cultivars Cougar and Sacramento were characterised by significantly higher HADg for the flag leaf than Dickens, Cashel and Evolution.

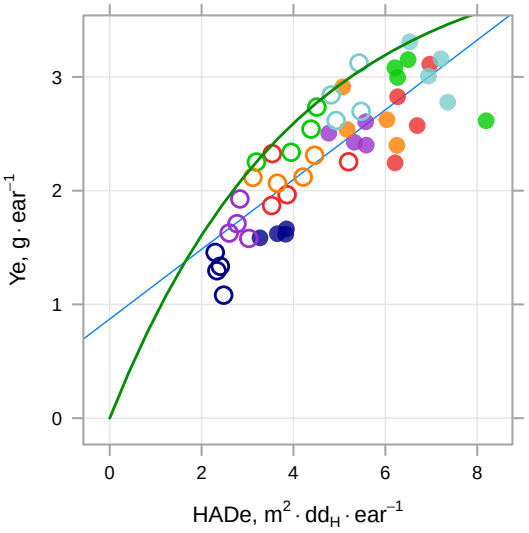
The source and sink relationships were also analysed through the correlations between source and sink traits at the different scales (crop, shoot and grain). Positive linear correlations were observed between HADm and Ym ($r = 0.82^{***}$, Fig. 6.7a), Ye to HADe ($r = 0.84$, Fig. 6.7b), and HADg and TGW ($r = 0.79$, Fig. 6.7c). In the last case only, however, the correlation was not significant when treated or untreated plots were analysed separately. Previously in the literature a saturating pattern has been proposed for the relationship from HADm to Ym which could be described by a boundary curve the experimental points could not exceed. Such a curve can be obtained by quantile regression: the curve above 95% of the observations (Gouache et al., 2014). The resulting fitting of this boundary curve was also reported in Figure 6.7. It should be noted, however, that the saturation is less obvious at the shoot scale than at grain or crop scale. Indeed, the coefficient of variation for HAD was close at the different scales (26% to 33%), whereas the resulting coefficient of variation for TGW was 12% only, close to that of Ym (15%), but much lower than that of Ye (25%). This scale effect will be discussed below.

Table 6.7: Pearson's correlation coefficient between source and with sink traits estimated on the treated and untreated plots (n = 48).

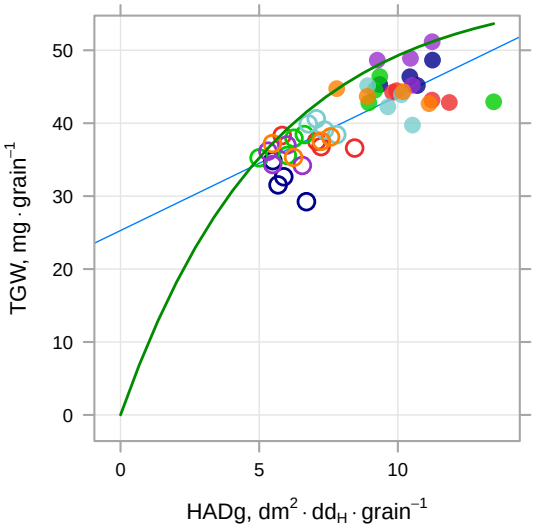
	I $°Cd_H$	D $°Cd$	HADe $m^2 \cdot °Cd$	HADm $m^2 \cdot °Cd$	HADg $dm^2 \cdot °Cd$	LAe cm^2	LAg cm^2	fLA 1
ENeq	-0.38^{**}	0.12^{ns}	-0.53^{***}	-0.08^{ns}	0.00^{ns}	-0.59^{***}	0.75^{***}	-0.40^{**}
GNe	0.45^{**}	-0.09^{ns}	0.65^{***}	0.27^{ns}	0.00^{ns}	0.75^{***}	-0.80^{***}	0.53^{***}
TGW	0.79^{***}	-0.52^{***}	0.61^{***}	0.62^{***}	0.79^{***}	-0.02^{ns}	-0.14^{ns}	0.06^{ns}
Ye	0.74^{***}	-0.33^{*}	0.84^{***}	0.51^{***}	0.35^{*}	0.63^{***}	-0.75^{***}	0.47^{***}
Ym	0.83^{***}	-0.34^{*}	0.83^{***}	0.82^{***}	0.63^{***}	0.45^{**}	-0.41^{**}	0.34^{*}



(a) Ym regarding HADm



(b) Ye regarding HADe



(c) TGW regarding HADg

Figure 6.7: Source/sink relation at square metre, shoot and grain scale. The colours represent the cultivars (dark blue, Cashel; red, Cougar; green, Dickens; purple, Evolution; light blue, Sacramento; orange, Zulu). The open/closed symbols represent the fungicide treatment (untreated/treated). Blue line is the ordinary least square regression line. The green curves are potential curves fitted for the current dataset (non-linear quantile regression, τ = 0.95, P or R^2 non-applicable).
a) Ym versus HADm: potential curve, $y = 1345(1 - exp(-1.06x/1345))$; regression line, $y = 508(\pm 42) + 0.214(\pm 0.022)x$ (R^2 = 0.68).
b) Ye versus HADe: potential curve, $y = 4.14(1 - exp(-1.02x/4.14))$; regression line, $y = 0.88(\pm 0.16) + 0.30(\pm 0.03)HADm$ (R^2 = 0.67).
c) TGW versus HADg: potential curve, $y = 51(1 - exp(-10.8x/51))$; regression line, $y = 25.3(\pm 1.8) + 1.84(\pm 0.21)x$ (R^2 = 0.62).

6.3.5 Tolerance

6.3.5.1 Cultivar tolerance estimation

Tolerance is defined by the ratio of grain yield to HAD differences between treated and untreated plots. It is usually estimated at the crop level (ΔHADm/ΔYm ratio), but can also be assessed at the grain level (ΔHADg/ΔTGWg ratio; cf section "Data analysis", see 6.2.3.2, p. 172). Different methods were applied to estimate the (in-) tolerance of cultivars to ensure the consistency of cultivar tolerance rankings.

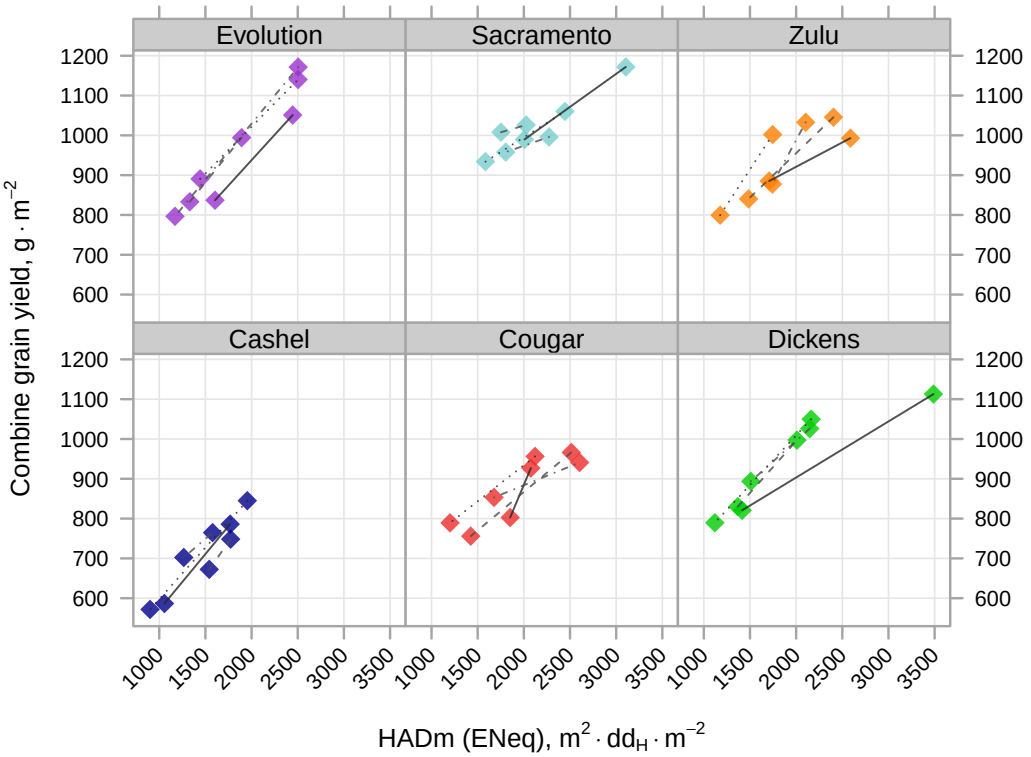


Figure 6.8: Grain yield per m^2 regarding the HADm (HAD per m^2), per cultivar and per block. The colours represent the cultivars (dark blue, Cashel; red, Cougar; green, Dickens; purple, Evolution; light blue, Sacramento; orange, Zulu). The different line types represent individual block comparison.

The usual method compared the ratios obtained in each block (method 1); the log transformation was required to run the ANOVA for tolerance and intolerance estimated at the m^2 scale (respectively Tm1 and inTm1). As intolerance is the inverse of tolerance, the statistics on the log transformed values of tolerance and intolerance are strictly equivalent.

The cultivar effect was detected at the crop level (Tm1 and inTm1; P = 0.034; Tab. 6.8). However, given the random effect of the block, the post-hoc Tukey HSD test could not conclude on the significance of cultivar pairwise comparisons on Tm1. Conversely, Evolution was characterized as more intolerant than the average of cultivars (P = 0.005, t-test effect of the cultivar statistical contrast was $\sum_i g_i = 0$). Regarding the tolerance or intolerance

Table 6.8: Tolerance estimations Tm1, Tg1, Tm2, Tg2 and inTg3. Values are least square mean estimations, and within each columns genotype values are compared according to Tukey's HSD.

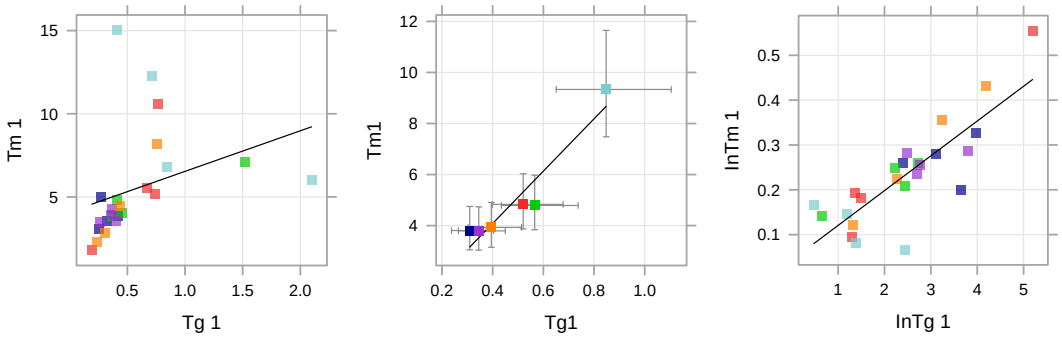
	Tm1	Tg1	Tm2	Tg2	inTg3
G	*	•	**	***	**
n	24	24	24	24	48
SE	0.22	0.26	0.15	0.10	-
Cashel	1.34 a	-1.17 a	1.29 a	0.32 a	2.94 b
Cougar	1.58 a	-0.65 a	1.66 ab	0.58 ab	1.39 ab
Dickens	1.57 a	-0.57 a	1.65 ab	0.59 ab	1.33 a
Evolution	1.33 a	-1.06 a	1.33 a	0.35 a	2.72 ab
Sacramento	2.23 a	-0.17 a	2.03 b	0.87 b	0.92 ab
Zulu	1.37 a	-0.93 a	1.37 ab	0.42 a	1.74 ab

at the grain level (Tg1 or inTg1) the cultivar effect was not significant.

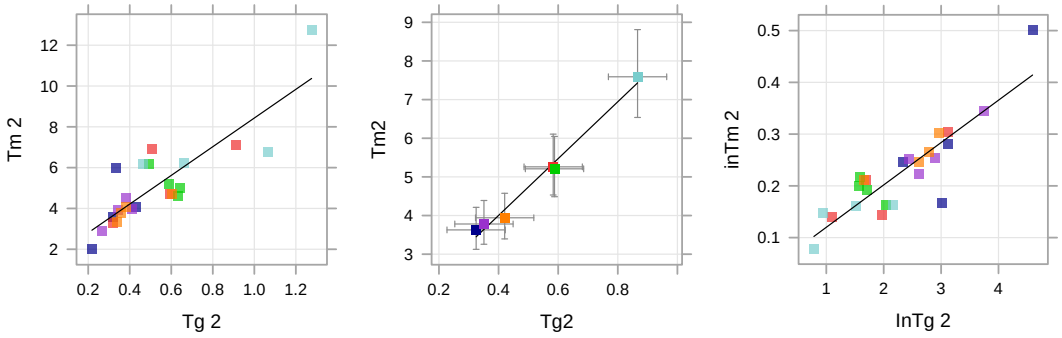
Alternatively, the four repetitions of control treated plots could be averaged (method 2). The variance homogeneity was improved using this method but log transformation was still required for crop tolerance or intolerance, therefore again, ANOVA was strictly equivalent between Tm2 and inTm2 (Tab. 6.8). Evolution and Cashel were found to be less tolerant than Sacramento, both at the crop level (Tm2, $P < 0.05$) and at grain level (Tg2, $P < 0.01$). Lastly the linear regression methods were used that pooled the four repetitions of a cultivar to obtain a single assessment of tolerance, that is the slope of grain yield to HAD. Slope comparisons then indicated no significant difference either at crop or at grain level could be found. Conversely, the intolerance slopes did not vary with cultivar at the crop level (Tm3, $P = 0.06$), but at grain level (Tg3) Sacramento exhibited a lower intolerance than Cashel and Dickens ($P < 0.001$; Tab. 6.8).

The different methods confirm tolerance contrasts between cultivars but only partially. The first method led to high variability in Sacramento where one of the treated plots was an outlier for Ym, and another for TGW, then Tm1 was not correlated with Tg1 ($r = 0.33$; $P > 0.05$; Fig. 6.9a). On the other hand, if the tolerance assessments obtained for each block were averaged, the resulting single tolerance values per cultivar were significantly correlated at crop and grain level ($P < 0.01$; Fig. 6.9b and Table 6.9). Lastly block assessments (and obviously cultivar means) of intolerance were also correlated ($r = 0.82$; $P < 0.001$; Fig. 6.9c, Table 6.9).

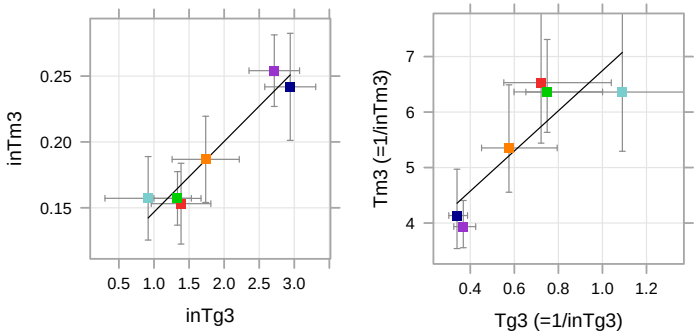
The third method based on the linear regression slopes gives rather different results which were linked to the reduced variability of yield compared to HAD. Consequently, the overal slopes were frequently lower than the average of block slopes (that can be seen on Fig. 6.8). Otherwise the outliers in Sacramento plots preclude Tm3 correlating with Tg3. Slopes are prone to uncertainty and therefore the ANOVA results must be treated cautiously as on the edge of normality and homoscedasticity hypotheses. Nonetheless, apart from Sacramento, the cultivars appeared similarly ranked in Figure 6.9g to that in Figures 6.9 a to f. The correlation of the ranks of cultivars regarding inTm3 (Spearman's rank correlation) was highest for the Tm1 ($\rho = -0.829$, $p = 0.058$), thus close



(a) Tolerance observations (b) Tolerance estimations (c) Intolerance observations



(d) Tolerance observations (e) Tolerance estimations (f) Intolerance observations



(g) Intolerance (h) Tolerance = 1/intolerance

Figure 6.9: Tolerance per m^2 (Tm) versus per grain (Tg), according various methods. The colours represent the cultivars (dark blue, Cashel; red, Cougar; green, Dickens; purple, Evolution; light blue, Sacramento; orange, Zulu). The y-axis represent observations at the m^2 scale and the x-axis represent observations at the grain scale. Method 1: (a) tolerance observations ($r = 0.33^{ns}$), (b) least square mean estimations of tolerance along with standard error bars ($r = 0.95^{**}$), (c) intolerance observations ($r = 0.82^{***}$). Method 2: (d) tolerance observations ($r = 0.85^{***}$), (e) least square mean estimations of tolerance along with standard error bars ($r = 0.99^{***}$), (f) intolerance observations ($r = 0.87^{***}$). Method 3: (g) intolerance was estimated by the regression between the grain yield and the HAD (crop or grain scale) and (h) tolerance was deduced from the inverse of the estimated slope and standard error interval.

to significance. For the grain intolerance estimated using this third method (inTg3), the ranks correlation was always significant, and the rank were the exact opposite of the grain tolerance (Tg1 and Tg2).

Table 6.9: Correlation matrix of tolerance estimations. Significance of the Pearson's correlation: |r| > 0.811, P < 0.05; |r| > 0.971, P < 0.01; |r| > 0.974, P < 0.001.

	Tm2	Tm1	Tg2	Tg1	inTm3	inTm2	inTm1	inTg3	inTg2	inTg1
inTg1	-0.943	-0.886	-1.000	-1.000	0.714	0.943	0.886	1.000	1.000	1.000
inTg2	-0.943	-0.886	-1.000	-1.000	0.714	0.943	0.886	1.000	1.000	
inTg3	-0.943	-0.886	-1.000	-1.000	0.714	0.943	0.886	1.000		
inTm1	-0.943	-1.000	-0.886	-0.886	0.829	0.943	1.000			
inTm2	-1.000	-0.943	-0.943	-0.943	0.771	1.000				
inTm3	-0.771	-0.829	-0.714	-0.714	1.000					
Tg1	0.943	0.886	1.000	1.000						
Tg2	0.943	0.886	1.000							
Tm1	0.943	1.000								
Tm2	1.000									

6.3.5.2 Tolerance and healthy crop traits

As tolerance assessments according to the first two methods (either at the crop level Tm1, Tm2; or at the grain level Tg1, Tg2) appeared closely related, a single value was obtained by normalizing the four preceding values, then averaging them. This averaged tolerance is hereafter called standard tolerance (Ts); genotypes could be ranked regarding the averaged tolerance Ts, from the least to the most tolerance: Cashel (Ts = -0.60), Evolution (Ts = -0.57), Zulu (Ts = -0.38), Dickens (Ts = 0.11), Cougar (Ts = 0.15), Sacramento (Ts = 1.29). Correlations were then calculated between a panel of cultivar traits observed in healthy plots and Ts as well as the four previous estimations of tolerance (Appendix 6.A.1, p.202). Figure 6.10 represents the association between the obtained correlation coefficients for traits with Ts (y-axis) and the correlation coefficients for traits with either Tm1 or Tg1 or Tm2 or Tg2 (x-axis). All points are close to the y=x line. Thus traits that modified any tolerance estimation also impacted the others. The trait correlation with Tg1, although still significantly related to the trait correlations with Ts, were more weakly associated than for the other estimates.

The crop STB tolerance Ts was positively correlated with senescence timings I, $I2$ and $I3$ in healthy plots (r = 0.65 to 0.68; P < 0.001, Table 6.10). A high correlation coefficient was also obtained from heading date that negatively correlated with the tolerance Ts (r = -0.67). The proportion of total leaf lamina area of the flag leaf (fLA1) was positively correlated with Ts (r = 0.65), while fLA3 was negatively correlated (r = -0.65). Although both senescence timings and leaf profile were highly correlated with heading date, the dry matter of lower internodes at anthesis and maturity (AMe and MMe), that correlated the best with heading date, was less tightly linked to Ts (r = 0.51; P < 0.05). The preceding traits were highly correlated not only with Ts, but also with the four toler-

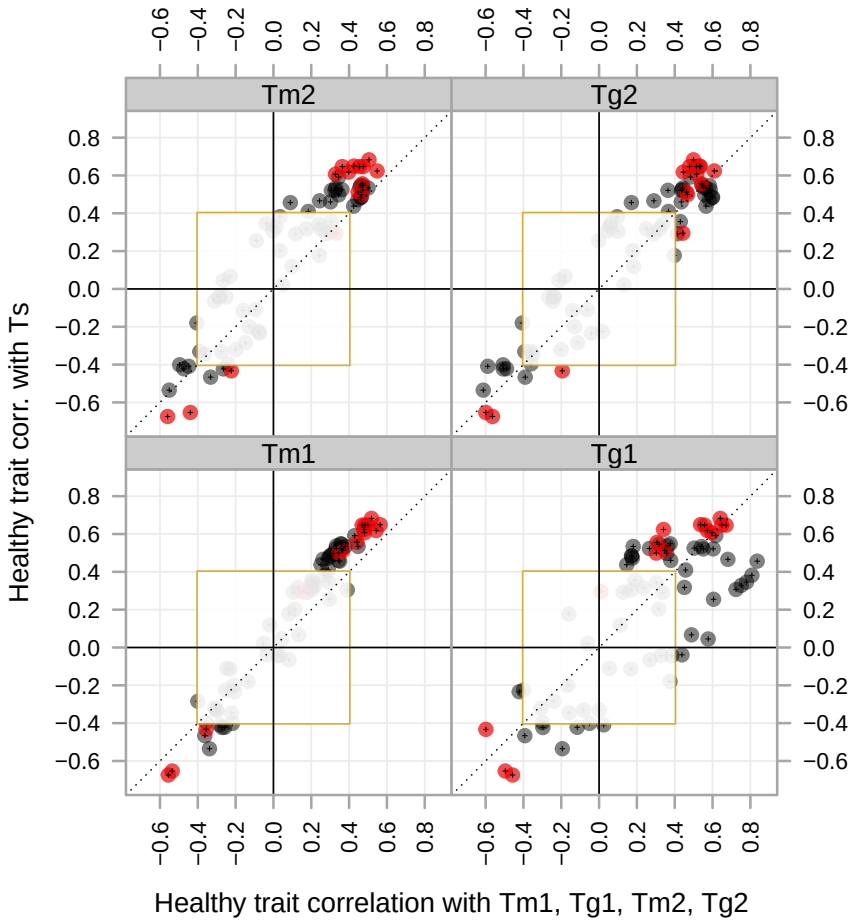


Figure 6.10: Correlation of healthy traits with average of normalized tolerance values (Ts) and with tolerance values (Tm1, Tg1, Tm2, Tg2). Each point is associated with a single healthy trait. The red dots correspond to variables cited in the paragraph "Tolerance and healthy crop traits". The yellow-delimited square represents the non-significance of the Pearson's correlation significance (for n = 24, $|r| > 0.404$ is associate with $P < 0.05$).

ance assessments. Above ground DM per shoot at anthesis (AMe) highly correlated with Ts ($r = 0.62$; $P < 0.001$), but not with Tg1. Another group of traits relative to flag leaf showed an especially high correlation with Tg1 that increased correlation with Ts; these traits were HADe1, LAe1 and DM of flag leaf at anthesis. Lastly many traits exhibited constant trends, but correlated with one or several tolerance assessments only. For instance TGW was always negatively correlated with tolerance, but significantly only with Tg1.

Multiple correlation was then tested to further explain tolerance. In Table 6.11 the best pairs and triplicates of traits are listed for each of the tolerance estimations considered. Numerous significant correlations were obtained, yet the retained traits varied between tolerances assayed, and for every tolerance for fits of close BIC (Bayesian Information Criterion). The low number of degrees of freedom gave too much weight to outliers, and

Table 6.10: Healthy trait correlations with tolerance estimations. The traits are: inflexion points of the senescence kinetics for the canopy (I), leaf 2 (I 2), leaf 3 (I3); the heading date, fractional contribution of leaf 1 (fLA 1) and leaf 3 (fLA 3) to the total leaf lamina area; total anthesis dry matter per ear-bearing shoot (AMe total), AMe of the lower internode (AMe lower internodes), the lamina of leaf 1 per ear-bearing shoot (AMe leaf 1), the ear (AMe ear); dry matter at maturity per ear-bearing shoot of the lower internodes (MMe lower internodes); HADe of the flag leaf, Leaf Lamina area of the flag leaf. Significance of the Pearson's correlation: $|r| > 0.404$, $P < 0.05$; $|r| > 0.515$, $P < 0.01$.

variable	Ts	Tm1	Tg1	Tm2	Tg2
I	0.65	0.47	0.65	0.45	0.48
I 2	0.68	0.52	0.64	0.51	0.50
I 3	0.65	0.48	0.56	0.47	0.53
LAe 1	0.61	0.48	0.60	0.33	0.52
fLA 1	0.65	0.56	0.54	0.43	0.53
fLA 3	-0.65	-0.54	-0.50.	-0.44	-0.60
HADe 1	0.65	0.50	0.67	0.36	0.52
Heading date (days)	-0.67	-0.56	-0.46	-0.56	-0.56
AMe lower internodes	0.50	0.35	0.30	0.47	0.47
AMe total	0.62	0.48	0.34	0.55	0.61
AMe leaf 1	0.62	0.54	0.57	0.40	0.45
AMe ear	0.56	0.44	0.31	0.47	0.54
TGW	-0.43	-0.36	-0.60	-0.22	-0.19
MMe lower internodes	0.51	0.37	0.35	0.45	0.46

consequently to variable combinations that by chance correlated with them. For instance although D did not correlate with Tm1, or D1 no D2, combinations D/D2 or D1/D2 were frequently retained. Conversely several traits that fitted tightly by simple correlation (e.g. heading date, fLA1 or fLA3) were not retained. Regarding Tg2, the DM of third leaf at maturity (MMe 3) combined very well to Ye and was systematically associated with tolerance estimations, despite MMe 3 clearly being of very low biological significance. Finally only Ts, that averaged casual variation of the four other tolerance assessments, led to results that were consistent with that obtained by simple correlation. The most retained trait was thus heading date, followed by traits representative of the previously characterized groups, i.e. flag leaf DM or stem DM at anthesis, and fLA1.

Table 6.11: Best multiple linear correlation combinations explaining the tolerance estimations. There were more than 40 000 combinations of two or three variables based on a pool of 62 explanatory variables. The models were ranked regarding the BIC (minimum BIC for the best combination). The explanotory variables: dry matter at anthesis or maturity per ear bearing shoot (AMe and MMe), also available per organ (b, lower internodes; s, stem; l1 to l3, leaf 1 to leaf 3; e, ear; c, chaff; g, grain); Net dry matter assimilation (NA) or Reserve Mobilisation (RM) per ear-bearing shoot, per grain or per m^2; inflexion point of the senescence kinetics for the canopy (I), leaf 2 (I.2), leaf 3 (I.3); the heading date, fractional contribution of leaf 1 (fLA 1) and leaf 3 (fLA 3) to the total leaf lamina area; grain yield per ear (Ye) or at the crop scale (Ym) or individual grain weight (TGW); grain number per ear or per m^2 (GNe and GNm).

Tolerance	Rank	model	BIC
Ts	1	Heading+AMe_s+HADg.1	44.84
Ts	2	HADe+MMe_c+LAI	45.03
Ts	3	fLA.1+AMe_e+MMe_c	45.31
Ts	4	LAg.3+AMe_l1+MMe_l3	45.46
Ts	5	Heading+MMe_b+LAe.2	45.80
Ts	6	HADe+LAI.3+MMe_c	45.83
Ts	7	fLA.1+RMe	46.05
Ts	8	Heading+AMe_l1+MMe_l3	46.12
Ts	9	Heading+AMe_s+LAg.1	46.12
Ts	10	Heading+LAe.1+RMg	46.15
Tm1	1	D+D.2+RMm	112.27
Tm1	2	RMe+D+D.2	114.33
Tm1	3	D+D.2+RMg	115.00
Tm1	4	AMe_b+D.2+D.1	115.67
Tm1	5	NAe+D.2+D.1	115.90
Tm1	6	fLA.1+AMe_l1+RMg	116.30
Tm1	7	fLA.1+RMe+D.2	116.31
Tm1	8	AMe_l1+LAe.2+RMg	116.64
Tm1	9	MMe_b+D.2+D.1	116.72
Tm1	10	AMe_l1+LAI.3+MMe_c	116.85
Tm2	1	GNe+D.2+MMe_l2	98.90
Tm2	2	I.2+ENeq+MMe_c	99.57
Tm2	3	GNe+D.2+MMe_l3	100.97
Tm2	4	Ye+D.2+MMe_l3	101.04
Tm2	5	I+ENeq+MMe_c	101.39
Tm2	6	Heading+AMe_s	101.94
Tm2	7	Heading+AMe_s+D.2	102.07
Tm2	8	Ye+D.2+MMe_l2	102.36
Tm2	9	NAe+D.2+D.1	102.64
Tm2	10	I.2+ENeq+MMe_l2	102.71
Tg1	1	I.1+HADm.1+LAI.1	-6.09
Tg1	2	TGW+HADm+LAe.3	-2.35
Tg1	3	HADm.1+Ym+HADg.1	1.61
Tg1	4	MMe_l1+MMe_l3+HADm.3	2.24
Tg1	5	LAe+TGW+HADm	2.77
Tg1	6	TGW+LAe.3+HADm.2	3.34
Tg1	7	MMe_s+MMe_l3+HADm	3.36
Tg1	8	TGW+LAe.2+HADm	3.76
Tg1	9	TGW+HADm.1+LAe.3	4.61
Tg1	10	GNe+Ye+HADm.1	4.90
Tg2	1	fLA.3+Ye+MMe_l3	-9.87
Tg2	2	Ye+MMe_l3+LAg.1	-8.76
Tg2	3	Ye+MMe_l3+HADg.1	-8.67

Continued on next page

Table 6.11: Best multiple linear correlation combinations explaining the tolerance estimations (next part).

Tolerance	Rank	model	BIC
Tg2	4	HADe.1+Ye+MMe_l3	-8.59
Tg2	5	Ye+LAe.1+MMe_l3	-8.28
Tg2	6	Ye+HADe+MMe_l3	-8.13
Tg2	7	Ye+D.2+MMe_l3	-7.69
Tg2	8	Ye+MMe_l3+HADg	-7.67
Tg2	9	Ye+HADe.2+MMe_l3	-7.48
Tg2	10	Ye+MMe_s+MMe_l3	-7.44

6.4 Discussion

The present field experiment aimed at confirming that traits observable in fungicide-protected plots could predict Septoria tritici blotch (STB) tolerance variation in a set of wheat cultivars. Thus, the ranges of the cultivars for phenology, source and sink traits and disease development were first considered and finally tolerance. Then tolerance traits were identified and compared to either the literature or other results of this thesis. Finally, after a methodological insight on the difficulties in assessing quantitatively tolerance with sufficient precision, the scales at which tolerance may be estimated — crop, ear or grain scales — were examined and discussed as a key point of the whole work.

6.4.1 Range of potential tolerance traits

- **Phenology**

As shown in Chapters 3 and 4, heading date is a key STB-tolerance trait through its impact on senescence time. This trait is easy to select and was not previously considered in the literature as a tolerance trait (Parker et al., 2004; Foulkes et al., 2006). Indeed, because genotypes varying in heading date actually experience varying epidemics (even when cultivated in a single experiment), experimental designs rather prevents this variation in phenology by the choice of relatively synchronous genotypes. In the 2015-16 field experiment, the cultivars were specifically chosen to contrast in heading date and showed a large range: 15 days or 200 °Cd between the extreme values. The same 200 °Cd range was observed between genotypes in the large French database (Chapter 3, p.53), while in the 2014-15 field experiment (Chapter 4, p.104) the maximum contrast between genotypes was 150 °Cd. In the 2015-16 experiment, however, the uneven distribution of cultivar heading dates was less favourable. The impact of heading date on STB tolerance relied on three groups of precocity, each differing from the others by 100 °Cd. Sacramento was early, Dickens was intermediate, while the four other cultivars Cashel, Cougar, Evolution and Zulu were very close for heading date. However, a trade-off might intervene between the grain yield and heading date in the absence of disease in some plant breeding

programmes if heading date is advanced significantly.

- **Grain source traits**

Cashel had a low Leaf Lamina Area per ear-bearing shoot (LAe, 59 cm^2 per shoot), while LAe was high in other cultivars (74 – 91 cm^2), larger than in the 2014-15 field experiment (63 – 85 cm^2) and in the French database (66 – 85 cm^2 for the three upper leaves). But the lower shoot number per m^2 in the UK led to Leaf Area Index (LAI) of 3.1 ± 0.5 $m^2 \cdot m^{-2}$, comparable to 2014-15 field experiment (2.6 ± 0.4 $m^2 \cdot m^{-2}$) but lower than in the French database (4.5 ± 0.5 $m^2 \cdot m^{-2}$). However, in the present experiment senescence timing was very long (I), between 665 and 881 °Cd_H for the canopy, although it was much shorter both in 2014-15 (577 to 683 °Cd_H) and in the database (525 to 613 °Cd_H, in this case over four upper leaves instead of three). Finally, the present 2015-16 field experiment was characterised by a high source availability for grain filling in healthy plots as shown by the mean HADm of 2300 ± 300 $m^2 \cdot °\,Cd \cdot m^{-2}$ versus. 1500 ± 200 $m^2 \cdot °\,Cd \cdot m^{-2}$ in 2014-15 field experiment, and 2400 ± 400 $m^2 \cdot °\,Cd \cdot m^{-2}$ in the database (for the three upper leaves). Flag-leaf LAI was 0.30 ± 0.03, less than in 2014-15 field experiment (0.35 ± 0.02) and in the database (0.32 ± 0.04).

- **Grain sink traits**

Associated with these source characteristics, the cultivars showed a large range in grain yield and yield components. The grain yield observed in 2015-16 was representative of the cultivar potentials: in fungicide treated plots Ym was 990 ± 110 $g \cdot m^{-2}$, and cultivar rankings were highly consistent with the UK cultivar Recommended List estimations (HGCA, 2015), and 20% higher than in the French database. This was linked to TGW that reached 45 ± 2 g in the 2015-16 experiment, versus 44 ± 3 g in 2014-15 and 37 ± 3 g in the database. Overall, comparable average values and variation in Grain Number per m^2 (GNm, around 20-22 thousand grains per m^2) was found amongst all the experiments and the database; but the UK genotypes and cultivars developed fewer (around 30% less ear per m^2) and larger ears (bearing around 50% more grains, GNe) than shown in the French database. Moreover, the reduced set of cultivars in 2015-16 experiment also combined different associations of yield components that may be of interest to identify tolerance traits. For example, high TGW was found in Cashel and Evolution, with, respectively, a low and a high GNm due to a 20% variation in Grain Number per ear-bearing shoot (GNe). In contrast, the other cultivars showed stable GNm and TGW but a 17% variation in GNe. Finally, if some characteristics of the cultivars seemed at first unevenly distributed, the diversity of combined traits may be of interest for the research of STB-tolerance traits.

- **Source to sink traits**

The HADg, a good indicator of source to sink ratio, was compared between healthy plots of the different experiments; an average value of 10.2 ± 0.4 $dm^2 \cdot ^\circ$ Cd per grain was found between cultivars in 2015-16, and showed limited variation between extreme values. Although TGW was in the same range, HADg was much lower in 2014-15 (7.1 ± 0.5 $dm^2 \cdot ^\circ$ Cd per grain in untrimmed ears). Conversely, HADg was higher in the French database (11.1 ± 1.6 $dm^2 \cdot ^\circ$ Cd per grain), despite TGW being much lower. Thus, although the relation between TGW and HADg was observed within each experiment, the source/sink ratio did not predict TGW between experiments. Besides, minor variations of grain source availability characterised the 2015-16 experiment (HADg), without any correlation with heading date variation.

- **Disease impacts on traits**

During the 2015-16 experiment, plants were exposed to a natural STB infection, which caused 36% mean losses both in HADm and HADg. Consistent with the STB epidemics damaging plant growth mainly after anthesis, grain number was unaffected by the disease and varied only with the cultivars. The STB was responsible for a 19 ± 9% TGW loss in untreated plots. Grain yield losses were in a medium range (170 ± 50 $g \cdot m^{-2}$), comparable between cultivars. But as the grain yield varied significantly amongst cultivars in treated plots, the relative yield losses represented 9 to 23% of the treated yield. In contrast, the French database recorded higher HADm losses that reached 44 ± 11% depending on the cultivar, and up to 18% losses in grain number (Bancal et al., 2015). Therefore, the HADg losses were less than HADm losses, at 38 ± 9%. The net result was that TGW decreased by 21 ± 6% leading to yield losses ranging from 15% to 44%.

To conclude, a sound choice of six cultivars based on key traits for tolerance succeeded in creating large ranges in some traits of interest, e.g. heading date, senescence timing and TGW, even if unevenly distributed. Conversely, relatively little variation in source/sink traits like HADg was generated in treated plots that moreover appeared much higher than observed during the 2014-15 experiment. Thus, the relation of tolerance to sink saturation level that was suggested from 2014-15 experiment could not be robustly explored using data from the 2015-16 experiment.

6.4.2 Insights on the estimation of tolerance

The tolerance could be estimated according to the equations in section 6.2.3.2, paragraph "Tolerance/intolerance"(p.172). The tolerance was estimated at the crop scale (ra-

tio of HADm reduction to Ym loss) and at the grain scale (ratio of HADg reduction to TGW loss).

- **Variability in quantitative assessments of tolerance**

As it is a ratio, the tolerance estimation was highly sensitive to a low denominator, i.e. to low range of yield or TGW losses — which occurs more often where tolerance is expressed. The calculation of intolerance ratios instead of tolerance was statistically helpful in the case of the 2015-16 experiment, but decreased the experiment sensitivity needed to characterize the genotypes. To ensure the reliability of the cultivar tolerance-ranking, three methods were used to calculate tolerance and their results were pairwise compared.

Despite the high positive correlation between TGW estimates in selected ears and in combine harvested grain, grain tolerance showed a large variability in cultivar Sacramento when considering blocks separately, so that Tg1 was not correlated with the crop tolerance Tm1. These same discrepancies were even increased when the slopes per cultivar were calculated, making the variations in Tg3 and Tm3 non-significant. Fortunately, no block effect was detected in treated plots of the 2015-16 experiment regarding yield or HAD, and thus variation in tolerance per cultivar could be attenuated by averaging block values of treated plots. So the values of Tm2 and Tg2 per repetition were largely stabilized and correlations of crop with grain tolerance strongly improved. Regardless of the calculation method used, tolerance grade was largely stabilized by averaging the repetitions per cultivar. However, the number of degrees of freedom was severely reduced: averaging was possible in Chapter 3, using a 60 genotype × site database, but not in the 2015-16 experiment with only 6 genotypes. This study nevertheless pointed out the difficulty in accurately quantifying tolerance, particularly in the conditions when tolerance occurs. Furthermore, a specific statistical study should be to estimate the precision needed on yield and HAD losses to capture the effect of small gains in tolerance. Conversely tolerance assessments can be combined over site-seasons as was done in Chapter 4, where a mean tolerance grade per genotype was calculated from different trials.

- **Close correlation between crop and grain tolerances**

Consistently with the results of the field experiment 2014-15 (Chapter 4, p.104), crop (i.e. per m^2) and grain tolerance were positively correlated, which may help in the investigation of the relevant source/sink balance studies. The 2015-16 experiment strengthened the relation of crop tolerance to grain tolerance in two ways. First, despite the problems encountered in quantitative estimations, significant correlations between crop and grain tolerances were always observed. Second and more interestingly, whichever the way tolerance was calculated, the traits correlated with tolerance were the same at crop and grain

scales further highlighting that the main key processes may be involved in both cases. Thus grain tolerance was shown as an alternative to crop tolerance for genotype or cultivar evaluation. On the other hand, the varying calculations failed statistical significance for different data, and therefore they were usefully averaged. The resulting Ts appeared less sensitive to casual data variation. Thus, after Chapter 4 had underlined the usefulness of aggregating tolerance estimates across experiments, the present chapter suggests the usefulness of combining various tolerance assessments within a trial.

6.4.3 Main results on tolerance and tolerance traits

The STB-tolerance contrast between the cultivars was generally low, but Sacramento appeared more tolerant than the other cultivars, especially in comparison to Cashel or Evolution which were the least tolerant cultivars. For the comparison, Zulu yield loss was 1.8 fold greater than Sacramento, while the HADm reduction was similar. The various cultivars also exhibited various STB-sensitivity, as deduced from HADm losses. Thus, although Cougar was included in the experiment as a resistant cultivar (HGCA, 2015), Sacramento was actually the most resistant amongst the cultivars. Zulu showed the second lowest HADm loss and Cougar ranked only third! Sacramento was released for the French market, where it was not expected to be particularly resistant (RAGT, 2016). Its resistance might therefore come from a low compatibility with UK STB-strains. Conversely, Cougar was recently removed from the HGCA recommended list (cropping season 2015-16, AHDB, 2016b), which suggests a drop in its resistance.

The Tolerance of STB was generally lower in cultivars that showed a late heading date. The tolerant cultivars Sacramento and, to a lesser extent, Cougar were associated with the earliest heading stage of the cultivar panel. The precocity for heading stage could therefore be a tolerance trait, beyond its well-known effect on STB-sensitivity (Murray et al., 1990; Shaw and Royle, 1993; AHDB, 2016a). Heading date was also negatively correlated with the senescence timing of the canopy, leaf 2 and leaf 3, confirming partially the findings of the Chapter 3 (p.53), that late senescence timing was correlated with early heading date. Based on the estimations of the six cultivars in 2015-16 experiment, tolerance was also higher in the cultivars that showed late senescence in healthy plots (i.e. Sacramento). Senescence timing actually applies to either canopy or any leaf layer, as senescence was correlated between leaf layers (e.g. leaf 1 senescence timing was highly correlated with leaf 3 senescence). The effect of heading date on tolerance could result from its correlation with senescence timing: early heading date would delay senescence and therefore increase the assimilate availability during the grain filling. This hypothesis was not confirmed by multiple correlation, where heading date appeared a better tolerance predictor than senescence timing. But as previously indicated multiple correlation should be cautiously regarded for 2015-16 experiment data, and additional assays are needed to

conclude on this hypothesis with confidence.

The canopy LAI was not correlated with tolerance which confirms the insight in Bancal et al. (2015): to promote tolerance, source availability might be increased, but rather by delaying the senescence than extending the leaf lamina area which could have a detrimental effect on STB epidemics. Conversely LAe and HADe moderately correlated with tolerance, as a secondary effect of their links to LAe 1 and HADe 1. The relative contribution of the flag-leaf layer to the LAI indeed appeared an interesting trait to increase tolerance. The cultivars Sacramento and Cashel had both contrasting tolerance and flag-leaf traits. The area distribution between the three studied leaf layers was variable and the tolerance positively correlated with higher proportion of the flag leaf (fLA 1). The two tolerant genotypes (Sacramento and Cougar) were characterised by the largest proportion fLA 1, while the less tolerant were associated with low fLA 1. Conversely, in the 2015-16 experiment tolerance correlated with low fractional leaf 3 (fLA 3). The opposite was observed in 2014-15 experiment Chapter 4, p.104), where fLA 3 was associated with tolerance and not fLA 1. However, the 2014-15 experiment was based on very low level of STB disease epidemic unlike the 2015-16 experiment, which could result in different disease distribution within the canopy layers. Interestingly, the fLA 1 was found to be negatively correlated with heading stage date in the French database. A complementary assessment of the light extinction coefficient would have been interesting to measure the association between the light interception and the fLA 1. Indeed, a higher contribution of the upper leaves could reduce the effect of disease epidemics which are expected more severe on the lower leaves (Bingham et al., 2009). A higher fLA 1 would increase the light interception by the upper leaf layer.

A higher remobilisation of dry matter from anthesis to maturity could buffer green leaf area reduction by the STB symptoms. However during 2015-16 experiment, variation amongst cultivars in vegetative DM mobilisation was not significant at the crop scale, and did not correlate with tolerance. This was consistent with Foulkes et al. (2006) who could not link higher stem carbohydrate remobilisation to STB-tolerance comparing a pair of near-isogenic lines with contrasting remobilisation (NILs: cv. Weston versus cv. Chaucer; two sites). Nevertheless, during the 2015-16 experiment, plants in the treated plots remobilized an average of 24% of their DM at anthesis, thus confirming the conclusion of Shearman et al. (2005) that modern UK cultivars are associated with high remobilisation of carbohydrate. However, average mobilisation, despite being significantly enhanced, was 28% only in untreated plots. According to one of the conclusions of the Chapter 4 and consistent with the findings of Shearman et al. (2005), the grain growth of UK-grown crops may be considered to be co-limited in optimal conditions as in the 2015-16 experiment, that could have limited the extent of remobilisation increase in untreated crops. In this study, the heading date range was the main rationale for cultivar selection while the

carbohydrate remobilisation was not the primary target. In order to address the relationship between tolerance of STB and carbohydrate remobilisation, the genotypes/cultivars should rather be chosen for their suspected wider range of carbohydrate remobilisation patterns.

In the 2015-16 experiment, the intolerant cultivar Evolution was associated with the heaviest grains in healthy conditions. Moreover TGW negatively correlated with every tolerance assessment, but this trend was significant only for Tg1 (probably due to outlier artefacts). Bancal et al. (2015) already indicated TGW as being negatively linked to tolerance. However, TGW influence mostly appeared in multiple correlations that were not consistent with the simple trait correlations in the 2015-16 data. Moreover, the data base reported by Bancal et al. (2015) included a N fertilisation effect. When restricting to assays receiving a standard N fertilisation, they no longer observed any TGW effect on tolerance. The 2015-16 experiment relies on genotypes expressing a limited range of grain weight and may not be well suited to address this hypotheses. If TGW modulates the tolerance, its best levels could have been missed in 2015-16 experiment which involved grains 20% heavier than in the French database.

Lastly, tolerance of wheat to STB was not correlated with the combine yield consistently with Chapter 4 (Field experiment 2014-15) or the recent study of (Castro and Simón, 2016). Therefore, encouragingly breeding for tolerance and high yield might be possible.

6.5 Conclusion

This study highlighted and confirmed that traits observable in fungicide-protected crops can predict STB-tolerance variations of cultivars. A large range of variation was produced for traits of interest. The results were generally consistent with the literature and the previous chapters, and confirmed the heading stage date precocity, the increased grain source availability, and the higher proportion of flag leaf as STB-tolerance traits. Finally, the estimation of tolerance and the research for tolerant traits can be improved if the results of multiple experiments are combined and, as shown in the present experiment, if several methods of estimations of the wheat STB-tolerance are combined.

References

AHDB. *Wheat disease maagement guide*. AHDB, 2016a. URL https://cereals.ahdb.org.uk/media/176167/g63-wheat-disease-management-guide-february-2016.pdf.

AHDB. Ahdb Recommended List - winter wheat 2016/17. tables, 2016b. URL https://cereals.ahdb.org.uk/media/883980/1-RLDL_2016-17_Winter_Wheat_RL-V6.pdf.

P. Bancal, M.-O. Bancal, F. Collin, and D. Gouache. Identifying traits leading to tolerance of wheat to Septoria tritici blotch. *Field Crops Research*, 180:176–185, 2015. doi: 10.1016/j.fcr.2015.05.006 .

D. Bates, M. Mächler, B. Bolker, and S. Walker. Fitting linear mixed-effects models using lme4. *Journal of Statistical Software*, 67(1):1–48, 2015. doi: 10.18637/jss.v067.i01 .

I. J. Bingham, D. R. Walters, M. J. Foulkes, and N. D. Paveley. Crop traits and tolerance of wheat and barley to foliar disease. *Annals of Applied Biology*, 154:159–173, 2009. doi: 10.1111/j.1744-7348.2008.00291.x .

A. C. Castro and M. R. Simón. Effect of tolerance to Septoria tritici blotch on grain yield, yield components and grain quality in Argentinean wheat cultivars. *Crop Protection*, 90: 66–76, 2016. ISSN 0261-2194. doi: 10.1016/j.cropro.2016.08.015 .

J. Conway, D. Eddelbuettel, T. Nishiyama, S. K. Prayaga, and N. Tiffin. *RPostgreSQL: R interface to the PostgreSQL database system*, 2016. URL https://CRAN.R-project.org/package=RPostgreSQL. R package version 0.4-1.

M. J. Crawley. *The R Book, 2nd Edition*, chapter Mixed-Effects Models, pages 681–714. Wiley, 2012. ISBN 978-0-470-97392-9.

M. J. Foulkes, N. D. Paveley, A. Worland, S. J. Welham, J. Thomas, and J. W. Snape. Major genetic changes in wheat with potential to affect disease tolerance. *Phytopathology*, 96:680–688, 2006. URL http://apsjournals.apsnet.org/doi/pdf/10.1094/PHYTO-96-0680.

D. Gouache, M. Bancal, B. de Solan, and P. Gate. Tolérance du blé tendre aux stress biotiques et abiotiques. *Innovations Agronomiques*, 35:75–87, 2014. URL https://hal.archives-ouvertes.fr/hal-01192469.

HGCA. HGCA recommended list - winter wheat 2015/16. tables, 2015. URL https://cereals.ahdb.org.uk/media/537620/winter-wheat-2015-16.pdf. Accessed 2017-07-04.

R. V. Lenth. Least-squares means: The R package lsmeans. *Journal of Statistical Software*, 69(1):1–33, 2016. doi: 10.18637/jss.v069.i01 .

D. J. Lovell, S. R. Parker, T. Hunter, D. J. Royle, and R. R. Coker. Influence of crop growth and structure on the risk of epidemics by Mycosphaerella graminicola (Septoria tritici) in winter wheat. *Plant Pathology*, 46(1):126–138, Feb 1997. ISSN 0032-0862. doi: 10.1046/j.1365-3059.1997.d01-206.x .

G. M. Murray, R. H. Martin, and B. R. Cullis. Relationship of the severity of Septoria tritici blotch of wheat to sowing time, rainfall at heading and average susceptibility of wheat cultivars in the area. *Australian journal of agricultural research*, 41(2):307–315, 1990. doi: 10.1071/AR9900307 .

S. R. Parker, S. Welham, N. Paveley, J. M. Foulkes, and R. K. Scott. Tolerance of Septoria leaf blotch in winter wheat. *Plant Pathology*, 53(1):1–10, 2004. doi: 10.1111/j.1365-3059.2004.00951.x .

R. Piessens, E. de Doncker-Kapenga, C. Uberhuber, and D. Kahaner. *Quadpack: a Subroutine Package for Automatic Integration*, springer verlag edition, 1983. ISBN: 978-3540125531.

R Core Team. *R: A Language and Environment for Statistical Computing*. R Foundation for Statistical Computing, Vienna, Austria, 2016. URL https://www.R-project.org/.

R Special Interest Group on Databases. *DBI: R Database Interface*, 2014. URL https://CRAN.R-project.org/package=DBI. R package version 0.3.1.

RAGT. Blé tendre d'hiver. Leaflet, 2016. URL http://www.ragtsemences.com/rs/pdf_fr/bth. accessed 2017-07-04.

D. Sarkar. *Lattice: Multivariate Data Visualization with R*. Springer, New York, 2008. URL http://lmdvr.r-forge.r-project.org. ISBN 978-0-387-75968-5.

M. W. Shaw and D. J. Royle. Factors determining the severity of epidemics of Mycosphaerella graminicola (Septoria tritici) on winter wheat in the UK. *Plant Pathology*, 42(6):882–899, 1993. ISSN 1365-3059. doi: 10.1111/j.1365-3059.1993.tb02674.x .

V. J. Shearman, R. Sylvester-Bradley, R. K. Scott, and M. J. Foulkes. Physiological processes associated with wheat yield progress in the UK. *Crop Science*, 45(1):175–185, 2005. doi: 10.2135/cropsci2005.0175 .

J. C. Zadoks, T. T. Chang, and C. F. Konzak. A decimal code for the growth stages of cereals. *Weed Research*, 44:415–421, 1974. doi: 10.1111/j.1365-3180.1974.tb01084.x .

6.A Appendix

6.A.1 Healthy trait correlation with tolerance estimates

Table 6.12: Healthy trait correlations with tolerance estimations. The tolerance values Tm1, Tg1, Tm2, Tg2 were obtained according to the "Material and Methods" (section 6.2.3.2, p.172). The tolerance value Ts was the average of the normalised Tm1, Tg1, Tm2, Tg2. Correlations were calculated with the variables: LAe (Leaf Lamina Area per ear-bearing shoot), Inflexion point of the senescence kinetics (I), Duration of the rapid senescence phase (D), equivalent Ear Number per m^2 (ENeq), the Grain Number (GN, GN), the Thousand Grain Weight (TGW), the grain yield (Y), the above-ground dry matter at anthesis or Maturity (AM or MM), the dry matter remobilisation between anthesis and maturity (maturity - anthesis, RM), the net assimilation between anthesis and maturity (NA), heading date (Heading, in days), Leaf Area per grain (LAg), Leaf Area Index (LAI), fraction of total Leaf lamina area of each leaf layer (fLA), Healthy Area Duration (HAD). Numbers following the variables indicate the leaf layer when relevant. Letters right after the variable indicate the scale of the variable (per grain, g; per ear-bearing, e; shoot, per m^2, m). The letters separated from the variable name indicate the organ when relevant (lower internodes, b; stem, s; ear, e; chaff, c; grain, g). Significance of the Pearson's correlation: $|r| > 0.404$, $P < 0.05$; $|r| > 0.515$, $P < 0.01$.

variable	Ts	Tm1	Tg1	Tm2	Tg2
LAe 1	0.61	0.48	0.60	0.33	0.52
I 1	0.52	0.36	0.60	0.33	0.36
D 1	-0.11	-0.25	0.05	-0.09	-0.06
LAe 2	0.29	0.18	0.34	0.12	0.29
I 2	0.68	0.52	0.64	0.51	0.50
D 2	0.30	0.39	0.17	0.31	0.10
LAe 3	0.20	0.11	0.32	0.03	0.18

Continued on next page

Table 6.12: Healthy trait correlations with tolerance estimations. Significance of the Pearson's correlation: |r| > 0.404, P < 0.05; |r| > 0.515, P < 0.01.

variable	Ts	Tm1	Tg1	Tm2	Tg2
I 3	0.65	0.48	0.56	0.47	0.53
D 3	-0.33	-0.30	0.00	-0.39	-0.36
LAe	0.41	0.29	0.46	0.18	0.37
I	0.65	0.47	0.65	0.45	0.48
D	-0.33	-0.30	-0.08	-0.28	-0.39
ENeq	-0.41	-0.28	0.02	-0.45	-0.59
GNe	0.55	0.36	0.32	0.47	0.58
GNm	0.47	0.26	0.68	0.24	0.29
TGW	-0.43	-0.36	-0.60	-0.22	-0.19
Ye	0.48	0.30	0.17	0.46	0.60
Ym	0.32	0.13	0.45	0.17	0.25
AMe 1	0.62	0.54	0.57	0.40	0.45
AMe 2	0.46	0.34	0.38	0.30	0.43
AMe 3	0.50	0.32	0.36	0.35	0.56
AMe b	0.50	0.35	0.30	0.47	0.47
AMe s	0.53	0.45	0.18	0.50	0.57
AMe e	0.56	0.44	0.31	0.47	0.54
AMe	0.62	0.48	0.34	0.55	0.61
MM 1	0.53	0.36	0.50	0.36	0.44
MM 2	0.34	0.21	0.30	0.24	0.34
MM 3	0.32	0.20	0.23	0.25	0.32
MM b	0.51	0.37	0.35	0.45	0.46
MM s	0.54	0.33	0.36	0.46	0.55
MM e	0.47	0.29	0.18	0.45	0.58
MM g	0.48	0.30	0.17	0.46	0.60
MM c	0.36	0.20	0.19	0.30	0.43
MM	0.52	0.33	0.27	0.47	0.59
MM veg	0.55	0.36	0.38	0.46	0.54
HI	0.18	0.08	-0.16	0.24	0.40
RMe l1	-0.28	-0.40	-0.24	-0.15	-0.11
RMe l2	-0.40	-0.36	-0.30	-0.24	-0.36
RMe l3	-0.42	-0.27	-0.30	-0.26	-0.51
RMe b	-0.35	-0.22	-0.16	-0.37	-0.35
RMe s	-0.11	-0.23	0.17	-0.16	-0.14
NAe e	0.44	0.25	0.15	0.42	0.57
NAe	0.29	0.11	0.13	0.28	0.41
Heading	-0.67	-0.56	-0.46	-0.56	-0.56
RMg	0.02	-0.05	-0.06	0.05	0.13
NAg	-0.23	-0.25	-0.40	-0.08	0.02
RMm	-0.23	-0.21	-0.42	-0.07	-0.04
NAm	0.12	-0.02	0.11	0.10	0.18
RMe	-0.47	-0.36	-0.39	-0.33	-0.39
RMe s	-0.20	-0.21	-0.17	-0.13	-0.13
LAg 3	-0.54	-0.34	-0.19	-0.55	-0.61
LAg 2	-0.42	-0.26	-0.12	-0.47	-0.49
LAg 1	-0.07	0.08	0.27	-0.31	-0.25
LAg	-0.40	-0.22	-0.05	-0.50	-0.51
LAI 3	-0.18	-0.14	0.38	-0.40	-0.41
LAI 2	-0.04	-0.03	0.44	-0.29	-0.24
LAI 1	0.35	0.29	0.78	-0.04	0.06
LAI	0.04	0.04	0.58	-0.27	-0.21
fLA 3	-0.65	-0.54	-0.50	-0.44	-0.60
fLA 2	-0.32	-0.31	-0.31	-0.20	-0.20
fLA 1	0.65	0.56	0.54	0.43	0.53
HADm 3	0.33	0.22	0.75	0.01	0.06
HADm 2	0.31	0.21	0.72	-0.00	0.04

Continued on next page

Table 6.12: Healthy trait correlations with tolerance estimations. Significance of the Pearson's correlation: $|r| > 0.404$, $P < 0.05$; $|r| > 0.515$, $P < 0.01$.

variable	Ts	Tm1	Tg1	Tm2	Tg2
HADm 1	0.46	0.35	0.84	0.09	0.17
HADm	0.38	0.27	0.81	0.03	0.10
HADg 3	-0.04	0.03	0.38	-0.29	-0.27
HADg 2	-0.04	0.02	0.33	-0.25	-0.24
HADg 1	0.25	0.30	0.61	-0.09	-0.00
HADg	0.07	0.13	0.49	-0.23	-0.18
HADe 3	0.53	0.38	0.54	0.33	0.44
HADe 2	0.52	0.36	0.55	0.31	0.44
HADe 1	0.65	0.50	0.67	0.36	0.52
HADe	0.59	0.43	0.62	0.34	0.48

Chapter 7

Discussion

The PhD project aimed at identifying traits and mechanisms which could improve the tolerance of wheat to STB. Relying on analysis of former experiments and three new experiments, new traits were identified. The results of the studies also underlined that environmental variations might alter the expression of the STB tolerance itself, but also that of tolerance traits. Finally, the quantification of tolerance itself will be also discussed.

Hypotheses of the rationale:

- Tolerance of STB relies on genotype traits therefore it is relevant to work with identified genotypes contrasting for tolerance of STB.
- Tolerance of STB relies on physiological processes (e.g. nitrogen metabolism, energetic transfers), responses to source/sink manipulations are therefore relevant to the study of tolerance.
- Glasshouse results obtained with mini-crop stands are consistent with the field studies.

7.1 Highlights of the results

The PhD project study started investigating the determinants of the senescence timings (I) and the mean grain weight (TGW) identified by Bancal et al. (2015) as tolerance traits. An attempt to identify the main traits altering TGW and I was performed (Chapter 3), leading to two principal outputs. Firstly, a data-mining method to investigate traits and environmental effects in a multiple genotypes and multiple seasons and locations dataset was developed. Secondly, traits influencing TGW and I were identified. The most important putative traits identified were the earliness of heading stage and the relative contribution to canopy green lamina area of the flag leaf (fLA 1); with earlier heading and proportionally more flag-leaf area delay senescence timing. Environmental variation, that influenced greatly the responses of I and TGW, was also considered.

In Chapter 4, the Field 2014-15 experiment at Hereford (F2015), including six tolerance-contrasting genotypes and a spikelet-removal treatment on field-grown plants, established that grain growth was co-limited by the source and the sink. Tolerance of genotypes was correlated with a low degree of source limitation. Finally, the putative STB tolerance at the crop scale was found to be correlated with tolerance of spikelet removal measured at the grain scale. The tolerance of both STB and spikelet removal was associated with traits of control crops, with greater tolerance associated with the higher individual grain weight and higher green leaf lamina area as a proportion of leaf 3.

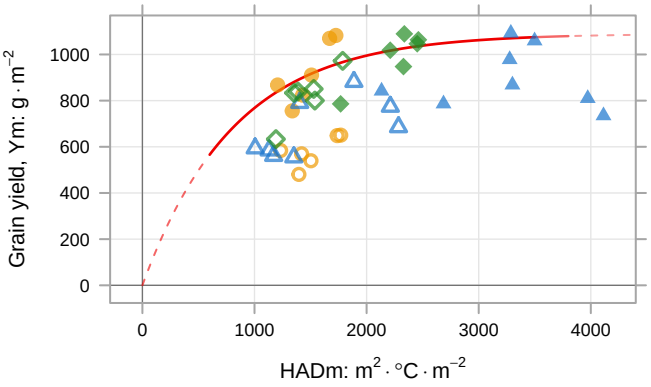
In Chapter 5, the Glasshouse 2014-15 experiment at Grignon (G2015) involved four of the six preceding genotypes grown in mini-crops. The N-fertilisation treatments differentiated from GS44. Estimates of N-tolerance at either the crop or the grain scale correlated positively, but each correlated negatively with putative STB tolerance.

In Chapter 6, the Field 2015-16 experiment held at Sutton Bonington (F2016) included six modern cultivars and generated severe STB symptoms and grain yield losses by fungicide treatments of field-grown crops. The range of STB tolerance was estimated using several methods (intolerance or tolerance ratios, slope based on linear regression results) and scales (the crop and the grain scale) whose results were generally converging. The STB tolerance was also correlated with heading date, the senescence timings, the fLA 1 and the TGW, underlining the consistency of the identified traits of tolerance.

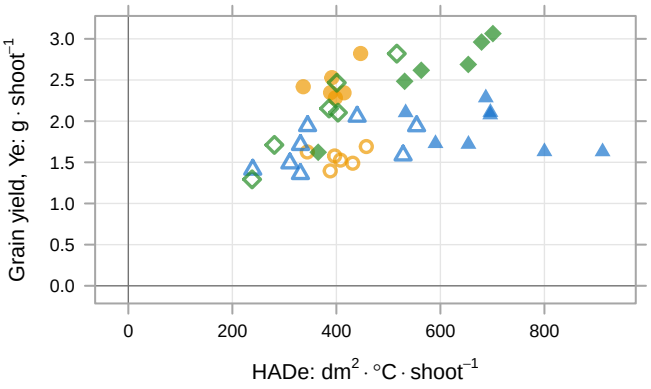
7.2 The range of source/sink balance generated

In order to analyze the scope of the results, the consistency of source/sink balances generated by the different experiments was first analysed. The three experiments generated new data based on source/sink balance that could be considered comparing source (HAD) to resulting grain yield (Y) at either the crop (HADm, Ym), the shoot (HADe, Ye) or the grain scale (HADg, TGW; Fig. 7.1). In the F2015 experiment, the main source/sink balance variability was obtained by a 50% spikelet-reduction, reducing the sink at the crop and the shoot scale, while increasing the source/sink balance at the grain scale. In the G2015 experiment, the largest variability in source/sink balance was generated by the N nutrition treatment after GS44. By comparison to N1, the N0 treatment largely reduced the source without affecting the grain number per ear. Both the F2015 and G2015 experiments included disease-contrasting treatments (fungicide-/inoculation- based, respectively), but the resulting disease severity was too low to be usefully considered. Finally, high STB symptoms were obtained by contrasting fungicide treatment in the F2016 experiment. At the crop scale (Fig. 7.1a), the grain source quantified by HADm in G2015 was comparable with the range of F2016 data, at least under N0 treatment, N1 inducing very large values for HADm. Regarding the obtained HADm, Ym in F2016 was close to

(a) Ym and HADm



(b) Ye and HADe



(c) TGW and HADg

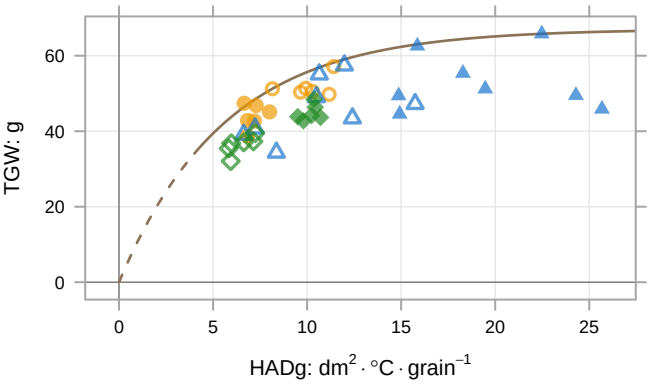


Figure 7.1: Source/sink balance comparison between experiments. The source/sink balance was calculated at (a) the crop scale, (b) the ear-bearing shoot scale and (c) the grain scale. At the crop scale, the potential curve (red curve) was defined (independently from the present experiments) as: $Ym = 1090 \cdot (-\exp(-1.33 \cdot HADm/1090))$ (Gouache et al., 2012). At the grain scale, a potential curve (brown) was fitted by quantile regression ($\tau = 0.95$): $TGW = 67 \cdot (-\exp(-11.9 \cdot HADg/67))$. The symbols represent the different experiments and respective main contrasting treatments:

- Orange circles: the F2015 experiment (Chapter 4), empty/closed for spikelet removal treatment and corresponding control (S1/S0).
- Blue triangles: the G2015 experiment (Chapter 5), empty/closed for N fertilisation treatments N0/N1.
- Green diamonds: the F2016 experiment (Chapter 6), empty/closed for STB-untreated/treated.

the theoretical boundary curve (Gouache et al., 2014), as expected from cultivars grown in intensive conditions. Conversely, Ym in G2015 was low under both N fertilisations. Data from F2015 were affected by poor establishment in some plots and low ear per m^2 (EN) that led to high Ye and Ym despite very low HADe and HADm. At the shoot scale (Fig. 7.1b) a large HADe variability was obtained in G2015 and F2016, while it was quite low in F2015 because the method included selection of average shoots for which HAD was hardly modified by the spikelet-removal treatment. In F2015, Ye of S0 treatment (control ears) was at the level obtained in F2016 for equivalent HADe, while Ye of the S1 (top spikelets removed) treatment was much lower than the control. Conversely, G2015 showed very low Ye as compared to the field studies; plants in the glasshouse accumulated less biomass relative to their green area than the field-grown plants grown, which could be related to the low PPFD they received per unit of thermal time. However, this effect was compensated at the grain scale: plants in glasshouse developed relatively smaller GNe. As a consequence, the relationships between HADg and TGW (Fig. 7.1c) appeared quite consistent between the three experiments. Very large HADg was obtained in G2015, even higher than that obtained by spikelet reduction in the F2015 study. Consequently, TGW was rather saturated, which would explain the low effect of GNe reduction by inoculation treatment observed in G2015.

7.3 The quantification of tolerance and the scale

In the literature, tolerance is generally estimated through the ratio (or slope) of yield loss to HAD reduction (Parker et al., 2004; Foulkes et al., 2006; Castro and Simón, 2016). This method constituted a milestone toward an absolute quantification of tolerance, whereas tolerance studies before relied mostly on disease/disease-free comparison (Schafer, 1971) or disease severity (% yield loss, Ziv and Eyal, 1978; AUDPC, Inglese and Paul, 2006) which does not quantify actual source reduction. However, the limitations of the current estimation method were addressed during the three experiments presently reported.

7.3.1 Limits of the single slope-based estimation of tolerance

The slope-based method for tolerance quantification at the crop scale relies on an hypothesis which is only partially verified. Indeed, mathematically, a slope (or a ratio) translates a linear conception of the source/sink balance. However, since Monteith and Moss (1977), light interception is known to be saturated at high canopy expansion. Slope- (or ratio-) based tolerance thus overlooks the saturating pattern which characterises the yield (Ym) to HADm relation (Fig. 7.1a; Monteith and Moss, 1977). The consequence is that tolerance slopes do not dissociate the source/sink balance of the crop (source limited

vs sink limited crops) from its conversion efficiency (every crop does not translate HAD into yield equally). Based on F2016 results, the Figure 7.2 exemplifies these consequences with regard to the two cultivars Cashel and Cougar. The slope-based estimations (green segments) did not account for the difference in source availability (HADm), which was larger for the Cougar than Cashel, neither did they identified the higher efficiency of Cougar that produced more Ym per unit HADm than Cashel.

Generally in the literature, the intolerance ($\Delta Y/\Delta HAD$) was estimated rather than the tolerance ($\Delta HAD/\Delta Y$). Following from the mathematical properties of the inverse function: for lower yield loss (as expected for tolerance scenario) slope-tolerance tends towards infinite values. Any data imprecision, such as encountered between replicates, led to large variation in obtained ratios. In contrast, for low HADm reduction (expected in a low epidemic context, plausible following the best agronomic practices), intolerance tends towards an infinite values, also precluding quantification. These estimation difficulties were encountered, for instance, in G2015 (Chapter 5) where the grain yield loss of C×L 7A due to the nitrogen treatment was very low, or also in F2015 (Chapter 4) where large variation of HADg was observed in comparison to TGW variations. In line with the ratio properties, the magnitude of estimated tolerance is largely impacted by the units of HAD or grain yield: Ym can be reported in $kg \cdot ha^{-1}$ (e.g. Castro and Simón, 2016) or in $g \cdot m^{-2}$ (e.g. Chapters 4 to 6), HADg can be reported in $cm^2 \cdot {}^\circ$ Cd (Chapter 4) or in $dm^2 \cdot {}^\circ$ Cd (Chapter 5) and so on. Therefore, the ratio might be well suited for comparison of genotypes and ranking within an experiment, but it should be admitted that the use of an absolute value is limited.

7.3.2 Improve the tolerance estimation

In F2015 and G2015, STB tolerance could not be estimated. Instead, STB-tolerance values were estimated from three independent experiments, where populations of doubled-haploid genotypes were screened for grain yield and STB tolerance. Within these three previous experiments, slope-based tolerance estimation was generally consistent across experiments (Fig. 5.1, p.129), but also showed some significant variation between experiments (e.g. for genotypes C×L 14B and 5H). This emphasizes the site-season variations and stresses the importance of experiment repetitions to obtain a robust estimation of crop STB tolerance, and a reliable STB-tolerance ranking. Despite relatively large intolerance variations between experiments, the genotype ranking was quite stable, which supported combining the data issued from these three experiments to estimate more robust tolerance-grades (Eq. 5.1, p.128).

In the F2016 experiment, no preliminary indication about the STB tolerance of cultivars tolerance was available from previous experiments; but based on the results of data-mining (Chapter 3), contrast in tolerance was expected in relation to the cultivar range

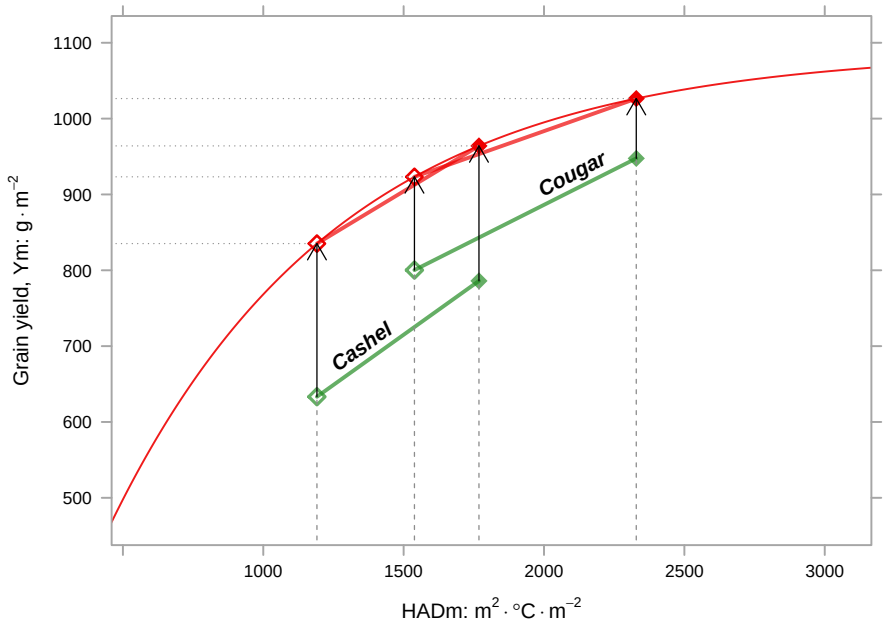


Figure 7.2: The Yield to HAD potential curve for tolerance of STB estimation. The y-axis represents the crop grain yield (500 to 1000 $g \cdot m^{-2}$) for a given source availability (HADm, x-axis, 500 to 3000 $m^2 \cdot^\circ \text{Cd} \cdot m^{-2}$). This example is based on the F2016 experiment, genotype Cashel (Ym: 633 and 816 $g \cdot m^{-2}$; HADm: 1191 and 2008 $m^2 \cdot^\circ \text{Cd} \cdot m^{-2}$; untreated and treated, respectively) and Cougar (Ym: 800 and 948 $g \cdot m^{-2}$; HADm: 1539 and 2329 $m^2 \cdot^\circ \text{Cd} \cdot m^{-2}$, untreated and treated, respectively), the empty/closed symbols represent the disease/disease-free treatments. The standard tolerance is estimated as the slope of the green segments. At the crop scale, the potential curve (red curve) was defined as: $Ym = 1090 \cdot \left(-\exp\left(-1.33 \cdot HADm/1090\right)\right)$ (Gouache et al., 2012). The arrows indicate the potential yield for the corresponding observed HADm.

in heading date. As reasonable disease severity was obtained, actual STB tolerance and intolerance slopes were estimated (unlike the two preceding experiments). Yet, they could not be strengthened by former comparison with former experiments. Instead, tolerance and intolerance were estimated at both the crop and the grain scale. Indeed tolerance at the crop and grain scale were highly correlated in G2015, and also in the datasets used in Chapter 3. This tight correlation was also found in F2016 and every tolerance estimation led to a similar contrast in STB tolerance between genotypes. Finally, the normalised average of these individual tolerance estimations (tolerance and intolerance, at the crop and the grain scale) resulted in a single more robust tolerance estimation, which was then used to identify tolerance traits.

Therefore, two methods were applied to increase robustness of the tolerance estimation: combining several site-season results and combining several estimations at the crop and the grain scale to ascertain the results. One problem remained unsolved as the resulting tolerance values were difficult to compare between different sets of genotypes exposed to different levels of epidemics, a problem that was corrected by an epidemiologic characterisation of the experiments by Bancal et al. (2015).

The potential curve approach (Gouache et al., 2014), which has not been used or

studied here, could provide an interesting alternative approach. This approach relies on the use of a constant reference curve, established on a large population of G and E, that avoids pair-wise comparison of genotypes. Potentially, this approach could improve the tolerance estimation as it can dissociate clearly the efficiency of the genotype (Yield per unit HAD), the level of source availability (HAD) and tolerance. However, this method also raises questions: how to define the reference? Gouache et al. (2014) investigated that question examining a total of 560 Ym - HADm pairs for multiple cultivar × site × season treatment combinations across a French field-scale experimental network. They proposed a monomolecular definition of the potential Ym, attainable for every HADm (Fig. 7.1a and 7.2). However, what was presented as a reference is likely to change with space and time. For instance: What would have been the potential curve before the introduction of the semi-dwarf cultivars on the market? Should the same function definition be used for the British or French field conditions, British and French genotypes? Nonetheless, the potential curve seemed largely consistent regarding the range of source/sink balances obtained during the PhD project (Fig. 7.1).

7.3.3 The grain scale relevance

The literature considering STB tolerance reports experiments varying source/sink balance that are generally conducted at the crop scale. The HAD was estimated in days (Parker et al., 2004; Foulkes et al., 2006; Castro and Simón, 2016), the yield in tonnes (Parker et al., 2004; Foulkes et al., 2006) or kilograms (Castro and Simón, 2016) per hectare or equivalent. Tolerance would arise either from compensations (increased radiation-use efficiency, Zuckerman et al., 1997; Scholes and Farrar, 1986; improved re-mobilisation of stem dry-matter reserves, Bingham et al., 2009) or from a large source availability relative to the sink (Parker et al., 2004; Ney et al., 2013). At the crop scale, because of self shading between leaf layers, intercepted light is not proportional to HADm. At higher HADm, saturation of the light interception occurs: the crop-source inevitably reaches a maximum light interception with canopy area increase (Fig. 7.1a). This explains that an asymptotic description of the relation, such as a monomolecular function, is an appropriate choice to describe the potential curve (Ym to HADm, Bryson et al., 1997).

Based on the present results, the source/sink balance at the grain scale was largely consistent with the crop tolerance (Fig. 7.1a). Moreover, the data collected also suggested an asymptotic relation between HADg and TGW (Fig. 7.1c). This his perhaps surprising as the nature of the saturating pattern is different at the crop and the grain scale. In this last case, a grain-sink saturation tending toward a physical/biological extension-limit of the grain-sink capacity should be suspected instead of the source saturation observed at the crop scale. Therefore, the spikelet-removal experiments, modifying sinks such as in F2015 are not directly equivalent to a disease experiment modifying sources such

as in F2016, although at the grain scale both of them could be regarded as inducing a modification of the degree of grain-source availability. In the literature, a nil to moderate grain growth increment is commonly observed by spikelet removal (Borrás et al., 2004) that has led to the common point of view: yield is sink saturated in intensive crops of elite cultivars. This point will be reexamined in Section 7.4.3 as results of F2015 tend to suggest the saturating relation of Ym to HADm is due both to a source limitation (limited by the light interception), and to sink limitation of TGW. A crop indeed regulates its grain number according to canopy expansion, thus maintaining a link between source and sink (Sinclair and Jamieson, 2006; Slafer et al., 2014). In control crops, grain number would be set in order that the growth of individual grains TGW in relation to the HADg is sink-limited or co-limited (by the degree of source availability per grain). Therefore, in a tolerance study focusing on source/sink balance, the reduction of the crop source (HADm) by disease symptoms would result in yield loss (Ym), only when it leads to a reduction of the grain-source availability (HADg) sufficient to reduce the individual grain yield (TGW). Briefly two cases could occur depending on the HADg obtained through HADm reduction:

- Either HADg still is high enough to saturate TGW: HADm reduction does not result in yield loss (tolerant crop).
- Or obtained HADg no longer saturates TGW: HADm reduction does result in yield loss (intolerant crop).

This rationale points out that tolerance would ultimately rely on the position of control crops on graphics such as Figure 7.1c: tolerant crops would lie in the right part, while intolerant crops in left part.

7.4 The STB-tolerance traits

7.4.1 Comparison of the experimental results

The tolerance estimation within the experiments was adapted to specific experimental constraints to allow for statistical analysis: mostly based on ratio, values do not vary linearly with ΔHADm or ΔYm and therefore are also highly susceptible to the units and extent of Δ (low/high yield loss, low/high HADm variations, etc). Within the chapters, the chosen tolerance quantification method varied to support statistical analysis requirement, i.e. to reduce the effect of outliers resulting from very low ΔY or very low ΔHAD. Nevertheless, for comparison between experiment, the tolerance was here homogeneously re-estimated between the experiments (Table 7.1) using the same units: Ym as $g \cdot m^2$, HADm as $m^2 \cdot^\circ \mathrm{Cd} \cdot m^{-2}$, TGW as g, HADg as $dm^2 \cdot^\circ \mathrm{Cd} \cdot grain^{-1}$. Regardless of the outliers they generated, two methods were applied to estimate tolerance across experiments:

- Method 1, the tolerance as a linear transformation of the intolerance ratio:

$$1 - intolerance \Longrightarrow Tm = 1 - \frac{\Delta Ym}{\Delta HADm}$$
$$Tg = 1 - \frac{\Delta TGW}{\Delta HADg}$$

- Method 2, the tolerance as intolerance inverse (non-linear transformation):

$$\frac{1}{intolerance} \Longrightarrow Tm = \frac{\Delta HADm}{\Delta Ym}$$
$$Tg = \frac{\Delta HADg}{\Delta TGW}$$

Tolerances calculated according to method 1 are reported in Table 7.1 in $g \cdot m^2 \cdot^\circ Cd^{-1}$ (Tm) and $mg \cdot dm^2 \cdot^\circ Cd^{-1}$ (Tg). Tolerances calculated according to method 2 are reported in Table 7.1 in $^\circ Cd \cdot g^{-1} \cdot m^{-2}$ (Tm) and $^\circ Cd \cdot mg^{-1} \cdot dm^{-2}$ (Tg).

The genotypes used in F2015 and G2015 were also studied in three external and independent UK experiments which resulted in STB effect on Ym and HADm (data presented Chapter 4, Table 4.1, p.112). However, HADm in these three independent experiments was only available in $m^2 \cdot days \cdot m^{-2}$ and could not be converted to thermal time. Despite the unit discrepancy, a genotype tolerance of STB was calculated. The genotype intolerance was first transformed into tolerance estimates (intolerance opposite and inverse transformations) within each experiment. Then, the results were combined to obtained a single genotype crop tolerance (Tuk) which was the genotype average of the tolerance estimations. The unit of Tuk in Table 7.1 are $t \cdot ha^1 \cdot^\circ Cd^{-1}$ (method 1) or $d \cdot t^{-1} \cdot ha^{-2}$ (method 2).

In F2015, the main source of variation of the source/sink balance was the spikelet removal treatment. Because the F2015 experiment manipulated sinks instead of sources, HADm was only marginally affected from feedback regulation of senescence while Ym was largely reduced, therefore method 1 resulted in extreme Tm values. Actually, the Tm estimation should be questioned in this experiment. Conversely, at the grain level, spikelet-removal led to an increase in the source/sink ratio, changing the nutrition of remaining grains in a way close to the other treatments (Fig. 7.1c). Tg was thus calculated, and amongst the main results of the study, Tg (an estimation of tolerance of spikelet removal) correlated with Tuk (an estimation of tolerance of STB).

In G2015 experiment, the source/sink balance was modified through a strong contrast in N supply. The treatment was applied after GS44 and did not change the grain number, thus affecting source but not sink. However, outliers appeared in the G2015 experiment, where the method 2 failed to provide satisfactory estimation for stay-green C×L 7A because of large ΔHAD associated with low ΔY. The method 1 seemed more appropriate in that case and tolerance classification regarding Tg was generally consistent with Tm.

Table 7.1: Tolerance values across experiments (Field 2014-15, F2015; Glasshouse 2014-15, G2015; Field 2015-16, F2016) and Tuk based on three independent UK experiments. Tolerance was firstly estimated as a linear transformation of intolerance ($1 - \Delta Ym/\Delta HADm$) and reported in $mg \cdot dm^2 \cdot^\circ \mathrm{Cd}^{-1}$ (Tg), in $g \cdot m^2 \cdot^\circ \mathrm{Cd}^{-1}$ (Tm) or in $t \cdot ha \cdot d^{-1}$ (Tuk). Alternatively, tolerance was estimated as an inverse transformation ($\Delta HADm/\Delta Ym$) so and reported in $^\circ\mathrm{Cd} \cdot mg^{-1} \cdot dm^{-2}$ (Tg), in $^\circ\mathrm{Cd} \cdot g^{-1} \cdot m^{-2}$ or in $d \cdot t^{-1} \cdot ha^{-1}$ (Tuk). Larger value is an expression of tolerance. Genotypes were ranked within experiments regarding tolerance estimation, starting from the least tolerant 1, to the most tolerant (4 or 6, regarding the number of genotype within the experiment). The median rank of the genotype across the tolerance estimations is given in the last column (Med.).

Trial	$1 - \Delta Ym/\Delta HADm$			$\Delta HADm/\Delta Ym$			
Genotype	Tg	Tm	Tuk	Tg	Tm	Tuk	Med.
F2015							
C×L 14B	-1.54 (4,5)	8.11 (4)	0.972 (3)	0.42 (4,5)	0.30 (6)	35 (3)	(4)
C×L 5H	-1.54 (4,5)	-6.91 (1)	0.975 (4)	0.42 (4,5)	-0.27 (2)	41 (4)	(4)
C×L 7A	-3.23 (1)	74.84 (6)	0.945 (1)	0.25 (1)	-0.02 (4,5)	18 (1)	(1)
LSP2×R 127	-1.74 (2)	6.20 (3)	0.986 (5)	0.39 (2)	-0.02 (4,5)	71 (5)	(4)
LSP2×R 16	-1.73 (3)	23.10 (5)	0.959 (2)	0.37 (3)	-0.20 (3)	24 (2)	(3)
LSP2×R 20	-0.54 (6)	1.56 (2)	0.989 (6)	0.67 (6)	-0.31 (1)	94 (6)	(6)
G2015							
C×L 14B	-0.16 (2)	0.83 (3)	0.972 (3)	0.86 (3)	5.99 (3)	35 (3)	(3)
C×L 7A	0.38 (3)	0.98 (4)	0.945 (1)	1.92 (4)	13.61 (4)	18 (1)	(4)
LSP2×R 127	1.71 (4)	0.69 (1)	0.986 (4)	0.65 (2)	3.99 (1)	71 (4)	(3)
LSP2×R 16	-0.63 (1)	0.75 (2)	0.959 (2)	0.55 (1)	4.33 (2)	24 (2)	(2)
F2016							
Cashel	-1.86 (3)	0.75 (3)		0.38 (2)	4.28 (3)		(3)
Cougar	-0.94 (5)	0.80 (5)		0.58 (4)	5.36 (5)		(5)
Dickens	-1.02 (4)	0.78 (4)		0.62 (5)	4.88 (4)		(4)
Evolution	-1.95 (2)	0.73 (2)		0.36 (1)	3.83 (1)		(1.5)
Sacramento	-0.53 (6)	0.86 (6)		3.95 (6)	9.78 (6)		(6)
Zulu	-2.21 (1)	0.66 (1)		0.44 (3)	4.13 (2)		(1.5)

Surprisingly, the tolerances Tg and Tm were not consistent with the tolerance — Tuk, even exhibiting negative correlation (not significant). Such inconsistency could be linked to differences in underlying mechanisms between tolerance of STB and tolerance of late N deficiency. Alternatively, the G2015 experiment can be considered as an extreme environment. Indeed, glasshouse growth induced phenotypes different from that in the field experiments, for instance, a generally larger flag leaf (LAe 1 and fLA 1) or the stay-green phenotype C×L 7A.

Lastly, in the F2016 experiment, STB epidemics generated both high ΔHADm and ΔYm. The two tolerance calculation methods were found to be very consistent, and Tm versus Tg as well.

7.4.2 Tolerance traits

A summary of the tolerance traits is reported in Table 7.2.

- **Senescence timings**

Bancal et al. (2015) identified the late senescence of the canopy as a tolerance trait, which could result from a higher source availability to grains during the grain filling phase, thus promoting tolerance (Ney et al., 2013). The senescence timings of the canopy (I) or the flag leaf ($I1$) were positively correlated with tolerance of STB. This was supported by the increased tolerance found in F2016 in the case of UK late-senescing cultivars exposed to natural STB epidemics. Furthermore, a late senescence was also found to increase tolerance of N deficiency in G2015 mini-crops. In turn, the senescence timings were delayed by early heading stage or for large flag-leaf area contribution (Chapter 3).

Table 7.2: Summary of the correlations between tolerance and genotype traits as estimated within respective chapters. In the F2015 and G2015, tolerances Tg and Tm were linear transformations while inverse transformation were applied in F2016. Only significant correlations ($P < 0.05$) were reported, brackets indicate trend (when $P<0.10$). Non-significant or non-tested (not measured variable) are left blank.

	F2015		G2015		F2016	
Trait	Tg	Tuk	Tg	Tm	Tg	Tm
Tg	1	0.98	1		1	0.94
Tm			0.94		0.94	1
Ym			-0.61	(-0.58)		
TGW	0.86	0.90				
ΔTGW	-0.92	-0.85				
GNm			-0.62	(-0.52)		
HADm				0.64		
HADe			0.61	0.78		0.48
HADg			0.86	0.90		
HADg 3	0.89	0.89				
I				0.67	0.48	0.45
$I1$			(0.52)	0.69		
LAg			0.95	0.88	-0.51	-0.50
LAe 1					0.52	
LAI						
LAI 1						
fLA 1			(-0.58)	(-0.55)	0.53	0.43
fLA 3	0.88	0.88			-0.60	-0.44
Heading			(0.58)	0.64	-0.56	-0.56
AN/m2			-0.75	-0.75		
dMv/m2						0.47
Pmax (L1)			-0.83	-0.84		

- **Canopy size**

Parker et al. (2004), Bingham et al. (2009) and Ney et al. (2013) suggested large canopy size could help maintain a maximum light interception and lead to STB tolerance. However, Foulkes et al. (2006) did not identify significant correlation between either LAI

or HADm and STB tolerance, but Bancal et al. (2015) reported a positive correlation of both LAI and HADm with tolerance. In the G2015 experiment, LAI was positively correlated with Tg and Tm. As reported previously, data in this experiment could be challenged, however, in F2016 experiment also both Tg and Tm correlated positively with LAI and HADm. In relation to breeding for STB tolerance the development of phenotypes of large LAI should also consider any possible effects of a lower dry-matter partitioning to the ear during the pre-anthesis phase which could potentially induce a lower yield potential (Reynolds et al., 2009).

- **Canopy vertical distribution**

Based on the upward propagation of STB, Parker et al. (2004) suggested that an increase in the relative contribution of the upper leaves to the canopy green area would maintain the radiation interception by healthy leaves. This could be achieved by selecting for vertical distribution of the leaf areas and Foulkes et al. (2006) observed a positive correlation between flag leaf area per shoot (LA1e) and STB tolerance. Bancal et al. (2015) found inconsistent correlation with intolerance of LAe 1 according to the sub-dataset examined. In the F2016 experiment, STB tolerance was correlated with a large flag-leaf as characterised by either LAe 1, LAI or fLA 1. Flag leaf could be involved in tolerance otherwise than its area. Bancal et al. (2015) developed models of diseased yields that always took account of flag-leaf traits but the authors did not find significant correlation with tolerance of LAe 1, LAI 1 or fLA 1. Bingham et al. (2009) suggested that differences in light-extinction coefficient (leaf inclinations) could also affect the flag-leaf photosynthetic contribution, despite the reduced genetic variability in the wheat cultivars in comparison to barley. The data-mining study identified a link between the canopy vertical distribution and the senescence timings: the larger the proportion of flag-leaf lamina in the LAI, the later the senescence time. Therefore, promoting large upper-leaf lamina also increased the green leaf-life during the grain filling phase.

- **Leaf photosynthetic rate**

Parker et al. (2004) proposed that high photosynthetic efficiency could be associated with intolerance as the loss of highly efficient green area (high RUE) might be associated with larger yield loss. Conversely, Bingham and Topp (2009) showed on a modelling study that high k (light-interception coefficient) or high RUE (radiation-use efficiency) would increase tolerance. These two traits were never observed during the PhD project, but direct Pmax measurement of the flag leaf was achieved during the G2015 experiment and estimation of Net Assimilation by the whole shoot DM increment during grain filling was obtained in the three experiments. Both Pmax and DM increase were associated with low Tg, Tm and high Tuk during G2015, while in the two other experiments DM increase

did not correlate with any tolerance estimates.

- **Dry-matter reserve**

Parker et al. (2004) proposed that compensation by stem soluble carbohydrate (WSC) reserves for loss in radiation interception could result in STB tolerance. Instead, Foulkes et al. (2006) identified a negative association between WSC content of stems and tolerance. This surprising result could be an indirect effect of genotype evolution through breeding. The range of both WSC content and tolerance were indeed related to the year of release from 1972 to 1996 of the studied cultivars. On the one hand breeding for shorter cultivars had led to a WSC increase (Shearman et al., 2005), while breeding strategies also decreased tolerance (Parker et al., 2004). Yet these two traits could have been selected by independent means. Stem WSC was only measured in some samples from the G2015 experiment and can't be usefully compared to tolerance in the present study. Conversely, a raw estimate of stored WSC was obtained in each experiment from the loss of DM by vegetative organs during grain filling. However, neither at the crop or at the grain scale could DM remobilisation be associated with tolerance in the case of one or the other stresses.

- **TGW and grain number**

Parker et al. (2004) and Foulkes et al. (2006) identified the grain sink size (index: GNm) as being negatively linked with STB tolerance. Bancal et al. (2015) did not, but in two of their three database subsets tolerance negatively correlated with GNe, while tolerance did correlate negatively with TGW in the third dataset subset. These two trends appeared to be contradictory, as TGW is generally reduced for higher grain number (Slafer et al., 2014). It should be noted also that these relations were no longer observed by Bancal et al. (2015) when restricted to standard N fertilisation treatment. In F2016, STB tolerance was negatively correlated with TGW, while in F2015 tolerance (Tg) positively correlated with the potential TGW. However, in the latter experiment the spikelet-removal treatment increased, theoretically, the TGW to its maximum attainable value; thus, the grain-sink was saturated and the variation observed reflects, therefore, the degree of source limitation to fully fill the grains. Interestingly, there was variability in the degree of source limitation for grain growth in cultivars having identical grain weight. For instance, in the standard conditions, the C×L 7A and C×L 14B showed identical TGW at the time of degraining, but responded very differently to the grain sink reduction: this could be explained by the lower HADg in C×L 7A than C×L 14B. Therefore, the TGW and GNm effect on STB-tolerance should be considered together with HADg variations.

7.4.3 Grain-source availability

The methods used during the project hypothesised that STB tolerance of wheat may rely on source/sink balance. The spikelet-removal experiment (F2015) concluded that tolerance was largely correlated with low grain-source limitation during the grain filling phase. Yet, the observed grain weight increase in response to spikelet removal was large in comparison to equivalent studies based on cultivars of wheat (Zhang et al., 2014; Serrago et al., 2013) or barley (Cartelle et al., 2006; Serrago et al., 2013). It should be noted that the F2015 experiment relied on six winter wheat genotypes selected in two doubled-haploid populations contrasting for STB-tolerance. Consequently, the genotypes were largely independent from breeding strategies and trends with year of release. The tolerance variability among these genotypes relied on the variability of their degree of source availability relative to grain sink. Breeding selection for reduced sink limitation, rather than a direct trade-off with yield, could explain the lower tolerance observed in modern cultivars by Parker et al. (2004). Indeed, four amongst the six genotypes used in F2015 were also observed in the G2015 experiment. The inoculation here resulted in a moderate *physiological* grain-sink reduction, but with low effects on TGW. Consequently, these crops were probably not limited by the grain source availability, due to growth conditions largely different from F2015. If new cultivars are being bred eliminating sink-limited TGW then a high gain in potential tolerance can't be expected from improvement of the grain-source availability. However, we should also consider that literature reporting spikelet-removal experiments may be biased. Indeed, in F2015, the treatment was quantified by its effect on grain source availability (HADg) since the time of the sink-reduction treatment, whereas literature generally reports only GNe variation. Firstly, the whole grain filling period is thus considered, and secondly possible compensation by development of ancillary grains or change in senescence are not regarded. Therefore, it is not possible to exclude a potential over-estimation of the sink limitation of the wheat grain yield in the literature.

7.4.4 Interaction between tolerance traits

Traits were regularly found to be interconnected. The most surprising was probably the link between heading date and the area proportion of flag leaf (fLA 1). This result could be compared to the observations by Steinfort et al. (2017) of a larger fLA 1 under short day conditions by 10 and 8 NILs of spring wheat in field and glasshouse experiments. Further confirmation using larger datasets selected for an appropriate variability on these two traits is needed, but it suggests the flag-leaf involvement in tolerance reported earlier is not necessarily linked to photosynthesis.

7.5 Environment effect

- **Tolerance and putative tolerance traits vary with environment**

Tolerance is characterised by a strong variability between environments (Parker et al., 2004; Bancal et al., 2015). Parker et al. (2004) underlined the importance of taking into account E variations, and, to do so, they used mixed models. Bancal et al. (2015) took into account E disease pressure by a local epidemic index, which enabled the identification of putative tolerance traits. Foulkes et al. (2006) also evoked a similar problem of variation in tolerance expression with the site, underlining again the need to ensure the robustness of tolerance grades. Therefore, quantifying the E effect on tolerance expression is required.

The data-mining chapter (Chapter 3) highlighted the environment variability of expression of putative tolerance traits, and proposed methods to take into account that variability in an attempt to explain *I* and TGW, which were identified as tolerance traits. Taking into account E variability allowed the identification of the putative traits such as heading stage, which would have been omitted otherwise. This could explain the relative incoherence of the G2015 experiment results with the expected STB-tolerance grades of the four genotypes, as the glasshouse E conditions led to specific source/sink responses which were shown to be strongly affecting the phenotypes.

- **Better understanding of E to discriminate/predict tolerance scenarios**

The tolerance has been studied with the objective of finding traits that could enhance genotype tolerance of STB. However, tolerance could also result from environmental variations. The environment generated a range of phenotypes. In the data-mining experiment the environment was, for instance, responsible for 60% of variation in heading date which was found to affect the senescence timings, and consequently the tolerance of STB. Improved understanding of the STB tolerance variability according to environment could allow for a better evaluation of the risk in yield loss and help to develop more appropriate fungicide protection strategies (Paveley et al., 2001). Therefore, the study of the genotype tolerance traits should be complemented by the study of the environmental effect that influences them. Such a study should include a large range of environments to detect the most important traits, as well as their variation with E. Using, for instance, a similar methodology as in Chapter 3, applied on the response variable tolerance or the key putative traits which influence tolerance, the origin of variations, i.e. either E or G or E×G, may help selecting either genotype tolerance traits useful in various or highly variable environments or environment tolerance traits useful to choose tolerant genotypes in specific environments.

7.6 Tolerance and trade-off

- **Grain yield**

Foulkes et al. (2006) found that STB tolerance negatively correlated with potential yield, and Parker et al. (2004) also reported a trend for a lower tolerance of the better yield-performing genotypes. However, they also reported a link with the release year which could explain the result as an effect of breeding strategy on source and sink traits rather than a strong association of tolerance with yield *per se*. Indeed, the potential-yield increase of UK cultivars from 1972 to 1995 was mainly associated with an enlargement of the grain sink (GNm, Shearman et al., 2005) potentially lowering the source availability in relation to grain sink (Foulkes et al., 2006) which was emphasized as a key determinant of STB tolerance according to F2015. Bancal et al. (2015) and Castro and Simón (2016) identified that there was no significant relation of potential yield with tolerance of STB (cultivars). In this PhD project as well no association between potential yield and STB tolerance was identified either in a subset of doubled-haploid genotypes independent from the general breeding strategies (F2015, G2015) and using recent cultivars (Chapter 6). These findings pointed out breeding could achieve high yield cultivars with increased levels of tolerance.

- **Stay green**

Tolerance is increased by late senescence timing, and very large delays in senescence timing correspond to stay-green phenotypes. The various physiological bases of these stay-green phenotypes were explored by Borrell et al. (2001) and Thomas and Ougham (2014). Borrell et al. (2001) suggested a physiological effect of higher specific leaf nitrogen content of the leaves of sorghum that would maintain a higher carbon assimilation and result, in turn, in higher capacity to extract N from the soil. Thomas and Ougham (2014) emphasized an alteration of hormone metabolism as a source of functional stay-green phenotypes. The most frequently studied case was described by Distelfeld et al. (2014) and Uauy et al. (2006). They reported the Gpc-1 allele modified nitrogen transfer to the grains, leading to both a lower N content of the grain and a later leaf senescence of wheat and barley. Therefore, a delayed senescence timing could be linked to lower N content of the grain. In the G2015 experiment, tolerance of late N deficiency correlated positively with N remobilisation from vegetative parts, but also with a delay in senescence. Interestingly, the higher the N remobilisation, the lower the relative contribution of leaves to N remobilisation, which may suggest the link to STB tolerance depended on the high stem N remobilisation. However, the genotypes ranked oppositely for their tolerance of N deficiency and their in STB tolerance in field, which precludes to any conclusion on the role of N remobilisation in stay-green genotypes. As underlined previously, however, both

F2015 and G2015 suffered from specific environmental conditions making generalisation difficult.

- **Tolerance and avoidance**

As mentioned by Bingham et al. (2009) and Bancal et al. (2015), a large canopy can also result in an increase of pathogen fitness associated with an increased epidemic (Lovell et al., 1997). Favouring large canopies, for instance, is likely to increase the epidemics by improving the chance of successful infection by the pathogen. Also, the microclimate within a lush canopy is more favourable for epidemic progress (Savary et al., 1995; Tompkins et al., 1993). Bancal et al. (2015) thus found HADm to be positively correlated with tolerance in a simple regression, but negatively correlated with yield of diseased crops in multiple regression. Another ambiguous tolerance trait is the heading date which had been associated with higher severity of the STB epidemics (Murray et al., 1990; Shaw and Royle, 1993; Robert et al., 2009). Therefore, the beneficial effect of tolerance traits must also be assessed in regard to avoidance strategy as the improvement of tolerance must not increase the chance for disease infection.

7.7 Perspectives

- **What is the actual degree of source limitation of modern cultivars?**

According to F2015 results, low source-limitation promoted STB-tolerance and should be regarded at the grain scale. The actual grain source-limitation of the existing cultivars should be investigated in spikelet-removal experiments with the objective of identifying genotypes tolerant to foliar diseases. To analyse properly the results of such experiments, grain number reduction is probably not a satisfactory estimation of the increase in grain source availability per remaining grain. The HADg seems a more reasonable alternative as it takes into account genotype variation in canopy senescence. However, spikelet-removal in association with appropriate HADg estimation increases substantially the experimental effort. Fortunately, remote-sensing technologies for canopy parameter estimations are increasingly being developed and becoming available in experimental platforms (Deswarte et al., 2015; Rebetzke et al., 2016); enabling more frequent and high-throughout measurements, which will provide adequate canopy characterisation during the grain-filling period.

- **Evaluation of the potential yield?**

The current quantification of tolerance is not fully satisfactory because of the mathematical properties of ratios. Moreover, it does not discriminate between origins of its variation, either the physiological states (source or sink limitations), the performance of

the crop (i.e. efficiency of conversion of HAD into yield) or the tolerance *sensus stricto*. The use of the potential curve, as proposed by Gouache et al. (2014), opens a promising alternative, but such a curve should be defined appropriately. Therefore, to improve further studies on tolerance, a deepened investigation of the potential curve, its evolution with the date of cultivar release (e.g. effect of semi-dwarf cultivar release), and its variation between environments is needed (maybe relying on the definition of the mega-environments supported by the CIMMYT, defined by Braun and Payne, 2012: "a broad, not necessarily continuous area, occurring in more than one country and frequently transcontinental, defined by similar biotic and abiotic stresses, cropping system requirements, consumer preferences, and, for convenience, by a volume of production"). Finally, for physiological use, a definition of such a potential curve at the grain scale would also be necessary. A first approach could consist in meta-analysis of available data and literature. However, accurate estimation of HADm is generally difficult to find in the literature, this would imply establishing new experiments. As evoked in the preceding paragraph, the proxy-measurement of the LAI, and green lamina area would be a major advance for the easier access to HADm.

- **Is there a trade-off between avoidance and tolerance?**

The preceding sections pointed out that the putative tolerance traits could also be associated with traits assumed to increase severity of disease epidemics. The potential for tolerance should be evaluated against the negative effects it has on disease escape strategy; therefore, assessing the actual net benefit of tolerance in disease management. Using existing models such as Septo-3D (Robert et al., 2009), a sensitivity analysis could possibly give a first estimation of disease-escape strategies when the putative tolerance traits are varied.

- **Characterisation of the *tolerant* environments?**

The data-mining study, Chapter 3, identified some putative tolerance traits, but also highlighted variables largely affected by the environment and G×E. The tolerance could thus also emerge from the specific environmental characteristics that require quantification using the procedure detailed in Chapter 3. Thereafter, a complementary study on the identification of environmental traits promoting tolerance would require a better environment characterisation than that used in Chapter 3. The database indeed lacked comparative data about crop management, soil, *etc* and finally mainly focused on meteorological data. Moreover, the very high number of meteorological data that can be incorporated raises a doubt about the interpretation of observed correlations. Do they indicate some physiological sensitivity or were they obtained by chance? Otherwise the year effect overwhelmed location effect in weather determinism. However, databases are

frequently built as the result of a project involving 2–3 years only. Characterisation of climate effect on tolerance would require compiling results collected over many different years, not only many locations.

- **How the agronomic practices could be used to enhance tolerance?**

In this PhD project the agronomic practices to manipulate directly tolerance were addressed in relation to N fertilisation. The larger canopy, or the higher contribution of the flag leaf could be achieved by N fertilisation strategies for instance. However, this strategy requires further study as general positive association between infection and nitrogen fertilisation was observed.

References

P. Bancal, M.-O. Bancal, F. Collin, and D. Gouache. Identifying traits leading to tolerance of wheat to Septoria tritici blotch. *Field Crops Research*, 180:176–185, 2015. doi: 10.1016/j.fcr.2015.05.006 .

I. J. Bingham and C. F. E. Topp. Potential contribution of selected canopy traits to the tolerance of foliar disease by spring barley. *Plant Pathology*, 58(6):1010–1020, Dec 2009. ISSN 0032-0862. doi: 10.1111/j.1365-3059.2009.02137.x .

I. J. Bingham, D. R. Walters, M. J. Foulkes, and N. D. Paveley. Crop traits and tolerance of wheat and barley to foliar disease. *Annals of Applied Biology*, 154:159–173, 2009. doi: 10.1111/j.1744-7348.2008.00291.x .

L. Borrás, G. A. Slafer, and M. E. Otegui. Seed dry weight response to source sink manipulations in wheat, maize and soybean: a quantitative reappraisal. *Field Crops Research*, 86(23):131–146, 2004. ISSN 0378-4290. doi: 10.1016/j.fcr.2003.08.002 .

A. Borrell, G. Hammer, and E. van Oosterom. Stay-green: A consequence of the balance between supply and demand for nitrogen during grain filling? *Annals of Applied Biology*, 138(1):91–95, 2001. doi: 10.1111/j.1744-7348.2001.tb00088.x .

H.-J. Braun and T. Payne. *Physiological breeding I: interdisciplinary approaches to improve crop adaptation*, chapter Mega-environment breeding, pages 6–17. CIMMYT, Mexico, Mexico, DF (Mexico), 2012. URL `http://repository.cimmyt.org/xmlui/bitstream/handle/10883/1288/96144.pdf`.

R. J. Bryson, N. D. Paveley, W. S. Clark, R. Sylvester-Bradley, and R. K. Scott. Use of in-field measurements of green leaf area and incident radiation to estimate the effects of yellow rust epidemics on the yield of winter wheat. *European Journal of Agronomy*, 7: 53–62, 1997. doi: 10.1016/S1161-0301(97)00025-7 .

J. Cartelle, A. Pedró, R. Savin, and G. A. Slafer. Grain weight responses to post-anthesis spikelet-trimming in an old and a modern wheat under mediterranean conditions. *European Journal of Agronomy*, 25(4):365–371, 2006. ISSN 1161-0301. doi: 10.1016/j.eja.2006.07.004 .

A. C. Castro and M. R. Simón. Effect of tolerance to Septoria tritici blotch on grain yield, yield components and grain quality in Argentinean wheat cultivars. *Crop Protection*, 90: 66–76, 2016. ISSN 0261-2194. doi: 10.1016/j.cropro.2016.08.015 .

J.-C. Deswarte, K. Beauchene, G. Arjaure, S. Jezequel, G. Meloux, Y. Flodrops, J. Landrieaux, A. Bouthier, S. Thomas, B. De Solan, and D. Gouache. Platform development for drought tolerance evaluation of wheat in france. *Procedia Environmental Sciences*, 29(Supplement C):93 – 94, 2015. ISSN 1878-0296. doi: 10.1016/j.proenv.2015.07.176 . Agriculture and Climate Change - Adapting Crops to Increased Uncertainty (AGRI 2015).

A. Distelfeld, R. Avni, and A. M. Fischer. Senescence, nutrient remobilization, and yield in wheat and barley. *Journal of experimental botany*, 65(14,SI):3783–3798, Jul 2014. ISSN 0022-0957. doi: 10.1093/jxb/ert477 .

M. J. Foulkes, N. D. Paveley, A. Worland, S. J. Welham, J. Thomas, and J. W. Snape. Major genetic changes in wheat with potential to affect disease tolerance. *Phytopathology*, 96:680–688, 2006. URL http://apsjournals.apsnet.org/doi/pdf/10.1094/PHYTO-96-0680.

D. Gouache, M. Bancal, and P. Bancal. Projet contrat de branche "Tolérance du blé tendre aux stress biotiques et abiotiques" C2008-02 blé tendre, october 2012. URL https://hal.archives-ouvertes.fr/hal-01192469/. Rapport final.

D. Gouache, M. Bancal, B. de Solan, and P. Gate. Tolérance du blé tendre aux stress biotiques et abiotiques. *Innovations Agronomiques*, 35:75–87, 2014. URL https://hal.archives-ouvertes.fr/hal-01192469.

S. J. Inglese and N. D. Paul. Tolerance of Senecio vulgaris to infection and disease caused by native and alien rust fungi. *Phytopathology*, 96(7):718–726, 2006. URL http://apsjournals.apsnet.org/doi/pdf/10.1094/PHYTO-96-0718.

D. J. Lovell, S. R. Parker, T. Hunter, D. J. Royle, and R. R. Coker. Influence of crop growth and structure on the risk of epidemics by Mycosphaerella graminicola (Septoria tritici) in winter wheat. *Plant Pathology*, 46(1):126–138, Feb 1997. ISSN 0032-0862. doi: 10.1046/j.1365-3059.1997.d01-206.x .

J. L. Monteith and C. J. Moss. Climate and the efficiency of crop production in Britain. *Philosophical Transactions of the Royal Society of London. Series B, Biological Sciences*, pages 277–294, 1977.

G. M. Murray, R. H. Martin, and B. R. Cullis. Relationship of the severity of Septoria tritici blotch of wheat to sowing time, rainfall at heading and average susceptibility of wheat cultivars in the area. *Australian journal of agricultural research*, 41(2):307–315, 1990. doi: 10.1071/AR9900307 .

B. Ney, M.-O. Bancal, P. Bancal, I. J. Bingham, J. M. Foulkes, D. Gouache, N. D. Paveley, and J. Smith. Crop architecture and crop tolerance to fungal diseases and insect herbivory. Mechanisms to limit crop losses. *European Journal of Plant Pathology*, 135(3): 561–580, 2013. ISSN 0929-1873. doi: 10.1007/s10658-012-0125-z .

S. R. Parker, S. Welham, N. Paveley, J. M. Foulkes, and R. K. Scott. Tolerance of Septoria leaf blotch in winter wheat. *Plant Pathology*, 53(1):1–10, 2004. doi: 10.1111/j.1365-3059.2004.00951.x .

N. D. Paveley, R. Sylvester-Bradley, R. K. Scott, J. Craigon, and W. Day. Steps in predicting the relationship of yield on fungicide dose. *Phytopathology*, 91(7):708–716, Jul 2001. ISSN 0031-949X. doi: 10.1094/PHYTO.2001.91.7.708 .

G. J. Rebetzke, J. A. Jimenez-Berni, W. D. Bovill, D. M. Deery, and R. A. James. High-throughput phenotyping technologies allow accurate selection of stay-green. *Journal of Experimental Botany*, 67(17):4919–4924, 2016. doi: 10.1093/jxb/erw301 .

M. Reynolds, M. J. Foulkes, G. A. Slafer, P. Berry, M. A. J. Parry, J. W. Snape, and W. J. Angus. Raising yield potential in wheat. *Journal of Experimental Botany*, 60(7): 1899–1918, 2009. doi: 10.1093/jxb/erp016 .

C. Robert, B. Andrieu, C. Fournier, D. Gouache, P. Gate, and B. Ney. Septo3D: un modèle pour analyser les effets de la structure des couverts de blé sur les épidémies de septoriose. In *9. Conférence internationale*, page np, Tours, France, Dec. 2009. Association Française de Protection des Plantes. URL `https://hal.archives-ouvertes.fr/hal-01192172`. Actes sous forme de cédérom + tome résumés.

S. Savary, N. P. Castilla, F. A. Elazegui, C. G. Mc Laren, M. A. Ynalvez, and P. S. Teng. Direct and indirect effects of nitrogen supply and disease source structure on rice sheath blight spread. *Phytopathology*, 85(9):959–965, Sep 1995. ISSN 0031-949X. doi: 10.1094/Phyto-85-959 .

J. Schafer. Tolerance to plant disease. *Annual review of phytopathology*, 9:235–252, 1971. ISSN 0066-4286. doi: 10.1146/annurev.py.09.090171.001315 .

J. D. Scholes and J. F. Farrar. Increased rates of photosynthesis in localized regions of a barley leaf infected with brown rust. *New Phytologist*, 104(4):601–612, 1986. doi: 10.1111/j.1469-8137.1986.tb00660.x .

R. A. Serrago, I. Alzueta, R. Savin, and G. A. Slafer. Understanding grain yield responses to source-sink ratios during grain filling in wheat and barley under contrasting environments. *Field Crops Research*, 150:42–51, August 2013. ISSN 0378-4290. doi: 10.1016/j.fcr.2013.05.016 .

M. W. Shaw and D. J. Royle. Factors determining the severity of epidemics of Mycosphaerella graminicola (Septoria tritici) on winter wheat in the UK. *Plant Pathology*, 42(6):882–899, 1993. ISSN 1365-3059. doi: 10.1111/j.1365-3059.1993.tb02674.x .

V. J. Shearman, R. Sylvester-Bradley, R. K. Scott, and M. J. Foulkes. Physiological processes associated with wheat yield progress in the UK. *Crop Science*, 45(1):175–185, 2005. doi: 10.2135/cropsci2005.0175 .

T. R. Sinclair and P. D. Jamieson. Grain number, wheat yield, and bottling beer: an analysis. *Field Crops Research*, 98(1):60–67, 2006. ISSN 0378-4290. doi: 10.1016/j.fcr.2005.12.006 .

G. A. Slafer, R. Savin, and V. O. Sadras. Coarse and fine regulation of wheat yield components in response to genotype and environment. *Field Crops Research*, 157(0): 71–83, 2014. ISSN 0378-4290. doi: 10.1016/j.fcr.2013.12.004 .

U. Steinfort, B. Trevaskis, S. Fukai, K. L. Bell, and M. F. Dreccer. Vernalisation and photoperiod sensitivity in wheat: Impact on canopy development and yield components. *Field Crops Research*, 201:108–121, 2017. doi: 10.1016/j.fcr.2016.10.012 .

H. Thomas and H. Ougham. The stay-green trait. *Journal of Experimental Botany*, 65(14): 3889–3900, 2014. doi: 10.1093/jxb/eru037 .

D. K. Tompkins, D. B. Fowler, and A. T. Wright. Influence of agronomic practices on canopy microclimate and Septoria development in no-till winter wheat produced in the Parkland region of Saskatchewan. *Canadian Journal of Plant Science*, 73(1):331–344, 1993. doi: 10.4141/cjps93-050 .

C. Uauy, J. C. Brevis, and J. Dubcovsky. The high grain protein content gene Gpc-B1 accelerates senescence and has pleiotropic effects on protein content in wheat. *Journal of Experimental Botany*, 57(11):2785–2794, Aug 2006. ISSN 0022-0957. doi: 10.1093/jxb/erl047 .

Y.-H. Zhang, N.-N. Sun, J.-P. Hong, Q. Zhang, C. Wang, X. Qing-Wu, Z. Shun-Li, H. Qin, and W. Zhi-Min. Effect of source-sink manipulation on photosynthetic characteristics of flag leaf and the remobilization of dry mass and nitrogen in vegetative organs of wheat. *Journal of integrative agriculture*, 13(8):1680–1690, 2014. ISSN 2095-3119. doi: 10.1016/S2095-3119(13)60665-6 .

O. Ziv and Z. Eyal. Assessment of yield component losses caused in plants of spring wheat cultivars by selected isolates of *Septoria tritici*. *Phytopathology*, 68(5):791–796, 1978. ISSN 0031-949X. URL http://apsnet.org/publications/phytopathology/backissues/Documents/1978Articles/Phyto68n05_791.pdf.

E. Zuckerman, A. Eshel, and Z. Eyal. Physiological aspects related to tolerance of spring wheat cultivars to Septoria tritici blotch. *Phytopathology*, 87(1):60–65, Jan. 1997. ISSN 0031-949X. URL http://apsjournals.apsnet.org/doi/pdf/10.1094/PHYTO.1997.87.1.60.

Chapter 8

Synthèse du manuscrit en français

This chapter is an overview of the manuscript addressed to the French reader.

La tolérance du blé à la septoriose

Résumé

La septoriose est la maladie foliaire responsable des plus grandes pertes de rendement du blé en Europe (Burke and Dunne, 2006; Fones and Gurr, 2015). Les méthodes de lutte disponibles (résistance variétale, stratégies d'évitement, fongicides) réduisent les symptômes, mais ne disent rien du rendement d'une culture infectée. L'objet de la tolérance est de satisfaire au remplissage des grains en dépit des symptômes. La prise en compte de la tolérance dans la sélection variétale et/ou les itinéraires techniques permettrait d'optimiser les stratégies de lutte (Paveley et al., 2001). Cela repose sur une optimisation des traits physiologiques de la plante. À partir d'un réseau d'essais expérimental, ainsi que d'essais ciblés au champ et en serre, il apparaît que la phénologie, le profil foliaire, la dynamique de la sénescence pendant le remplissage et le Poids de Mille Grains (PMG) offrent des pistes prometteuses pour accroître la tolérance.

8.1 Introduction

Le concept de tolérance est basé sur une observation simple : des cultures de blé touchées par des épidémies de septoriose comparables (en quantité de symptômes) accusent des pertes de rendement variables (Cobb, 1894; Salmon and Laude, 1932). La tolérance, définie comme la capacité à maintenir le rendement en présence de symptômes (Foulkes et al., 2006; Ney et al., 2013), a très tôt été associée à des approches écophysiologiques de type source/puits (Ellis, 1954) qui décrivent les relations entre organes exportateurs/importateurs d'assimilats. Comme la septoriose est une maladie de

fin de cycle, l'essentiel des dégâts est donc fonction des symptômes qui s'étendent sur les feuilles supérieures. Ceux-ci limitent la photosynthèse et par conséquent l'assimilation de carbone durant la période de remplissage du grain (Serrago et al., 2009). La tolérance vise à assurer qu'en dépit d'une réduction des sources (diminution des surfaces de feuilles vertes), le remplissage des grains (puits) soit maintenu.

Actuellement, deux principales voies sont explorées pour accroître la tolérance (Bingham et al., 2009; Ney et al., 2013). Tout d'abord, les réserves carbonées, essentiellement localisées dans les tiges, constitueraient une source alternative mobilisable lorsque la photosynthèse est limitée par la maladie (Zilberstein et al., 1985; Blum, 1997; Parker et al., 2004). Par ailleurs, un accroissement de la disponibilité des sources permettrait à la culture de supporter une perte liée à l'extension des symptômes (Bingham et al., 2009) ; l'augmentation de la disponibilité des sources est obtenue par une optimisation du profil foliaire (Bingham et al., 2009; Bancal et al., 2015), un élargissement des surfaces photosynthétiques (Foulkes et al., 2006), un allongement de la durée de vie des feuilles pendant le remplissage (Bancal et al., 2015) ou encore une efficacité accrue de la photosynthèse (Zuckerman et al., 1997). Enfin, le niveau de disponibilité en assimilats par grain conditionnerait les pertes observées (van den Berg et al., 2017) : s'il est pléthorique les pertes seront nulles ou faibles ; s'il est limitant, la réduction des sources par les maladies se traduira par une diminution du PMG. Ce sont les principales hypothèses explorées au cours de cette thèse.

Le manuscrit se compose d'une revue de la littérature scientifique (Chapitre 1, p.1) visant à définir les concepts sur lesquels repose la tolérance du blé à la septoriose, décrire les processus physiologiques invoqués dans le manuscrit, et identifier les manques scientifiques et les enjeux qui justifient les objectifs de ce travail de thèse. Les méthodologies déployées et l'articulation des études menées sont présentées dans le Chapitre 2 (p.43) avec une description générale des outils, des matériels et des méthodes utilisés. Les quatre chapitres suivants (chapitres 3 – 6, p.53) constituent les synthèses des quatre études misent en œuvre lors de ce projet. Enfin, une large discussion des résultats est proposée au Chapitre 7 (p.205), où les faits saillants de la thèse sont mis en lumière, ressitués dans un cadre général afin d'appréhender la portée du travail réalisé mais aussi de suggérer de nouvelles hypothèses et perspectives à l'aune de ces nouveaux résultats.

8.2 Les études réalisées

8.2.1 Présentation générale du matériel et des méthodes

Un retard de la sénescence foliaire allonge la durée de la photosynthèse durant le remplissage des grains, accroît la disponibilité des ressources et constitue un trait potentiel de tolérance (Bancal et al., 2015). Cette piste privilégiée a été l'objet d'une première

étude qui consista en une tâche de datamining exploitant des données historiques tirées du travail de Bancal et al. (2015). À cette occasion, une stratégie d'analyse de données a été développée et appliquée aux données d'essais impliquant neuf cultivars dans neuf environnements (cinq localisations et deux saisons) en l'absence de maladie. Cette stratégie a permis d'identifier des traits génotypiques et des variables environnementales qui affectent la sénescence, et a fourni ainsi de nouvelles hypothèses de traits de tolérance du blé à la septoriose. Ensuite, afin de comprendre le lien entre la tolérance et le métabolisme azoté, un essai a été conduit en serre (2014–2016, S2015) sur des mini-couverts cultivés à l'UMR ÉcoSys Grignon, France). Quatre génotypes, de niveau de tolérance connue et contrastée, ont été soumis à un arrêt brutal de la nutrition azotée (cultures semi-hydroponiques) et inoculé de septoriose à l'émission de la dernière feuille. Dans un autre essai mené au champ (2014–2015) sur six génotypes (C2015 ; Herefordshire, Royaume Uni), une manipulation d'égrainage a exploré la relation entre les équilibres source/puits et la tolérance à la septoriose. Finalement, les résultats et hypothèses résultants de ces études ont été confrontés à ceux obtenus pour six cultivars modernes dans un essai final au champ (2015–2016) à Nottingham (Royaume Uni ; C2016). Un récapitulatif des études menées est proposé Tab. 2.1 (p.44).

Génotypes et cultivars

Les neuf cultivars de l'étude de datamining constituaient une gamme commune à neuf essais (notés "Expe.C" dans Bancal et al., 2015), ce jeu de données relativement équilibré a permis une étude confortable des interactions génotypes × environnements. Qui plus est, et contrairement à l'usage, ces cultivars étaient de précocité variable et caractérisés par une large fenêtre de dates d'épiaison.

Les essais au champ et en serre de 2014–15 (C2015 et S2015) ont employé des génotypes qui faisaient parti d'un panel dérivé de deux populations d'haploïdes doubles, testés et sélectionnés selon le potentiel de rendement et l'expression de tolérance. La première population est issue du croisement entre Cadenza (blé de printemps panifiable britannique) et Lynx (blé d'hiver britannique), la seconde du croisement entre Rialto (blé d'hiver de biscuiterie/panifiable, britannique) et LSP2, blé de printemps mexicain obtenu par le CIMMYT et caractérisé par de gros épis. La seconde population visait à étendre la gamme de phénotypes et d'équilibres source/puits pour du blé d'hiver à haut potentiel de rendement. Les données de trois essais indépendants ont été utilisées pour estimer une note de tolérance (voir paragraphe 4.2.1, p.107). Par conséquent, bien que les essais en serre et au champ de 2014–15 (S2015, C2015) aient généré des épidémies de septoriose de faible incidence et sévérité, la note de tolérance ainsi obtenue (Tab. 4.1 et Fig. 5.1, p.112 et p.129 respectivement) a été utilisée pour identifier des traits de tolérance observés par ailleurs dans ces couverts sains. Ce raisonnement fait écho à la démarche

publiée par Bancal et al. (2015).

Finalement, le dernier essai examina des cultivars de blés modernes, actuellement cultivés et recommandés au Royaume Uni (HGCA, 2015; RAGT, 2016; AHDB, 2016). Il s'appuie sur les essais précédents qui ont démontré un lien possible entre la précocité épiaison et le potentiel de tolérance à la septoriose. Les cultivars ont donc été choisi pour exprimer une longue gamme de précocité, avec une différence de date d'épiaison de 15 jours entre les cultivars les plus précoces et les plus tardifs.

Analyse de croissance

Les méthodes expérimentales des deux essais au champs (C2015, C2016) et de l'essai en serre (S2015) reposent sur un échantillonnage de brins débutant de manière générale autour de la date d'épiaison. Les brins étaient sélectionnés/identifiés selon des méthodes visant à réduire la variabilité aléatoire de la taille des brins. Les échantillons étaient généralement disséqués, de manière à fournir des informations sur l'évolution de la biomasse par organe, y compris l'évolution des composantes de rendement (nombre de grains et poids de grain). En plus de la masse de matière sèche acquise systématiquement, des mesures de teneurs en azote ont été réalisées en serre.

Healthy Area Duration, HAD/Indice foliaire vert intégré, IFVI

L'estimation des sources disponibles lors du remplissage des grains est basée sur le calcul de l'IFVI (équivalent en anglais au HAD dans le manuscrit), c'est à dire l'aire sous la courbe de l'évolution des surfaces vertes depuis l'épiaison. Ceci est justifié par la sénescence monocarpique qui caractérise le cycle de vie du blé. La surface des trois feuilles supérieures a été mesurée, et l'évolution des surfaces vertes/malades/sénescentes suivie lors de 5 à 8 évaluations du pourcentage de surface du limbe selon l'expérimentation et la modalité. Les cinétiques d'évolution des surfaces vertes ont été ajustées à une fonction de Gompertz, permettant une estimation de l'air sous la courbe (IFVI, Eq.2.1 p.50 et Eq.2.2 p.51). Qui plus est, la fonction est basée sur des paramètres I et D, qui correspondent respectivement à une approximation de la durée de la phase de sénescence depuis l'épiaison, et de la phase de sénescence rapide (Fig. 2.1 p.50). L'IFVI a été calculé d'abord à l'échelle du brin puis rapporté à l'échelle de la culture et du grain en ayant recours aux estimations de densité d'épis par unité de surface et du nombre de grains par épi.

Tolérance

L'estimation de la tolérance a connu des évolutions importantes. En effet, Schafer (1971) considéra que la tolérance s'estime par comparaison du rendements de culti-

vars exposés à des épidémies de septoriose comparables. Ceci limite considérablement l'extrapolation des valeurs de tolérance ainsi obtenues. Depuis, Kramer et al. (1980) ou encore Inglese and Paul (2006) ont suggéré d'utiliser la relation entre l'aire sous la courbe de l'évolution des symptômes de la maladie (AUDPC : Area Under the Disease Progress Curve) et le rendement pour évaluer la tolérance de l'orge à la rouille, ou du sèneçon (*Senecio vulgaris*) à une maladie. Ceci représente un progrès, néanmoins une estimation de la sévérité de la maladie telle que le AUDPC ne prend pas compte les sources finalement disponibles. Contrairement au AUDPC, l'IFVI (ou HAD) quantifie les ressources disponibles lors de la phase de remplissage en tenant compte des dimensions du couvert, variable d'un génotype — ou d'un environnement — à l'autre et des symptômes de septoriose. La tolérance a donc été estimée par des rapports entre évolution des puits (rendement grain) et évolution des sources (IFVI) en réponse à un traitement (maladie, égrainage, arrêt de la nutrition azotée) conformément aux études publiées de tolérance du blé à la septoriose (Parker et al., 2004; Foulkes et al., 2006; Castro and Simón, 2016). Le rapport décrit généralement la perte de rendement au regard d'une diminution des sources. Plusieurs alternatives ont été utilisées, et les différentes échelles (culture, brin, grain) ont été considérées. La méthode d'estimation de la tolérance a fait l'objet d'une discussion approfondie.

8.2.2 Datamining : effets du génotype et de l'environnement sur la sénescence et le poids des grains

Cette étude a fait l'objet de deux posters présentés lors des conférences :

- the 9th International Symposium on Septoria Diseases of Cereals, 7–9 April 2016, Paris, France, (Collin et al., 2016b).
- the 14th Congress of the European Society for Agronomy, 5–9 September 2016, Edinburgh, Scotland (Collin et al., 2016a).

Bancal et al. (2015) identifièrent que la sénescence et le poids des grains (PMG, Poids de Mille Grains) sont des traits potentiel de tolérance. Si les mécanismes physiologiques qui régissent la sénescence et le PMG sont globalement connus, il n'en est pas de même quant aux relations quantitatives ou leur plasticité, c'est à dire leur réponse aux variations environnementales. Plus concrètement, l'objectif est d'identifier des traits qui influencent la sénescence et qui sont probablement, par extension, des traits de tolérance. À partir d'un jeu de données présentant de bonnes propriétés, 6–9 génotypes cultivés dans 9 environnements (Fig. 3.1 p.58 ; 2 saisons, 5 sites répartis dans le Nord de la France, correspondant à "Expe.C" dans l'article de Bancal et al. 2015), trois outils ont été déployés pour répondre à des questions spécifiques :

1. **Variables importantes ?** Tout d'abord, parce qu'on a voulu étudier l'impact potentiel d'un grand nombre de variables (climatiques, génétiques) sur la sénescence ou le PMG, une méthode de machine learning a été employée : les modèles Random Forest (Breiman, 2001). Cet outil a identifié, sans *a priori*, les variables importantes dans ce jeu de données, influençant la sénescence et le PMG.

2. **Relations linéaires ?** Néanmoins, les modèles Random Forest sont des modèles qualifiées de "boîtes noires", ils peuvent identifier les variables importantes et il est même possible de les utiliser pour fournir des prédictions, mais on n'a pas accès à la nature de la relation entre la variable réponse et les variables explicatives (*comment varie y en fonction de x ?*). Par conséquent, des modèles de régressions multiples ont été ajustés estimant les relations linéaires entre sénescence ou PMG et les variables explicatives importantes selon les modèles Random Forest.

3. **Génotype**, **Environnement et interactions ?** Finalement, parce que le jeu de données comportent plusieurs environnements et génotypes, il convenait de déterminer dans quelle mesure les variables et relations importantes variaient avec l'environnement ou le génotype. Une analyse des composantes de la variance (Crawley, 2012) et une étude des régressions entre résidus partiels ont été employées à cette fin.

La méthode elle-même constitue un développement intéressant pour identifier des variables d'intérêt et estimer la variabilité G×E, ce point est discuté et approfondi au paragraphe 3.4.1 (p.92). Les principaux résultats suggèrent que la phénologie tient un rôle important dans la sénescence. En effet, la précocité de la date d'épiaison (qui variait de 10 à 15 jours selon l'essai, 40% de variation expliqués par la variété, Fig. 3.6 p.75) permettrait d'améliorer les conditions lors de la période de remplissage du grain. Par ailleurs, le profile foliaire influence également la sénescence. Une large proportion de surface de feuille représentée par la feuille étendard (fLA1) retarderait la sénescence. Cependant, de manière surprenante, la date d'épiaison et fLA1 sont liées (Fig. 3.5 p.73). Si la raison demeure largement inconnue (association génétique, réponse à la phénologie, *etc*) les variétés précoces étaient néanmoins associées aux variétés à grande fLA1. Il s'agit là d'un résultat surprenant mais aussi partiellement cohérent avec les résultats de Steinfort et al. (2017) qui ont i) identifié une relation entre la durée du jour au semis de blés de printemps et la surface de la feuille étendard, et ii) reporté les données nécessaires au calcul variétal de fLA1 qui confirment nos résultats. L'intérêt de la fraction de feuille étendard est également accentué puisque ce trait varie essentiellement avec la variété : c'est un trait largement héritable. Les variables de nombre de grains par épi ou par unité de surface sont également associées à la sénescence du couvert. Plusieurs variables climatiques ont été sélectionnées, l'explication biologique est parfois peu évidente ou même pertinente, mais elles renvoient aux contrastes importants entre les deux années

de l'expérimentation. S'agissant de la variable réponse PMG, peu de résultats concluant sont reportés, seule la relation aux nombre de grains par unité de surface est pertinente (Fig. 3.9 p.79) et permet, sur un cas connu, d'apprécier i) les résultats fournis par ces méthodes d'analyses et ii) l'importance ou les implications des interactions génotypes environnements sur une relation bivariée.

8.2.3 Champ 2014-15 (C2015)

Ce chapitre est l'objet d'un article scientifique à comité de lecture, voir Collin et al. (2018).

La principale hypothèse de travail était que des génotypes contrastés pour la tolérance sont également contrastés du point de vue des équilibres source/puits.

Cet essai est basé sur des génotypes contrastés pour la tolérance à la septoriose. Ils sont issus de deux populations de génotypes haploïdes doubles issues des croisements entre les génotypes Cadenza × Lynx (blé de printemps de qualité boulangère × blé d'hiver) et LSP2 × Rialto (blé de printemps mexicain à gros épis × blé d'hiver de qualité boulangère/biscuiterie) afin d'obtenir une gamme étendue de phénotypes. Parmi ces populations, 6 génotypes ont été sélectionnés sur le haut potentiel de rendement et le contraste pour la tolérance. Ils ont été exposés à un traitement fongicide dont le but était de générer des épidémies de septoriose mais en maintenant les autres maladies à un niveau négligeable. Pour générer des gammes d'équilibres sources/puits au champ, ces génotypes ont été exposés à une fertilisation azotée tardive et un traitement d'égrainage pour lequel la moitié supérieure de l'épi a été retirée 200 degrés jours après la floraison.

L'épidémie naturelle de septoriose a été particulièrement faible cette année et n'a pas pu être exploitée pour estimer la tolérance *in situ* des génotypes. Néanmoins, la tolérance des génotypes a été estimée durant trois expérimentations préliminaires au champ. La tolérance à la septoriose était corrélée avec des traits des microparcelles saines : Poids de Mille Grain (PMG) et importante proportion de surface foliaire représentée par la feuille 3 (fLAI3). Par ailleurs, la modalité d'égrainage a démontré que ces génotypes présentaient un degré de limitation du remplissage des grains par les sources très variable et corrélé à leur tolérance. Par conséquent, nous avons proposé un index de tolérance basé sur une modalité d'égrainage qui est beaucoup plus accessible et répétable que l'estimation directe de la tolérance à la septoriose. D'un point de vue méthodologique, l'estimation de l'IFVI par grain pour estimer l'accroissement du rapport source/puits suite à la manipulation d'égrainage est également discuté. Finalement, le potentiel de rendement de ces génotypes n'était pas corrélé à la tolérance, il serait donc possible de sélectionner des variétés pour leur tolérance sans compromis avec leur potentiel de rendement.

8.2.4 Serre 2014-15 (S2015)

Cet essai a été motivé par le lien qui existe entre les flux d'azote et de carbone dans la plante. En effet, le grain est composé de 10 à 15% de protéines. L'essentiel du flux d'azote vers le grain après floraison est alimenté par la remobilisation depuis les organes végétatifs (e.g. tiges, feuilles). Or, l'essentiel de l'azote est également associé aux fonctions photosynthétiques (Evans, 1989). Par conséquent, la remobilisation de l'azote induit une diminution de la photosynthèse et une diminution du flux de carbone post-floraison qui alimente le grain en amidon (ce dont il est composé à plus de 80%). Les sorts de l'azote et du carbone après floraison sont donc liés, de leur interaction dépend le rendement en grains (Zhang et al., 2014). L'objectif principal de l'essai était d'étudier le lien entre tolérance et métabolisme azoté. Un essai en conditions contrôlées (serre + semi-hydroponie) est justifié par le contrôle de l'alimentation en azote de la culture qu'il offre.

L'essai en serre s'appuie sur quatre hypothèses :

- la tolérance reposant sur des équilibres source/puits, il est possible de produire en serre des couverts semblables à ceux généralement obtenus au champ, avec des paramètres cohérents (architecture, nombre d'épis, nombre de grains, *etc*).
- les variations génotypiques observées au champ se traduisent par des variations génotypiques cohérentes en serre.
- les traits des génotypes associés à une faible limitation du remplissage des grains par les sources sont des traits de tolérance potentiels.
- les variations de tolérance à la septoriose dépendent du génotype et sont liées au métabolisme azoté.

Quatre génotypes contrastés pour la tolérance parmi les six utilisés dans l'essai au champ 2014-15 (C2015) ont été exploités ici. La méthode de culture en serre en semi-hydroponie a assuré l'obtention d'un couvert dense assez semblable au champs. Au stade GS44, immédiatement après un échantillon initial, l'alimentation azotée a été stoppée pour la moitié des plantes et suivie par une inoculation au pinceau des deux feuilles supérieures par une solution de spores de *Septoria tritici*. Ensuite, une analyse de la croissance a été réalisée, en suivant l'évolution des surfaces vertes, les masses de biomasses sèches, les teneurs en azote et les composantes de rendement.

L'inoculation n'a pas généré de maladie mais a induit un égrainage physiologique expliqué par l'avortement de fleurs probablement associé à l'extinction des lampes que la méthode d'inoculation nécessitait (Demotes-Mainard et al., 1995, 1996; Fischer and Stockman, 1980). Le traitement azoté a quant à lui engendré une sénescence précoce

réduisant fortement la disponibilité des sources (IFVI) et résultant en une diminution du rendement variable. Le contraste azoté a donc été utilisé pour estimer un ratio de tolérance (perte de rendement par unité de réduction des sources). Les génotypes ont produit une gamme étendue de phénotypes. L'expérimentation, conduite en conditions hivernales, a été exposée a des niveaux de radiations relativement faibles induisant une faible biomasse associée à une nombre de grains faible en comparaison de l'essai au champ. Néanmoins, le couvert produit était caractérisé par un nombre de talles réduit contrairement aux plantes isolées généralement étudiées lors d'essais en serre. Les traitements ont généré des phénotypes variés, dont un effet stay-green pour l'un des génotypes. De l'indice de nutrition azotée (INN, Justes et al., 1994) nous avons déduit que les plantes n'étaient généralement pas sur-fertilisées, même lorsque l'alimentation azotée était maintenue en post-floraison. Les relations source/puits à l'échelle du brin étaient peu cohérentes étant donnés les faibles niveau de biomasses, les larges feuilles étendards et les contrastes importants d'IFVI résultant du traitement azoté. Néanmoins, rapporté au nombre de grains ou à l'échelle de la culture, les résultats obtenus étaient comparables à l'essai réalisé au champ (2014-15). En serre, le potentiel de rendement n'était pas associé à la note de tolérance des génotypes. La forte remobilisation azotée observée pour les génotypes tolérants était tout à fait surprenante. Qui plus est, la forte remobilisation azotée était associée à une sénescence tardive de la feuille étendard. En effet, il est attendu de génotypes stay-green, porteurs du gène NAM-B1, une sénescence tardive associée à une faible remobilisation de l'azote pénalisant le rendement protéique du grain par un mécanisme de dilution. Or, dans notre essai, les génotypes tolérants présentaient une longue durée de vie des feuilles et une meilleure remobilisation de l'azote. D'autre traits on été soulignés mais de portée plus limitée.

8.2.5 Champ 2014-16 (C2016)

Les études précédentes ont identifié des traits potentiels de tolérance à la septoriose, soit en se basant sur des données historiques, soit en utilisant des dispositifs expérimentaux dédiés, étudiant les relations sources/puits de génotypes contrastés pour la tolérance (C2015 et S2015). Ce dernier essai au champ visa à vérifier si les résultats basés, entre autres, sur des génotypes sont valides sur une gamme de variétés modernes cultivées. Au contraire des essais en serre (S2015) et au champ (C2015) précédents, la tolérance de ces variétés n'était pas connue. Néanmoins, selon les résultats de l'étude de datamining, la précocité épiaison serait un trait de tolérance. De ce fait, les variétés ont été choisies de manière à représenter une large gamme de précocité épiaison, supposée associée à une large gamme de tolérance.

Plus spécifiquement, dans cet essai on a cherché à vérifier si :

- la tolérance à la septoriose est associée à un degré de limitation des puits par les

sources réduit.

- le faible limitation de la croissance des grains par les sources disponibles peut être obtenue par un IFVI élevé.
- la précocité épiaison est associée à une sénescence tardive et une augmentation des sources.
- pour les maladies de fin de cycle (telles que la septoriose), l'étude de la tolérance à l'échelle de la culture ou rapportée à l'échelle du grain sont équivalentes.

Six variétés de précocité épiaison contrastée ont été cultivées dans un essai en blocs randomisés, comprenant une modalité fongicide destinée à produire un contraste de septoriose. C'est le seul essai qui a généré une forte épidémie de septoriose. Plusieurs méthodes d'estimation de la tolérance ont été testées. Dans l'ensemble, le rang des cultivars pour la tolérance est stable, et les estimations de la tolérance rapportées à l'échelle de la culture ou bien à l'échelle du grain étaient très corrélées. Ces différents indicateurs de tolérance ont été synthétisé dans une estimation standard, qui s'est révélée corrélée à un certain nombre de traits, dont la date d'épiaison.

8.3 Discussion

De nouvelles données source/puits

Les trois expérimentations ont généré de nouvelles données sources/puits aux échelles du brin, du grain ou de la culture. Dans l'essai au champ 2014–15 (C2015), l'égrainage a été le principal facteur générant une gamme étendue d'équilibres source/puits. En C2015, les puits (les épis) ont été diminués à l'échelle du brin et de la culture par le traitement d'égrainage alors que le rapport source/puits a été fortement accru à l'échelle du grain. Dans l'essai en serre (S2015), la gamme d'équilibres source/puits a été accentuée par la modalité d'arrêt de la nutrition azotée à GS44 en réduisant la disponibilité des sources durant la période post-épiaison (IFVI) sans modifier le nombre de grains par épi. Dans les deux essais C2015 et S2015 les modalités de contraste de septoriose (fongicide et inoculation, respectivement) n'ont pas permis d'obtenir une sévérité de maladie suffisante pour qu'elles soient utilisées en tant que telles. Au contraire, les traitements fongicides appliqués dans l'essai au champ 2015–2016 (C2016) ont abouti à de forts contrastes entre microparcelles saines et malades.

À l'échelle de la culture, les sources (IFVI) obtenues en S2015 étaient comparables aux données obtenue en C2015. En C2016, compte tenu des IFVI élevés, les rendements obtenus étaient eux aussi élevés et proches du plateau théorique conformément aux attentes pour des cultivars à haut potentiel en conditions de cultures intensives (Gouache

et al., 2014, Fig.7.1 p.207). Au contraire, en S2015, les rendements étaient faibles sous les deux modalités de nutrition azotés. En C2015, les mauvaises conditions d'implantation de la culture ont été responsable d'une densité d'épis assez faible, maintenant néanmoins un rendement par épi (ou de la culture) élevé au regard de l'IFVI. En S2015, la biomasse accumulée par brin était faible, expliquée par le faible rayonnement au moment de la culture. Mais les conséquences du faible rayonnement ne s'arrêtent pas aux biomasses puisque le nombre de grains était lui aussi faible en comparaison des essais au champ. Par conséquent, ramené à l'échelle du grain, les données des trois essais étaient cohérentes.

Estimation de la tolérance

Plusieurs méthodes d'estimation de la tolérance ont été employées, basées sur des rapports entre perte de rendement et diminution d'IFVI causées par un stress (égrainage, azote, maladie). Il faut admettre que cette estimation pause des problèmes d'ordre mathématique, liés aux propriétés de la fonction inverse. Ainsi, si ces rapports sont utiles pour comparer et classer des génotypes selon leur tolérance, les valeurs absolues obtenues sont d'utilité limitée. Voir paragraphe 7.3.1 p.208.

Plusieurs méthodes pour améliorer les estimations de la tolérance ont été proposées. La première consiste à utiliser les données de plusieurs essais. En effet, si les variations environnementales sont en générale grandes, le classement des génotypes inclus dans les essais C2015 et S2015 s'est révélé relativement stable selon les résultats de trois essais indépendants antérieurs. Plusieurs essais peuvent ainsi fournir une estimation plus robuste d'une note de tolérance génotypique. Néanmoins, en C2016, aucune estimation antérieure de la tolérance n'était disponible pour les cultivars testés. L'utilisation de plusieurs méthodes et plusieurs échelles ont renforcé l'estimation de la tolérance au cours de ce dernier essai.

Une autre limite à l'utilisation des ratios pour estimer la tolérance repose dans la confusion qui est entretenue entre : disponibilité des sources (IFVI), efficacité de la culture (conversion de l'IFVI en rendement) et tolérance. Une approche basée sur l'utilisation des courbes potentielles (Gouache et al., 2014) permettrait de lever cette ambigüité et d'apporter de nouvelle informations sur les performances de la cultures. Voir paragraphe 7.3.2 p.209.

Enfin, ce manuscrit étudie la tolérance selon différentes échelles. L'échelle du brin est peu pertinente pour les études écophysiologiques d'ordre source/puits puisqu'elle ne prend pas en compte les paramètres du peuplement (densité d'épis / nombre de grains par épi et compétition pour la ressource). En revanche, l'échelle de la culture et l'échelle du grain sont cohérentes entre elles et apportent un éclairage complémentaire aux études de tolérance. En effet, il ne s'agit pas simplement d'un changement d'échelle puisque les facteurs limitant en jeu ne sont pas les mêmes. À l'échelle de la culture, l'augmentation de

l'IFVI tend vers une saturation de l'interception lumineuse : les sources à l'échelle de la culture tendent donc inévitablement vers un maximum. À l'échelle du grain, le processus en jeu implique la limite physiologique d'expansion du grain, la capacité même du grain à accumuler des assimilats : la taille du puits tend vers un maximum. Ceci explique que l'égrainage appliqué lors de C2015 est en réalité associé à une augmentation des ressources par grain restant. L'égrainage induit un surplus de croissance des grains plus ou moins important, selon le degré de saturation par les sources. Voir paragraphe 7.3.3 p.211.

Les traits de tolérance à la septoriose

Les résultats des différents essais sont comparés au paragraphe 7.4.1 p.212. Des traits de tolérance ont été identifiés. Ainsi, alors qu'il est généralement admis que la croissance du grain est limitée par les puits, l'essai au champ (C2015), et dans une moindre mesure celui en serre (S2015), montrent que le contraste avéré de tolérance entre ces génotypes est lié à la variabilité du degré de limitation de la croissance des grains par la disponibilité d'assimilats provenant des sources. D'autre part, une sénescence tardive du couvert, ou de la feuille étendard, est un trait de tolérance confirmé dans les essais au champ. La sénescence tardive est elle-même promue par une épiaison précoce ou encore par la taille de la feuille étendard (en proportion de la surface totale représentée par les feuilles supérieures). La distribution verticale de la surface foliaire serrait aussi directement liée à la tolérance ; la sévérité des symptômes de septoriose est généralement plus faible sur la feuille étendard, étant donnée la propagation du bas vers le haut de la maladie. Les deux effets ont pu s'additionner dans l'essai au champ (C2016) où la proportion de feuille étendard était corrélée à la tolérance observée. Par ailleurs, les gammes générées dans nos essais ne permettaient pas de confirmer le lien entre tolérance et efficacité photosynthétique ou remobilisation des réserves des tiges. Enfin, parmi les essais entrepris, potentiel de rendement et tolérance n'on jamais été antagonistes ; la recherche de génotypes et/ou d'itinéaires techniques tolérants n'impliquent pas de renoncer à un haut niveau de performance agricole.

Environnement

L'estimation de la tolérance à la septoriose est caractérisée par une forte variabilité environnementale (E). Parker et al. (2004) ont eu recours à des modèles mixtes pour tenir compte de l'effet aléatoire de l'environnement ; Bancal et al. (2015) ont calculé des indices épidémiques pour estimer la variabilité de la sévérité des épidémies de septoriose d'un essai à l'autre ; Foulkes et al. (2006) ont évoqué eux aussi le problème de la prise en compte de E. Le Chapitre 3 a pris en compte la variabilité E entre neuf essais pour déterminer des traits génotypiques et effets environnementaux affectant la sénescence et

le PMG. C'est bien la prise en compte de E qui a permis l'identification de traits, tels que la date d'épiaison, qui n'auraient sinon pas été détectés.

La tolérance a été étudiée ici dans l'objectif d'identifier des traits de tolérance. Pourtant, la tolérance serait également une propriété émanant de l'environnement : certains environnements étant plus propices à l'expression de tolérance que d'autres. Par exemple, si la précocité épiaison (probable trait de tolérance) varie significativement avec le génotype, le Chapitre 3 montre également que 60% de la variabilité de la précocité épiaison observée dans le jeu de données correspondant était due à E.

8.4 Conclusion

La tolérance à la septoriose et le potentiel de rendement du blé ne sont pas incompatibles. Des traits de tolérance du blé à la septoriose ont été identifiés ; la principale voie pour générer de la tolérance serait d'accroître la disponibilité des sources en regard de la demande des grains.

L'étude de la tolérance à la septoriose est avant tout une étude des relations source/puits et peut donc être réalisée à l'échelle du grain ou de la culture. L'échelle du brin n'est pas utilisable en raison des compensations physiologiques entre source et puits. Par ailleurs, l'estimation des sources durant le remplissage bénéficierait grandement de l'emploi de méthodes de phénotypage haut débit. Cela constituerait un progrès significatif dans la mesure et la prise en compte de la tolérance comme un caractère mesurable des variétés.

Finalement, la première analyse de données réalisée incluant plusieurs génotypes et environnements démontre également la plasticité de la tolérance, qui dépend à un certain degré de l'environnement. Par extension, chaque environnement est caractérisé par un potentiel de tolérance. Ceci ouvre la voie à un raisonnement exigeant et justifié pour ajuster les itinéraires techniques et l'emploi de fongicides en réponse à un risque de perte de rendement.

References

AHDB. Ahdb Recommended List - winter wheat 2016/17. tables, 2016. URL https://cereals.ahdb.org.uk/media/883980/1-RLDL_2016-17_Winter_Wheat_RL-V6.pdf.

P. Bancal, M.-O. Bancal, F. Collin, and D. Gouache. Identifying traits leading to tolerance of wheat to Septoria tritici blotch. *Field Crops Research*, 180:176–185, 2015. doi: 10.1016/j.fcr.2015.05.006 .

I. J. Bingham, D. R. Walters, M. J. Foulkes, and N. D. Paveley. Crop traits and tolerance of wheat and barley to foliar disease. *Annals of Applied Biology*, 154:159–173, 2009. doi: 10.1111/j.1744-7348.2008.00291.x .

A. Blum. Improving wheat grain filling under stress by stem reserve mobilisation. In *Wheat: Prospects for Global Improvement*, pages 135–141. Springer, 1997. URL https://link.springer.com/article/10.1023%2FA%3A1018303922482.

L. Breiman. Random forests. *Machine Learning*, 45(1):5–32, 2001. ISSN 1573-0565. doi: 10.1023/A:1010933404324 .

J. Burke and B. Dunne. Septoria tritici in winter wheat – to spray or not to spray? *Irish farmer*, pages 14–18, April 2006.

A. C. Castro and M. R. Simón. Effect of tolerance to Septoria tritici blotch on grain yield, yield components and grain quality in Argentinean wheat cultivars. *Crop Protection*, 90: 66–76, 2016. ISSN 0261-2194. doi: 10.1016/j.cropro.2016.08.015 .

N. A. Cobb. *Contributions to an economic knowledge of Australian rusts (Uredineae)*, chapter Chapter 10, pages 239–250. Agricultural Gazette of New South Wales, 1894.

F. Collin, P. Bancal, J. Foulkes, and M. O. Bancal. A statistical analysis of gxe contribution to leaf senescence during grain filling in wheat. In *ESA 14 - Growing landscapes - Cultivating innovative agricultural systems*, pages 13–14, Edinburgh, Scotland, September 2016a. ESA. Poster presentation - session 12.

F. Collin, D. Gouache, M.-O. Bancal, and P. Bancal. Tolerance of wheat to Septoria tritici blotch; genetic vs environmental variations of key traits. In *9th International Symposium on Septoria Diseases of Cereals*, page 76, Paris, France, April 2016b. ISSDC. Poster presentation.

F. Collin, P. Bancal, J. Spink, P. Kock Appelgren, J. Smith, N. D. Paveley, M.-O. Bancal, and M. J. Foulkes. Wheat lines exhibiting variation in tolerance of Septoria tritici blotch differentiated by grain source limitation. *Field Crops Research*, 217:1– 10, March 2018. ISSN 0378-4290. doi: 10.1016/j.fcr.2017.11.022 . URL https://www.sciencedirect.com/science/article/pii/S0378429017312078.

M. J. Crawley. *The R Book, 2nd Edition*, chapter Mixed-Effects Models, pages 681–714. Wiley, 2012. ISBN 978-0-470-97392-9.

S. Demotes-Mainard, G. Doussinault, and J. M. Meynard. Effects of low radiation and low temperature at meiosis on pollen viability and grain set in wheat. *Agronomie*, 15:357–365, 1995. URL https://hal.archives-ouvertes.fr/hal-00885691/document.

S. Demotes-Mainard, G. Doussinault, and J. M. Meynard. Abnormalities in the male developmental programme of winter wheat induced by climatic stess at meiosis. *Agronomie*, 15:357–365, 1996. URL https://hal.archives-ouvertes.fr/hal-00885813/document.

R. T. Ellis. Tolerance to the maize rust *Puccinia polysora* underw. *Nature*, 174:1021, 1954.

J. R. Evans. Photosynthesis and nitrogen relationships in leaves of C3 plants. *Oecologia*, 78: 9–19, 1989. URL https://link.springer.com/article/10.1007%2FBF00377192?LI=true.

R. A. Fischer and Y. M. Stockman. Kernel number per spike in wheat (*Triticum aestivum* l.): responses to preanthesis shading. *Australian Journal of Plant Physiology*, 7(2):169–180, 1980. doi: 10.1071/PP9800169 .

H. Fones and S. Gurr. The impact of Septoria tritici blotch disease on wheat: An EU perspective. *Fungal Genetics and Biology*, 79:3 – 7, 2015. ISSN 1087-1845. doi: 10.1016/j.fgb.2015.04.004 . Septoria tritici blotch disease of wheat: Tools and techniques to study the pathogen Zymoseptoria tritici.

M. J. Foulkes, N. D. Paveley, A. Worland, S. J. Welham, J. Thomas, and J. W. Snape. Major genetic changes in wheat with potential to affect disease tolerance. *Phytopathology*, 96:680–688, 2006. URL http://apsjournals.apsnet.org/doi/pdf/10.1094/PHYTO-96-0680.

D. Gouache, M. Bancal, B. de Solan, and P. Gate. Tolérance du blé tendre aux stress biotiques et abiotiques. *Innovations Agronomiques*, 35:75–87, 2014. URL https://hal.archives-ouvertes.fr/hal-01192469.

HGCA. HGCA recommended list - winter wheat 2015/16. tables, 2015. URL https://cereals.ahdb.org.uk/media/537620/winter-wheat-2015-16.pdf. Accessed 2017-07-04.

S. J. Inglese and N. D. Paul. Tolerance of Senecio vulgaris to infection and disease caused by native and alien rust fungi. *Phytopathology*, 96(7):718–726, 2006. URL http://apsjournals.apsnet.org/doi/pdf/10.1094/PHYTO-96-0718.

E. Justes, B. Mary, J. M. Meynard, J. M. Machet, and L. Thelierhuche. Determination of a critical nitrogen dilution curve for winter-wheat crops. *Annals of Botany*, 74(4):397–407, Oct 1994. ISSN 0305-7364. doi: 10.1006/anbo.1994.1133 .

T. Kramer, B. H. Gildemacher, M. Van der Ster, and J. E. Parlevliet. Tolerance of spring barley cultivars to leaf rust, Puccinia hordei. *Euphytica*, 29(2):209–216, 1980. ISSN 1573-5060. doi: 10.1007/BF00025116 .

B. Ney, M.-O. Bancal, P. Bancal, I. J. Bingham, J. M. Foulkes, D. Gouache, N. D. Paveley, and J. Smith. Crop architecture and crop tolerance to fungal diseases and insect herbivory. Mechanisms to limit crop losses. *European Journal of Plant Pathology*, 135(3):561–580, 2013. ISSN 0929-1873. doi: 10.1007/s10658-012-0125-z .

S. R. Parker, S. Welham, N. Paveley, J. M. Foulkes, and R. K. Scott. Tolerance of Septoria leaf blotch in winter wheat. *Plant Pathology*, 53(1):1–10, 2004. doi: 10.1111/j.1365-3059.2004.00951.x .

N. D. Paveley, R. Sylvester-Bradley, R. K. Scott, J. Craigon, and W. Day. Steps in predicting the relationship of yield on fungicide dose. *Phytopathology*, 91(7):708–716, Jul 2001. ISSN 0031-949X. doi: 10.1094/PHYTO.2001.91.7.708 .

RAGT. Blé tendre d'hiver. Leaflet, 2016. URL http://www.ragtsemences.com/rs/pdf_fr/bth. accessed 2017-07-04.

S. C. Salmon and H. H. Laude. Twenty years of testing varieties and strain of winter wheat at the Kansas agricultural experiment station. Technical bulletin 80, Kansas state college of agriculture and applied science, Manhattan, Kansas, February 1932. URL https://www.k-state.edu/historicpublications/pubs/STB030.PDF.

J. Schafer. Tolerance to plant disease. *Annual review of phytopathology*, 9:235–252, 1971. ISSN 0066-4286. doi: 10.1146/annurev.py.09.090171.001315 .

R. A. Serrago, R. Carretero, M.-O. Bancal, and D. J. Miralles. Foliar diseases affect the eco-physiological attributes linked with yield and biomass in wheat (Triticum aestivum L.). *European Journal of Agronomy*, 31(4):195–203, 2009. doi: 10.1016/j.eja.2009.06.002 .

U. Steinfort, B. Trevaskis, S. Fukai, K. L. Bell, and M. F. Dreccer. Vernalisation and photoperiod sensitivity in wheat: Impact on canopy development and yield components. *Field Crops Research*, 201:108–121, 2017. doi: 10.1016/j.fcr.2016.10.012 .

F. van den Berg, N. D. Paveley, I. J. Bingham, and F. van den Bosch. Physiological traits determining yield tolerance of wheat to foliar diseases. *Phytopathology*, 2017. URL https://apsjournals.apsnet.org/doi/pdfplus/10.1094/PHYTO-07-16-0283-R. Accepted for publication - first look.

Y.-H. Zhang, N.-N. Sun, J.-P. Hong, Q. Zhang, C. Wang, X. Qing-Wu, Z. Shun-Li, H. Qin, and W. Zhi-Min. Effect of source-sink manipulation on photosynthetic characteristics of flag leaf and the remobilization of dry mass and nitrogen in vegetative organs of wheat. *Journal of integrative agriculture*, 13(8):1680–1690, 2014. ISSN 2095-3119. doi: 10.1016/S2095-3119(13)60665-6 .

M. Zilberstein, A. Blum, and Z. Eyal. Chemical desiccation of wheat plants as a simulator of postanthesis speckled leaf blotch stress. *Phytopathology*, 75(2):226–230, 1985. URL http://apsnet.org/publications/phytopathology/backissues/Documents/1985Articles/Phyto75n02_226.PDF.

E. Zuckerman, A. Eshel, and Z. Eyal. Physiological aspects related to tolerance of spring wheat cultivars to Septoria tritici blotch. *Phytopathology*, 87(1):60–65, Jan. 1997. ISSN 0031-949X. URL http://apsjournals.apsnet.org/doi/pdf/10.1094/PHYTO.1997.87.1.60.

Glossary

%GLA percentage of Green Leaf Lamina Area.

%IncMSE Percentage Increase of the Mean Square Error.

ADAS rebranded National Agricultural Advisory Service (1971).

AMT Ammonium transporter.

AUDPC Area Under the Disease Progress Curve.

BIC Bayesian information criterion is a criterion for model selection among a finite set of models; the model with the lowest BIC is preferred. It is based, in part, on the likelihood function. When fitting models, it is possible to increase the likelihood ($\ln L$) by adding parameters, but doing so may result in overfitting. BIC resolves this problem by introducing a penalty term for the number of independant parameters in the model (K) and the number of individuals used to fit the model (n).

$$BIC = -2 \cdot \ln V + K \cdot \ln n$$

CIMMYT Centro Internacional de Mejoramiento de Maíz y Trigo (International Maize and Wheat Improvement Center).

CTPS Comité Technique Permanent de la Sélection des plantes cultivées (permanent technical committee for plant breeding).

D Duration of rapid senescence phase (approximately between 80% and 20% GLA. See Gompertz['s function].

DEFRA Department for Environment Food & Rural Affairs.

DH Doubled-Haploid.

ECOSYS ÉCOlogie fonctionnelle et ÉCOtoxicologie des agroécoSYStemes (functional ecology and ecotoxicology of agroecosystems).

EN Ear Number per m^2.

ENeq equivalent Ear Number per m^2. When independent estimations of the grain yield per m^2 (Ym, combine-harvested) and the grain yield per ear (Ye, based on identified sampled shoots) are available, the ratio Ym/Ye is an appropriate estimation of the ear density (ENeq) to estimate at the crop scale, the estimations based on the shoot samples (e.g. LAI, HADm).

fGLA fraction of Green Leaf Lamina Area.

fLA Generally fLA l, with l the leaf layer. Contribution of leaf layers to canopy leaf area. In this document, the total leaf lamina area represents generally the cumulated area of the three upper leaves, except in the case of the French data base analysis (Chapter 3) where the four upper leaves were taken into account.

G×E Genotype Environment Interaction. The effect of a genotype (G) varies according to the environmental conditions (E) it is exposed.

GNe Grain Number per ear-bearing shoot.

GNm Grain Number per m^2.

Gompertz's function Adaptation of the Gompertz's function for the description of senescence / green leaf lamina area kinetics since heading stage:

$$\%GLA(t,K,D,I) = K \cdot \exp\left(-\exp\left(\frac{2\times(I-t)}{D}\right)\right)$$

With: %GLA, percentage of green leaf lamina area; t, thermal time since heading stage (unit °Cd_H: degree-days since heading stage, base temp. 0 °C); K, left asymptote set to 100%; D, the duration of rapid senescence (approximately between 80% and 20% GLA; unit °Cd: degree-days base temp. 0 °C); I, inflexion point of the kinetic which happens when 37% of the lamina area is green, indicating the time of the senescence (unit °Cd_H).

GS Glutamate synthethase.

GS Growth Stage, in this document followed by the decimal code for the growth stages of cereals (Zadoks et al., 1974).

HAD Healthy Area Duration. In the literature, it refers generally to the area under the curve of the green leaf lamina area per unit of ground area, from heading date to maturity (time expressed in days). In the experiments, the closest indicator was the HADm (see HADm) while the HAD described the percentage of green leaf lamina, integrated from heading to matururity (time expressed as degree days since heading stage).

HADe Healthy Area Duration per ear-bearing shoot. The area under the curve of the green leaf lamina area per shoot, from heading date to maturity (time expressed degree-days since heading stage).

HADg Healthy Area Duration per grain. The area under the curve of the green leaf lamina area per grain, from heading date to maturity (time expressed degree-days since heading stage).

HADm Healthy Area Duration per crop m^2. The area under the curve of the green leaf lamina area per unit of ground area, from heading date to maturity (time expressed degree-days since heading stage).

I Senescence timing. In this document, it corresponds to the inflexion point of the green leaf lamina area kinetic which happens when 37% of the lamina area is green. See Gompertz[']s function]. Ix, is the senescence timing of the leaf layer x.

INRA Institut National de la Recherche Agronomique (National Institute of Agricultural Research).

k Light-extinction coefficient.

LAe Leaf Lamina Area per ear-bearing shoot. LAe x, is the LAe for the leaf layer x.

LAg Leaf Lamina Area per grain. LAg x, is the LAg for the leaf layer x.

LAI Leaf Area Index. Leaf lamina area per unit of ground area, without unit. LAI x is the LAI for the leaf layer x.

MSE Mean Square Error:

$$MSE = \frac{1}{n}\sum_{i=1}^{n}(\hat{y}_i - y_i)^2$$

With: n, the number of observations; y_i, the ith observation; $\hat{y}_i$, the ith estimation.

NIL Near Isogenic Line.

NUE Nitrogen Use Efficiency.

NUpE Nitrogen Uptake Efficiency.

NUtE Nitrogen Utilisation Efficiency.

PPFD Photosynthetic Photon Flux Density.

QoI Quinone outside Inhibitors.

RF Random Forest (Breiman, 2001).

RMSE Root Mean Square Error of estimation:

$$RMSE = \sqrt{\frac{1}{n}\sum_{i=1}^{n}(\hat{y}_i - y_i)^2}$$

With: n, the number of observations; y_i, the ith observation; $\hat{y}_i$, the ith estimation.

RMSEP Root Mean Square Error of Prediction:

$$RMSE = \sqrt{\frac{1}{n}\sum_{i=1}^{n}(\hat{y}_i - y_i)^2}$$

With: n, the number of observations; y_i, the ith observation; $\hat{y}_i$, the ith prediction.

Rubisco Ribulose-Bisphosphate-Carboxylase-Oxygenase.

STB Septoria tritici blotch, nomenclature according to Cunfer (1995).

Teagasc means "Instruction" (Irish), the official title of the body is Teagasc — The Agriculture and Food Development.

TGN Thousand Grain Nitrogen amount.

TGW Thousand Grain Weight, ofter expressed in g. TGW is actually equivalent to single grain weight expressed in mg.

VCA Variance Component Analysis, see Crawley (2007).

Ye grain yield per ear-bearing shoot.

Ym grain yield per crop m^2.

Complete list of references

M. M. Acreche and G. A. Slafer. Variation of grain nitrogen content in relation with grain yield in old and modern Spanish wheats grown under a wide range of agronomic conditions in a Mediterranean region. *The Journal of Agricultural Science*, 147(6):657–667, 2009. doi: 10.1017/S0021859609990190 .

T. B. Adhikari, J. M. Anderson, and S. B. Goodwin. Identification and molecular mapping of a gene in wheat conferring resistance to Mycosphaerella graminicola. *Phytopathology*, 93(9):1158–1164, 2003. URL http://apsjournals.apsnet.org/doi/pdfplus/10.1094/PHYTO.2003.93.9.1158.

T. B. Adhikari, J. R. Cavaletto, J. Dubcovsky, J. O. Gieco, A. R. Schlatter, and S. B. Goodwin. Molecular mapping of the Stb4 gene for resistance to Septoria tritici blotch in wheat. *Phytopathology*, 2004. URL http://apsjournals.apsnet.org/doi/pdfplus/10.1094/PHYTO.2004.94.11.1198.

AHDB. *Wheat disease maagement guide*. AHDB, 2016a. URL https://cereals.ahdb.org.uk/media/176167/g63-wheat-disease-management-guide-february-2016.pdf.

AHDB. Ahdb Recommended List - winter wheat 2016/17. tables, 2016b. URL https://cereals.ahdb.org.uk/media/883980/1-RLDL_2016-17_Winter_Wheat_RL-V6.pdf.

AHDB. Ahdb Recommended List for cereals and oilseed 2017/18. Internet, Stoneleigh Park, Warwickshire, CV8 2TL, UK, 2017. URL https://cereals.ahdb.org.uk/media/800462/lr-ahdb-recommended-list-2017-18.pdf. Accessed 2017-08-11.

K. A. B. Aisawi, M. P. Reynolds, R. P. Singh, and M. J. Foulkes. The physiological basis of the genetic progress in yield potential of CIMMYT spring wheat cultivars from 1966 to 2009. *Crop Science*, 55:1749–1764, 2015. doi: 10.2135/cropsci2014.09.0601 .

K. Ando, R. Grumet, K. Terpstra, and J. D. Kelly. Manipulation of plant architecture to enhance crop disease control. *CABI*, 2(26):8 pp., 2007. ISSN 1749-8848. doi: 10.1079/PAVSNNR20072026 .

J. Angus, R. Jones, and J. Wilson. A comparison of barley cultivars with different leaf inclinations. *Crop and Pasture Science*, 23:945–957, 1972. doi: 10.1071/AR9720945 .

I. Aranjuelo, L. Cabrera-Bosquet, R. Morcuende, J. C. Avice, S. Nogués, J. L. Araus, R. Martínez-Carrasco, and P. Pérez. Does ear C sink strength contribute to overcoming photosynthetic acclimation of wheat plants exposed to elevated CO2? *Journal of Experimental Botany*, 62(11):3957–3969, 2011. doi: 10.1093/jxb/err095 .

I. Aranjuelo, L. Cabrera-Bosquet, J. L. Araus, and S. Noguès. Carbon and nitrogen partitioning during the post-anthesis period is conditioned by N fertilisation and sink

strength in three cereals. *Plant Biology*, 15(1):135–143, 2013. ISSN 1438-8677. doi: 10.1111/j.1438-8677.2012.00593.x .

L. Arraiano, A. Worland, C. Ellerbrook, and J. Brown. Chromosomal location of a gene for resistance to Septoria tritici blotch (Mycosphaerella graminicola) in the hexaploid wheat 'Synthetic 6x'. *TAG Theoretical and Applied Genetics*, 103(5):758–764, 2001. doi: 10.1007/s001220100668 .

R. B. Austin, J. Bingham, R. D. Blackwell, L. T. Evans, M. A. Ford, C. L. Morgan, and M. Taylor. Genetic improvements in winter wheat yields since 1900 and associated physiological changes. *The Journal of Agricultural Science*, 94(3):675–689, 1980. doi: 10.1017/S0021859600028665 .

R. Baccar, C. Fournier, T. Dornbusch, B. Andrieu, D. Gouache, and C. Robert. Modelling the effect of wheat canopy architecture as affected by sowing density on Septoria tritici epidemics using a coupled epidemic × virtual plant model. *Annals of Botany*, 108(6): 1179–1194, 2011. doi: 10.1093/aob/mcr126 .

B. Baltazar, A. Scharen, and W. Kronstad. Association between dwarfing genes 'rht1'and 'rht2'and resistance to Septoria tritici blotch in winter wheat (Triticum aestivum L. em Thell). *Theoretical and applied genetics*, 79(3):422–426, 1990. doi: 10.1007/BF01186089 .

M.-O. Bancal, R. Roche, and P. Bancal. Late foliar diseases in wheat crops decrease nitrogen yield through N uptake rather than through variations in N remobilization. *Annals of Botany*, 102(4):579–590, Oct 2008. ISSN 0305-7364. doi: 10.1093/aob/mcn124 .

M.-O. Bancal, R. B. Slimane, and P. Bancal. Zymoseptoria tritici development induces local senescence in wheat leaves, without affecting their monocarpic senescence under two contrasted nitrogen nutrition. *Environmental and Experimental Botany*, 132:154–162, 2016. doi: 10.1016/j.envexpbot.2016.09.002 .

P. Bancal. Positive contribution of stem growth to grain number per spike in wheat. *Field Crops Research*, 105(1–2):27–39, 2008. doi: 10.1016/j.fcr.2007.06.008 .

P. Bancal. Data: Précocité et surface de feuille étendard. Personal communication, project CP2P2, Aug 2017.

P. Bancal, M.-O. Bancal, F. Collin, and D. Gouache. Identifying traits leading to tolerance of wheat to Septoria tritici blotch. *Field Crops Research*, 180:176–185, 2015. doi: 10.1016/j.fcr.2015.05.006 .

A. Barbottin, C. Lecomte, C. Bouchard, and M. H. Jeuffroy. Nitrogen remobilization during grain filling in wheat: Genotypic and environmental effects. *Crop Science*, 45(3): 1141–1150, May–Jun 2005. doi: 10.2135/cropsci2003.0361 .

A. J. Barneix. Physiology and biochemistry of source-regulated protein accumulation in the wheat grain. *Journal of plant physiology*, 164(5):581–590, May 2007. ISSN 0176-1617. doi: 10.1016/j.jplph.2006.03.009 .

L. Bastiaans. Ratio between virtual and visual lesion size as a measure to describe reduction in leaf photosynthesis of rice due to leaf blast. *Phytopathology*, 81:611–615, 1991. URL `http://apsnet.org/publications/phytopathology/backissues/Documents/1991Articles/Phyto81n06_611.PDF`.

L. Bastiaans. Effects of leaf blast on growth and production of a rice crop. 1. Determining the mechanism of yield reduction. *Netherland journal of plant pathology*, 99(5–6):323–334, 1993. ISSN 0028-2944. doi: 10.1007/BF01974313 .

D. Bates, M. Mächler, B. Bolker, and S. Walker. Fitting linear mixed-effects models using lme4. *Journal of Statistical Software*, 67(1):1–48, 2015. doi: 10.18637/jss.v067.i01 .

R. Ben Slimane , P. Bancal, and M. Bancal. Down-regulation by stems and sheaths of grain filling with mobilized nitrogen in wheat. *Field Crops Research*, 140(0):59 – 68, 2013. ISSN 0378-4290. doi: 10.1016/j.fcr.2012.10.006 .

R. Ben Slimane. *Effets de la septoriose foliaire sur la sénescence et les flux d'azote pendant le remplissage des grains chez le blé tendre*. PhD thesis, AgroParisTech, 2010. URL https://hal.archives-ouvertes.fr/pastel-00560282/.

I. J. Bingham and C. F. E. Topp. Potential contribution of selected canopy traits to the tolerance of foliar disease by spring barley. *Plant Pathology*, 58(6):1010–1020, Dec 2009. ISSN 0032-0862. doi: 10.1111/j.1365-3059.2009.02137.x .

I. J. Bingham, D. R. Walters, M. J. Foulkes, and N. D. Paveley. Crop traits and tolerance of wheat and barley to foliar disease. *Annals of Applied Biology*, 154:159–173, 2009. doi: 10.1111/j.1744-7348.2008.00291.x .

A. Blum. Improving wheat grain filling under stress by stem reserve mobilisation. In *Wheat: Prospects for Global Improvement*, pages 135–141. Springer, 1997. URL https://link.springer.com/article/10.1023%2FA%3A1018303922482.

A. Boonman, N. P. R. Anten, T. A. Dueck, W. J. R. M. Jordi, A. van der Werf, L. A. C. J. Voesenek, and T. L. Pons. Functional significance of shade-induced leaf senescence in dense canopies: an experimental test using transgenic tobacco. *The American Naturalist*, 168(5):597–607, 2006. doi: 10.1086/508633 .

B. Borghi, M. Corbellini, C. Minoia, M. Palumbo, N. Di Fonzo, and M. Perenzin. Effects of Mediterranean climate on wheat bread-making quality. *European journal of agronomy*, 6(3-4):145–154, May 1997. ISSN 1161-0301. doi: 10.1016/S1161-0301(96)02040-0 .

L. Borrás, G. A. Slafer, and M. E. Otegui. Seed dry weight response to source sink manipulations in wheat, maize and soybean: a quantitative reappraisal. *Field Crops Research*, 86(23):131–146, 2004. ISSN 0378-4290. doi: 10.1016/j.fcr.2003.08.002 .

A. Borrell, G. Hammer, and E. van Oosterom. Stay-green: A consequence of the balance between supply and demand for nitrogen during grain filling? *Annals of Applied Biology*, 138(1):91–95, 2001. doi: 10.1111/j.1744-7348.2001.tb00088.x .

A. K. Borrell and G. L. Hammer. Nitrogen dynamics and the physiological basis of stay-green in sorghum. *Crop science*, 40(5):1295–1307, 2000. doi: 10.2135/cropsci2000.4051295x .

P. A. Brading, E. C. Verstappen, G. H. Kema, and J. K. Brown. A gene-for-gene relationship between wheat and Mycosphaerella graminicola, the Septoria tritici blotch pathogen. *Phytopathology*, 92(4):439–445, 2002. URL http://apsjournals.apsnet.org/doi/pdfplus/10.1094/PHYTO.2002.92.4.439.

H.-J. Braun and T. Payne. *Physiological breeding I: interdisciplinary approaches to improve crop adaptation*, chapter Mega-environment breeding, pages 6–17. CIMMYT, Mexico, Mexico, DF (Mexico), 2012. URL http://repository.cimmyt.org/xmlui/bitstream/handle/10883/1288/96144.pdf.

L. Breiman. *Manual On Setting Up, Using, And Understanding Random Forests*. URL https://www.stat.berkeley.edu/~breiman/Using_random_forests_V3.1.pdf. V3.1.

L. Breiman. Random forests. *Machine Learning*, 45(1):5–32, 2001. ISSN 1573-0565. doi: 10.1023/A:1010933404324 .

J. K. Brown, L. Chartrain, P. Lasserre-Zuber, and C. Saintenac. Genetics of resistance to Zymoseptoria tritici and applications to wheat breeding. *Fungal Genetics and Biology*, 79:33–41, 2015. doi: 10.1016/j.fgb.2015.04.017 .

R. J. Bryson, N. D. Paveley, W. S. Clark, R. Sylvester-Bradley, and R. K. Scott. Use of in-field measurements of green leaf area and incident radiation to estimate the effects of yellow rust epidemics on the yield of winter wheat. *European Journal of Agronomy*, 7: 53–62, 1997. doi: 10.1016/S1161-0301(97)00025-7 .

J. Burke and B. Dunne. Septoria tritici in winter wheat – to spray or not to spray? *Irish farmer*, pages 14–18, April 2006.

D. F. Calderini, R. Savin, L. G. Abeledo, M. P. Reynolds, and G. A. Slafer. The importance of the period immediately preceding anthesis for grain weight determination in wheat. *Euphytica*, 119(1–2):199–204, 2001. ISSN 0014-2336. doi: 10.1023/A:1017597923568 .

R. Carretero, R. A. Serrago, M. O. Bancal, A. E. Perelló, and D. J. Miralles. Absorbed radiation and radiation use efficiency as affected by foliar diseases in relation to their vertical position into the canopy in wheat. *Field Crops Research*, 116(1):184–195, 2010. doi: 10.1016/j.fcr.2009.12.009 .

J. Cartelle, A. Pedró, R. Savin, and G. A. Slafer. Grain weight responses to post-anthesis spikelet-trimming in an old and a modern wheat under mediterranean conditions. *European Journal of Agronomy*, 25(4):365–371, 2006. ISSN 1161-0301. doi: 10.1016/j.eja.2006.07.004 .

A. C. Castro and M. R. Simón. Effect of tolerance to Septoria tritici blotch on grain yield, yield components and grain quality in Argentinean wheat cultivars. *Crop Protection*, 90: 66–76, 2016. ISSN 0261-2194. doi: 10.1016/j.cropro.2016.08.015 .

H. F. Causin, R. N. Jauregui, and A. J. Barneix. The effect of light spectral quality on leaf senescence and oxidative stress in wheat. *Plant Science*, 171(1):24–33, Jul 2006. ISSN 0168-9452. doi: 10.1016/j.plantsci.2006.02.009 .

L. Chartrain, P. A. Brading, J. C. Makepeace, and J. K. M. Brown. Sources of resistance to Septoria tritici blotch and implications for wheat breeding. *Plant Pathology*, 53(4): 454–460, 2004. ISSN 1365-3059. doi: 10.1111/j.1365-3059.2004.01052.x .

J. Chen, Y. Liang, X. Hu, X. Wang, F. Tan, H. Zhang, Z. Ren, and P. Luo. Physiological characterization of 'stay green'wheat cultivars during the grain filling stage under field growing conditions. *Acta physiologiae plantarum*, 32(5):875–882, 2010. doi: 10.1007/s11738-010-0475-0 .

P. Cheval, A. Siah, M. Bomble, A. D. Popper, P. Reignault, and P. Halama. Evolution of QoI resistance of the wheat pathogen *Zymoseptoria tritici* in Northern France. *Crop protection*, 92:131–133, Feb 2017. ISSN 0261-2194. doi: 10.1016/j.cropro.2016.10.017 .

N. A. Cobb. *Contributions to an economic knowledge of Australian rusts (Uredineae)*, chapter Chapter 10, pages 239–250. Agricultural Gazette of New South Wales, 1894.

F. Collin, P. Bancal, J. Foulkes, and M. O. Bancal. A statistical analysis of gxe contribution to leaf senescence during grain filling in wheat. In *ESA 14 - Growing landscapes - Cultivating innovative agricultural systems*, pages 13–14, Edinburgh, Scotland, September 2016a. ESA. Poster presentation - session 12.

F. Collin, D. Gouache, M.-O. Bancal, and P. Bancal. Tolerance of wheat to Septoria tritici blotch; genetic vs environmental variations of key traits. In *9th International Symposium on Septoria Diseases of Cereals*, page 76, Paris, France, April 2016b. ISSDC. Poster presentation.

F. Collin, P. Bancal, J. Spink, P. Kock Appelgren, J. Smith, N. D. Paveley, M.-O. Bancal, and M. J. Foulkes. Wheat lines exhibiting variation in tolerance of Septoria tritici blotch differentiated by grain source limitation. *Field Crops Research*, 217:1– 10, March 2018. ISSN 0378-4290. doi: 10.1016/j.fcr.2017.11.022 . URL https://www.sciencedirect.com/science/article/pii/S0378429017312078.

J. Conway, D. Eddelbuettel, T. Nishiyama, S. K. Prayaga, and N. Tiffin. *RPostgreSQL: R interface to the PostgreSQL database system*, 2016. URL https://CRAN.R-project.org/package=RPostgreSQL. R package version 0.4-1.

H. J. Cools and B. A. Fraaije. Are azole fungicides losing ground against Septoria wheat disease? resistance mechanisms in Mycosphaerella graminicola. *Pest Management Science*, 64(7):681–684, 2008. ISSN 1526-4998. doi: 10.1002/ps.1568 .

H. J. Cools and B. A. Fraaije. Update on mechanisms of azole resistance in Mycosphaerella graminicola and implications for future control. *Pest management science*, 69(2):150–155, 2013. doi: 10.1002/ps.3348 .

F. Cormier, J. Foulkes, B. Hirel, D. Gouache, Y. Moënne-Loccoz, and J. Le Gouis. Breeding for increased nitrogen-use efficiency: a review for wheat T. aestivum L.). *Plant Breeding*, 135:255–278, 2016. doi: 10.1111/pbr.12371 .

P. S. Cornish, G. R. Baker, and G. M. Murray. Physiological responses of wheat (triticum aestivum) to infection with Mycosphaerella graminicola causing Septoria tritici blotch. *Australian Journal of Agricultural Research*, 41(2):317–327, 1990. doi: 10.1071/AR9900317 .

C. Cowger, M. Hoffer, and C. Mundt. Specific adaptation by Mycosphaerella graminicola to a resistant wheat cultivar. *Plant Pathology*, 49(4):445–451, 2000. doi: 10.1046/j.1365-3059.2000.00472.x .

M. Cox, C. Qualset, and D. Rains. Genetic-variation for nitrogen assimilation and translocation in wheat. 2. Nitrogen assimilation in relation to grain-yield and protein. *Crop science*, 25(3):435–440, 1985. ISSN 0011-183X. doi: 10.2135/cropsci1985.0011183X002500030003x .

S. J. Crafts-Brandner, F. E. Below, V. A. Wittenbach, J. E. Harper, and R. H. Hageman. Differential senescence of maize hybrids following ear removal II. Selected leaf. *Plant Physiology*, 74(2):368–373, 1984. doi: 10.1104/pp.74.2.368 .

S. J. Crafts-Brandner, R. Hölzer, and U. Feller. Influence of nitrogen deficiency on senescence and the amounts of RNA and proteins in wheat leaves. *Physiologia Plantarum*, 102(2):192–200, 1998. ISSN 1399-3054. doi: 10.1034/j.1399-3054.1998.1020206.x .

M. Crawley. *Statistics: an introduction using R*, chapter Mixed-effects models, pages 627–660. Wiley, 2007.

M. J. Crawley. *The R Book, 2nd Edition*, chapter Mixed-Effects Models, pages 681–714. Wiley, 2012. ISBN 978-0-470-97392-9.

B. M. Cunfer. Taxonomy and nomenclature of Septoria and Stagonospora species on small grain cereals. *Plant Disease*, 81(5):427–428, May 1995.

T. Curtis and N. Halford. Food security: the challenge of increasing wheat yield and the importance of not compromising food safety. *Annals of applied biology*, 164(3):354–372, 2014. doi: 10.1111/aab.12108 .

J. C. Dawson, D. R. Huggins, and S. S. Jones. Characterizing nitrogen use efficiency in natural and agricultural ecosystems to improve the performance of cereal crops in low-input and organic agricultural systems. *Field Crops Research*, 107(2):89–101, 2008. doi: 10.1016/j.fcr.2008.01.001 .

S. Demotes-Mainard, G. Doussinault, and J. M. Meynard. Effects of low radiation and low temperature at meiosis on pollen viability and grain set in wheat. *Agronomie*, 15:357–365, 1995. URL `https://hal.archives-ouvertes.fr/hal-00885691/document`.

S. Demotes-Mainard, G. Doussinault, and J. M. Meynard. Abnormalities in the male developmental programme of winter wheat induced by climatic stess at meiosis. *Agronomie*, 15:357–365, 1996. URL `https://hal.archives-ouvertes.fr/hal-00885813/document`.

A. P. Derkx, S. Orford, S. Griffiths, M. J. Foulkes, and M. J. Hawkesford. Identification of differentially senescing mutants of wheat and impacts on yield, biomass and nitrogen partitioning. *Journal of integrative plant biology*, 54(8):555–566, Aug 2012. ISSN 1672-9072. doi: 10.1111/j.1744-7909.2012.01144.x .

J.-C. Deswarte, K. Beauchene, G. Arjaure, S. Jezequel, G. Meloux, Y. Flodrops, J. Landrieaux, A. Bouthier, S. Thomas, B. De Solan, and D. Gouache. Platform development for drought tolerance evaluation of wheat in france. *Procedia Environmental Sciences*, 29(Supplement C):93 – 94, 2015. ISSN 1878-0296. doi: 10.1016/j.proenv.2015.07.176 . Agriculture and Climate Change - Adapting Crops to Increased Uncertainty (AGRI 2015).

L. Ding, K. Wang, G. Jiang, D. Biswas, H. Xu, L. Li, and Y. Li. Effects of nitrogen deficiency on photosynthetic traits of maize hybrids released in different years. *Annals of Botany*, 96(5):925–930, 2005. doi: 10.1093/aob/mci244 .

A. Distelfeld, R. Avni, and A. M. Fischer. Senescence, nutrient remobilization, and yield in wheat and barley. *Journal of experimental botany*, 65(14,SI):3783–3798, Jul 2014. ISSN 0022-0957. doi: 10.1093/jxb/ert477 .

H. Dooley, M. Shaw, J. Spink, and S. Kildea. Effect of azole fungicide mixtures, alternations and dose on azole sensitivity in the wheat pathogen Zymoseptoria tritici. *Plant Pathology*, 65(1):124–136, 2016a. doi: 10.1111/ppa.12395 .

H. Dooley, M. W. Shaw, J. Mehenni-Ciz, J. Spink, and S. Kildea. Detection of Zymoseptoria tritici SDHI-insensitive field isolates carrying the SdhC-H152R and SdhD-R47W substitutions. *Pest management science*, 72(12):2203–2207, 2016b. doi: 10.1002/ps.4269 .

K. E. Duncan and R. J. Howard. Cytological analysis of wheat infection by the leaf blotch pathogen Mycosphaerella graminicola. *Mycological Research*, 104(9):1074 – 1082, 2000. ISSN 0953-7562. doi: 10.1017/S0953756299002294 .

F. M. Dupont and S. B. Altenbach. Molecular and biochemical impacts of environmental factors on wheat grain development and protein synthesis. *Journal of Cereal Science*, 38 (2):133–146, September 2003. ISSN 0733-5210. doi: 10.1016/S0733-5210(03)00030-4 .

L. Echarte, S. Rothstein, and M. Tollenaar. The response of leaf photosynthesis and dry matter accumulation to nitrogen supply in an older and a newer maize hybrid. *Crop Science*, 48(2):656–665, 2008. doi: 10.2135/cropsci2007.06.0366 .

D. B. Egli and W. P. Bruening. Source-sink relationships, seed sucrose levels and seed growth rates in soybean. *Annals of botany*, 88(2):235–242, Aug 2001. ISSN 0305-7364. doi: 10.1006/anbo.2001.1449 .

R. T. Ellis. Tolerance to the maize rust *Puccinia polysora* underw. *Nature*, 174:1021, 1954.

L. Eriksen, M. W. Shaw, and H. Østergård. A model of the effect of pseudothecia on genetic recombination and epidemic development in populations of Mycosphaerella graminicola. *Phytopathology*, 91(3):240–248, 2001. doi: 10.1094/PHYTO.2001.91.3.240 .

J. R. Evans. Photosynthesis and nitrogen relationships in leaves of C3 plants. *Oecologia*, 78: 9–19, 1989. URL https://link.springer.com/article/10.1007%2FBF00377192?LI=true.

R. E. Evenson and D. Gollin. Assessing the impact of the green revolution, 1960 to 2000. *Science*, 300(5620):758–762, 2003. doi: 10.1126/science.1078710 .

Z. Eyal, I. Maize, and W. I. Center. *The Septoria diseases of wheat : concepts and methods of disease management / International Maize and Wheat Improvement Center.* CIMMYT Mexico, D.F, 1987. ISBN 9686127062.

Z. Eyal et al. Integrated control of Septoria diseases of wheat. *Plant Disease*, 65(9):763–768, 1981.

FAO. *FAO Statistical pocketbook - World food and Agriculture*, chapter Crops, pages 28–29. Food and Agriculture Organization of the United Nations, Rome, 2015.

FAOSTAT. Faostat database. Internet, 2017. URL http://www.fao.org/faostat/. Accessed 2017-07-20.

U. Feller and A. Fischer. Nitrogen-metabolism in senescing leaves. *Critical reviews in plant sciences*, 13(3):241–273, 1994. ISSN 0735-2689. doi: 10.1080/713608059 .

R. A. Fischer. Understanding the physiological basis of yield potential in wheat. *The Journal of Agricultural Science*, 145(2):99–113, 2007. doi: 10.1017/S0021859607006843 .

R. A. Fischer and Y. M. Stockman. Kernel number per spike in wheat (*Triticum aestivum* l.): responses to preanthesis shading. *Australian Journal of Plant Physiology*, 7(2):169–180, 1980. doi: 10.1071/PP9800169 .

H. Fones and S. Gurr. The impact of Septoria tritici blotch disease on wheat: An EU perspective. *Fungal Genetics and Biology*, 79:3 – 7, 2015. ISSN 1087-1845. doi: 10.1016/j.fgb.2015.04.004 . Septoria tritici blotch disease of wheat: Tools and techniques to study the pathogen Zymoseptoria tritici.

M. J. Foulkes, N. D. Paveley, A. Worland, S. J. Welham, J. Thomas, and J. W. Snape. Major genetic changes in wheat with potential to affect disease tolerance. *Phytopathology*, 96:680–688, 2006. URL http://apsjournals.apsnet.org/doi/pdf/10.1094/PHYTO-96-0680.

M. J. Foulkes, M. J. Hawkesford, P. B. Barraclough, M. J. Holdsworth, S. Kerr, S. Kightley, and P. R. Shewry. Identifying traits to improve the nitrogen economy of wheat: Recent advances and future prospects. *Field crops research*, 114(3):329–342, Dec 2009. ISSN 0378-4290. doi: 10.1016/j.fcr.2009.09.005 .

B. Fraaije, H. Cools, J. Fountaine, D. Lovell, J. Motteram, J. West, and J. Lucas. Role of ascospores in further spread of QoI-resistant cytochrome b alleles (G143A) in field populations of Mycosphaerella graminicola. *Phytopathology*, 95(8):933–941, Aug 2005. ISSN 0031-949X. URL http://apsjournals.apsnet.org/doi/pdfplus/10.1094/PHYTO-95-0933.

B. A. Fraaije, J. A. Lucas, W. S. Clark, and F. J. Burnett. QoI resistance development in populations of cereal pathogens in the UK. In *Proceedings of the BCPC International Congress, Crop Science and Technology*, 689–694, Alton, Hampshire, UK, 2003. The British Crop Protection Council.

B. A. Fraaije, C. Bayon, S. Atkins, H. J. Cools, J. A. Lucas, and M. W. Fraaije. Risk assessment studies on succinate dehydrogenase inhibitors, the new weapons in the battle to control Septoria leaf blotch in wheat. *Molecular Plant Pathology*, 13(3):263–275, 2012. ISSN 1364-3703. doi: 10.1111/j.1364-3703.2011.00746.x . URL http://dx.doi.org/10.1111/j.1364-3703.2011.00746.x.

V. Fröhlich and U. Feller. Effect of phloem interruption on senescence and protein remobilization in the flag leaf of field-grown wheat. *Biochemie und Physiologie der Pflanzen*, 187(2):139–147, 1991. doi: 10.1016/S0015-3796(11)80118-6 .

J.-D. Fu and B.-W. Lee. Changes in photosynthetic characteristics during grain filling of a functional stay-green rice SNU-SG1 and its F1 hybrids. *Journal of crop science and biotechnology*, 11:75–82, 2008. URL http://www.cropbio.org/contribute/paperfiles/Jin-Dong%20Fu.pdf.

O. Gaju, V. Allard, P. Martre, J. W. Snape, E. Heumez, J. LeGouis, D. Moreau, M. Bogard, S. Griffiths, S. Orford, S. Hubbart, and M. J. Foulkes. Identification of traits to improve the nitrogen-use efficiency of wheat genotypes. *Field Crops Research*, 123(2):139 – 152, 2011. ISSN 0378-4290. doi: 10.1016/j.fcr.2011.05.010 .

O. Gaju, V. Allard, P. Martre, J. Le Gouis, D. Moreau, M. Bogard, S. Hubbart, and M. J. Foulkes. Nitrogen partitioning and remobilization in relation to leaf senescence, grain yield and grain nitrogen concentration in wheat cultivars. *Field Crops Research*, 155:213 – 223, 2014. ISSN 0378-4290. doi: 10.1016/j.fcr.2013.09.003 .

Y. Gan, B. D. Gossen, L. Li, G. Ford, and S. Banniza. Cultivar type, plant population, and Ascochyta blight in chickpea. *Agronomy journal*, 99(6):1463–1470, 2007. doi: 10.2134/agronj2007.0105 .

R. E. Gaunt and A. C. Wright. Disease-yield relationship in barley. II. Contribution of stored stem reserves to grain filling. *Plant Pathology*, 41(6):688–701, 1992. ISSN 1365-3059. doi: 10.1111/j.1365-3059.1992.tb02552.x .

R. Genuer, J.-M. Poggi, and C. Tuleau-Malot. Variable selection using random forests. *Pattern Recogn. Lett.*, 31(14):2225–2236, Oct. 2010. ISSN 0167-8655. doi: 10.1016/j.patrec.2010.03.014 . URL http://dx.doi.org/10.1016/j.patrec.2010.03.014.

H. C. J. Godfray. The challenge of feeding 9–10 billion people equitably and sustainably. *The Journal of Agricultural Science*, 152(S1):2–8, 2014. doi: 10.1017/S0021859613000774 .

M. J. Gooding, P. J. Gregory, K. E. Ford, and S. Pepler. Fungicide and cultivar affect post-anthesis patterns of nitrogen uptake, remobilization and utilization efficiency in wheat. *Journal of Agricultural Science*, 143(6):503–518, Dec 2005. ISSN 0021-8596. doi: 10.1017/S002185960500568X .

D. Gouache. Toward a new indicator of cultivar resistance to Septoria tritici blotch accounting for cultivar phenology. *unpublished*, 2009.

D. Gouache, M. Bancal, and P. Bancal. Projet contrat de branche "Tolérance du blé tendre aux stress biotiques et abiotiques" C2008-02 blé tendre, october 2012. URL https://hal.archives-ouvertes.fr/hal-01192469/. Rapport final.

D. Gouache, A. Bensadoun, F. Brun, C. Pagé, D. Makowski, and D. Wallach. Modelling climate change impact on Septoria tritici blotch (STB) in France: accounting for climate model and disease model uncertainty. *Agricultural and Forest Meteorology*, 170:242–252, 2013. doi: 10.1016/j.agrformet.2012.04.019 .

D. Gouache, M. Bancal, B. de Solan, and P. Gate. Tolérance du blé tendre aux stress biotiques et abiotiques. *Innovations Agronomiques*, 35:75–87, 2014. URL https://hal.archives-ouvertes.fr/hal-01192469.

P. Gregersen, P. Holm, and K. Krupinska. Leaf senescence and nutrient remobilisation in barley and wheat. *Plant Biology*, 10(s1):37–49, 2008. doi: 10.1111/j.1438-8677.2008.00114.x .

P. L. Gregersen. *The Molecular and Physiological Basis of Nutrient Use Efficiency in Crops*, chapter 5. Senescence and Nutrient Remobilization in Crop Plants, pages 83–102. Wiley-Blackwell, 2011. ISBN 9780470960707. doi: 10.1002/9780470960707.ch5 .

P. L. Gregersen, A. Culetic, L. Boschian, and K. Krupinska. Plant senescence and crop productivity. *Plant Molecular Biology*, 82(6):603–622, Aug 2013. ISSN 0167-4412. doi: 10.1007/s11103-013-0013-8 .

M. J. Griffin and N. Fischer. Laboratory studies on benzimidazole resistance in Septoria tritici. *EPPO Bulletin*, 15:505–511, 1985. doi: 10.1111/j.1365-2338.1985.tb00262.x .

Y. Guo and S.-S. Gan. Convergence and divergence in gene expression profiles induced by leaf senescence and 27 senescence-promoting hormonal, pathological and environmental stress treatments. *Plant, Cell & Environment*, 35(3):644–655, 2012. doi: 10.1111/j.1365-3040.2011.02442.x .

A. J. Hall and R. A. Richards. Prognosis for genetic improvement of yield potential and water-limited yield of major grain crops. *Field Crops Research*, 143:18–33, 2013. doi: 10.1016/j.fcr.2012.05.014 .

A. J. Hall, R. Savin, and G. A. Slafer. Is time to flowering in wheat and barley influenced by nitrogen? A critical appraisal of recent published reports. *European Journal of Agronomy*, 54:40–46, Mar 2014. ISSN 1161-0301. doi: 10.1016/j.eja.2013.11.006 .

J. P. Hébrard. Azote et qualité des blés: fractioner pour plus de protéines. *Perspectives Agricoles*, (68):21–29, 1999.

HGCA. HGCA recommended list - winter wheat 2015/16. tables, 2015. URL `https://cereals.ahdb.org.uk/media/537620/winter-wheat-2015-16.pdf`. Accessed 2017-07-04.

S. J. Inglese and N. D. Paul. Tolerance of Senecio vulgaris to infection and disease caused by native and alien rust fungi. *Phytopathology*, 96(7):718–726, 2006. URL `http://apsjournals.apsnet.org/doi/pdf/10.1094/PHYTO-96-0718`.

C. F. Jenner, T. D. Ugalde, and D. Aspinall. The physiology of starch and protein deposition in the endosperm of wheat. *Australian journal of plant physiology*, 18(3):211–226, 1991. ISSN 0310-7841. doi: 10.1071/PP9910211 .

A. K. Joshi, M. Kumari, V. P. Singh, C. M. Reddy, S. Kumar, J. Rane, and R. Chand. Stay green trait: variation, inheritance and its association with spot blotch resistance in spring wheat (Triticum aestivum L.). *Euphytica*, 153(1):59–71, 2007. ISSN 1573-5060. doi: 10.1007/s10681-006-9235-z .

E. Justes, B. Mary, J. M. Meynard, J. M. Machet, and L. Thelierhuche. Determination of a critical nitrogen dilution curve for winter-wheat crops. *Annals of Botany*, 74(4):397–407, Oct 1994. ISSN 0305-7364. doi: 10.1006/anbo.1994.1133 .

G. H. J. Kema, D. Z. Yu, F. H. J. Rijkenberg, M. W. Shaw, and R. P. Baayen. Histology of the pathogenesis of Mycosphaerella graminicola in wheat. *Phytopathology*, 86(7):777–786, Jul 1996. ISSN 0031-949X. doi: 10.1094/Phyto-86-777 .

J. Keon, J. Antoniw, R. Carzaniga, S. Deller, J. L. Ward, J. M. Baker, M. H. Beale, K. Hammond-Kosack, and J. J. Rudd. Transcriptional adaptation of Mycosphaerella graminicola to programmed cell death (PCD) of its susceptible wheat host. *Molecular plant-microbe interactions*, 20(2):178–193, Feb 2007. ISSN 0894-0282. doi: 10.1094/MPMI-20-2-0178 .

T. Kichey, B. Hirel, E. Heumez, F. Dubois, and J. Le Gouis. In winter wheat (Triticum aestivum L.), post-anthesis nitrogen uptake and remobilisation to the grain correlates with agronomic traits and nitrogen physiological markers. *Field Crops Research*, 102(1):22–32, Apr 2007. ISSN 0378-4290. doi: 10.1016/j.fcr.2007.01.002 .

E. J. M. Kirby. Analysis of leaf, stem and ear growth in wheat from terminal spikelet stage to anthesis. *Field Crops Research*, 18(2):127–140, 1988. ISSN 0378-4290. doi: 10.1016/0378-4290(88)90004-4 .

T. Kramer, B. H. Gildemacher, M. Van der Ster, and J. E. Parlevliet. Tolerance of spring barley cultivars to leaf rust, Puccinia hordei. *Euphytica*, 29(2):209–216, 1980. ISSN 1573-5060. doi: 10.1007/BF00025116 .

M. Kremer and G. M. Hoffmann. Effects of leaf infections of Drechslera tritici-repentis on the carbohydrate and nitrogen metabolism of wheat plants. *Journal of Plant Diseases and Protection*, 100(3):259–277, 1993. ISSN 0340-8159.

R. Lemoine, S. La Camera, R. Atanassova, F. Dédaldéchamp, T. Allario, N. Pourtau, J.-L. Bonnemain, M. Laloi, P. Coutos-Thévenot, L. Maurousset, et al. Source-to-sink transport of sugar and regulation by environmental factors. *Frontiers in Plant Science*, 4: 1–21, 2013. doi: 10.3389/fpls.2013.00272 .

R. V. Lenth. Least-squares means: The R package lsmeans. *Journal of Statistical Software*, 69(1):1–33, 2016. doi: 10.18637/jss.v069.i01 .

J. Levitt. *Stress and strain terminology*, chapter Chapter 1, pages 1–8. New York Academic Press Physiological Ecology, 1972.

A. Liaw and M. Wiener. Classification and regression by Rrandom Forest. *R News*, 2(3): 18–22, 2002. URL `http://CRAN.R-project.org/doc/Rnews/`.

D. J. Lovell, S. R. Parker, T. Hunter, D. J. Royle, and R. R. Coker. Influence of crop growth and structure on the risk of epidemics by Mycosphaerella graminicola (Septoria tritici) in winter wheat. *Plant Pathology*, 46(1):126–138, Feb 1997. ISSN 0032-0862. doi: 10.1046/j.1365-3059.1997.d01-206.x .

J. P. Lynch, E. Glynn, S. Kildea, and J. Spink. Yield and optimum fungicide dose rates for winter wheat (Triticum aestivum L.) varieties with contrasting ratings for resistance to Septoria tritici blotch. *Field Crops Research*, 204:89–100, 2017. doi: 10.1016/j.fcr.2017.01.012 .

Y.-Z. Ma, C. T. MacKown, and D. A. van Sanford. Differential effects of partial spikelet removal and defoliation on kernel growth and assimilate partitioning among wheat cultivars. *Field Crops Research*, 47:201–209, 1996. ISSN 0378-4290. doi: 10.1016/0378-4290(96)00016-0 .

A. Martin, X. Belastegui-Macadam, I. Quilleré, M. Floriot, M.-H. Valadier, B. Pommel, B. Andrieu, I. Donnison, and B. Hirel. Nitrogen management and senescence in two maize hybrids differing in the persistence of leaf greenness: agronomic, physiological and molecular aspects. *New Phytologist*, 167(2):483–492, 2005. doi: 10.1111/j.1469-8137.2005.01430.x .

C. Masclaux-Daubresse, M. Reisdorf-Cren, and M. Orsel. Leaf nitrogen remobilisation for plant development and grain filling. *Plant Biology*, 10:23–36, 2008. ISSN 1438-8677. doi: 10.1111/j.1438-8677.2008.00097.x .

C. Masclaux-Daubresse, F. Daniel-Vedele, J. Dechorgnat, F. Chardon, L. Gaufichon, and A. Suzuki. Nitrogen uptake, assimilation and remobilization in plants: challenges for sustainable and productive agriculture. *Annals of Botany*, 105(7):1141–1157, Jan 2010. ISSN 0305-7364, 1095-8290. doi: 10.1093/aob/mcq028 .

C. McCartney, A. Brûlé-Babel, and L. Lamari. Inheritance of race-specific resistance to Mycosphaerella graminicola in wheat. *Phytopathology*, 92(2):138–144, 2002. URL `http://apsjournals.apsnet.org/doi/pdfplus/10.1094/PHYTO.2002.92.2.138`.

J. L. Monteith and C. J. Moss. Climate and the efficiency of crop production in Britain. *Philosophical Transactions of the Royal Society of London. Series B, Biological Sciences*, pages 277–294, 1977.

G. M. Murray, R. H. Martin, and B. R. Cullis. Relationship of the severity of Septoria tritici blotch of wheat to sowing time, rainfall at heading and average susceptibility of wheat cultivars in the area. *Australian journal of agricultural research*, 41(2):307–315, 1990. doi: 10.1071/AR9900307 .

B. Ney, M.-O. Bancal, P. Bancal, I. J. Bingham, J. M. Foulkes, D. Gouache, N. D. Paveley, and J. Smith. Crop architecture and crop tolerance to fungal diseases and insect herbivory. Mechanisms to limit crop losses. *European Journal of Plant Pathology*, 135(3): 561–580, 2013. ISSN 0929-1873. doi: 10.1007/s10658-012-0125-z .

L. D. Noodén, J. W. Hillsberg, and M. J. Schneider. Induction of leaf senescence in Arabidopsis thaliana by long days through a light-dosage effect. *Physiologia Plantarum*, 96(3):491–495, 1996. ISSN 1399-3054. doi: 10.1111/j.1399-3054.1996.tb00463.x .

K. Ono, I. Terashima, and A. Watanabe. Interaction between nitrogen deficit of a plant and nitrogen content in the old leaves. *Plant and Cell Physiology*, 37(8):1083–1089, 1996. doi: 10.1093/oxfordjournals.pcp.a029057 .

S. R. Parker, S. Welham, N. Paveley, J. M. Foulkes, and R. K. Scott. Tolerance of Septoria leaf blotch in winter wheat. *Plant Pathology*, 53(1):1–10, 2004. doi: 10.1111/j.1365-3059.2004.00951.x .

D. L. Parrott, J. M. Martin, and A. M. Fischer. Analysis of barley (Hordeum vulgare) leaf senescence and protease gene expression: a family C1A cysteine protease is specifically induced under conditions characterized by high carbohydrate, but low to moderate nitrogen levels. *New Phytologist*, 187(2):313–331, 2010. ISSN 0028-646X. doi: 10.1111/j.1469-8137.2010.03278.x .

Parry, M. Reynolds, M. Salvucci, C. Raines, P. Andralojc, X.-G. Zhu, D. Price, A. Condone, and R. Furbank. Raising yield potential of wheat. II. Increasing photosynthetic capacity and efficiency. *Journal of Experimental Botany*, 62:453–467, 2001. doi: 10.1093/jxb/erq30410.1093/jxb/erq304 .

A. Pask. *Optimising nitrogen storage in wheat canopies for genetic reduction in fertiliser nitrogen inputs*. PhD thesis, University of Nottingham, December 2009. URL `http://eprints.nottingham.ac.uk/12567/`.

A. J. D. Pask, R. Sylvester-Bradley, P. D. Jamieson, and M. J. Foulkes. Quantifying how winter wheat crops accumulate and use nitrogen reserves during growth. *Field crops research*, 126:104–118, Feb 2012. ISSN 0378-4290. doi: 10.1016/j.fcr.2011.09.021 .

J. B. Passioura. Soil conditions and plant growth. *Plant, Cell & Environment*, 25(2):311–318, 2002. doi: 10.1046/j.0016-8025.2001.00802.x .

N. D. Paveley, R. Sylvester-Bradley, R. K. Scott, J. Craigon, and W. Day. Steps in predicting the relationship of yield on fungicide dose. *Phytopathology*, 91(7):708–716, Jul 2001. ISSN 0031-949X. doi: 10.1094/PHYTO.2001.91.7.708 .

R. Piessens, E. de Doncker-Kapenga, C. Uberhuber, and D. Kahaner. *Quadpack: a Subroutine Package for Automatic Integration*, springer verlag edition, 1983. ISBN: 978-3540125531.

J. Pinheiro, D. Bates, S. DebRoy, D. Sarkar, and R Core Team. *nlme: Linear and Nonlinear Mixed Effects Models*, 2017. URL https://CRAN.R-project.org/package=nlme. R package version 3.1-131.

R Core Team. *R: A Language and Environment for Statistical Computing*. R Foundation for Statistical Computing, Vienna, Austria, 2016. URL https://www.R-project.org/.

R Core Team. *R: A Language and Environment for Statistical Computing*. R Foundation for Statistical Computing, Vienna, Austria, 2017. URL https://www.R-project.org/.

R Special Interest Group on Databases. *DBI: R Database Interface*, 2014. URL https://CRAN.R-project.org/package=DBI. R package version 0.3.1.

RAGT. Blé tendre d'hiver. Leaflet, 2016. URL http://www.ragtsemences.com/rs/pdf_fr/bth. accessed 2017-07-04.

I. Rajcan and M. Tollenaar. Source: sink ratio and leaf senescence in maize: II. Nitrogen metabolism during grain filling. *Field Crops Research*, 60(3):255–265, 1999. doi: 10.1016/S0378-4290(98)00143-9 .

R. Rakotomalala. Pratique de la régression linéaire multiple — Diagnostic et sélection de variables. Version 2.1, May 2015. URL https://eric.univ-lyon2.fr/~ricco/cours/cours/La_regression_dans_la_pratique.pdf.

G. J. Rebetzke, J. A. Jimenez-Berni, W. D. Bovill, D. M. Deery, and R. A. James. High-throughput phenotyping technologies allow accurate selection of stay-green. *Journal of Experimental Botany*, 67(17):4919–4924, 2016. doi: 10.1093/jxb/erw301 .

S. Recous, P. Loiseau, J. M. Machet, and B. Mary. Transformations et devenir de l'azote de l'engrais sous cultures annuelles et sous prairies. *Les colloques de l'INRA*, 83:105–120, 1997.

M. Reynolds, M. J. Foulkes, G. A. Slafer, P. Berry, M. A. J. Parry, J. W. Snape, and W. J. Angus. Raising yield potential in wheat. *Journal of Experimental Botany*, 60(7):1899–1918, 2009. doi: 10.1093/jxb/erp016 .

M. Reynolds, A. Pask, and D. Mullan. *Physiological breeding I: interdisciplinary approaches to improve crop adaptation*. CIMMYT, Mexico, Mexico, DF (Mexico), 2012. URL http://repository.cimmyt.org/xmlui/bitstream/handle/10883/1288/96144.pdf.

M. P. Reynolds, A. Pellegrineschi, and B. Skovmand. Sink-limitation to yield and biomass: a summary of some investigations in spring wheat. *Annals of applied biology*, 146(1):39–49, 2005. ISSN 0003-4746. doi: 10.1111/j.1744-7348.2005.03100.x .

S. Rieben, O. Kalinina, B. Schmid, and S. L. Zeller. Gene flow in genetically modified wheat. *Plos One*, 6(12):1–7, 12 2011. doi: 10.1371/journal.pone.0029730 .

C. Robert, C. Fournier, B. Andrieu, and B. Ney. Coupling a 3D virtual wheat (Triticum aestivum) plant model with a Septoria tritici epidemic model (Septo3D): a new approach to investigate plant–pathogen interactions linked to canopy architecture. *Functional Plant Biology*, 35:997–1013, 2008. doi: 10.1071/FP08066 .

C. Robert, B. Andrieu, C. Fournier, D. Gouache, P. Gate, and B. Ney. Septo3D: un modèle pour analyser les effets de la structure des couverts de blé sur les épidémies de

septoriose. In *9. Conférence internationale*, page np, Tours, France, Dec. 2009. Association Française de Protection des Plantes. URL https://hal.archives-ouvertes.fr/hal-01192172. Actes sous forme de cédérom + tome résumés.

A. A. Rosielle and W. J. R. Boyd. Genetics of host-pathogen interactions to the Septoria species of wheat. Technical report, 1985.

M. C. Rousseaux, A. J. Hall, and R. A. Sánchez. Far-red enrichment and photosynthetically active radiation level influence leaf senescence in field-grown sunflower. *Physiologia Plantarum*, 96(2):217–224, 1996. ISSN 1399-3054. doi: 10.1111/j.1399-3054.1996.tb00205.x .

S. A. Ruuska, G. J. Rebetzke, A. F. van Herwaarden, R. A. Richards, N. A. Fettell, L. Tabe, and C. L. Jenkins. Genotypic variation in water-soluble carbohydrate accumulation in wheat. *Functional Plant Biology*, 33(9):799–809, 2006. doi: 10.1071/FP06062 .

S. C. Salmon and H. H. Laude. Twenty years of testing varieties and strain of winter wheat at the Kansas agricultural experiment station. Technical bulletin 80, Kansas state college of agriculture and applied science, Manhattan, Kansas, February 1932. URL https://www.k-state.edu/historicpublications/pubs/STB030.PDF.

R. Sanchez-Bragado, G. Molero, M. P. Reynolds, and J. L. Araus. Relative contribution of shoot and ear photosynthesis to grain filling in wheat under good agronomical conditions assessed by differential organ δ13c. *Journal of experimental botany*, 65(18): 5401–5413, 2014. doi: 10.1093/jxb/eru298 .

R. Sanchez-Bragado, M. D. Serret, and J. L. Araus. The nitrogen contribution of different plant parts to wheat grains: Exploring genotype, water, and nitrogen effects. *Frontiers in Plant Science*, 7:1986, 2017. ISSN 1664-462X. doi: 10.3389/fpls.2016.01986 .

M. Sanchez-Garcia, C. Royo, N. Aparicio, J. Martin-Sanchez, and F. Alvaro. Genetic improvement of bread wheat yield and associated traits in Spain during the 20th century. *The Journal of Agricultural Science*, 151(1):105–118, 2013. doi: 10.1017/S0021859612000330 .

A. Sánchez-Vallet, M. C. McDonald, P. S. Solomon, and B. A. McDonald. Is Zymoseptoria tritici a hemibiotroph? *Fungal Genetics and Biology*, 79:29 – 32, 2015. ISSN 1087-1845. doi: 10.1016/j.fgb.2015.04.001 . Septoria tritici blotch disease of wheat: Tools and techniques to study the pathogen Zymoseptoria tritici.

D. Sarkar. *Lattice: Multivariate Data Visualization with R*. Springer, New York, 2008. URL http://lmdvr.r-forge.r-project.org. ISBN 978-0-387-75968-5.

D. Sarkar and F. Andrews. *latticeExtra: Extra Graphical Utilities Based on Lattice*, 2016. URL https://CRAN.R-project.org/package=latticeExtra. R package version 0.6-28.

S. Savary, N. P. Castilla, F. A. Elazegui, C. G. Mc Laren, M. A. Ynalvez, and P. S. Teng. Direct and indirect effects of nitrogen supply and disease source structure on rice sheath blight spread. *Phytopathology*, 85(9):959–965, Sep 1995. ISSN 0031-949X. doi: 10.1094/Phyto-85-959 .

J. Schafer. Tolerance to plant disease. *Annual review of phytopathology*, 9:235–252, 1971. ISSN 0066-4286. doi: 10.1146/annurev.py.09.090171.001315 .

A. L. Scharen and J. M. Krupkinsk. Effect of Septoria nodorum infection on CO2 absorption and yield of wheat. *Phytopathology*, 59(9):1298–&, 1969. ISSN 0031-949X.

M. Schierenbeck, M. C. Fleitas, D. J. Miralles, and M. R. Simón. Does radiation interception or radiation use efficiency limit the growth of wheat inoculated with tan spot or leaf rust? *Field Crops Research*, 199:65–76, 2016. doi: 10.1016/j.fcr.2016.09.017 .

J. D. Scholes and J. F. Farrar. Increased rates of photosynthesis in localized regions of a barley leaf infected with brown rust. *New Phytologist*, 104(4):601–612, 1986. doi: 10.1111/j.1469-8137.1986.tb00660.x .

R. A. Serrago, R. Carretero, M.-O. Bancal, and D. J. Miralles. Foliar diseases affect the eco-physiological attributes linked with yield and biomass in wheat (Triticum aestivum L.). *European Journal of Agronomy*, 31(4):195–203, 2009. doi: 10.1016/j.eja.2009.06.002 .

R. A. Serrago, R. Carretero, M. O. Bancal, and D. J. Miralles. Grain weight response to foliar diseases control in wheat (triticum aestivum l.). *Field Crops Research*, 120(3):352 – 359, 2011. ISSN 0378-4290. doi: 10.1016/j.fcr.2010.11.004 .

R. A. Serrago, I. Alzueta, R. Savin, and G. A. Slafer. Understanding grain yield responses to source-sink ratios during grain filling in wheat and barley under contrasting environments. *Field Crops Research*, 150:42–51, August 2013. ISSN 0378-4290. doi: 10.1016/j.fcr.2013.05.016 .

M. W. Shaw and D. J. Royle. Factors determining the severity of epidemics of Mycosphaerella graminicola (Septoria tritici) on winter wheat in the UK. *Plant Pathology*, 42(6):882–899, 1993. ISSN 1365-3059. doi: 10.1111/j.1365-3059.1993.tb02674.x .

V. J. Shearman, R. Sylvester-Bradley, R. K. Scott, and M. J. Foulkes. Physiological processes associated with wheat yield progress in the UK. *Crop Science*, 45(1):175–185, 2005. doi: 10.2135/cropsci2005.0175 .

P. R. Shewry. Wheat. *Journal of experimental botany*, 60(6):1537–1553, 2009. doi: 10.1093/jxb/erp058 .

P. R. Shewry, R. A. C. Mitchell, P. Tosi, Y. Wan, C. Underwood, A. Lovegrove, J. Freeman, G. A. Toole, E. N. C. Mills, and J. L. Ward. An integrated study of grain development of wheat (cv. Hereward). *Journal of Cereal Science*, 56(1):21–30, 2012. ISSN 0733-5210. doi: 10.1016/j.jcs.2011.11.007 .

M. R. Simón, A. E. Perelló, C. A. Cordo, S. Larrán, P. E. van der Putten, and P. C. Struik. Association between Septoria tritici blotch, plant height, and heading date in wheat. *Agronomy Journal*, 97(4):1072–1081, 2005. doi: 10.2134/agronj2004.0126 .

T. R. Sinclair and P. D. Jamieson. Grain number, wheat yield, and bottling beer: an analysis. *Field Crops Research*, 98(1):60–67, 2006. ISSN 0378-4290. doi: 10.1016/j.fcr.2005.12.006 .

G. A. Slafer and F. H. Andrade. Changes in physiological attributes of the dry matter economy of bread wheat (Triticum aestivum) through genetic improvement of grain yield potential at different regions of the world. *Euphytica*, 58(1):37–49, 1991. URL https://link.springer.com/article/10.1007%2FBF00035338?LI=true.

G. A. Slafer and R. Savin. Postanthesis green area duration in a semidwarf and a standard-height wheat cultivar as affected by sink strength. *Australian Journal of Agricultural Research*, 1994a. doi: 10.1071/AR9941337 .

G. A. Slafer and R. Savin. Source-sink relationships and grain mass at different positions within the spike in wheat. *Field Crops Research*, 37:39–49, 1994b. doi: 10.1016/0378-4290(94)90080-9 .

G. A. Slafer, R. Savin, and V. O. Sadras. Coarse and fine regulation of wheat yield components in response to genotype and environment. *Field Crops Research*, 157(0): 71–83, 2014. ISSN 0378-4290. doi: 10.1016/j.fcr.2013.12.004 .

R. J. Smith. Use and misuse of the reduced major axis for line-fitting. *American Journal of Physical Anthropology*, 140(3):476–486, 2009. ISSN 1096-8644. doi: 10.1002/ajpa.21090 .

O. A. Somasco, C. O. Qualset, and D. G. Gilchrist. Single-gene resistance to Septoria tritici blotch in the spring wheat cultivar 'Tadinia'. *Plant Breeding*, 115(4):261–267, 1996. ISSN 1439-0523. doi: 10.1111/j.1439-0523.1996.tb00914.x .

G. Spano, N. Di Fonzo, C. Perrotta, C. Platani, G. Ronga, D. W. Lawlor, J. A. Napier, and P. R. Shewry. Physiological characterization of 'stay green' mutants in durum wheat. *Journal of Experimental Botany*, 54(386):1415–1420, 2003. doi: 10.1093/jxb/erg150 .

J. Spiertz and N. Devos. Agronomical and physiological-aspects of the role of nitrogen in yield formation of cereals. *Plant and soil*, 75(3):379–391, 1983. ISSN 0032-079X. doi: 10.1007/BF02369972 .

G. Steinberg. Cell biology of Zymoseptoria tritici: Pathogen cell organization and wheat infection. *Fungal Genetics and Biology*, 79:17–23, 2015. ISSN 1087-1845. doi: 10.1016/j.fgb.2015.04.002 .

U. Steinfort, B. Trevaskis, S. Fukai, K. L. Bell, and M. F. Dreccer. Vernalisation and photoperiod sensitivity in wheat: Impact on canopy development and yield components. *Field Crops Research*, 201:108–121, 2017. doi: 10.1016/j.fcr.2016.10.012 .

V. Svetnik, A. Liaw, C. Tong, and T. Wang. *Multiple Classifier Systems: 5th International Workshop, MCS 2004, Cagliari, Italy, June 9-11, 2004. Proceedings*, chapter Application of Breiman's Random Forest to Modeling Structure-Activity Relationships of Pharmaceutical Molecules, pages 334–343. Springer Berlin Heidelberg, Berlin, Heidelberg, 2004. ISBN 978-3-540-25966-4. doi: 10.1007/978-3-540-25966-4_33 .

S. M. Tabib Ghaffary, J. D. Faris, T. L. Friesen, R. G. F. Visser, T. A. J. van der Lee, O. Robert, and G. H. J. Kema. New broad-spectrum resistance to Septoria tritici blotch derived from synthetic hexaploid wheat. *Theoretical and Applied Genetics*, 124(1):125–142, Jan 2012. ISSN 1432-2242. doi: 10.1007/s00122-011-1692-7 .

L. Taiz and E. Zeiger. *Plant physiology and development*, chapter Plant senescence and cell death, pages 665–692. Sinauer Associates, Inc., 6th edition edition, 2014.

E. A. Tambussi, J. Bort, J. Jose Guiamet, S. Nogues, and J. Luis Araus. The photosynthetic role of ears in C3 cereals: Metabolism, water use efficiency and contribution to grain yield. *Critical reviews in plant sciences*, 26(1):1–16, 2007. ISSN 0735-2689. doi: 10.1080/07352680601147901 .

H. Thomas and L. de Villiers. Gene expression in leaves of Arabidopsis thaliana induced to senesce by nutrient deprivation. *Journal of Experimental Botany*, 47(12):1845–1852, 1996. doi: 10.1093/jxb/47.12.1845 .

H. Thomas and C. J. Howarth. Five ways to stay green. *Journal of Experimental Botany*, 51 (S1):329–337, Feb 2000. ISSN 0022-0957. doi: 10.1093/jexbot/51.suppl_1.329 .

H. Thomas and H. Ougham. The stay-green trait. *Journal of Experimental Botany*, 65(14): 3889–3900, 2014. doi: 10.1093/jxb/eru037 .

D. K. Tompkins, D. B. Fowler, and A. T. Wright. Influence of agronomic practices on canopy microclimate and Septoria development in no-till winter wheat produced in the Parkland region of Saskatchewan. *Canadian Journal of Plant Science*, 73(1):331–344, 1993. doi: 10.4141/cjps93-050 .

S. F. F. Torriani, J. P. E. Melichar, C. Mills, N. Pain, H. Sierotzki, and M. Courbot. Zymoseptoria tritici: A major threat to wheat production, integrated approaches to control. *Fungal Genetics and Biology*, 79:8–12, 2015. ISSN 1087-1845. doi: 10.1016/j.fgb.2015.04.010 .

C. Uauy, J. C. Brevis, and J. Dubcovsky. The high grain protein content gene Gpc-B1 accelerates senescence and has pleiotropic effects on protein content in wheat. *Journal of Experimental Botany*, 57(11):2785–2794, Aug 2006. ISSN 0022-0957. doi: 10.1093/jxb/erl047 .

F. van den Berg, N. D. Paveley, I. J. Bingham, and F. van den Bosch. Physiological traits determining yield tolerance of wheat to foliar diseases. *Phytopathology*, 2017. URL https://apsjournals.apsnet.org/doi/pdfplus/10.1094/PHYTO-07-16-0283-R. Accepted for publication - first look.

D. A. Vansanford and C. T. MacKown. Cultivar differences in nitrogen remobilization during grain fill in soft red winter-wheat. *Crop science*, 27(2):295–300, MAr-Apr 1987. ISSN 0011-183X. doi: 10.2135/cropsci1987.0011183X002700020035x .

P. M. Vitousek. Beyond global warming: ecology and global change. *Ecology*, 75(7): 1861–1876, 1994. doi: 10.2307/1941591 .

J. Voltas, I. Romagosa, and J. L. Araus. Grain size and nitrogen accumulation in sink-reduced barley under Mediterranean conditions. *Field Crops Research*, 52:117–126, 1997. ISSN 0378-4290. doi: 10.1016/S0378-4290(96)01067-2 .

L. Weaver and R. Amasino. Senescence is induced in individually darkened Arabidopsis leaves, but inhibited in whole darkened plants. *Plant Physiology*, 127:876–886, 2001. doi: 10.1104/pp.010312 .

R. E. Wilson. Inheritance of resistance to Septoria tritici in wheat. In *Septoria of Cereals*, 1985.

A. Wingler, S. Purdy, J. A. MacLean, and N. Pourtau. The role of sugars in integrating environmental signals during the regulation of leaf senescence. *Journal of Experimental Botany*, 57(2):391–399, Jan. 2006. ISSN 0022-0957, 1460-2431. doi: 10.1093/jxb/eri279 .

J. C. Zadoks, T. T. Chang, and C. F. Konzak. A decimal code for the growth stages of cereals. *Weed Research*, 44:415–421, 1974. doi: 10.1111/j.1365-3180.1974.tb01084.x .

J. Zhan and B. A. McDonald. The interaction among evolutionary forces in the pathogenic fungus Mycosphaerella graminicola. *Fungal Genetics and Biology*, 41(6):590–599, 2004. ISSN 1087-1845. doi: 10.1016/j.fgb.2004.01.006 .

Y.-H. Zhang, N.-N. Sun, J.-P. Hong, Q. Zhang, C. Wang, X. Qing-Wu, Z. Shun-Li, H. Qin, and W. Zhi-Min. Effect of source-sink manipulation on photosynthetic characteristics of flag leaf and the remobilization of dry mass and nitrogen in vegetative organs of wheat. *Journal of integrative agriculture*, 13(8):1680–1690, 2014. ISSN 2095-3119. doi: 10.1016/S2095-3119(13)60665-6 .

M. Zilberstein, A. Blum, and Z. Eyal. Chemical desiccation of wheat plants as a simulator of postanthesis speckled leaf blotch stress. *Phytopathology*, 75(2):226–230, 1985. URL http://apsnet.org/publications/phytopathology/backissues/Documents/1985Articles/Phyto75n02_226.PDF.

O. Ziv and Z. Eyal. Assessment of yield component losses caused in plants of spring wheat cultivars by selected isolates of *Septoria tritici*. *Phytopathology*, 68(5):791–796, 1978. ISSN 0031-949X. URL http://apsnet.org/publications/phytopathology/backissues/Documents/1978Articles/Phyto68n05_791.pdf.

E. Zuckerman, A. Eshel, and Z. Eyal. Physiological aspects related to tolerance of spring wheat cultivars to Septoria tritici blotch. *Phytopathology*, 87(1):60–65, Jan. 1997. ISSN 0031-949X. URL http://apsjournals.apsnet.org/doi/pdf/10.1094/PHYTO.1997.87.1.60.